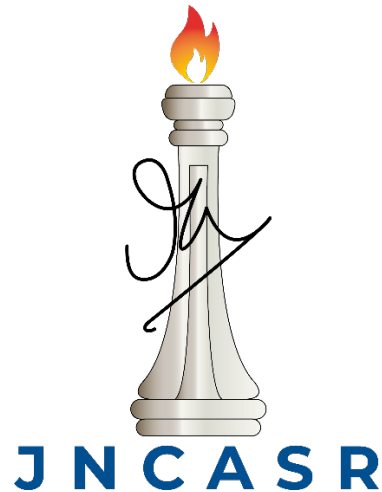# Investigating the role of Innexins in *Drosophila melanogaster* circadian pacemaker neurons

JNCASR

Thesis submitted for the degree of

Doctor of Philosophy

By

Iyer Aishwarya Ramakrishnan

Neuroscience Unit
Jawaharlal Center for Advanced Scientific Research
Bengaluru, Karnataka-560 064, India.

October 2021

Dedicated to my parents,

T.V. Ramakrishnan and Usha Ramakrishnan,

For being my source of strength and inspiration.

Table of Contents

Chapter 2: Examining the effect of RNAi mediated knockdown of *Innexin* genes on circadian clock properties

Chapter 3: Role of Innexin2 in modulating the free-running period of activity-rest rhythms.

Chapter 4: Role of Innexin1 in modulating the free-running period of activity-rest rhythms.

7. Appendices

Declaration

I hereby declare that the thesis entitled "**Investigating the role of Innexins in *Drosophila melanogaster* circadian pacemaker neurons**" submitted towards the fulfillment of the Ph.D. degree is the result of investigations carried out by me at the Neuroscience Unit of the Jawaharlal Nehru Centre for Advanced Scientific Research, Bangalore, India. The work incorporated in this thesis did not form the subject matter of any thesis submitted by me for any other degree elsewhere.

Due care has been taken to acknowledge the work and findings of other investigators in the light of the present study, keeping in view the practice of reporting scientific observations. Any omission that may have occurred due to misjudgment or oversight is deeply regretted.

Iyer Aishwarya Ramakrishnan

Place: Bangalore

Date: 20th October, 2021

Chronobiology and Behavioural Neurogenetics Laboratory

Neuroscience Unit

Jawaharlal Nehru Centre for Advanced Scientific Research

Jakkur, Bangalore – 560064, India

CERTIFICATE

This is to certify the work described in this thesis entitled "**Investigating the role of Innexins in *Drosophila melanogaster* circadian pacemaker neurons**" is the result of studies carried out by Ms. Iyer Aishwarya Ramakrishnan in the Chronobiology and Behavioural Neurogenetics Laboratory, of Jawaharlal Nehru Centre for Advanced Scientific Research, Jakkur, Bangalore, 560064, under my supervision, and that the results discussed in the thesis have not previously formed the basis for award of any other diploma, degree or fellowship.

Dr. Sheeba Vasu

Associate Professor

Acknowledgements

The journey to obtain a Ph.D. is a long one filled with emotions of uncertainty, anxiety, long working hours, and sleepless nights but also with moments of excitement, pure joy, and contentment. I consider myself lucky to be able to undertake this journey in JNC surrounded by wonderful people without whom this would not have been possible. Firstly, I would like to thank my guide, Dr. Sheeba Vasu, for having so much faith in my ability to design and explore a scientific question on my own. The trust and patience she had in me while I navigated through the many hurdles of this project have played a huge role in cultivating the attribute of independent thinking. I'm ever inspired by her strength and quiet resolve, and to undertake and perform so much work without even complaining a little bit about it.

I want to thank Prof. Vijay Kumar Sharma, Prof. Amitabh Joshi, Dr. Ravi Manjithaya, and Dr. James Chelliah for their coursework; Prof. Anand, Dr. Ravi, and Dr. James for being a part of my thesis committee. I would also like to thank Prof. Gaiti Hasan for various discussions and inputs in the initial stages of the project. Many thanks to fly biologists worldwide for generously providing us fly lines and antibodies, which has enabled us to carry out our work in a timely manner. Mr. Sunil Kumar, Ms. Keerthana, and Ms. Suma of the JNC confocal facility have helped me take beautiful images of the *Drosophila* brain, and I am grateful to them for that. I want to acknowledge DST-INSPIRE for fellowship, and DST-SERB and JNCASR for funding; SRBR for granting me the fellowship that enabled me to attend the SRBR 2020 Conference, which was hugely beneficial. I want to thank Rajanna and Muniraju for working tirelessly in the fly kitchen and going out of their way to ensure that our experiments and maintenance of fly lines were never affected.

List of publications

1. **Ramakrishnan, A., & Sheeba, V.** (2021). Gap junction protein Innexin2 modulates the period of free-running rhythms in *Drosophila melanogaster*. iScience, Volume 24, Issue 9, 103011.

2. **Ramakrishnan, A., & Sheeba, V.** Role of gap junction protein Innexin1 in the circadian pacemaker circuit of *Drosophila melanogaster* (*In preparation*).

3. **Ramakrishnan, A., & Sheeba, V.** A new player in circadian pacemaker networks-electrical synapses and the role of gap junction proteins (Invited review*, Frontiers in Physiology, in preparation*).

Synopsis

Circadian systems are endogenous timekeeping mechanisms that restrict physiological and behavioural processes of organisms to specific times of the day. The central circadian clock in mammals is located at the base of the hypothalamus, in bilaterally located structures called the Suprachiasmatic nuclei, made up of about 20,000 neurons which regulate many rhythmic metabolic, behavioural, and physiological processes. In contrast, the central clock in *Drosophila melanogaster* comprises around 150 neurons, organized into distinct subsets, distributed bilaterally in the brain, and controls many robust circadian behaviours. Several decades of work focusing on the genetic and neuronal basis of how rhythms are generated using *Drosophila* have been instrumental in advancing our understanding of the organization and functioning of circadian systems across organisms. Each of the 150 neurons in the *Drosophila* brain is characterized by a molecular clock made up of core clock proteins forming a self-sustaining Transcription Translation Feedback Loop (TTFL). However, several studies have shown that coherent rhythms in behaviour are generated only when these subsets of neurons function as a network and communicate with each other. *Drosophila* circadian neurons are known to communicate amongst each other via neuropeptides and neurotransmitters extensively. One such well-studied neuropeptide is the Pigment Dispersing Factor (PDF), secreted by a subset of circadian neurons called the ventral lateral neurons. Our current understanding of the *Drosophila* circadian network posits that PDF secreted by these ventral lateral neurons acts to synchronize the molecular clocks of the entire neuronal network, thus bringing about coherent rhythms in behaviour. Flies lacking PDF show arrhythmic circadian activity-rest behaviour, thus underscoring the importance of communication among neurons in this network.

Several decades of research have focused on how neurons communicate amongst each other in specialized synaptic compartments using neuropeptides and neurotransmitters. We now understand in great detail the underlying molecular and physiological mechanisms of how action potentials are generated and transmitted in neuronal networks via the release of neuromodulators. However, neuronal networks across most organisms are composed of chemical and electrical synapses that function together intricately to regulate various behaviours. Electrical synapses are direct cell-to-cell connections made up of gap junction proteins (called Connexins in vertebrates and Innexins in invertebrates) which facilitate the exchange of ions and small molecules (< 1 kDa) between cells, thus coupling them "electrically." Because these cells are electrically connected, there is little to no delay in the transfer of information from one cell to another. Hence, electrical synapses were traditionally studied for their roles in circuits demanding fast responses, e.g., the escape networks found in both invertebrate and vertebrate nervous systems. Over time, it became apparent that the functions of electrical synapses are not just limited to escape responses, but they play important roles both during the development of nervous systems and in the adult nervous system to modulate several behaviours in both vertebrates and invertebrates. Yet, compared to its chemical counterparts, the contribution made by electrical synapses to nervous system functioning remains highly underrated.

There are eight genes coding for gap junction proteins in *Drosophila*, named from *Innexin1-8*. These are mostly studied for their roles in development, but in recent years, there have been a few studies that establish their contribution in adult circuits for behaviours such as learning, memory, and sleep. Although the adult *Drosophila* circadian circuit is studied in great detail, there are no reports to date which examine a role for gap junctions in this circuit for regulating circadian behaviours. This motivated me to ask if gap junctions play a role in the circadian circuits of *Drosophila melanogaster* to modulate

various clock properties. A comprehensive review of the current understanding of how the *Drosophila* circadian pacemaker circuit functions as a network to generate rhythmic activity-rest behaviours and the roles played by electrical synapses in nervous systems during development and in the mature, adult stages in both vertebrate and invertebrate model systems are discussed in detail in the introductory chapter, Chapter 1.

To identify the roles played by gap junctions in the *Drosophila* circadian circuit, I carried out an unbiased knockdown screen and examined clock properties under two external environments representing the two essential functions of the clock, 1. Under constant conditions (constant darkness and ambient temperature of 25°C), the clock is devoid of all external periodic cues and manifests its inherent properties. 2. Under entrained conditions, the internal clock synchronizes its activity to the external, periodic cue (under daily light or temperature cycles). I found that knockdown of 2 gap junction genes, *innexin1* and *Innexin2,* lengthens the free-running period of flies under constant conditions, i.e., their clocks now run with a speed that is lengthened by about an hour as compared to control flies. This suggests that Innexin1 and Innexin2 are required in the clock cells to determine the normal speed of the clock and a near 24-hour period, as seen in wild-type flies. I also found that downregulation of the levels of *Innexin2* and *Innexin4* in clock neurons interferes with its ability to phase activity appropriately with reference to an external, cyclic periodic cue; in this case, cycling of Light and Dark in the external environment. These flies now phase their activity about 45 minutes later than the wild-type flies, thus suggesting that Innexins also affect circadian behaviour under entrained conditions. Therefore, my results report for the first time that gap junction genes function in the circadian circuit of *Drosophila* to modulate clock properties. The experiments and results of the genetic screen are discussed in detail in Chapter 2.

Next, I wanted to examine the distribution and mechanisms by which Innexin2 functions in the circadian circuit. To begin with, I use genetic methods to restrict the knockdown of *Innexin2* to either the adult stage or the developmental stages to ask if the period lengthening seen in case of Innexin2 downregulation are due to its roles during development or its functions in the adult circadian circuit. I then proceeded to systematically target the knockdown of *Innexin2* to different subsets of clock neurons and found that Innexin2 functions only in the ventral lateral subsets, the cluster of neurons that have previously been reported to play important roles in regulating activity under constant conditions. I also show the presence of Innexin2 protein in these cell groups. Further, to understand the mechanism by which Innexin2 functions in the circadian neurons, I examine the status of oscillation of a core molecular clock protein Period in all the clock neuronal subsets and find that the phase of oscillation is affected in flies when *Innexin2* is downregulated. I also examine the levels and oscillation of the circadian neuropeptide PDF in the neuronal terminals of ventral lateral neurons and find that downregulation of *Innexin2* affects the levels of PDF compared to control flies. Finally, using a mutant of *Innexin2* that alters channel-based functions, I show that Innexin2 functions as gap junctions/hemi channels in the ventral lateral neurons. The experiments, results, and discussion addressing the function and mechanism of action of Innexin2 in the circadian neurons are described in detail in Chapter 3.

In the next chapter, I proceed to investigate the roles of Innexin1 in the clock network. Developmental versus adult-specific knockdown of *Innexin1* in the clock neurons reveals that Innexin1 functions at both stages to regulate the free-running period. I restricted the knockdown of *Innexin1* to subsets of clock neurons and found its function to be important in the ventral lateral neurons. Apart from the ventral lateral neurons, I found that the function of Innexin1 was important in astrocytes, a subset of glial cells, in modulating the

free-running period. I examined the oscillations of the molecular clock protein Period in clock neurons and found that the downregulation of *Innexin1* in these neurons phase-shifts the molecular clocks and affects the levels of neuropeptide PDF in the axonal terminals of the ventral lateral neurons. I also found that Innexin1 functions as gap junctions/hemi channels in the ventral lateral neurons. The details of the roles of Innexin1 in the clock network are described in detail in Chapter 4.

In summary, my studies reveal important roles for *Innexin* genes in determining core clock properties like free-running period and phase of the rhythm in *Drosophila melanogaster*. I found that the levels of *Innexin1* and *Innexin2* in the ventral lateral clock neurons determine the free-running period. Several previous reports have shown that these neuronal subsets are important to regulate rhythm properties under constant conditions. My experiments uncover a novel mechanism by which these neurons regulate the free-running period of the network. Membrane electrical properties of the clock neurons modulate several aspects of circadian behaviour under free-running conditions. Since gap junctions function to couple cells electrically, I hypothesize that Innexin1 and Innexin2 could be involved in regulating the electrical properties of these neurons, such as firing frequency or pattern, which could, in turn, affect the molecular clocks and the free-running rhythms. Alternatively, disruption of the synchronous firing of these clock neurons in the absence of gap junction proteins could also affect the molecular clock and its free-running period. In the last chapter, Chapter 5, I summarize my findings on the roles of Innexin1 and Innexin2 in the circadian network. I place my results in the context of various previous studies on the roles of gap junctions in vertebrate and invertebrate nervous systems and discuss the possible mechanisms by which these proteins modulate the free-running period of the *Drosophila* circadian network. Overall, my studies highlight the importance of gap junction proteins in regulating circadian rhythms and reveal that circadian timekeeping is

brought about by a combination of electrical and chemical synapses in the underlying neuronal network.

Chapter 1: Introduction

1.1 Introduction to circadian clocks and their properties

The 24-hour rotation of the earth on its axis has resulted in daily variations in different biotic and abiotic factors in the environment such as light, temperature, and humidity. To adapt to such daily variations, it is hypothesized that organisms ranging from bacteria to humans evolved to have endogenous timekeeping mechanisms of about 24 hours to restrict most of their behavioural and physiological activities to appropriate times of the day (reviewed in K L Nikhil and Sharma V.K., 2017). These timekeeping mechanisms are called circadian clocks, and the processes they regulate are known as circadian rhythms. Franz Halberg coined the term 'circadian' (Latin, 'circa'-about, 'diem'-day) to emphasize that the periodicity of the endogenous rhythms are approximately 24 hours, as opposed to exact 24 hours (reviewed in Daan, 2010). This is regarded as a fundamental property of circadian clocks, to persist with a near 24-hour periodicity in the absence of any cyclic, external periodic cues under constant conditions (e.g., constant light or constant darkness and constant temperature). These conditions are called free-running conditions, and the period exhibited under these conditions is called the 'free-running period'. Most organisms in nature exhibit a free-running period of near 24-hours with some exceptions (Dunlap et al., 2004). Under free-running conditions, circadian clocks are also shown to have the properties of persistence, innateness, and temperature compensation (ability to maintain a near 24-hour period under different temperatures). Apart from its persistence under free-running conditions, a vital function of the circadian clock is to synchronize the processes of an organism to the cyclic, external environmental cues. This phenomenon is called entrainment, and the periodic environmental signals which provide time information to the clock are called *Zeitgebers* (from German, time-giver). Light and Dark alterations in the environment are probably the most prominent and well-studied as a *Zeitgeber* out of all the cyclic factors. The clock synchronizes its activity to the external light: dark

cycles such that a particular phase (any point in time) of the clock has a stable and reproducible relationship with the phase of the *Zeitgeber*.

1.2 Anatomical organization of the circadian clock

For a long time after the discovery of endogenous rhythms, researchers did not try to find the anatomical location of the circadian clock, partially because it was thought that rhythms were generated in the body of the organism as a whole and not in any particular anatomical location. The idea of a pacemaker that controls an organism's circadian rhythms was put forth by Pittendrigh (Daan, 2010; Pittendrigh, 1960). An organ can be called a pacemaker if it is rhythmic by itself and responsive to external Light: Dark cycles and can restore rhythmicity with a phase or period dictated by the donor when transplanted into a host that lacks a pacemaker. One of the first transplantation experiments was carried out in cockroaches, which led to the identification of the accessory medulla of the optic lobe as the site of circadian pace making (Nishiitsutsuji-Uwo and Pittendrigh, 1968, Page T, 1982). Similar transplantation studies also led to the discovery of the Suprachiasmatic nucleus, the mammalian circadian pacemaker located at the base of the hypothalamus (Ralph et al., 1990). We now know that the central pacemaker, which regulates most physiological processes, is located in the central nervous system in organisms. They are either directly photosensitive or strategically placed to form connections to major photoreceptive organs, e.g., the optic lobe medulla behind the compound eyes in cockroach (Nishiitsutsuji-Uwo and Pittendrigh, 1968, Page , 1982), the basal neurons behind the eyes of the mollusk *Bulla gouldiana* (Block and Wallace, 1982) and the synaptic connections from the mammalian retina to the SCN (Moore and Lenn, 1972). However, over time, researchers have found that circadian systems are not composed of one single oscillator in the central nervous system but are a multi-oscillatory system with clocks in several other organs and tissues (Bell-Pedersen et al., 2005). The central clocks in the brain and the

peripheral clocks in different tissues coordinate to generate coherent rhythms in various behavioural and metabolic processes (Kumar, 2017). In mammals, circadian clocks were found to be present in other tissues such as lung, liver, skeletal muscles (Stokkan et al., 2001; Yamazaki et al., 2000), kidney, cornea, pituitary glands, etc. in mammals (Kumar, 2017; Yoo et al., 2004). Similar evidence of multi-oscillatory systems was also found in *Drosophila melanogaster* (Ito and Tomioka, 2016), Zebrafish (Whitmore et al., 1998), Xenopus (Andreazzoli and Angeloni, 2017), birds (Cassone et al., 2017) and even in the case of the unicellular marine dinoflagellate, *Gonyaulax polyedra* (Roenneberg and Morse, 1993).

1.3 Clock genes: defining the cogs and gears of the circadian clock

The idea that circadian clocks are innate gives rise to the question of the identity of the underlying genetic components regulating circadian behaviour. In the 1950s and 1960s, Seymour Benzer had started forward genetic screens in *Drosophila melanogaster* by carrying out random mutagenesis and assaying for behavioural defects. Ron Konopka, then working in the lab of Benzer, had taken up the task of conducting such forward genetic mutagenesis screens to identify genes regulating circadian behaviour. The behaviour of interest was *Drosophila* eclosion rhythms, which Pittendrigh earlier showed to be under the control of circadian clocks. These screens produced surprising results that formed the basis of most future studies investigating the genetic regulation of circadian rhythms in *Drosophila* and other organisms. Konopka identified three different mutants one with a long free-running period of eclosion (28-hr) (per^L), another with a short (20-hr) period of eclosion (per^S) and a third with no rhythmicity (per^0) (Konopka and Benzer, 1971). All three mutations were mapped to the same locus that was named *period (per),* which is now identified as one of the core clock genes in *Drosophila*. Several years later, the *per* locus was cloned, and researchers started examining the mechanisms that enable *per* to regulate

properties of circadian rhythms. A breakthrough in figuring out the mechanism was made when it was found that PER protein was expressed rhythmically in the adult *Drosophila* brain, 6 hours later than the peak phase of per mRNA. This finding led to the hypothesis of a Transcription-Translation feedback loop (TTFL) by Paul Hardin, Jeff Hall, and Michael Rosbash in the early 1990s (Hardin et al., 1990). The following two decades were dedicated to discovering elements of the TTFL in *Drosophila* and other organisms. Genetic screens uncovered many other clock genes in *Drosophila* such as *timeless (tim)* (Sehgal et al., 1994), *Clock (Clk)* (Allada et al., 1998), *cycle (cyc)* (Rutila et al., 1998), *doubletime (dbt)* (Kloss et al., 1998; Price et al., 1998), *shaggy (sgg)* (Martinek et al., 2001) and *cryptochrome (cry)* (Emery et al., 1998; Stanewsky et al., 1998). The core clock genes in *Drosophila* as we know it today are *Clock, cycle, period and timeless. Clock* and *cycle* act as the positive arm of the feedback loop and form a heterodimer that binds to the E-boxes of the *per* and *tim* promoters and activates its transcription. per and tim mRNA peak at late night, around *Zeitgeber* time (ZT 16) and their protein products peak 6 hours later at ZT22 (reviewed in Hardin, 2011). PER and TIM proteins form a heterodimer, translocate into the nucleus, and bind to CLOCK and CYCLE, thus inhibiting their own transcription, thereby acting as the negative arm of the feedback loop. This entire process of TTFL takes about 24 hours to complete such that the rhythms of mRNA and protein accumulation mirror the rhythms in activity-rest. The entire TTFL is self-sustaining even in the absence of external Light: Dark cycles, i.e., under constant darkness (DD) with a near 24-hour period (Hardin, 2011). Several post-transcriptional and post-translational modifications like phosphorylation of PER and TIM by kinases like DBT and SGG are now known to be involved in the functioning of this self-sustaining oscillator (Curtin et al., 1995; Kloss et al., 2001, 1998; Patke et al., 2020; Price et al., 1998; Price et al., 1995). The TTFL involving the core clock genes is the simplest mechanism by which timekeeping

by a self-sustaining oscillator can be explained. However, many studies over the years have revealed that circadian timekeeping at the molecular level consists of many such interlocked feedback loops, which are necessary to keep the core TTFL functioning properly (reviewed in Hardin, 2011, Patke et al., 2020). Around the same time, genetic screens in other model organisms have also led to the identification of analogous clock genes. In the mold *Neurospora crassa,* mutagenesis screens led to the identification of the core clock gene *frequency (frq)* (Feldman and Hoyle, 1973); similar mutagenesis screens identified Clock as a positive regulator of the TTFL in mammals (Vitaterna, M.H et al., 1994), while the other components of the mammalian TTFL were discovered via homology with known clock elements in *Drosophila* (Herzog et al., 2017). Although the specific mechanisms and finer details of the molecular clock are different among organisms, core timekeeping can be explained by self-sustaining transcriptional-translational feedback loops in most eukaryotes.

1.4 From genes to circuits: The *Drosophila melanogaster* circadian pacemaker neuronal circuitry

The discovery of central pacemaker neurons in the *Drosophila* brain followed the discovery of *per* gene as a core circadian clock component. Antibodies raised against PER protein detected its expression in about 150 neurons in the adult brain distributed in the lateral brain close to the optic lobe and the posterior dorsal cortex. PER protein levels were also found to be cycling in these cells both under Light: Dark cycles (LD) and under constant conditions (DD) (Ewer et al., 1992; Siwicki et al., 1988; Zerr et al., 1990). These neurons in the brain are classified into two major subsets based on their anatomical location as the lateral neurons and dorsal neurons. Each of these classes are further sub-divided based on their size and anatomical locations. The lateral neurons consist of the small ventral lateral neurons (s-LNv), the large ventral lateral neurons (l-LNv), the dorsal

lateral neurons (LNd), and the lateral posterior neurons (LPNs). The dorsal neurons are further subdivided into the DN1, DN2, and DN3 clusters (reviewed in Sheeba, 2008) (Fig. 1.1). The functions of each of these clusters are important in regulating various aspects of circadian behaviour under different external environments. Even though these neuronal subsets have a functional, ticking cellular clock composed of the core and accessory TTFL loops, coherent rhythms in behavioural outputs are manifested only when these neurons communicate amongst each other and function as a network (reviewed in Beckwith and Ceriani, 2015). In *Drosophila,* blocking the communication among circadian neurons by expressing the tetanus toxin light chain (TeTxLC) results in about 80-90% of flies becoming arrhythmic under constant conditions (DD 25°C) and about 60% of flies failing to entrain to Light: Dark cycles (Kaneko et al., 2000), thus underscoring the importance of synaptic transmission among neurons in the network. Under constant darkness (DD), the ventral lateral neurons (LNv) and the molecular clock in these cells were shown to be necessary and sufficient for rhythmicity of activity-rest rhythms (Grima et al., 2004; Helfrich-Förster, 1998; Renn et al., 1999; Stoleru et al., 2004); however, recent studies have shown that clock properties under DD are also regulated by the non-LNv neuronal clusters (Bulthuis et al., 2019; Delventhal et al., 2019; Schlichting et al., 2019). The ventral lateral neurons secrete the neuropeptide Pigment Dispersing Factor (PDF), which is necessary for rhythmicity under constant conditions (DD 25°C) (Renn et al., 1999) (Fig. 1.1). s-LNv secrete PDF in the dorsal part of the brain through their axonal terminals, henceforth referred to as dorsal projections (DP) (Park et al., 2000); and most circadian neurons except the l-LNv, some LNds and, DN1ps are responsive to PDF via expression of its receptor PDFR (Hyun et al., 2005; Mertens et al., 2005; Shafer et al., 2008). PDF is shown to rhythmically accumulate in the s-LNv dorsal terminals both under LD and DD (Park et al., 2000). It is probably also secreted rhythmically, as evidenced by the high

amounts of rhythmic fasciculation of the s-LNv dorsal terminals observed, coinciding with the peak of accumulation (Fernandez et al., 2008). However, the functional role of the morphological changes in DD continues to be debated (Fernandez et al., 2020). Not surprisingly, PDFR expression is also found to be rhythmic in non-LNv cells, with the peak expression coinciding with the peak of PDF accumulation in the DP (Klose et al., 2016). PDF functions as a synchronizing factor in the circadian network, with complex effects on downstream neurons such as required for maintaining rhythmicity in some clock cells, including the s-LNv themselves and adjusting the phase of the molecular clock in some other cells (Yoshii et al., 2009). The small percentage of rhythmic flies among *Pdf/ PdfR* mutants show a short period of free-running rhythms, suggesting that PDF acts to lengthen the period of the circadian network(Hyun et al., 2005; Mertens et al., 2005; Renn et al., 1999) (Lear et al., 2005b). Overexpression or ectopic expression of PDF in the dorsal region lengthens the free-running period while also desynchronizing the network (Helfrich-Förster et al., 2000; Wülbeck et al., 2008). PDF acts via the PDFR, a G-protein coupled receptor that further activates the adenylate cyclase (AC) pathway with different subunits of AC recruited for signalling in different clock neurons, thus bringing about differences downstream (Duvall and Taghert, 2012, 2011). Furthermore, increasing the speed of the molecular clock specifically within the PDF neurons by overexpression of kinases shortens the free-running period of locomotor rhythms and speeds up the molecular clocks within most PDF-negative clock neuron classes, an effect that requires PDF signalling (Yao and Shafer, 2014). Although coherent rhythms in DD is a network property, s-LNv play a major role in setting the free-running period of the circuit by regulating the phase of molecular clocks of other non-LNv neurons via PDF (Yao and Shafer, 2014). Thus, it is now well-established that PDF acts as a major synchronizing factor in the circadian network. Apart from its role as a synchronizing factor in the circuit,

PDF also acts as an output factor of the clock to regulate various overt rhythms like activity-rest and sleep (Cavanaugh et al., 2014; Pírez et al., 2013). Based on the above evidence, it is reasonable to suggest that the ventral lateral neurons and PDF secreted by these cells are major players that regulate clock properties under constant conditions. However, studies from the past few years have compelled researchers to appreciate that circadian rhythmicity, free-running period, and rhythm power under constant conditions (an indicator of how well-consolidated activity and rest are to a particular time of the day) are determined by the entire network of clock cells and not just the ventral lateral neurons (Bulthuis et al., 2019; Delventhal et al., 2019; Dissel et al., 2014; Nettnin et al., 2021; Schlichting et al., 2019; Yao et al., 2016; Yao and Shafer, 2014). Tissue-specific CRISPR-Cas9 based mutagenesis study of clock proteins revealed that not just the ventral lateral neurons but the dorsal lateral subsets are also necessary to maintain rhythmicity under constant darkness (Delventhal et al., 2019; Schlichting et al., 2019). Similarly, the non-LNv cells were found to be important to regulate the power of the rhythm which is an important property of circadian rhythms (Bulthuis et al., 2019; Nettnin et al., 2021).
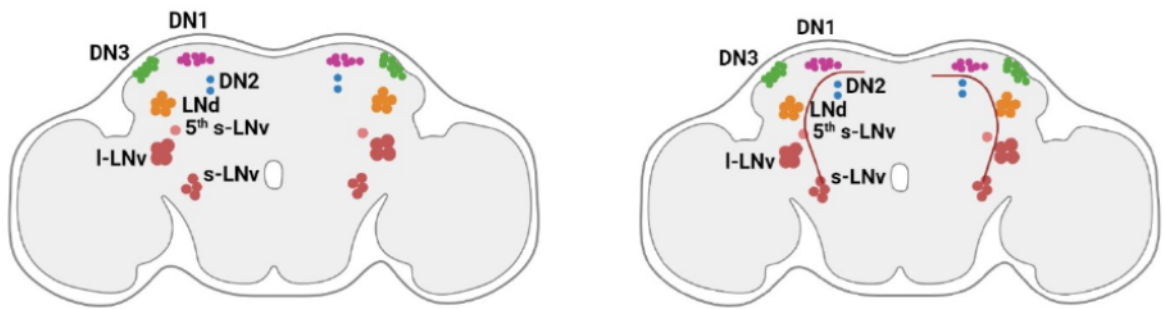
Figure 1.1: Adult *Drosophila* brain depicting the distribution of circadian clock neuronal subsets **(left)**. The subsets are divided broadly into ventral and lateral neuronal groups based on their anatomical location. The lateral neurons are further subdivided into ventral subsets (LNv) and dorsal subsets (LNd). The ventral subsets are comprised of the small ventral lateral neurons (s-LNv) and the large ventral lateral neurons (l-LNv). The dorsal subsets are subdivided into DN1, DN2 and DN3 groups. **(Right)** The small ventral lateral neurons secrete the neuropeptide Pigment Dispersing Factor (PDF) via its dorsal neuronal terminals into the dorsal part of the brain. PDF acts to synchronize the molecular clocks of most clock neurons in the circadian circuit.

On the same lines, other neuropeptides and neurotransmitters apart from PDF were also found to have roles in the circadian network, although they are not as well-studied as PDF. Small neuropeptide F (sNPF) is expressed by s-LNv and some subsets of LNd among the clock neurons (reviewed in Beckwith and Ceriani, 2015). sNPF has been shown to have some sleep-promoting roles in the circuit (Shang et al., 2013) apart from acting as an output signal from the clocks to the motor centers (Vecsey et al., 2014). It has also been shown to have significant roles in another clock-controlled behaviour: the rhythmic eclosion of *Drosophila melanogaster* (Selcho et al., 2017). Neuropeptide F (NPF) is expressed in some LNds, 5th s-LNv, and some l-LNvs. Lack of NPF in these clock cells lengthens the free-running period and modulates the phase of activity under Light: Dark cycles, suggesting its roles in regulating rhythm properties (Hermann et al., 2012). Similarly, Ion Transport Peptide (ITP), secreted by one LNd and the 5th s-LNv, is involved in the modulation of the free-running period as well as the phasing of activity under LD cycles,

thus suggesting that it plays complementary roles to PDF as a synchronizer in the clock circuit and as an output molecule for the clock network (Hermann-Luibl et al., 2014; Johard et al., 2009). Apart from neuropeptides, neurotransmitters have also been shown to play certain specific roles in the circadian network in *Drosophila*. Acetylcholine and glutamate secreted by a subset of LNds and DN1ps are important for their communication with the s-LNv, which regulates the phasing of activity under LD cycles (Duhart et al., 2020). Additionally, glutamate also has roles in modulating the free-running period of clocks, as evidenced by the lengthened period of rhythms seen in the case of glutamate receptor mutants (Hamasaka et al., 2007). It is also involved in relaying temperature information from DN1p to s-LNv to modulate activity-rest rhythms under temperature cycles (Fernandez et al., 2020). Dopamine and GABA are shown to play important roles in regulating the timing of sleep, which is a critical output of the circadian clock (reviewed in Shafer and Keene, 2021). GABAergic inputs are shown to be required in the s-LNv for maintenance of rhythmicity and modulation of the period of free-running rhythms (Dahdal et al., 2010). Thus, communication among neurons in the circadian network mediated by chemical synapses via neuropeptides and neurotransmitters play essential roles in the circadian pacemaker circuit of *Drosophila melanogaster*.

1.5 Membrane electrical properties of the clock neurons and circadian rhythms

Apart from the role of molecular clocks and several neuropeptides and neurotransmitters in modulating circadian rhythm properties, electrical properties of the LNv membranes have also been shown to contribute to regulating clock properties. The resting membrane potential in the case of s-LNv and l-LNv was found to oscillate in a time-of-day dependent manner. It is more depolarized during the day and hyperpolarized during the night under Light: Dark cycles (Cao and Nitabach, 2008; Sheeba et al., 2008b). The l-LNv also shows

a day versus night variation in the firing rates and pattern with more burst and tonic firing during the day that decreases progressively towards the night (Sheeba et al., 2008b). These variations in the firing pattern in l-LNv persist under constant darkness (DD day 15) and are abolished in the core clock mutant *per⁰*, suggesting that the variation in membrane properties is under circadian clock control (Cao and Nitabach, 2008; Sheeba et al., 2008b). Constitutive expression of a potassium channel, Kir2.1, in the ventral lateral neurons renders the flies arrhythmic and abolishes molecular rhythms in the ventral lateral neurons (Nitabach et al., 2002). A similar study was carried out, which examined the effect of LNv membrane silencing by expression of Kir2.1 only during the adult stages to avoid triggering compensatory mechanisms during development that may affect cell viability. Silencing the LNv membrane only during the adult stages using an inducible system also led to behavioural arrhythmicity but did not affect the molecular clock protein oscillations in these cells. However, there was an effect on the complexity of arborisations of the PDF termini in the dorsal side of the brain in the experimental flies, suggesting that membrane electrical state could directly affect the output of the clock (Depetris-Chauvin et al., 2011). An opposite kind of genetic manipulation, the constitutive activation of the membrane via expression of a voltage-gated Na^+ channel, NaChBac, in the ventral lateral neurons, results in complex rhythms in behaviour (activity-rest rhythms composed of multiple free-running periods), shifted phase of molecular oscillations in the dorsal neurons and a higher accumulation of PDF in the s-LNv dorsal terminals (Nitabach et al., 2006). This again implies that interference with the membrane electrical states can affect behavioural rhythms and the underlying molecular clock, clock outputs, or both. Finally, the link between membrane states and circadian clock gene expression was established by performing microarrays on circadian neurons after hyperexcitation or hyperpolarization of these cells (Mizrak et al., 2012). The authors conclude that altering the membrane

electrical states can lead to changes in the transcription of many genes, including circadian clock genes. They also show that hyper exciting the neurons causes a 'morning-like' transcription profile, whereas hyperpolarizing the neurons can generate an 'evening-like' transcription profile, thus suggesting that membrane electrical states and transcriptional profiles are intricately linked with each other (Mizrak et al., 2012).

Several ion channels have been implicated in contributing to this daily variation in membrane properties of the clock neurons. They are required for the maintenance of appropriate resting membrane potential in *Drosophila*. The sodium channels *Narrow abdomen* (NA) (Lear et al., 2005a) and *NA/NACLN* (Flourakis et al., 2015), hyperpolarization-induced cation channel I_h (Fernandez-Chiappe et al., 2021) as well as the potassium channels *slowpoke* (Fernández et al., 2007), inward rectifying channel *Ir* (Ruben et al., 2012), *shaw* and *shal* (Smith et al., 2019) have all been shown to play important roles in the regulation of membrane properties and can affect various aspects of circadian rhythms. *Narrow abdomen (na)* is a gene encoding a sodium channel expressed in the circadian neurons. *na* mutants are arrhythmic in DD and show decreased anticipation to light and dark transitions in LD. Although the molecular clock oscillations are intact in *na* mutants, they show higher level of PDF in the dorsal terminals, which could desynchronize the clocks in the non-LNv neurons leading to arrhythmicity in behaviour (Lear et al., 2005a). Another recent study shows that a reduction of a hyperpolarization-activated cation channel (I_h) in the LNvs leads to arrhythmicty, reduction in the burst firing pattern of both s-LNv and l-LNv neurons, and reduced levels of PDF accumulation in the s-LNv dorsal terminals (Fernandez-Chiappe et al., 2021). Similar studies have been performed in the case of K channel mutants in *Drosophila* circadian neurons. A mutation in the gene encoding the K channel, *slowpoke*, reduces the rhythmicity of flies and PDF levels in the dorsal terminals. However, the molecular clocks

in the LNv were found to be intact. This suggests that slowpoke acts by altering the output of the circadian clocks and does not affect the underlying molecular clocks (Fernández et al., 2007). Similar observations were made for mutants lacking the inward rectifier potassium channel I_r. Mutants of this channel have lengthened period of activity-rest rhythms, while overexpression of this channel leads to arrhythmicity and dampening of molecular oscillations in DD (Ruben et al., 2012). Voltage-gated potassium channels shaw and shal were also shown to be important for the daily variation in the rhythmic firing of the LNv and absence of these channels in the LNv result in differences in the activity levels under LD cycles (Smith et al., 2019). While the above studies have examined the roles of individual ion channels on circadian rhythm properties, a somewhat complete model of the regulation of the daily variation in membrane potential was given by Flourakis et al., 2015. This study proposed the 'bicycle model' of membrane excitability where during the day, the sodium leak channels NA/NALCN are active allowing for depolarization of the neuron to promote elevated firing rates. During the night, the resting K currents are elevated, hyperpolarizing the cell to decrease the firing rate. They also found that Na/NALCN activity was controlled by *NCA localization factor1* (*Nlf1*), which is directly modulated by the core clock gene *Clock* (Flourakis et al., 2015). However, this model to explain daily variation in membrane excitability was proposed after recording from the DN1p neurons and not from the LNv neurons, which have been well-studied previously and are shown to have rhythms in membrane electrical activity.

Taken together, all the above studies suggest that electrical activity of the clock cells has profound effects on the circadian rhythms under both entrained and free-running conditions by either affecting the core molecular clocks or the output pathway mediated by PDF or both. Although few studies focus on the roles of membrane electrical states in circadian behaviour in *Drosophila*, because of the technical difficulty in obtaining

electrophysiological recordings from these neurons, one can expect that the core molecular clock and membrane potential are likely to be intricately linked and reciprocally regulate each other.

1.6 Communication in neural networks: Overview of electrical synapses

Neural networks made up of neurons and glia are known to extensively communicate amongst themselves. This is crucial for regulating several processes from development to behaviour and plasticity. Interaction between neurons occurs at specialized cellular regions called synapses. Across organisms and behaviours, most studies have focused on the role of chemical synapses among neurons in a circuit, even though electrical and chemical synapses have been known to co-exist in neural networks of most metazoans (reviewed in Nagy et al., 2018; Pereda, 2014). In this section, I will review the literature revealing roles played by the lesser-understood mode of communication in neural networks, the electrical synapses. While chemical synapses are made up of sophisticated molecular machinery where information is transferred from the pre-synaptic cell to the post-synaptic cell via the release of neuropeptides or neurotransmitters, electrical synapses are direct cell-cell connections made up of specialized structures called gap junctions (Figure 1.2). The first evidence of direct communication between cells via gap junctions was discovered in invertebrates. Furshpan and Potter recorded electrical activity from one-way synapses in the abdominal nerve cord of the crayfish (*Astacus fluviatilis*) and showed that action potentials directly pass between the giant axons to the motor neurons (Furshpan and Potter, 1957). Similar "electrical connections" were shown to be present in the lobster cardiac ganglion cells when electrodes were inserted into one cell, and recordings from the other cell showed an action potential of lower amplitude and delayed time course (Watanabe A, 1958). This form of electrical communication was thought to be mediated by direct connections between adjacent cells, called 'nexus' or 'gaps.' These connections

were observed using electron microscopy in several tissues such as smooth and cardiac muscles in mammals, rat epithelia, giant axon in the earthworm, mouse heart and liver cells, etc. (Dewey and Barr, 1964; Revel and Karnovsky, 1967). However, there was no one-to-one correlation reported between the existence of these nexuses and the electronic coupling of these cells (Dewey and Barr, 1964), suggesting that these intercellular connections may have other roles to play in cell-cell coupling and adherence of cells. Although electrical connections between cells were first observed in invertebrates, the genes responsible for these cell-to-cell connections were first identified and isolated in vertebrates where they are called Connexins. Innexin genes were discovered much later, probably because of a lack of sequence similarity between these two gene families (Bauer et al., 2005). As we know now, gap junctions are clusters of intercellular channels made up of proteins called Connexins in vertebrates, Innexins in invertebrates, and Pannexins, which share sequence similarity to Innexins and are found in some chordates (reviewed in Beyer and Berthoud, 2018). Each cell expresses one unit of the channel, known as the hemichannel, and two such hemichannels in adjacent cells interact to form functional gap junctions (Figure 1.2). Gap junction hemichannels could be made up of the same protein subunit (homomeric) or different protein subunits (heteromeric); similarly, gap junctions could be composed of the same subunits of hemichannels (homotypic) or different subunits of hemichannels (heterotypic) (Goodenough and Paul, 2009). Gap junctions can be in the 'open' state or 'closed' state depending on the cellular needs and external and internal conditions including pH, voltage, calcium concentrations and protein phosphorylation (Dbouk et al., 2009). Gap junctions in cells are usually present as clusters on the cell membrane (called gap junctional plaques), and the recruitment and assembly of gap junction proteins is a highly regulated process (Martin and Evans, 2004). There are about 20 *Connexin* genes reported to be expressed in humans and mice. Several of the 25

members of the *Innexin* gene family are expressed in flies, leech, and the worm *C. elegans*. The various biochemical and physiological properties of gap junctions have been studied by expressing them in heterologous systems like paired Xenopus oocytes which do not express these proteins. These studies reveal that both Connexins and Innexins can only selectively form channels with certain other Connexins or Innexins. These combinations determine the properties of the resulting channels and are essential for their proper physiological functioning. However, it is worth mentioning that these specific combinations can change across developmental stages, across tissues, and with changes in external conditions and internal states, as seen with *C. elegans* electrical connectome, revealing the plasticity of electrical synapses (Bhattacharya et al 2019). Although gap junctions are present and function in many tissues and organs across several organisms, in this chapter, I will focus on and restrict my discussion to the roles of gap junctions in nervous systems and their interaction with chemical synapses.
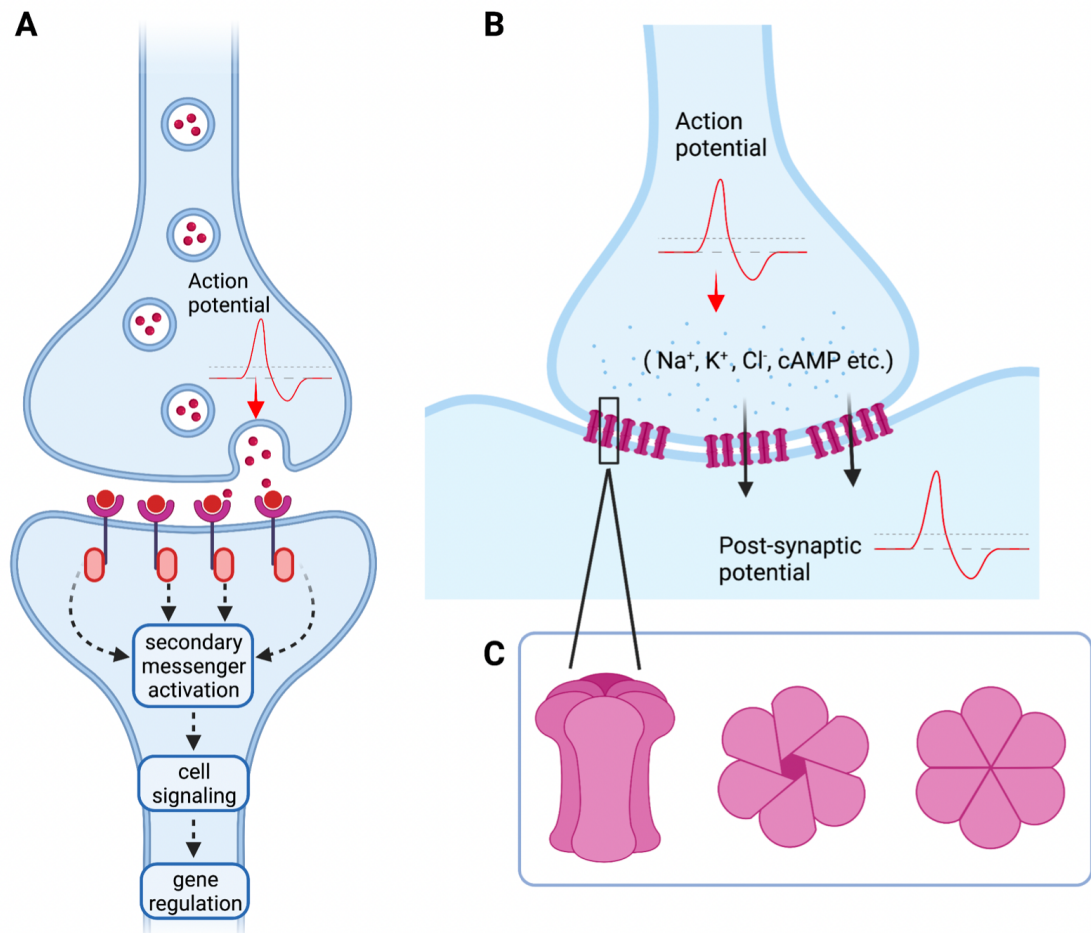
Figure 1.2: An overview of chemical and electrical synapses: (A) Chemical synapses consist of a pre-synaptic and post-synaptic cell, where an action potential in the pre-synaptic cell is propagated to the post-synaptic cell via release of chemicals like neuropeptides and neurotransmitters. These chemical transmitters bind to their cognate receptors on the post-synaptic cells and activate secondary messengers and signal transduction pathways to activate/repress expression of specific genes **(B)** Electrical synapses form direct cell-cell connections via gap junction proteins made up of Connexins or Innexins. The action potential/sub-threshold potential from the pre-synaptic cell, in this case, is directly transferred to the post-synaptic cell by passage of ions or small molecules, such that these cells are "electrically coupled." **(C)** Inset: (left) Structure of a gap junction hemichannel (Connexon/Innexon) made up of six units of Connexin or Innexin proteins. Top view of Connexon in Open (middle) and Closed (right) configurations.

1.7 Functional roles of electrical synapses

The roles of electrical synapses in nervous systems can be broadly classified into three categories: 1) Alteration of the membrane properties of communicating cells. 2) Changing the conductance properties of gap junctions and 3) Changing the expression levels of the gap junction protein itself (O'Brien, 2014). Functionally, electrical synapses facilitate direct bi-directional communication between multiple cells, thus "coupling" the cells electrically. Electrical synapses communicate with little to no delay in the transmission rate (~0.1 ms), which warrants its presence in networks controlling escape responses in some invertebrates (Edwards et al., 1999; Herberholz et al., 2002). Electrical coupling is not just restricted to action potentials but even to subthreshold currents like depolarization, hyperpolarization and, changes in membrane potentials (Faber and Pereda, 2018). Electrical synapses are not mere passive conductors, but themselves contribute to electrical communication. An important property of gap junction channels is the rectification of electrical transmission. Rectification is the property of electric currents to preferentially flow in one direction in a coupled system. Molecular differences between the hemichannels making up the gap junction are involved in rectification (Barrio et al., 1991) (Versalis et al., 1994); and this phenomenon has been observed both in case of Connexins (Rash et al., 2013) and Innexins (Phelan et al., 2008). Gap junctions have also been shown to be involved in synchronous firing (either with fast or slow time scales) of adjacent neurons in a network (Curti et al., 2012; Galarreta and Hestrin, 2001; Veruki et al., 2002). Although the functional significance of such firing synchrony is not very clear, some modelling studies (Lewis and Rinzel, 2000) and experimental evidence has indicated that synchronous firing reduces noise in neuronal networks and facilitates the efficient release of hormones/neurotransmitters to drive downstream neurons (e.g., communication between rod cells and bipolar cells in the retina; Attwell et al., 1987) release of hormones

in the locus coeruleus (Christie et al., 1989) and substantia nigra (Grace and Bunney, 1983). Such networks of synchronously firing neurons are also present in vertebrate motor systems (Li and Rekling, 2017).

Apart from the well-studied roles of gap junctions in the electrical coupling of cells, these proteins are also implicated in several non-channel based functions (reviewed in Dbouk et al., 2009) like cell growth and migration (Kalra et al., 2006), cell division, and cell differentiation (Gu et al., 2003), cell signalling (Richard and Hoch, 2015) and, regulation of gene expression (Iacobas et al., 2004; Stains et al., 2003; Stains and Civitelli, 2005). Some gap junction proteins also function as hemi channels. These hemi channels are present in a 'closed' state on the cell membrane. Their opening/closing is regulated by changes in membrane potential, ionic concentrations, metabolic state, and mechanical stimuli (reviewed in Dbouk et al., 2009; Scemes et al., 2009). Hemi channels regulate the transport of small molecules like ATP and NAD+ between the cell and the extracellular milieu. They are also involved in regulating calcium signalling, cell signalling and differentiation (Belliveau et al., 2006; Evans et al., 2006) and apoptosis (Hur et al., 2003).

1.8 Interactions of chemical and electrical synapses during development

Gap junctions play significant roles during the development of the nervous system. Gap junctional coupling among neurons was observed to be much higher during early development before the appearance of chemical synapses and decreases progressively decreases during the later stages (Kandler and Katz, 1995; Montoro and Yuste, 2004). This initial gap junctional coupling enables the developing neurons to fire synchronously, forming functional domains (Yuste et al., 1992), which lays out the blueprint for several processes like neuronal differentiation, migration, circuit formation, and the elimination of chemical synapses (Montoro and Yuste, 2004; Pereda, 2014). This transient gap

junctional network formation is seen in both invertebrates (Chuang et al., 2007; Marin-burgin et al., 2005, 2006) and vertebrates (Bittman et al., 1997; Kandler and Katz, 1995; Montoro and Yuste, 2004; Penn et al., 1994; Yuste et al., 1992). An example of a transient gap junction network during development would be in *C. elegans* where Innexin19 in Amphid Wing C cell (AWC) neurons is required to generate an asymmetrical pattern of gene expression. The absence of this gap junction gene leads to a failure in the establishment of asymmetry resulting in developmental defects (Chuang et al., 2007). Gap junctional networks have also been shown to be important in developing mammalian spinal cord, where it is essential for the conversion of innervation of muscle fibers from multiple to single nerve innervations (Chang et al., 1999; Personius et al., 2009). The elimination of a large number of electrical synapses and the appearance of an increased number of chemical synapses are highly correlated events during both vertebrate (Maher et al., 2009; Mentis et al., 2002) and invertebrate (Szabo et al., 2004; Todd et al., 2010) development. Furthermore, several studies have suggested that electrical synapses are essential for developing chemical synapses in the nervous system. *Drosophila* gap junction genes *Innexin1* and *Innexin2* were found to be important in glial cells for the proper development of nervous systems (Holcroft et al., 2013). Similarly, flies lacking *Innexin8* and *Innexin1* failed to form appropriate synaptic connections in the visual system leading to defects in visual transduction (Curtin et al., 2002). Similar examples exist in vertebrate nervous systems where the lack of *Connexin36* (*Cx36*) gene results in defective development of the mouse olfactory bulb (Maher et al., 2009) as well as an impairment of long term potentiation of glutamatergic neurons in the hippocampus (Wang and Belousov, 2011). A similar requirement for electrical coupling was also seen in the developing mouse neocortex, where blockade of electrical coupling leads to defective development of chemical synapses (Yu Y C et al., 2012).

1.9 Interactions of chemical and electrical synapses in adult neural circuits.

Electrical synapses are abundantly present in the adult nervous systems and play essential roles in regulating behaviour and physiological processes. Mixed synapses are now being discovered in the nervous systems of animals, where components of both chemical and electrical synapses co-exist and interact with each other (reviewed in Pereda, 2014). e.g., the retinal cells of rabbits, rod and cone inputs converge on the bipolar cells. This connection from the rod to the bipolar cells is mediated by gap junctions, which are under the regulation of dopamine (Mills and Massey 1995; Xia and Mills, 2004). Mixed synapses comprising Connexins and chemical synapses that use glutamate as the transmitter are also found in myelinated club endings of primary auditory efferents of teleost Mauthner cells. Activation of these terminals by high-frequency burst firing leads to long-term potentiation of both electrical and glutamatergic synapses, which is eliminated by using NMDA antagonists, suggesting that glutamatergic synapses are required for the potentiation of electrical synapses. Several other examples of mixed synapses exist where glutamate regulates the activity and plasticity of electrical synapses (Kothmann et al., 2012; Rash et al., 2004; Landisman and Connors, 2005). Mixed synapses were also found in invertebrates like *Drosophila*. The *Drosophila* antennal lobe neurons are coupled with each other via gap junctions made up of Innexin8 proteins, which is additionally modulated by acetylcholine (Yaksi and Wilson, 2010). These modulations of electrical synapses by chemical modulators can fine-tune the number of cells electrically coupled to each other and their coupling strength, which can reconfigure neural networks and create functional compartmentalization in them. The ' shunting effect ' is a different kind of interaction between electrical and chemical synapses observed in the nervous systems (reviewed in Pereda, 2014). Neuronal networks consisting of inhibitory synapses made up of neuromodulators like GABA can reduce coupling among cells connected by

electrical synapses by 'shunting' (by locally increasing the membrane conductance) the electric current. These combinations of inhibitory synapses and gap junctions giving rise to synchronized oscillations are found in the cerebellum and are important for cognitive processing (Bartos et al., 2002). Alteration of this synchronized oscillatory activity also underlies disorders like schizophrenia (Gonzalez-burgos et al., 2010; Nakazawa et al., 2012), autism spectrum disorder (Welsh et al., 2005), and Parkinson's disease (Hammond et al., 2007).

1.10 Gap junctions and circadian rhythms

Most of the current literature which suggests a role for gap junctions in circadian behaviour is based on studies carried out in the mammalian system. Perhaps the earliest evidence of non-synaptic coupling among neurons in the Suprachiasmatic nucleus (SCN), the central clock in mammals, came from studies on the development of fetal SCN. It was observed that rat fetal SCN show rhythms in glucose metabolism and neuronal firing as early as embryonic day E19 and E22, respectively (Shibata and Moore, 1987; Reppert and Schwartz, 1984), while synaptogenesis in the SCN happens much later postnatally between P4-P10 (Moore and Bernstein, 1989). This suggests that SCN behaves as a functional oscillator even before the synapses are completely developed in these animals, thus giving rise to the question of how SCN cells are coupled before chemical synapses are formed. An early study looked at neuronal firing rhythms in rat SCN neuronal cultures in a Ca^{+2}-free medium which blocks synaptic transmission and found that these neurons fire synchronously even in the absence of synaptic transmission, suggesting that some form of coupling mechanism other than chemical transmission exists in the SCN (Bouskila and Dudek, 1993). Electrical synapses made up of gap junctions could be a potential mechanism by which these cells in the SCN are coupled. Studies that followed started looking at gap junctions as a potential coupling mechanism. While previous studies using

immunohistochemistry have shown that gap junctions abundantly couple SCN astrocytes, there were no reports of gap junctional coupling among SCN neurons (Welsh and Reppert, 1996). However, this could just be due to the dissociation and culturing procedures that make the low density of gap junctional proteins present on the surface of neurons more scarce and undetectable in the background of astrocytes where they are abundantly expressed. Hence, further studies examined if adult rat SCN tissues are coupled via gap junctions by injecting a tracer molecule, Neurobiotin, and tracing its passage through the cells in the tissue (Jiang et al., 1997). The logic behind this experiment is that Neurobiotin is a small molecule (molecular weight < 1000 Dalton) that can travel from cell to cell via gap junctions. If one cell is injected with Neurobiotin and is coupled to the other cell via gap junctions, then one could now observe Neurobiotin in the coupled cell as well. This study reported that about 30% of SCN neurons show dye coupling. Furthermore, they show that these neurons show synchronous oscillations of their membrane potentials detected using electrophysiological recordings, suggesting that the neurons in the SCN are also coupled via gap junctions (Jiang et al., 1997). A later study complemented this by systematically examining the dye coupling among neurons in the rat SCN using a different tracer molecule, biocytin. This study confirms that SCN neurons are indeed extensively coupled via gap junctions. Dye filling experiments with biocytin revealed that about 73% of SCN cells showed dye coupling, which was abolished on bath application of known gap junction blockers, thus confirming that these cells were indeed coupled by gap junctions (Colwell, 2000). Furthermore, these cells show time-of-day dependent differences in dye coupling such that the cells are more coupled to each other during the day than night both in Light: Dark (LD) as well as constant darkness (DD), suggesting that this preferential coupling is under the control of the circadian clock. Using antibodies against Connexins, they also show that SCN neurons show positive immunoreactivity to Connexin32, whereas

Connexin43 was found abundantly present in SCN astrocytes (Colwell, 2000). Connexin32 and Connexin36 gap junctions were found to be present in both rat and mice SCN slices using fluorescence and freeze-fracture electron microscopy (Rash et al., 2007). While immunocytochemical and physiological studies indicated the presence of gap junctions in the SCN, there were no reports on the functional roles of these proteins in circadian behaviour. The first report on behavioural rhythms in *Connexin* mutants appeared in 2005. This study investigated behavioural rhythms in mice along with electrophysiological recordings of the SCN neurons in the absence of *Connexin36 (Cx36),* which is the most abundantly present in SCN (Long et al., 2005). *Cx36* mutant mice show defects in synchronous firing of neurons, with wild-type mice SCN showing significantly higher synchrony among neurons in the firing of action potentials, suggesting that gap junction composed of Cx36 are involved in the electrical coupling of SCN neurons (Long et al., 2005) (Figure 1.3). Further, they record the wheel-running behaviour of both wild-type and Cx36 mutant mice under both entrained (LD) and free-running (DD) conditions. The rhythm properties were not observed to be significantly different among the genotypes under LD conditions. Under DD, the mutant mice have significantly reduced circadian amplitude, low consolidation of activity – (activity is dispersed over both day and night) and a transient but significantly lengthened period of free-running activity rhythms. Thus, Cx36 was found to be important in the SCN for electrical synchrony and proper consolidation of activity (Long et al., 2005). Similarly, another study examined the requirement of gap junctions for synchrony in calcium oscillations among the SCN neurons, an important physiological readout of neuronal cells (Wang et al., 2014). They found that application of a known gap junction blocker, Carbenoxolone in the bath when recording from slices decreases the synchronous activity of SCN neurons as measured by two photon imaging experiments, which also indicates that gap junctions are required for

synchronous activity of SCN cells (Wang et al., 2014). Lastly, a somewhat recent study now re-examined the *Cx36* mutants used in Long et al., 2005 to understand the changes happening at the molecular and cellular level in these mice (Figure 1.3). This report shows that the desynchrony observed at the level of electrical coupling in Cx36 mutants is not seen at the level of molecular oscillations measured by PER-luciferase imaging of SCN slices. The PER protein oscillations in all the cells in the SCN slices appears to oscillate in phase, and there is no desynchrony in the network. Further, they also observe that the behavioural rhythm period and the period of PER oscillations of *Cx36* mutants are slightly lengthened as compared to the wild-type mice, suggesting that gap junctions are possibly involved in modulating the free-running period via the molecular clocks (Figure 1.3) (Diemer et al., 2017). To summarize, although there are many studies which report the presence of gap junctions in the SCN and describe its functional roles in the circuit and behavioural levels, our understanding of how gap junctions modulate circadian behaviour is very preliminary. There are very few, to no reports where each of the Connexins are systematically eliminated, and their effect on behaviour is assessed. Moreover, there are no studies that examine the mechanisms by which gap junctions may modulate circadian behaviour in mammals.
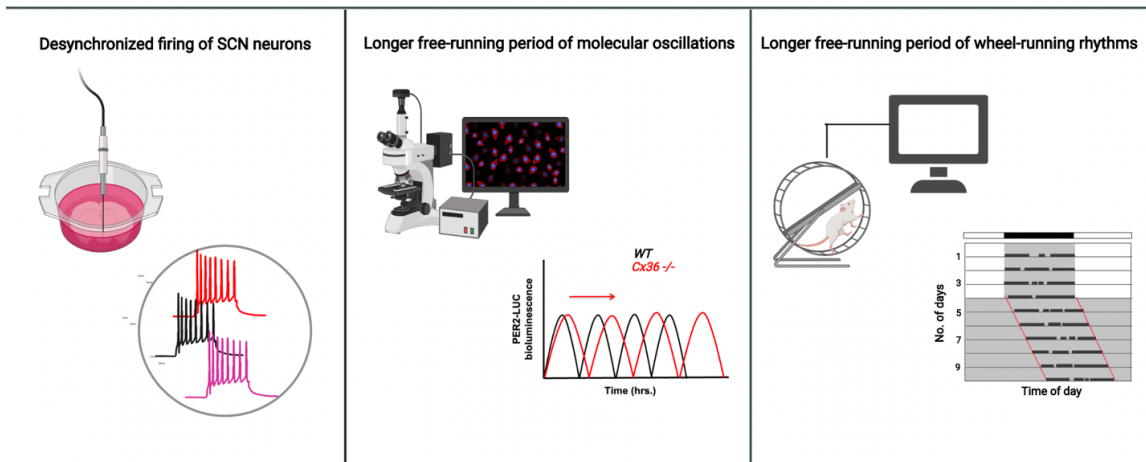
Figure 1.3: Summary of the circadian phenotypes observed in *Connexin36* mutant mice: (A) Electrophysiological recordings from SCN slices of *Cx36^-/-^* mice show desynchronized firing of SCN neurons (Long et al., 2005) **(B)** PER2-Luc rhythms in *Cx36^-/-^* mice (red traces) oscillate with a longer free-running period compared to WT mice (black traces) over days (Diemer et al., 2017) **(C)** The wheel-running activity of adult mice with *Connexin36* mutation runs with a longer free-running period compared to WT mice under constant darkness (Long et al., 2005, Diemer et al., 2017).

In the case of invertebrates, to the best of our knowledge, there is only one study that looks at the role of gap junctions in circadian circuits of the cockroach, *Leucophaea maderae*. The use of gap junction blockers eliminates the synchronous firing of neurons in the accessory medulla region, which is the circadian pacemaker center in insects (Schneider and Stengl, 2006). Thus, it appears that gap junctions in both vertebrates and invertebrates perform similar functions of synchronizing the electrical activity of circadian neurons. However, more evidence is required to generalize the functions of these proteins across organisms and taxa.

1.11 Gap junction genes in *Drosophila*

Mutagenesis screens in the late 1900s in *Drosophila* discovered many genes that gave rise to defective developmental phenotypes (Homyk et al., 1980). Molecular characterization of some of these genes and loci led to the identification of *Innexin* genes (**In**vertebrate analogs of Co**nnexin**s) in *Drosophila melanogaster* and *C. elegans* (Phelan et al., 1998). Later, protein products of these genes were shown to form functional intercellular channels when expressed in a heterologous system like *Xenopus* oocytes (Landesman et al., 1999; Phelan et al., 1998; Stebbings et al., 2000), similar to what was observed in the case of Connexin proteins (Swenson et al., 1989). Although the gene sequences of *Innexins* are not similar to the *Connexins*, the structure and function of Innexin proteins in cells are surprisingly similar to those of Connexins. They are characterized by two extracellular domains, four membrane-spanning domains, three cytoplasmic domains, an intracellular loop and carboxy and amino termini (Bauer et al., 2005). Innexins can work as gap junctions or hemichannels in cells and tissues. Innexin proteins form hemichannels in cells, and two hemichannels in adjacent cells combine to form functional gap junctions (Bauer et al., 2005; Phelan and Starich, 2001). They could also function as hemichannels by facilitating the passage of ions and small molecules and metabolites like ATP, glutamate, $NAD^+,$ etc. between the cell and the surrounding extracellular space (Phelan and Starich, 2001; Scemes et al., 2009). *Drosophila* has eight *Innexin* genes named from *Innexin1 - Innexin8* (Bauer et al., 2005). After their discovery, Innexins were studied extensively for their roles during developmental processes. A comprehensive list of all the *Innexins* and their known functions is described in Table 1.1.

Gene	Functions	References
Innexin1 (ogre)	Development of and optic lobes and proper signal transduction in the visual system, development of nervous system, escape response to sound stimuli	Lipshitz & Kankel, 1985, Curtin et al., 2002, Han et al., 2017, Holcroft et al., 2013, Spéder and Brand, 2014, Kottmeier et al., 2020, Pézier et al., 2016.
Innexin2	Development of gut, tracheal systems, salivary glands, epithelial tissue morphogenesis, development of nervous system, development of eye and proper signal transduction in the visual system, proper growth and development of follicle cells in the ovary	Bauer et al., 2003, Bauer et al., 2004. Holcroft et al., 2013, Speder and Brand, 2014, Richard & Hoch, 2015, Chaturvedi et al., 2014, Bohrmann and Zimmermann, 2008, Sahu et al., 2017.
Innexin3	Dorsal closure in embryonic stages, escape response to sound stimuli	Giuliani et al., 2013, Pézier et al., 2016.
Innexin4 (zpg)	Germline cell development	Bohrmann & Zimmermann, 2008.
Innexin5	Visual learning and memory	Liu et al., 2016.
Innexin6	Associative learning and anaesthesia-resistant memory, visual learning and memory, escape response to sound stimuli, modulating behavioural responses during sleep	Wu et al., 2011, Liu et al., 2016, Pézier et al., 2016, Troup et al., 2018.
Innexin7	Development of nervous system, associative learning and anaesthesia-resistant memory	Ostrowski et al., 2008, Wu et al., 2011.
Innexin8 (shakB)	Synaptic transmission in the giant fibre system, transmission of olfactory information in the antennal lobe	Phelan et al., 2008, Yaksi & Wilson, 2010.

Table 1.1: Table representing the known roles of *Innexin* (*Innexin* 1-8) genes in *Drosophila melanogaster* both during development and adult stages.

Apart from their roles in developmental processes, some Innexins were recently investigated for their contribution to adult-specific behaviours. mRNA quantification from adult *Drosophila* heads shows the presence of all the eight *Innexin* genes in the adult stages, suggesting that the expression of these genes is not just restricted to early developmental stages (Liu et al., 2016; Wu et al., 2011). *Innexin8* or *shakB* was necessary for transferring information from the local excitatory neurons (eLN) to projection neurons (PN) and among two sets of projection neurons in the antennal lobe of *Drosophila*. While wild-type flies elicit appropriate and robust responses to odour stimuli, *shakB* mutants fail to show this response, suggesting that electrical synapses are required to properly process olfactory information in the antennal lobes of *Drosophila* (Yaksi and Wilson, 2010). Similarly, gap junction genes *Innexin6* and *Innexin7* were found to be present in the mushroom body neurons in *Drosophila*. RNAi-mediated knockdown of *Innexin7* in the Anterior Paired Lateral (APL) and of *Innexin6* in the Dorsal Paired Medial (DPM) neurons in the mushroom bodies failed to form anesthesia-sensitive memory to olfactory associative learning (Wu et al., 2011). A few years later, another study showed that Kenyon cells (KC) and Mushroom body output neurons (MBON) are coupled by gap junctions through dye coupling experiments. They further showed that these cells are coupled by Innexin5, and Innexin6 proteins, and downregulation of these *Innexins* impairs the visual learning and memory in flies (Liu et al., 2016). Innexin5 in the mushroom body cells was also necessary for retrieving anaesthesia-resistant olfactory memory in *Drosophila* (Shyu et al., 2019). Gap junction proteins Innexin1 and Innexin2 are present in the glial cells of the blood-brain barrier (BBB), where they regulate the permeability of the BBB in a time-of-day dependent manner to different drugs and small molecules. This

is particularly important in the case of targeted delivery of drugs for neurological disorders where the drugs need to cross the BBB to reach the brain tissues (Zhang et al., 2018). Innexin6 was found to be important in the homeostatic control of sleep in *Drosophila*. Innexin6 is expressed in the dorsal fan-shaped body cells (dFB), and its downregulation resulted in decreased sleep intensity and increased behavioural responsiveness in flies (Troup et al., 2018). Similarly, Innexin2 in cortical glial cells was shown to be important in regulating sleep, where downregulation of its expression leads to increased amounts of sleep (Farca Luna et al., 2017). Thus although *Drosophila Innexins* were initially studied in the context of their roles in development, there is increasing evidence in recent years to suggest that they play active roles during the adult stages to regulate various behaviours. These studies, although very few in number, seem to suggest that electrical synapses function along with chemical synapses in nervous systems of *Drosophila melanogaster*, and an absence of these electrical synapses could can behavioural defects. Importantly, there have been no studies investigating the roles of Innexins in the very well characterized circadian pacemaker circuit of *Drosophila*. This motivated me to ask if circadian pacemaking in *Drosophila* is brought about by chemical and electrical synapses functioning together in the underlying neuronal circuitry and what roles Innexins play in modulating circadian behaviour in *Drosophila melanogaster*.

Chapter 2. Examining the effect of RNAi-mediated knockdown of *Innexin* genes on circadian clock properties.

2.1 Introduction

The genetic basis and neural circuitry underlying circadian behaviour in *Drosophila melanogaster* has been studied extensively for about three decades now, which has been instrumental in understanding how circadian clocks function across organisms. Although the individual neurons and the interneuronal connectivity in the network are well-studied in *Drosophila*, there are no reports that systematically investigate the roles of electrical synapses made up of gap junction proteins in regulating rhythm properties. Several previous studies show that neuronal networks in most organisms function due to the complex interplay of underlying chemical and electrical synapses (Pereda, 2014). Moreover, membrane electrical properties of clock neurons also play important roles in regulating various clock properties. Hence, to examine if gap junctions have any functional role in the circadian neurons in *Drosophila*, I carried out a systematic RNA-interference mediated knockdown screen of all the eight *Innexin* genes in *Drosophila* and assayed clock properties under different external environments. Broadly, I examined clock properties under two different conditions, (i) under free-running conditions where the inherent properties of the underlying clock are manifested and (ii) under entraining conditions, where the internal clock synchronizes to external cyclic, periodic cues. This chapter focuses on the knockdown screen of all eight *Innexin* genes and the behaviour of these flies under both free-running and entrained conditions. Under free-running conditions, I examined the % rhythmicity, free-running period, and power of rhythm of flies in which each of the *Innexin* genes are downregulated. I have also assayed two other important clock properties under constant conditions, the precision of activity rhythms which is a measure of the day-to-day stability of the free-running period, and temperature compensation which is a property of the clock to maintain near 24-hour period under different external temperatures. Next, I have assayed the behaviour of *Innexin* knockdown

flies under the influence of an external cyclic, periodic cue like light and temperature cycles. I examined the ability of flies lacking *Innexins* to entrain to the periodic, external cycles as well as to phase activity under these conditions appropriately. The details of the results of these screens are described in this chapter.

2.2 Materials and Methods

2.2.1 Fly lines and husbandry

All genotypes were reared on standard cornmeal medium under LD (12 hr **L**ight: 12 hr **D**ark) cycles and 25 °C. The transgenic lines used in this study were obtained from the Bloomington Stock center (Indiana, USA). They were UAS *Innexin1* RNAi (BL 44048), UAS *Innexin2* RNAi (BL 42645), UAS *Innexin3* RNAi (BL 60112), UAS *Innexin4* RNAi (BL 27674), UAS *Innexin5* RNAi (BL 28042), UAS *Innexin6* RNAi (BL 44663), UAS *Innexin7* RNAi (BL 26297), and UAS *Innexin8* RNAi (BL 57706). *tim Gal4* was obtained from the lab of Todd Holmes, University of California, Irvine.

2.2.2 Activity-rest assay set-up

Individual virgin male flies (4-6 days old) were housed in glass tubes (length 65mm, diameter 7mm) with corn food and a cotton plug on the other end. Locomotor activity was recorded using the ***Drosophila*** **A**ctivity **M**onitors (DAM, Trikinetics, Waltham, United States of America). Experiments were conducted in incubators manufactured by Sanyo (Japan) or Percival (USA) under controlled light, humidity, and temperature conditions. For experiments involving Light: Dark (LD) cycles, the incubator was set to 70 lux light intensity at a constant temperature of 25°C, and flies were recorded for 7 days followed by transfer to continuous darkness (DD) at 25°C for 7 days. For experiments involving temperature (TC) cycles, the incubator was maintained under constant darkness, and flies

were assayed under temperature cycles of 21°C: 29°C for 7 days and then transferred to DD 21°C for 7 days.

2.2.3 Activity data analysis

Raw data obtained from the DAM system were scanned and binned into activity counts of 15-minute intervals using a DAM file scanner. Data were analysed using CLOCKLAB software (Actimetrics, Wilmette, IL) or RhythmicAlly (Abhilash and Sheeba, 2019). Values of period and power of rhythm were calculated for 7-8 days using the Chi-square periodogram with a cut-off of $p=0.05$. The period and power values of all the flies for a particular experimental genotype were compared against the parental controls using one-way ANOVA with genotype as the fixed factor followed by post-hoc analysis using Tukey's Honest Significant Difference (HSD) test. For precision analysis, onsets and offsets of activity were marked manually from actograms for a period of 7 days using RhythmicAlly. τ_{onset} was calculated as the duration between successive phases of activity onsets under constant conditions. Similarly, τ_{offset} was calculated as the duration between successive phases of activity offsets. Precision was calculated as the inverse of Standard deviation (SD) in τ_{onset} and τ_{offset} across days.

Onset Precision = $1/SD$ $(\tau_{onset)}.$

Offset Precision = $1/SD$ $(\tau_{offset)}.$

The precision values obtained were then compared using one-way ANOVA with genotype as the main factor, followed by post-hoc comparisons using Tukey's HSD test.

For experiments involving LD data analysis, raw data obtained for 7 days of LD from the DAM system were scanned and binned into activity counts of 15-minute intervals using the DAM file scanner. Periodicity and power of rhythm under LD cycles were calculated using Chi-square periodogram analysis in RhythmicAlly. For phase-control analysis,

onsets of activity were marked for all the flies of a genotype for LD day7 and DD days 2-5 from actograms using RhythmicAlly. Regression analysis was then performed on the onset phases for DD day 2-5 using custom codes in R to obtain the onset phase for DD day1. These DD day1 phase values were then statistically compared to LD day7 phase values for all the flies of a particular genotype using one-way ANOVA with the light condition as the main factor, followed by post-hoc Tukey's HSD test to check for phase control.

Activity profiles for each genotype were generated by pasting the 15-minutes binned activity data on an excel template which calculates average activity across all the flies and 7 days of recording. Actograms were observed visually to identify channels with dead flies which were not included while calculating average data across flies. The activity profiles of experimental genotypes were then compared with control parental genotypes to identify the differences. For comparison of onset phases of evening activity among genotypes, evening onsets (activity onset after the afternoon siesta) were visually marked in actograms of individual flies using RhythmicAlly. These phases were then subtracted from the Lights-OFF timing for all the genotypes and statistically compared using one-way ANOVA with genotype as the main factor, followed by post-hoc Tukey's HSD test. Morning anticipation values were calculated by dividing activity levels three hours before Lights-On to six hours before the Lights-On timing. Similarly, evening anticipation values were calculated by dividing activity levels three hours before Lights-Off to six hours before the Lights-Off timing. Morning and evening anticipation values were transformed using the arcsine transformation and compared among relevant genotypes using Welch ANOVA followed by Games-Howell post-hoc test.

For TC data analyses, raw data obtained for 7 days of TC from the DAM system were scanned and binned into activity counts of 15-minute intervals using the DAM file scanner.

Periodicity and power of rhythm under TC cycles were calculated using Chi-square periodogram analysis in RhythmicAlly. Activity profiles for each genotype were generated by pasting the 15-minutes binned activity data on an excel template which calculates average activity across all the flies and 7 days of recording. Actograms were observed visually to identify channels with dead flies to be excluded while calculating averages across flies. The activity profiles of experimental genotypes were then compared with control parental genotypes to identify the differences.

2.3 Results

2.3.1 RNAi-mediated knockdown screen of *Innexins* under DD 25°C

To examine the contributions of *Innexins* in modulating the properties of the circadian clock under free-running conditions, I systematically downregulated the expression of each of the eight *Innexin* genes using a broad driver, *timGal4* (expressed under the promoter of a core clock gene, *timeless*). This driver targets all the known 150 clock neurons and additionally also targets some glial cells and cells of the optic lobe (Kaneko and Hall, 2000). Initially, I examined the properties of rhythm under free-running conditions, wherein the inherent properties of the clock are manifested in the absence of any external environmental cue or *Zeitgeber*. Knockdown of the gap junction gene *Innexin1* (*ogre*) resulted in a lengthening of the free-running period of the experimental flies by about 2 hours as compared to its respective Gal4 and UAS parental controls (Fig. 2.1A left, Table 2.1, Appendix 2.1). Similarly, knockdown of the second gap junction gene *Innexin2* also resulted in a lengthening of the free-running period of activity-rest rhythms of the experimental flies by about an hour as compared to its respective parental controls (Fig. 2.1B left, Table 2.1, Appendix 2.1). By contrast, knockdown of the other gap junction genes (*Innexins 3-8*), did not significantly affect the free-running period of the experimental flies as compared to their respective parental controls (Fig. 2.1 C-H left,

Table 2.1, Appendix 2.1), suggesting that only Innexin 1 and Innexin2 were involved in the modulation of the period of the free-running rhythms in *Drosophila*. I also examined the power of the rhythm, which is the amplitude value of the periodogram analysis and an indicator of how robust the underlying clock is and how well it can consolidate activity over a 24-hour period (Klarsfeld et al., 2003). The power of the rhythm of experimental flies were not significantly different as compared to parental controls when *Innexin1* is downregulated (Fig. 2.1A right, Table 2.1, Appendix 2.2) even though the free-running period of these flies are lengthened, suggesting that Innexin1 probably does not affect the robustness of the clock. Similarly, the power of the rhythm of experimental flies was not significantly different in the case of downregulation of *Innexin2* (Fig.2.1 B right, Table 2.1, Appendix 2.2), although the free-running period was lengthened suggesting that Innexin2 also affects the free-running period without affecting the underlying robustness of the clock. Experimental flies where the other *Innexin* genes (*Innexin 3-8*) were downregulated also did not show any significant difference in the power of the rhythm as compared to their respective parental controls suggesting that Innexins are probably not involved in regulating the robustness of the circadian clock (Fig.2.1 C-H right, Table 2.1, Appendix 2.2). Finally, I also examined the percentage of rhythmic flies when each of the *Innexin* genes are downregulated in the clock neurons. The percentage of rhythmic flies were not different upon knockdown of any of the *Innexin* genes (*Innexin1-8*) (Fig. 2.1I, Table 2.1), suggesting that reduction in *Innexin* levels does not disrupt the *Drosophila* circadian clock machinery to such an extent as to disrupt rhythmicity. Thus, our results from the RNAi knockdown screen of *Innexins* in DD reveals a role for 2 gap junction genes *Innexin1* and *Innexin2* in modulating the free-running period.
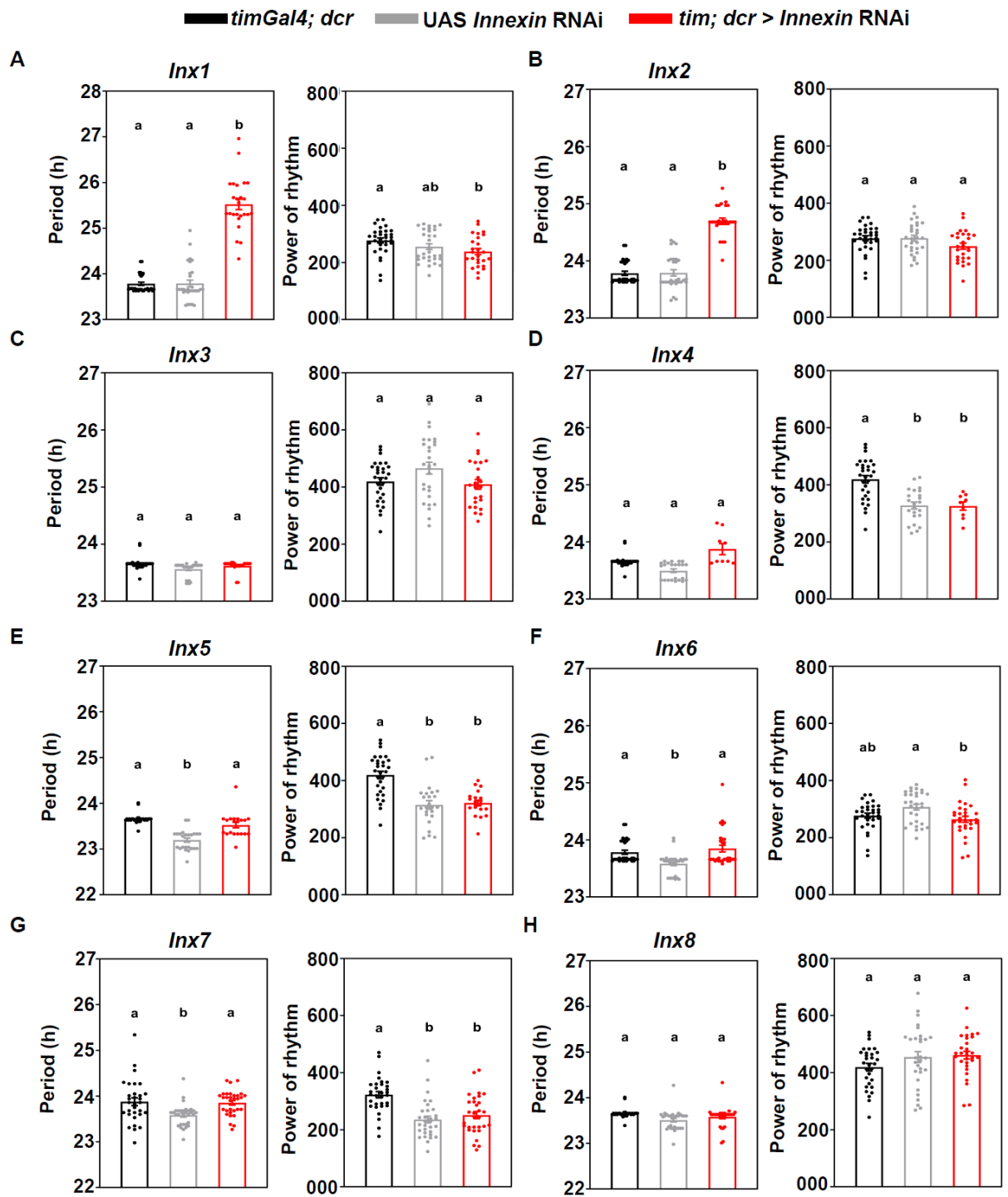
I
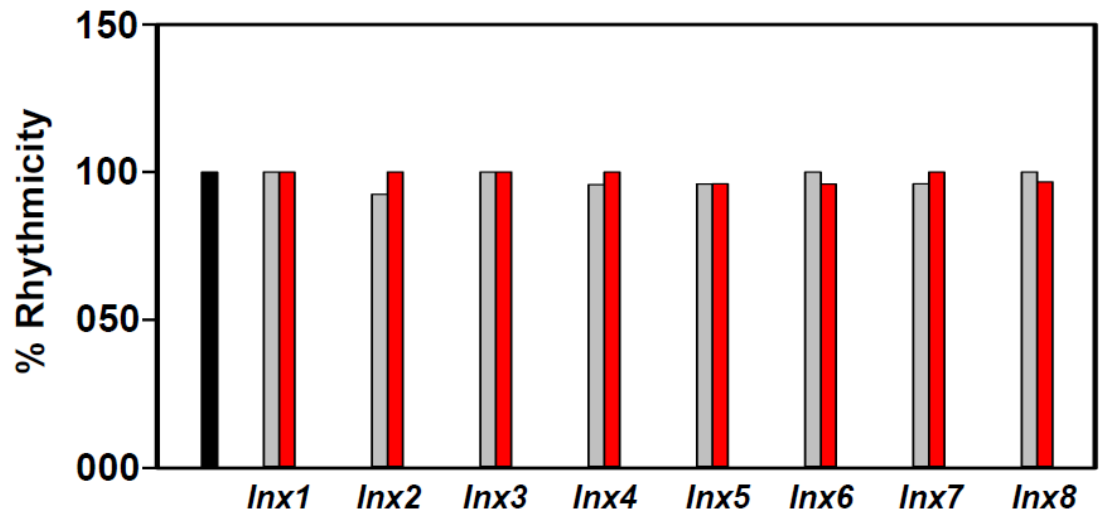
Figure 2.1: Knockdown screen of Innexins under DD 25°C (A) Free-running period (left) and power of rhythm (right) of experimental flies (*tim; dcr > Inx1* RNAi) (*n*=26) flies is plotted along with its Gal4 (*n*=31) and UAS (*n*=30) control flies. **(B)** Free-running period (left) and power of rhythm (right) of experimental flies (*tim; dcr > Inx2* RNAi) (*n*=27) flies is plotted along with its Gal4 (*n*=31) and UAS (*n*=29) control flies **(C)** Free-running period (left) and power of rhythm (right) of experimental flies (*tim; dcr > Inx3* RNAi) (*n*=28) is plotted along with its Gal4 (*n*=30) and UAS control (*n*=28) genotypes. **(D)** Free-running period (left) and power of rhythm (right) of experimental flies (*tim; dcr > Inx4* RNAi) (*n*=16) flies is plotted along with its Gal4 (*n*=30) and UAS control (*n*=24) genotypes. **(E)** Free-running period (left) and power of rhythm (right) of experimental flies (*tim; dcr > Inx5* RNAi) (*n*=26) flies is plotted along with its Gal4 control (*n*=30) and UAS control (*n*=25) genotype. **(F)** Free-running period (left) and power of rhythm (right) of experimental flies (*tim; dcr > Inx6* RNAi) (*n*=30) flies is plotted along with its Gal4 control (*n*=31) and UAS control (*n*=30) genotype **(G)** Free-running period (left) and power of rhythm (right) of experimental flies (*tim; dcr > Inx7* RNAi) (*n*=26) flies is plotted along with its Gal4 control (*n*=30) UAS control (*n*=26) genotypes. **(H)** Free-running period (left) and power of rhythm (right) of experimental flies (*tim; dcr > Inx8* RNAi) (*n*=31) flies is plotted along with its Gal4 control (*n*=30) and UAS control (*n*=30) genotypes. Error bars are SEM. Period and power values are calculated using Chi-squared periodogram for a period of 7 days. All statistical comparisons were performed using one-way ANOVA with genotype as a fixed factor, followed by post-hoc analysis using Tukey's Honest Significant Difference (HSD) test.

(I) Percentage (%) rhythmicity values of flies with individual *Innexin* (*Innexin* 1-8) genes downregulated are being plotted along with their common Gal4 control (*timGal4; dcr*) and respective UAS controls (UAS *Innexin* RNAi) flies. *n* > 20 flies for each genotype. See Table 2.1 for more details.

Genotype	n	Period ± SEM	POR ± SEM	% Rhythmicity
w; timGal4; dcr	30	23.65 ± 0.01	419.2 ± 13.19	100
tim; *dcr* > *Inx1* RNAi	25	25.78 ± 0.07	385.3 ± 14.55	100
tim; *dcr* > *Inx2* RNAi	26	24.61 ± 0.07	377 ± 13.5	100
tim; *dcr* > *Inx3* RNAi	28	23.62 ± 0.01	409.4 ± 16.76	100
tim; *dcr* > *Inx4* RNAi	16	23.87 ± 0.09	325.8 ± 14.28	100
tim; *dcr* > *Inx5* RNAi	26	23.52 ± 0.03	321.2 ± 6.9	96
tim; *dcr* > *Inx6* RNAi	25	23.8 ± 0.06	376.5 ± 18.17	96
tim; *dcr* > *Inx7* RNAi	26	23.73 ± 0.05	337.2 ± 91.18	100
tim; *dcr* > *Inx8* RNAi	30	23.58 ± 0.04	461.3 ± 13.44	100
UAS *Inx1* RNAi	24	23.5 ± 0.03	393.8 ± 13.24	100
UAS *Inx2* RNAi	27	23.54 ± 0.02	424.2 ± 16.55	100
UAS *Inx3* RNAi	28	23.56 ± 0.02	466.1 ± 20.9	100
UAS *Inx4* RNAi	24	23.49 ± 0.03	327.5 ± 11.34	100
UAS *Inx5* RNAi	25	23.19 ± 0.04	314.6 ± 14.84	96
UAS *Inx6* RNAi	31	23.43 ± 0.02	437.2 ± 14.4	100
UAS *Inx7* RNAi	26	23.56 ± 0.03	410.9 ± 51.2	100
UAS *Inx8* RNAi	30	23.5 ± 0.03	454.6 ± 19.17	100

Table 2.1: Table representing the no. of flies (*n*), average period (±SEM), power of the rhythm (POR ± SEM) and % rhythmicity values of all the experimental (*tim; dcr > Inx1-8* RNAi) lines used for the screen along with their respective Gal4 (*w; timGal4; dcr*) and UAS controls (UAS *Inx 1-8* RNAi).

2.3.2 Knockdown of *Innexin1* and *Innexin2* does not affect the precision of free-running activity-rest rhythms.

Precision is a measure of the stability of the free-running period across days. Previous studies have shown that precision is correlated with the free-running period such that precision is maximum when the period is close to 24 hours and decreases as the period deviates from 24 hours in both directions (Nikhil et al., 2020; Pittendrigh and Daan, 1976; Sharma and Chandrashekaran, 1999). There are very few reports on the neuronal or cellular mechanisms of how the circadian clock maintains precision in rhythms. One such study shows the importance of coupling among individual oscillators for the generation of precise rhythms in the Suprachiasmatic nucleus (SCN), the mammalian circadian clock (Herzog et al., 2004). The authors calculate precision at three levels of organization: at

the single neuron level, by measuring the precision of electrical activity of single neurons across days, at the network level, by measuring the PER-bioluminescence rhythm in SCN slices, and at the organismal level, by measuring the precision of wheel-running activity rhythms. After measuring across all three levels, the authors concluded that single neurons show the lowest precision while activity rhythms of organisms show the highest precision with SCN slices showing intermediate precision, suggesting that precision increases as the coupling among oscillators increases. Keeping this in mind, I decided to estimate the precision of clocks of experimental flies which have *Innexin1* and *Innexin2* downregulated for 2 reasons. Firstly, I wished to examine if lengthened free-running period due to *Innexin* knockdown is correlated with lower precision. Secondly, since Innexins are gap junction proteins, and gap junctions are known to be involved in electrical coupling and synchronization among neurons, I wanted to examine if knockdown of *Innexin1* and *Innexin2* could lead to a reduction in the precision of activity-rest rhythms due to reduced coupling. I measured precision using two phase markers- onset of activity and offset of activity. I observed that the offset of activity is a more precise marker than the onset (Fig. 2.2 B, Fig. 2.2D), as reported previously for *Drosophila* activity rhythms (Srivastava et al., 2019). Knockdown of *Innexin1* did not significantly reduce the precision of activity-rest rhythms, measured with both activity onsets and offsets (Fig. 2.2 A, Fig. 2.2 B, Appendix 2.3, Appendix 2.4). However, a trend towards lowered precision was seen for offsets, suggesting that loss of *Innexin1* possibly does not strongly affect rhythm precision. Similarly, in the case of knockdown of *Innexin2*, the experimental flies do not show any reduction in the precision of activity rhythms as compared to its parental controls, both in case of onsets and offsets (Fig. 2.2C, Fig. 2.2D, Appendix 2.3, and Appendix 2.4), again suggesting that Innexin2 is not involved in the modulation of precision.
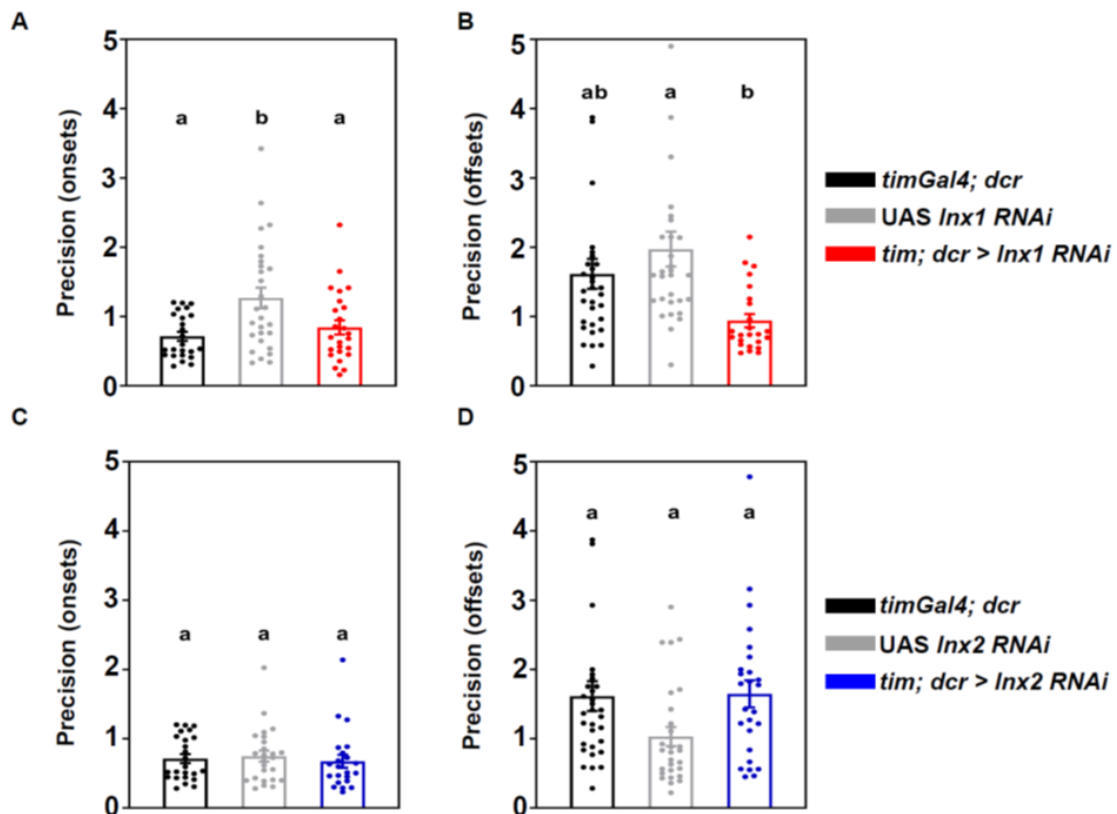
Figure 2.2: Knockdown of *Innexin1* and *Innexin2* does not affect the precision of activity-rest rhythms Precision of activity-rest rhythms calculated from phases of onsets of activity (A) and offsets of activity (B) of experimental flies (*tim; dcr > Inx1* RNAi) (*n*=26) is plotted along with its UAS (*n*=30) and Gal4 parental (*n*=31) controls. Precision of activity-rest rhythms calculated from phases of onsets of activity (C) and offsets of activity (D) of experimental flies (*tim; dcr > Inx2* RNAi) (*n*=27) is plotted along with its Gal4 control (*n*=31) and UAS control (*n*=27) genotypes.
Error bars are SEM. Phase values of onsets and offsets of activity was subjectively marked for each fly and each genotype for a period of 8 days using RhythmicAlly (Abhilash and Sheeba, 2019). All statistical comparisons were made using one-way ANOVA with genotype as a fixed factor, followed by post-hoc Tukey's HSD test.

2.3.3 Effect of knockdown of *Innexin1* and *Innexin2* on temperature compensation

Temperature compensation is a fundamental property of the circadian clock to maintain a near 24-hour free-running period under a wide range of physiological temperatures exhibited in organisms ranging from Cyanobacteria to homeothermic mammals. While most biochemical reactions follow the Arrhenius equation of temperature dependence on reaction rates such that higher temperatures lead to faster reaction rates and vice versa,

circadian clocks have a unique property of period stability under changing external temperatures. Currently, we do not understand the exact mechanism by which circadian clock periods are resistant to temperature changes. Several models have been proposed to explain this phenomenon, and there is empirical evidence to support some of these hypotheses in different model systems. It was proposed that positive and negative feedback loops of the molecular clock react in opposite ways to temperature changes which maintain a stable 24-hour period (Ruoff P, 1992; Hastings and Sweeney, 1957). Studies in *Drosophila* have implicated roles for various post-transcriptional and post-translational modifications of core clock genes *per* and *tim* in modulating temperature compensation (Hong and Tyson, 1997; Majercak et al., 1999; Singh et al., 2019). Similarly, in *Neurospora crassa*, the two isoforms of the core clock gene *frequency (frq)* have been shown to have roles in the temperature compensation of the system. In the plant *Arabidopsis thaliana*, the negative regulators of the feedback loop, CCA1 and LHY, have been shown to have roles in temperature compensation, such that mutants in genes *prr6* and *prr7,* which regulate levels of CCA1 and LHY show temperature overcompensation (Gould et al., 2006; Salome, 2010). In mammalian systems, a phosphoswitch mediates differential phosphorylation of PER2 protein at two sites at different temperatures, and this could play a role in the stability of PER2 and free-running period under different temperatures (Narasimamurthy and Virshup, 2017). A general theoretical model predicts that temperature-sensitive switch-like mechanisms acting on processes affecting the stability of core clock proteins like phosphorylation, complex formation, nuclear accumulation, ubiquitination, etc., could potentially regulate the temperature compensation abilities of the clock (Hong et al., 2007). Interestingly, each of these processes that affect the stability of core clock proteins, could in principle, affect the free-running period irrespective of the temperatures, and mutations that affect these processes

could affect temperature compensation. However, there have been no systematic studies investigating these questions, and no correlation has been observed between the free-running period and temperature compensation abilities of mutants that affect clock functions (Hong et al., 2007; Kidd et al., 2015).

Since knockdown of *Innexin1* and *Innexin2* leads to significant lengthening of the free-running period, I was curious to examine if these genes play any roles in the temperature compensation ability of the clock. I examined the free-running period of experimental and control flies under two different temperatures of 25°C and 29°C. Knockdown of *Innexin1* using *timGal4* results in lengthening of the free-running period as compared to both its parental controls under both temperatures of 25°C and 29°C (Fig. 2.3A). The free-running period of experimental flies at 29°C was significantly different from its period at 25°C (Fig. 2.3A). To examine if the experimental genotype was also compromised in maintaining its period length in a temperature-dependent manner, I calculated the difference between the free-running period at 29°C and 25°C for all the genotypes. Although the period differences at these two temperatures were significantly different in experimental flies as compared to both parental controls, it was significantly lower than the Gal4 control but higher than the UAS control (Fig. 2.3C, Appendix 2.5), suggesting that knockdown of *Innexin1* does not particularly affect the temperature compensation ability of the clock at 29°C. Similarly, in the case of knockdown of *Innexin2*, the free-running period of experimental flies was significantly longer than parental controls at both temperatures of 25°C and 29°C (Fig. 2.3B). The free-running period of experimental flies at 29°C was found to be significantly different from its period at 25°C (Fig. 2.3B). Similar to the *Innexin1* knockdown, I calculated the difference between the free-running period at 29°C and 25°C for all the genotypes and compared the values of experimental flies to both parental controls. The period differences were significantly higher in experimental flies

than both the parental controls (Fig. 2.3D, Appendix 2.5), suggesting that knockdown of *Innexin2* possibly affects the temperature compensation ability of the circadian clock, leading to temperature overcompensation.
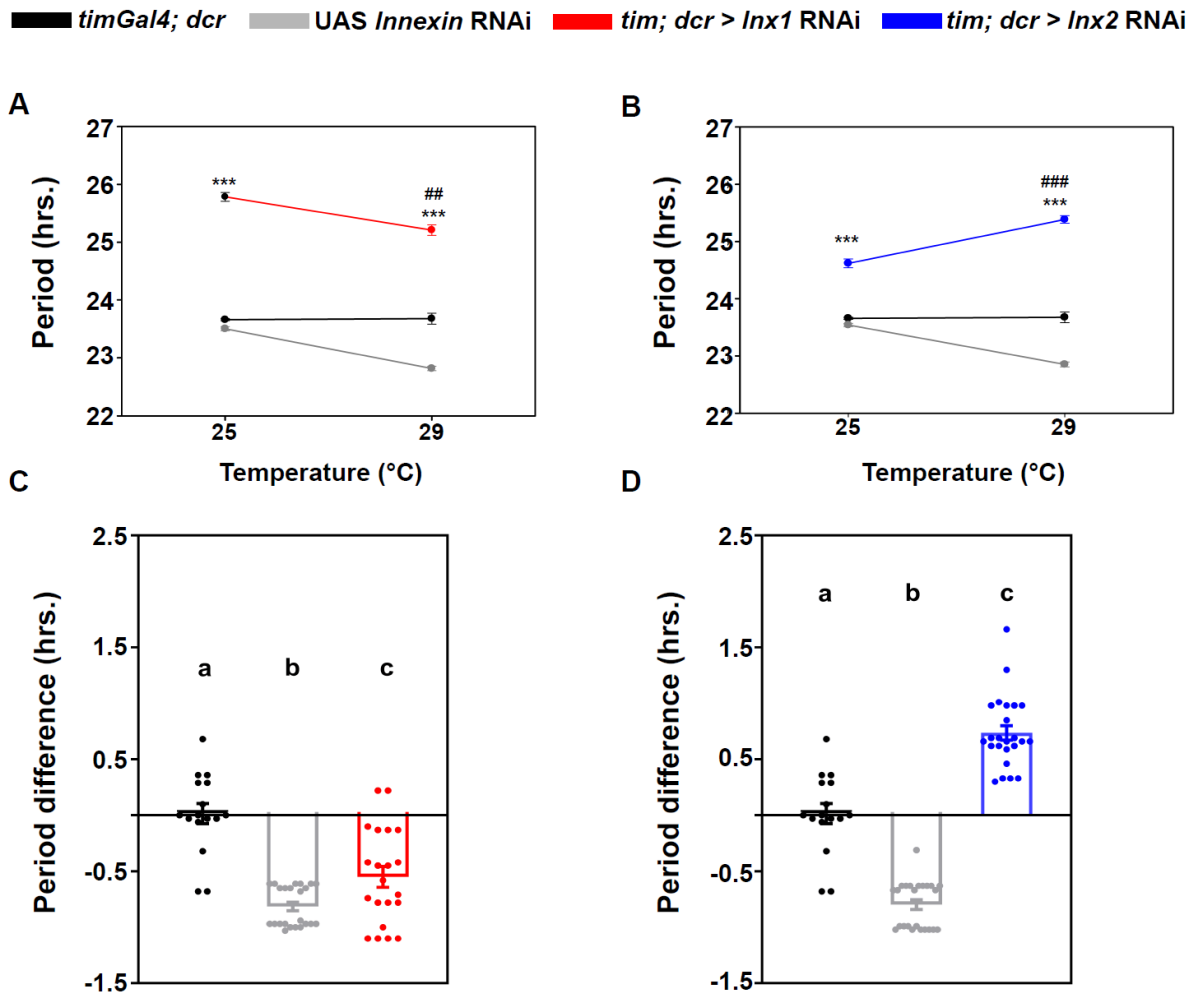
Figure 2.3: Effect of knockdown of *Innexin1* and *Innexin2* on temperature compensation (A) Knockdown of *Innexin1* in all clock neurons (*tim; dcr > Inx1* RNAi) lengthens the period of free-running rhythms at both 25°C and 29°C as compared to both its Gal4 and UAS parental controls. The free-running period of experimental flies at 29°C is significantly different than at 25°C. **(B)** Knockdown of *Innexin2* in all clock neurons (*tim; dcr > Inx2* RNAi) lengthens the period of free-running rhythms at both 25°C and 29°C as compared to both its Gal4 and UAS parental controls. The free-running period of experimental flies at 29°C is significantly different than at 25°C. **(C)** The difference between free-running period values at 29°C and 25°C is plotted for all the genotypes. This difference in free-running period is significantly different in experimental (*tim; dcr > Inx1* RNAi) flies as compared to both its parental control genotypes (one-way ANOVA, post-

hoc Tukey's test $p < 0.05$). **(D)** The difference between free-running period values at 29°C and 25°C is plotted for all the genotypes. This difference in free-running period is significantly different in experimental (*tim; dcr > Inx2* RNAi) flies as compared to both its parental control genotypes (one-way ANOVA, post-hoc Tukey's test $p < 0.001$). Asterisks indicate significant difference between experimentals and control genotypes at $p<0.001$,# indicates significant difference between experimentals at *25*°C and a higher temperature of 29°C ($p<0.01$ **(for A)** and $p<0.001$ **(for B)**), error bars are SEM, period values are determined using Chi-square periodogram for a period of 8 days, all comparisons were made using one-way ANOVA with post-hoc Tukey's test, $n > 21$ flies for all genotypes at all temperatures.

2.3.4 RNAi-mediated knockdown screen of *Innexins* under LD 25°C.

After examining the properties of *Innexin* downregulated flies under free-running conditions, I next proceeded to ask if these flies show any defects under entrained conditions. It is well-known that organisms can synchronize their internal circadian clocks to external, cyclic environmental cues, a phenomenon termed as entrainment. These cyclic, environmental cues that provide time information to the clock are termed as *Zeitgebers*. Light is the most important and well-studied *Zeitgeber* in most organisms, including *Drosophila melanogaster*. The receptors and pathways mediating light input to the circadian clocks and the activity-rest rhythms under different durations and intensities of light are very well-characterized in *Drosophila* (Förster, 2019). Similarly, the importance of communication among the neurons in the circadian network to modify behaviour to different durations of light and dark cycles has been well-studied in *Drosophila* (Shiga, 2013; Stoleru et al., 2007). Hence, I wanted to examine if the knockdown of gap junction genes affects the activity-rest behaviour of *Drosophila* under Light: Dark cycles. I downregulated the expression of all the eight *Innexin* genes individually using the *timGal4* driver and examined the flies under 12 hours of Light: 12 hours of darkness (LD 12:12) at 70 lux light intensity. First, I investigated if knockdown of any of the *Innexins* affected the entrainment of flies to Light: Dark cycles. The circadian

clock of an organism is entrained to the external cyclic periodic cue if the following conditions are satisfied: 1) $\tau=T$. If an organism is entrained to an external cycle, the internal periodicity of the organism (τ) should exactly match the periodicity of the external cycle (T), which in this case is 24 hours (LD 12:12). 2) Phase control. If the circadian clock of an organism is truly entrained to the external cycle, then the phase of activity (onset or offset) on the first day of free-run (constant darkness, DD) should follow the phase of the last day of the Light: Dark cycle (Dunlap et al., 2004). I examined if *Innexin* downregulated flies fulfill the criteria mentioned above for entrainment. All the flies of the experimental genotype where each of the eight *Innexin* genes are downregulated show almost 100% rhythmicity and have a 24-hour periodicity under Light-dark cycles (Fig. 2.4, Table 2.2), suggesting that they fulfill the first criteria for entrainment. For the second criteria, I marked the phases of activity onsets for all the flies of each experimental genotype from day 2 - day 5 in DD, which were then used to estimate the onset phase on DD day 1 by fitting a line of regression. These DD day 1 phases were then compared to the onset phases of the last day of the LD cycle to examine if they were statistically different from each other. If DD day 1 phase is not significantly different from the phases in LD, then the flies of that particular genotype can be classified as entrained. Experimental genotypes where *Innexin1* and *Innexin2* were downregulated show significantly different phases of onset between the last day of LD and first day of DD (Fig. 2.4, Appendix 2.6), suggesting that flies which lack *Innexin1* and *Innexin2* do not entrain well to LD 12:12 cycles and possibly show a certain component of masking. Experimental flies where the other six *Innexin* genes are downregulated (*Innexins* 3-8) do not show any significant difference between onset phases on the last day of LD and the first day of DD (Fig. 2.4, Appendix 2.6), suggesting that these flies show true entrainment by fulfilling the above criteria.

A *tim; dcr > Inx1* RNAi

B *tim; dcr > Inx2* RNAi

C *tim; dcr > Inx3* RNAi

D *tim; dcr > Inx4* RNAi

E *tim; dcr > Inx5* RNAi

F *tim; dcr > Inx6* RNAi

G *tim; dcr > Inx7* RNAi

H *tim; dcr > Inx8* RNAi

No. of days

Time of Day (hrs.)
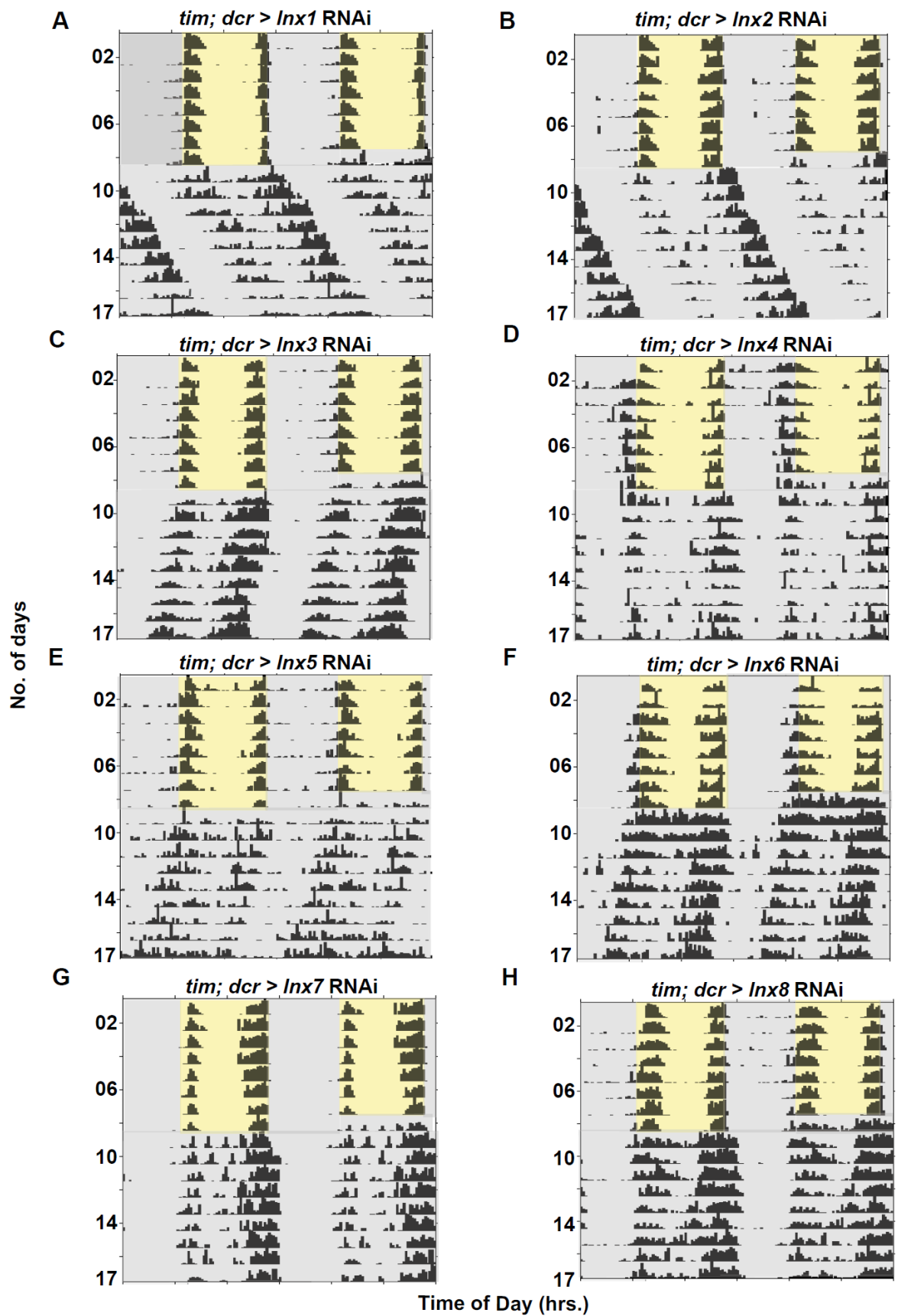
Figure 2.4: RNAi mediated knockdown screen of *Innexins* under LD 25°C (A-H)
Average double-plotted actograms of flies of each indicated genotype with each of the 8 *Innexin* (*Innexin 1-8*) genes downregulated using a driver that targets all clock neurons (*timGal4*). On each day, activity is depicted as black vertical bars across the time of day which is double plotted such that 2 consecutive days are shown on the *x*-axis. Flies were recorded under Light: Dark (LD) cycles for the first 7 days. The yellow shading depicts the light part of the day and the gray shading depicts the dark part. Following the LD cycle, the flies were transferred to constant darkness (DD 25°C) for a period of 8 days, depicted here as gray shading.

Genotype	*n*	Period ± SEM	POR ± SEM	% Rhythmicity
tim; *dcr* > *Inx1* RNAi	24	24 ± 0.0	513.6 ± 21.3	100
tim; *dcr* > *Inx2* RNAi	29	24 ± 0.0	558.7 ± 16.1	100
tim; *dcr* > *Inx3* RNAi	30	24 ± 0.0	618.19 ± 9.5	100
tim; *dcr* > *Inx4* RNAi	26	24 ± 0.0	490.1 ± 16.17	100
tim; *dcr* > *Inx5* RNAi	16	24 ± 0.0	486.3 ± 22.19	94
tim; *dcr* > *Inx6* RNAi	29	24 ± 0.0	584.7 ± 15.85	97
tim; *dcr* > *Inx7* RNAi	25	23.9 ± 0.01	558.5 ± 12.13	100
tim; *dcr* > *Inx8* RNAi	25	24 ± 0.0	587.4 ± 12.87	100

Table 2.2: Table representing the *n*, average period (±SEM), power of the rhythm (POR) (± SEM) and % rhythmicity values of all the experimental (*tim; dcr > Inx1-8* RNAi) lines used for the screen under LD 25°C.

2.3.5 Knockdown of *Innexin2* and *Innexin4* delays the phase of onset of evening activity under LD 25°C.

Next, I examined the activity profiles of experimental flies with *Innexins* downregulated and compared them with their respective parental controls. Wild type *Drosophila* typically shows two activity bouts, one during the dawn transition (Lights-Off to Lights-On transition in the lab), also known as the morning activity bout, and the other during the dusk transition (Lights-On to Lights-Off transition in the lab), also known as the evening activity bout. The neuronal mechanisms governing these two activity bouts are well-studied in *Drosophila*, with specific subsets of circadian neurons in the brain responsible

for modulating the features of the morning activity known as the morning neurons and certain other subsets responsible for evening activity known as the evening neurons (Grima et al., 2004; Stoleru et al., 2004). To compare among genotypes, I plotted the activity profiles of flies averaged across seven days and compared the activity profiles of control flies with experimental flies. Knockdown of *Innexin2* shows a visibly delayed onset of evening activity compared to its respective parental controls (Fig. 2.5B, arrow mark). Hence, I quantified the onset of activity phases for the control and parental genotypes and found that the onset of evening activity in the case of *Innexin2* knockdown is significantly delayed by about 45 minutes compared to its respective parental controls (Fig. 2.6A, Appendix 2.7). Similarly, knockdown of *Innexin4* also shows a visibly delayed phase of evening onset as compared to its parental genotypes (Fig. 2.5D, arrow mark). Upon quantification, I find that the evening activity onset in the case of knockdown of *Innexin4* is significantly delayed by about an hour compared to its parental control genotypes (Fig. 2.6B, Appendix 2.7). In case of experimental flies where the other *Innexins* (*Innexin1*, *Innexin3*, *Innexins 5-8*) are downregulated, I do not observe any changes in the activity profiles of experimental flies as compared to their respective parental controls (Fig. 2.5A, Fig. 2.5C, Fig. 2.5E-H).

Further, I also calculated the morning and evening anticipation of flies where *Innexin2* and *Innexin4* are downregulated. Anticipation is the property of the circadian clock to predict the transitions of environmental variables and modulate activity accordingly. It is a distinguishing feature that separates circadian clocks from mutants without a functional clock. While mutants lacking circadian clock components could also immediately respond to environmental transitions by increasing or decreasing activity levels, only animals with intact clocks can anticipate and modulate activity to transitions of environmental variables (Grima et al., 2004; Vanin et al., 2012). Since knockdown of *Innexin2* and *Innexin4* affect

the phase of onset of activity, a circadian clock property, I wanted to examine if they also affect the anticipation to LD cycles. Knockdown of *Innexin2* does not affect the anticipation to morning Lights Off-On transition (Fig. 2.7A left, Appendix 2.8). Similarly, knockdown of *Innexin2* does not affect the evening anticipation to Lights On-off transition as the anticipation values are not significantly different from the respective parental controls (Fig. 2.7A right, Appendix 2.9). Knockdown of *Innexin4* also does not affect the morning anticipation of experimental flies compared to their respective parental controls (Fig. 2.7B left, Appendix 2.8). In the case of evening anticipation, I find that experimental flies in which *Innexin4* is downregulated show slightly but significantly increased anticipation to the Lights-On to Lights-Off transition (Fig.2.7B right, Appendix 2.9).

Legend: timGal4; dcr (black) — UAS Innexin RNAi (grey) — tim; dcr > Innexin RNAi (red)

A — *Inx1*
B — *Inx2*
C — *Inx3*
D — *Inx4*
E — *Inx5*
F — *Inx6*
G — *Inx7*
H — *Inx8*

Y-axis: Activity Counts/15 mins.
X-axis: Zeitgeber time (hrs.)
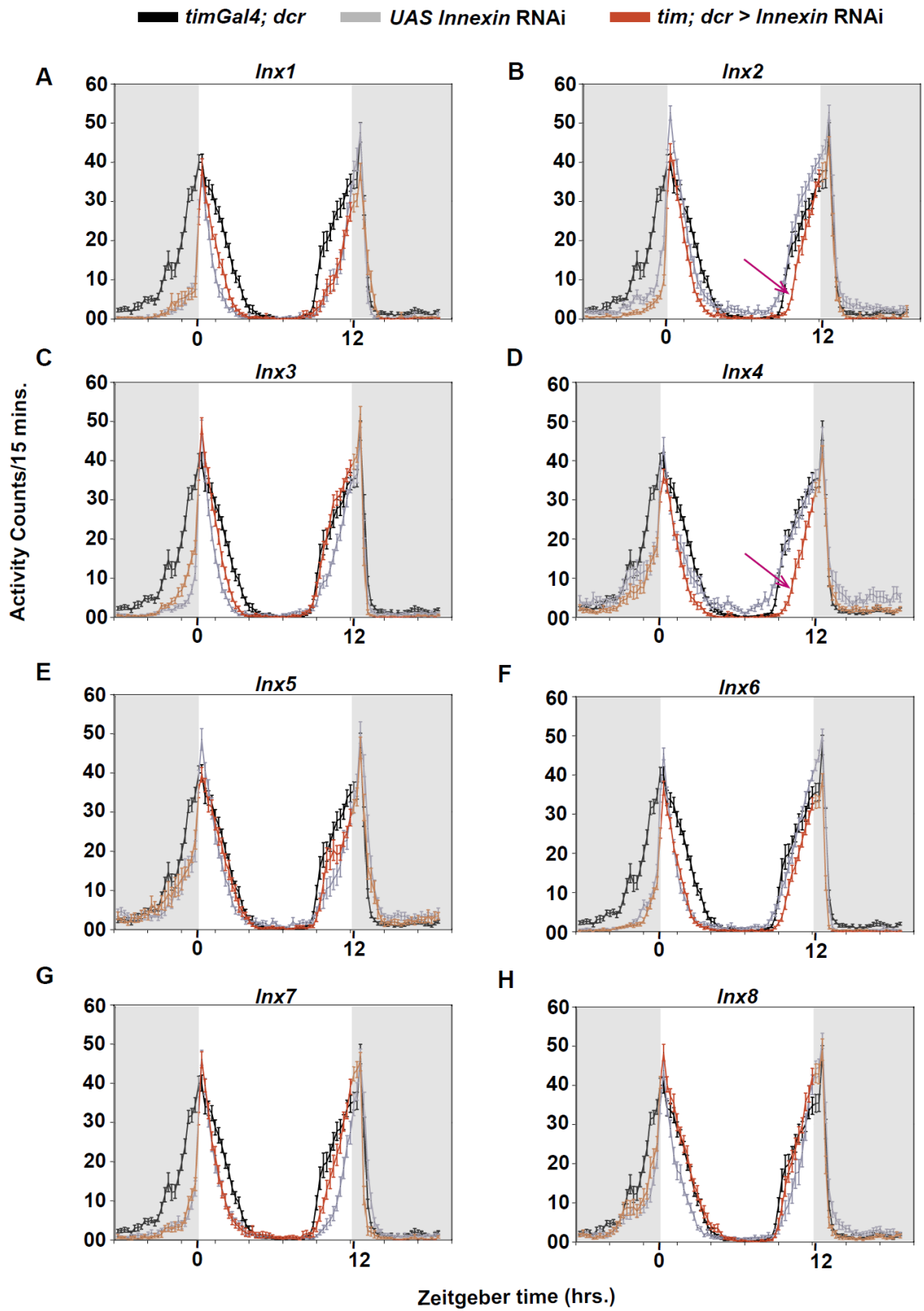
Figure 2.5: RNAi mediated knockdown screen of *Innexins* under LD 25°C (A-H)
Average activity profiles of flies across 7 days in which each of the eight *Innexins* (*Innexin 1-8*) are downregulated using a broad driver (*timGal4*) are plotted along with their respective parental controls. Gray shading depicts the 12 hours of dark phase and white shading depicts the 12 hours of light phase of the Light: Dark cycle. Arrows indicate the delay in the onset of evening activity in case of knockdown of *Innexin2* **(B)** and *Innexin4* **(D)** genes. Error bars depicted on the activity profiles are SEM values.

A

B
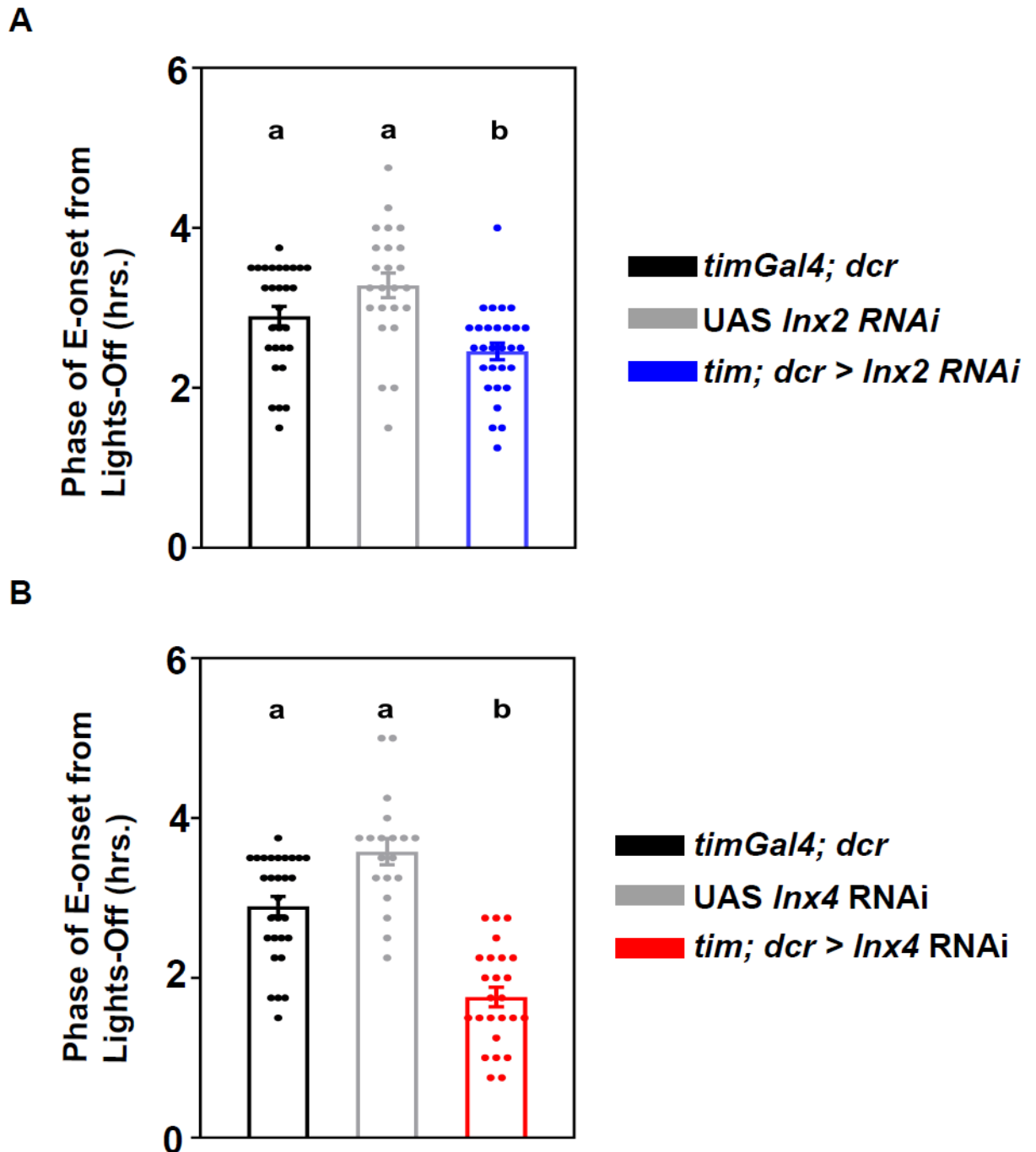
Figure 2.6: Knockdown of *Innexin2* and *Innexin4* delays the onset of evening activity
Difference of phases of onset of evening activity from the time of Lights-Off are plotted for individual flies. **(A)** Difference of phases of onset of evening activity from the time of Lights-Off are plotted for experimental (*tim; dcr > Inx2* RNAi) (*n*=29) and its Gal4 (*n*=29) and UAS (*n*=24) parental control genotypes **(B)** Difference of phases of onset of evening activity from the time of Lights-Off are plotted for experimental (*tim; dcr > Inx4* RNAi) (*n*=25) and its Gal4 (*n*=29) and UAS (*n*=21) parental control genotypes.
Error bars are SEM. Phase values were obtained by subjectively marking the onset of evening activity of individual flies in actograms generated using ClockLab. All statistical comparisons were made using one-way ANOVA with genotype as a fixed factor, followed by post-hoc Tukey's HSD test.
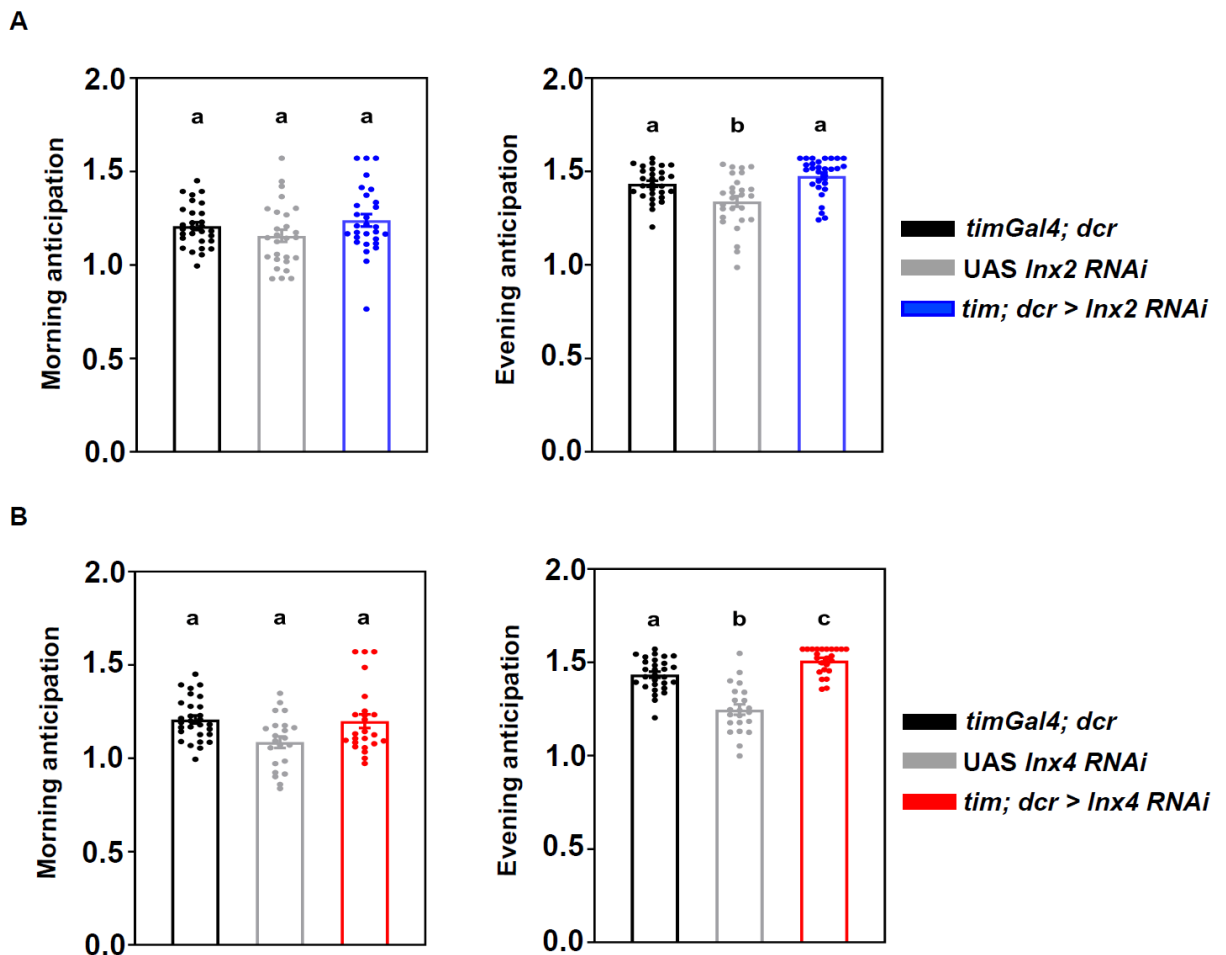
Figure 2.7: Knockdown of *Innexin2* and *Innexin4* does not affect the anticipation of morning or evening activity under LD 25°C. Anticipation of morning activity (A) and evening activity (B) for experimental (*tim; dcr > Inx2* RNAi) (*n*=29) and its respective Gal4 (*n*=29) and UAS control (*n*=27) genotypes are being plotted. **)** Anticipation of morning activity (C) and evening activity (D) for experimental flies (*tim; dcr > Inx4* RNAi) (*n*=24) is plotted along with its Gal4 (*n*=29) and UAS control (*n*=22) genotypes. Error bars are SEM. Anticipation values are a ratio of 3 hours of activity of the flies before Lights-On time to 6 hours of activity before Lights-On time recorded for a period of 7 days. All statistical comparisons are being made on the arcsine transformed values using Welch ANOVA with genotype as the main factor, followed by Games-Howell post-hoc test.

2.3.6 RNAi-mediated knockdown screen of *Innexins* under temperature cycles.

Similar to LD cycles, temperature can also provide periodic environmental input to the circadian clock such that cycles of high and low temperatures (Thermophase: Cryophase; TC) can act as *Zeitgebers* to circadian clocks. Temperature cycles with as low as 2°C amplitude can entrain the circadian clock under constant conditions of DD or LL (Yoshii et al., 2005). In *Drosophila,* specific subsets of clock neurons are important for entrainment to temperature cycles, although the input pathways and neuronal mechanisms of entrainment to temperature cycles are not as well-understood as light entrainment (George and Stanewsky, 2021). To examine if the lack of *Innexins* could affect the activity rhythms under TC, I downregulated *Innexin* expression in clock neurons using *timGal4* and examined behaviour under TC cycles of 21°C: 29°C. All the experimental flies with *Innexins 1-8* downregulated synchronize to the TC cycles, as evidenced by their 24 hour period under TC conditions (Table 2.3). Similar to LD cycles, wild-type *Drosophila* show two prominent peaks of activity under temperature cycles, one marking the cryophase - thermophase transition (known as the morning peak) and the other marking the thermophase - cryophase transition (known as the evening peak). I compared the activity profiles of experimental flies with each of the *Innexin* genes downregulated with their respective parental controls. None of the experimental flies show any significant

difference in their activity profiles compared to their respective parental controls (Fig. 2.8 A-H), suggesting that Innexins possibly do not have any role to play in modulating activity rhythms under this particular temperature cycle.

Genotype	*n*	Period ± SEM	POR ± SEM	% Rhythmicity
tim; *dcr > Inx1* RNAi	15	24.02 ± 0.02	409.4 ± 37.87	100
tim; *dcr > Inx2* RNAi	27	23.99 ± 0.009	453.5 ± 23.17	100
tim; *dcr > Inx3* RNAi	30	23.98 ± 0.016	532.5 ± 21.67	100
tim; *dcr > Inx4* RNAi	25	24 ± 0.0	425.3 ± 24.61	100
tim; *dcr > Inx5* RNAi	28	24.01 ± 0.012	466.2 ± 17.56	100
tim; *dcr > Inx6* RNAi	26	23.96 ± 0.01	416 ± 16.51	100
tim; *dcr > Inx7* RNAi	29	24 ± 0.0	487.9 ± 20.84	96.5
tim; *dcr > Inx8* RNAi	27	23.91 ± 0.02	359.6 ± 14.19	100

Table 2.3: Table representing the *n*, average period (±SEM), power of the rhythm (POR) (± SEM) and % rhythmicity values of all the experimental (*tim; dcr > Inx1-8* RNAi) lines used for the screen under TC 21°C: 29°C.

Legend: *timGal4; dcr* (black) — UAS *Innexin* RNAi (grey) — *tim; dcr > Innexin* RNAi (red)

A — *Inx1*
B — *Inx2*
C — *Inx3*
D — *Inx4*
E — *Inx5*
F — *Inx6*
G — *Inx7*
H — *Inx8*

Activity Counts/15 mins.

Zeitgeber time (hrs.)
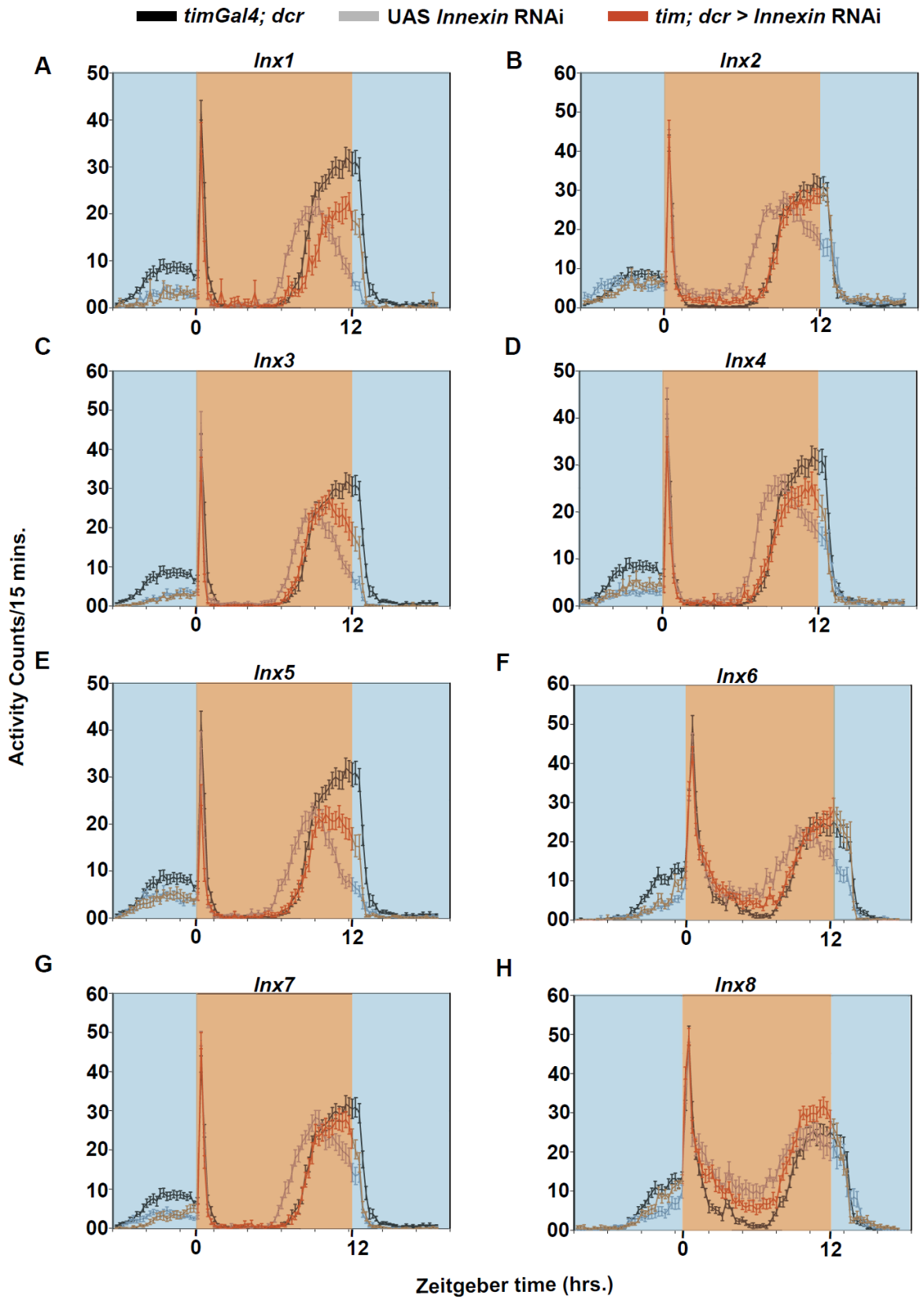
Figure 2.8: RNAi mediated knockdown screen of *Innexins* under TC 21°C : 29°C (A-H) Average activity profiles of flies across 7 days in which each of the eight *Innexins* (*Innexin 1-8*) are downregulated using a broad driver (*timGal4*) are plotted along with their respective parental controls. Blue shading depicts the 12 hours of cryophase (21°C) and orange shading depicts the 12 hours of thermophase (29°C) of the Thermophase: Cryophase cycle. Error bars depicted on the activity profiles are SEM values.

2.4 Discussion

The neuronal and molecular mechanisms underlying circadian rhythms have been extensively studied in *Drosophila melanogaster* for many years now. Although intercellular communication in the circadian network via chemical synapses is known to be important in modulating various properties of circadian rhythms, there have been no reports of the involvement of electrical synapses or gap junction proteins in circadian behaviour. I wanted to investigate if gap junction proteins play any role in modulating circadian rhythm properties in *Drosophila* since chemical and electrical synapses are known to co-exist and function together in the nervous systems of most organisms. *Drosophila* has eight gap junction genes which are mostly studied for their roles in developmental processes. As a first step to investigate their roles in circadian behaviour, I performed a RNAi knockdown screen by downregulating each of the eight *Innexin* genes using a broad driver which targets all the clock neurons and examined clock properties under different external environments.

2.4.1 Innexin1 and Innexin2 modulate the free-running period.

From the initial knockdown screen for *Innexins* under constant darkness and temperature (DD 25°C), I have identified two potential candidate *Innexin* genes that have a role in determining the period of free-running rhythms. Endogenous or free-running period of an organism is an important clock property, and we report for the first time a role for

members of the gap junction gene family in regulating a core clock property. Knockdown of *Innexin1* and 2 did not however affect the power of the rhythm, suggesting that the underlying robustness of the clock to keep time is not affected. Similarly, I did not observe any change in the percentage rhythmicity values upon knockdown of *Innexin1* and *Innexin2,* suggesting that lack of these gap junction genes does not affect the ability of the clock to be rhythmic. Knockdown of the other gap junction genes (*Innexins 3-8*) did not affect any of the clock properties in DD such as free-running period, power of the rhythm or the percentage rhythmicity, suggesting that these Innexins possibly do not contribute to determining clock properties under free-running conditions. However, one cannot conclude this firmly based on the results from a knockdown screen using a single RNAi construct. Further assays using multiple RNAi constructs and mutants for these genes will be required to rule out their contribution to circadian behaviour.

Since the free-running period of the clock and coupling among oscillators in the network are both correlated with clock precision, I wanted to examine the effect of knockdown of *Innexin1* and *2* on the precision of activity-rest rhythms. Free-running period is correlated with precision such that, as the period deviates from 24-hour, precision reduces (Kondo et al., 1994; Nikhil et al., 2020; Pittendrigh and Daan, 1976; Sharma and Chandrashekaran, 1999). This correlation of free-running period with precision has been observed with several short and long period clock mutants, although many reports have also observed a weak correlation (Srivastava et al., 2019) or a complete absence of this correlation with some mutants, e.g., the *duper* mutant hamsters (Bittman, 2013) (also, Nikhil et al., 2020). In our case, I observe that knockdown of *Innexin1* and *Innexin2* does not affect the precision of activity-rest rhythms, suggesting that the correlation between free-running period and precision is not always strictly maintained and could perhaps depend on the underlying mechanisms by which the period change occurs or on the phase markers used

for the quantification of precision. Gap junction proteins couple cells electrically thus facilitating communication among them. Hence, I wanted to examine if the lack of gap junction genes *Innexin1* and *2* would result in lowered precision of activity rhythms, as previous reports have shown that lowered coupling could lead to a decrease in precision (Herzog et al., 2004). While I find no differences in the precision between the controls and experimental flies, it cannot be concluded that the electrical coupling among the cells is not affected. It is possible that the differences in coupling due to lack of gap junction genes is not reflected at the level of behaviour due to multiple, redundant coupling mechanisms that compensate for the lack of *Innexins*. Perhaps a more efficient method would be to examine precision changes upon knockdown of multiple *Innexin* genes in combinations.

I also examined the effect of knockdown of *Innexin1* and *2* on the property of the clock to compensate for changes in free-running period under different temperatures. While knockdown of *Innexin1* did not significantly affect the compensation abilities of the clock at a higher temperature, knockdown of *Innexin2* leads to overcompensation at a higher temperature. It would be interesting to examine the reasons behind the differential effects of Innexin1 and 2 on the property of temperature compensation. Does Innexin2 affect temperature compensation via the molecular clock by affecting the stability of core clock proteins? Further experiments using many different ranges of temperatures would be helpful to examine the roles of Innexins in temperature compensation.

2.4.2 Innexin2 and Innexin4 affect the phase of activity rhythms under LD 25°C.

Apart from screening for the roles of Innexins under free-running conditions, I also asked if they contribute to regulating activity rhythms under cyclic external environments like Light: Dark cycles. My preliminary results from the screen indicate that specific *Innexin*

genes could affect both the ability of the clock to entrain to external LD cycles and its ability to phase activity rhythms with reference to a particular phase of the external Light: Dark cycle. While most experimental genotypes with each of the *Innexin* genes downregulated do not show any defects in entrainment to the LD cycle, flies that lack *Innexin1* and *Innexin2* do not show phase control with respect to onsets of activity when they are introduced into constant conditions after the entraining stimulus is removed. This could suggest that these flies are not truly entrained to the Light: Dark cycle, and some component of masking could be involved in the synchronization of these flies to the entraining stimulus. Further experiments need to be done to understand how lack of *Innexin1* and *Innexin2* could affect the ability of the clock to entrain to LD cycles. A well-established model of entrainment known as the non-parametric model hypothesizes that entrainment of the circadian clocks to external periodic cues like Light: Dark cycles are accomplished by accumulating phase shifts of the appropriate amount in response to light pulses at different times of the day (Pittendrigh and Daan, 1976). To understand the mechanism of entrainment in flies bearing the knockdowns of *Innexin1* and *Innexin2*, it would be interesting to conduct such an experiment by providing light pulses at different times of the day and calculating and comparing the amount of resulting phase-shift in both experimental flies and its respective parental controls. Importantly, flies with *Innexin4* and *Innexin2* downregulated have a delayed onset of evening activity, suggesting that lack of these *Innexins* could affect the phasing of activity relative to the external environmental light cycle. They, however do not affect the anticipation of the clock to light-dark and dark-light transitions. Future experiments such as examining the activity of mutants under long and short photoperiods, low-intensity Light: Dark cycles, etc., would be required to probe the specific roles of Innexin2 and Innexin4 in the circadian network and understand the mechanism by which it affects the phasing of activity under LD cycles. It would also

be important to investigate the distribution of these proteins in the circadian neurons to better understand the cellular and neuronal mechanisms by which these proteins affect phasing of behaviour under LD cycles.

Chapter 3: Role of Innexin2 in modulating the free-running period of activity-rest rhythms.

3.1 Introduction

A screen for identifying the members of the gap junction (*Innexin*) gene family began in *Drosophila melanogaster* after discovering two genes from this family in a mutagenesis screen. *ogre* (now *Innexin1*) and *ShakingB* (now *Innexin8*) were some of the first genes to be discovered as members of the *Drosophila Innexin* family of genes. Soon after, several groups started amplifying these genes based on sequence homology and subsequently cloning, sequencing, and mapping these sequences to the chromosome to identify new members of the *Innexin* gene family. One such study identified a gene on the X-chromosome very close to the *ogre* locus and named it as *pars related protein 33* (*prp33*, now also known as *Innexin2* or *Inx2*) (Curtin et al., 1999). A study carried out a year later after its discovery confirmed that Innexin2 could form a functional gap junction channel. Expression of Inx2 mRNA in a heterologous system like paired *Xenopus* oocytes results in the formation of voltage sensitive channels suggesting that Innexin2 is a component of the gap junction gene family and can form functional channels (Stebbings et al., 2000). Innexin2 mRNA was also found to be expressed in *Drosophila* in the epidermal cells bordering each segment throughout embryogenesis where it is found to be co-localized with Innexin3 (Stebbings et al., 2000). Several studies that followed examined the requirement of Innexin2 for many processes in *Drosophila* development. Antibodies generated against Innexin2 proteins revealed its expression in several organs and tissues such as epidermis, gut, salivary glands (Bauer et al., 2003), ovaries (Bohrmann and Zimmermann, 2008; Sahu et al., 2017), glial cells in the nervous system (Holcroft et al., 2013; Spéder and Brand, 2014), satellite glial cells in the lamina of the eye (Chaturvedi et al., 2014), glial cells of the blood-brain barrier (Spéder and Brand, 2014; Zhang et al., 2018), cortical glial cells (Farca Luna et al., 2017), and wrapping glial cells (Kottmeier et al., 2020). Over the years, many functional roles of Innexin2 were characterized in

multiple tissues. Innexin2 was shown to be a part of the Wingless signalling pathway in the development of foregut in *Drosophila* (Bauer et al., 2002), for epithelial morphogenesis (Bauer et al., 2004), for proper growth and development of follicle cells, nurse cells and oocytes in the *Drosophila* ovary (Bohrmann and Zimmermann, 2008), and for proper transmission of calcium flux across follicle cells, which is required for border cell specification during oogenesis (Sahu et al., 2017). Innexin2 is present in multiple types of glial cell subtypes and plays essential roles during development and in the adult central nervous systems. Innexin2 forms functional gap junctions along with Innexin1 in glial cells and is required during early developmental stages for proper development of nervous systems (Holcroft et al., 2013). Knockdown of *Innexin2* using glial specific driver leads to developmental lethality (Chaturvedi et al., 2014; Holcroft et al., 2013). Whole-body mutants of *Innexin2* are lethal, and this lethality can be partially rescued by expression of the functional Innexin2 protein only in glial cells (Chaturvedi et al., 2014), underscoring the importance of Innexin2 in glial cells for proper development. Similarly, gap junctions comprising of Innexin1 and Innexin2 proteins in the glia of blood-brain barrier are required for the reactivation of neural stem cells, an important step in the development of nervous systems (Spéder and Brand, 2014). Innexin2 was also shown to be present in the glial cells of the lamina in *Drosophila* eye, where it is important for the uptake of neurotransmitter histamine by the glial cell network (Chaturvedi et al., 2014). Innexin2 in the perineurial and sub-perineurial glial cells of the blood brain barrier is also important for regulating the permeability of the barrier to metabolites and drugs in a time-of-day dependent manner (Zhang et al., 2018). Innexin2 in cortex glial cells is important in the regulation of sleep via the glutamate recycling pathway (Farca Luna et al., 2017). Thus, studies so far have reported crucial roles for Innexin2 both during development and for adult specific behaviours. Our RNAi knockdown screen reveals a potential role for

Innexin2 in modulating clock properties like free-running period and entrained phase under LD cycles (See Chapter 2). In this chapter, I present the details of my findings detailing the distribution and function of Innexin2 in the circadian circuit as well as the potential mechanisms by which it modulates circadian behaviour.

3.2 Materials and methods

3.2.1 Fly lines and husbandry

All genotypes were reared on standard cornmeal medium under LD (12 hr **L**ight: 12 hr **D**ark) cycles and 25 °C, unless specified otherwise. The transgenic lines used in this study are UAS *Innexin2* RNAi (BL 42645), UAS *Innexin2* RNAi (BL 80409), *Innexin2 KO* (Drosophila Genomics Resource Centre (DGRC)111858), UAS *eGFP* (BL 6874), *Clk4.1MGal4 (BL 36316),* UAS *tubGal80^{ts} (BL 7017)* were all obtained from Bloomington *Drosophila* stock centre. *pdfGal4* and *timGal4* were obtained from the lab of Todd Holmes, UC Irvine, *Clk856Gal4* was obtained from Orie Shafer, ASRC, CUNY, *pdfGal80* was obtained from Charlotte Helfrich-Forster (University of Wurzburg), *dvpdfGal4* was obtained from Micahel Rosbash (Brandeis University), *LNdGal4* was obtained from Daniel Cavanaugh (Loyola University), *pdfGal4 (GS)* was obtained from Fernanda Ceriani (Leloir Institute, Argentina). UAS *RFP-Inx2* was obtained from Andrea Brand (Cambridge University), UAS *Inx2-GFP w*as obtained from Michael Hoch and Reinhard Bauer (University of Bonn).

For experiments involving temporal knockdown during the adult stages, flies were reared at a permissive temperature of 19°C from embryonic stages till 3 days after eclosion to allow for repression of Gal4 by *tubGal80^{ts}* and facilitate proper development, including the final pruning of synaptic connections in the nervous system. The flies were then transferred to LD 12:12 at 29°C and assayed under constant darkness and restrictive

temperature of 29°C. For experiments involving temporal knockdown of *Innexin2* during developmental stages, the flies were reared at restrictive temperature of 29°C from embryonic stages till 3 days after eclosion to allow for Gal4 expression. The flies were then transferred to LD 12:12 at 19°C and then assayed under constant darkness and permissive temperature of 19°C.

3.2.2 Temporal knockdown using the gene-switch method

For experiments involving temporal knockdown using the gene switch method, flies were reared in normal corn food until pupariation. After pupariation, pupae from each genotype were collected individually and transferred to an empty vial containing blotting paper soaked in water for moisture. Upon emergence, virgin male flies were collected and transferred to food containing either RU486 (Mifepristone, an analog of the hormone progesterone, 200µg/ml) prepared in 80% ethanol or food containing the same concentration of vehicle (80% ethanol). These flies were then allowed to stay in these vials for at least 3 days before transferring them to locomotor tubes containing RU food or vehicle respectively and assaying activity-rest rhythms under DD 25°C.

3.2.3 Locomotor activity rhythm assay

Virgin male flies (4-6 days old) were used for all experiments unless mentioned otherwise. Virgin female flies (3-5 days old) were used for experiments involving the *Innexin2* mutant (Inx2 KO, DGRC). All the flies were individually housed in glass tubes (length 65mm, diameter 7mm) with corn food and a cotton plug on the other end. Locomotor activity was recorded using the ***Drosophila* A**ctivity **M**onitors (DAM, Trikinetics, Waltham, United States of America). Experiments were conducted in incubators manufactured by Sanyo (Japan) or Percival (USA) with controlled light and temperature conditions.

3.2.4 Immunohistochemistry

Adult *Drosophila* brains were dissected in ice-cold Phosphate buffered saline (PBS) and fixed immediately after dissection in 4% Paraformaldehyde (PFA) for 30 min. The fixed brains were then treated with blocking solution (10% horse serum) for 1-h at room temperature and an additional 6-h at 4 °C (additional incubation is only given in case of staining with anti-PER antibody to reduce staining of non-specific background elements), followed by incubation with primary antibodies at 4°C for 24-48 h. The primary antibodies used were anti-PER (rabbit, 1:20,000, kind gift from Jeffrey Hall, Brandeis University), anti-PDF (mouse, 1:5000, C7, DSHB), anti-GFP (chicken, 1:2000, Invitrogen), anti-Innexin2 (guinea pig, 1:50, kind gift from Michael Hoch, University of Bonn). After incubation, the brains were given 6-7 washes with 0.5% PBS + Triton-X (PBT) after which they were incubated with Alexa-fluor conjugated secondary antibodies for 24-hour at 4°C. The following secondary antibodies were used, goat anti-chicken 488 (1:3000, Invitrogen), goat anti-rabbit 488 (1:3000, Invitrogen), goat anti-mouse 546 (1:3000, Invitrogen), goat anti-mouse 647 (1:3000, Invitrogen), goat anti-guinea pig 546 (1:3000, Invitrogen). The brain samples were further washed 6-7 times with 0.5% PBT and cleaned and mounted on a clean glass slide in mounting media (7:3 glycerol: PBS). The same procedure was followed for experiments where immunostaining of larval brains (L3 stage) was required.

3.2.5 Quantification and Statistical Analysis

3.2.5.1 Activity data analysis

Raw data obtained from the DAM system were scanned and binned into activity counts of 15-minute intervals using DAM Filescan. Data were analysed using the CLOCKLAB software (Actimetrics, Wilmette, IL) or RhythmicAlly (Abhilash and Sheeba, 2019).

Values of period and power of rhythm were calculated for 7-8 days using the Chi-square periodogram with a cut-off of *p=0.05*. The period and power values of all the flies for a particular experimental genotype were compared against the parental controls using one-way ANOVA with genotype as the fixed factor followed by post-hoc analysis using Tukey's Honest Significant Difference (HSD) test. The details on the statistical comparisons and the number of flies used in a given experiment are indicated in the respective figure legends section.

3.2.5.2 Image acquisition and analysis

The slides prepared for immunohistochemistry were imaged using confocal microscopy in a Zeiss LSM880 microscope with 20X, 40X (oil-immersion), or 63X (oil-immersion) objectives. Image analysis was performed using Fiji software (Schindelin et al., 2012). In the samples, clock neurons were classified based on their anatomical locations and expression of PER/PDF. PER intensity in these neurons was measured by selecting the slice of the Z-stack, which shows maximum intensity, drawing a Region of Interest (ROI) around the cells, and measuring their intensities. 3-6 separate background values were also measured around each cell and the final intensity was taken as the difference between the cell intensity and the background. For PDF quantification in the dorsal projections, a rectangular box was drawn as ROI starting from the point where the PDF projection turns into the dorsal brain, and intensity was measured. 3-6 background values were also calculated around the projection. The intensity values obtained from both the hemispheres for each cell type for each brain were averaged and used for statistical analysis. I used a COSINOR based curve-fitting method (Cornelissen, 2014) to estimate different aspects of rhythmicity like presence of a 24-hour periodicity, phase and amplitude values of the oscillation. COSINOR analysis was implemented using the CATCosinor function from the CATkit package written for R (Lee Gierke and Cornelissen, 2016).

3.3 Results

3.3.1 Knockdown of *Innexin2* in all clock neurons lengthens the free-running period

Although it would be ideal to check for expression pattern of the proteins before downregulating them in different cell types, it is extremely tedious and practically difficult to obtain antibodies/reporters for all the eight Innexin proteins from labs and sources all over the world without a good reason to do so. A genetic knockdown screen, on the other hand, is a simple technique to assess the importance of a particular gene in a behaviour of interest. Once the candidate genes are identified from the screen, I have obtained antibodies/reporters to ensure that these proteins are being expressed in the relevant cells to corroborate the results from the behavioural RNAi knockdown experiments. Our genetic knockdown screen of *Innexins* in all clock neurons identifies Innexin2 as a potential candidate in regulating free-running period of activity-rest rhythms (Fig. 2.1). But *timGal4* drives expression in many cells in the brain, most of the circadian pacemaker neurons, neurons in the optic lobe, and some glial cells (Kaneko and Hall, 2000). Hence, I also used another driver, *Clk856Gal4* which has a narrower expression pattern than *timGal4* but nevertheless targets most clock neurons, except a few DNs (Gummadova et al., 2009). *Innexin2* knockdown using *Clk856Gal4* also resulted in the lengthening of the free-running period compared to their respective parental controls (Fig. 3.1A, Fig. 3.1C, Table 3.1, and Appendix 3.1). Consistent with previous results, no significant difference in the power of the rhythm was observed in case of *Innexin2* knockdown using *Clk856Gal4* (Fig. 3.1B, Table 3.1, and Appendix 3.2). I also used a second *Innexin2* RNAi construct (BL 80409) on a different chromosome to verify if the period lengthening obtained is an effect of *Innexin2* knockdown and not because of positional effects of transgene insertion. Knockdown of *Innexin2* using a second RNAi construct (BL 80409) in all clock neurons with *timGal4* resulted in lengthening of the free-running period as compared to its parental

controls (Fig. 3.2A) with no significant difference in the power of rhythm from both the parental controls (Fig. 3.2B). Similarly, knockdown of *Innexin2* (BL 80409) using *Clk856Gal4* also resulted in lengthening of the free-running period as compared to its parental control genotypes (Fig. 3.2C) with no significant difference in the power of rhythm compared to both its parental control genotypes (Fig. 3.2D). I also used a previously characterized mutant of *Innexin2* (Sahu et al., 2017) to verify the period lengthening phenotype seen with *Innexin2* RNAi experiments. Innexin2 has been reported to have essential roles in development. Previous studies have shown that *Innexin2* mutants are lethal such that homozygous mutants die during early larval stages (Chaturvedi et al., 2014; Holcroft et al., 2013). I also observe something similar with our *Innexin2* mutant flies (*Inx2 KO*, DGRC 111858). Homozygous females (*Inx2 KO*/*Inx2 KO*) and hemizygous males (*Inx2 KO/ y*) do not survive and die during the early larval stages. Heterozygous *Innexin2* mutant female flies (*Inx2 KO / +*) show a significantly lengthened period of free-running rhythms as compared to their parental control flies (Fig. 3.2E), and the power of rhythm of these mutant flies was not different from its parental control genotype (Fig. 3.2F).
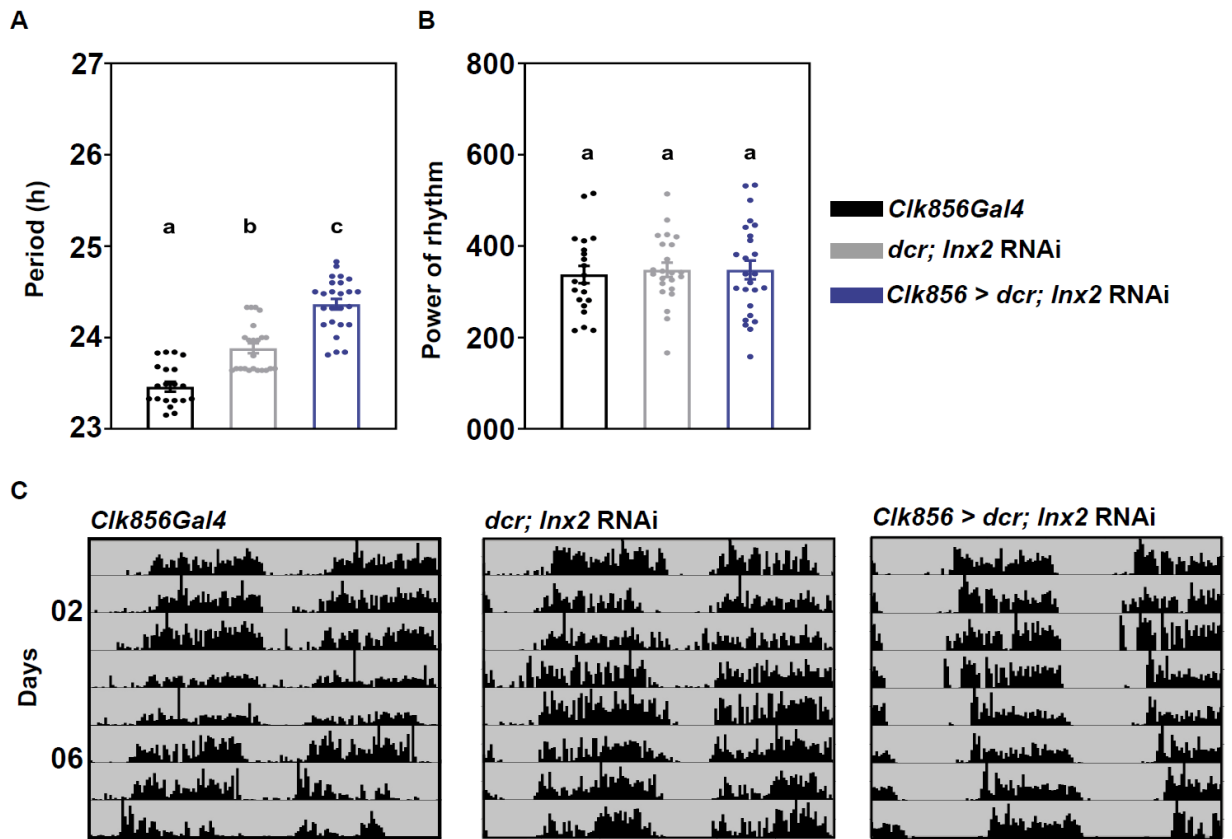
Figure 3.1: Knockdown of *Innexin2* in all clock neurons lengthens the free-running period Free-running period **(A)** and power of rhythm **(B)** of experimental flies (*Clk856 > dcr; Inx2* RNAi) (*n=27*) is plotted along with its Gal4 (*n=22*) and UAS parental control (*n=23*) flies **(C)** Representative double-plotted actograms of individual flies of each indicated genotype under constant darkness.

Error bars are SEM, period and power values are determined using Chi-square periodogram for a period of 7 days. All statistical comparisons were performed using one-way ANOVA with genotype as a fixed factor followed by post-hoc Tukey's HSD test. Data representative from 3 independent experiments. See Table 3.1 for more details.
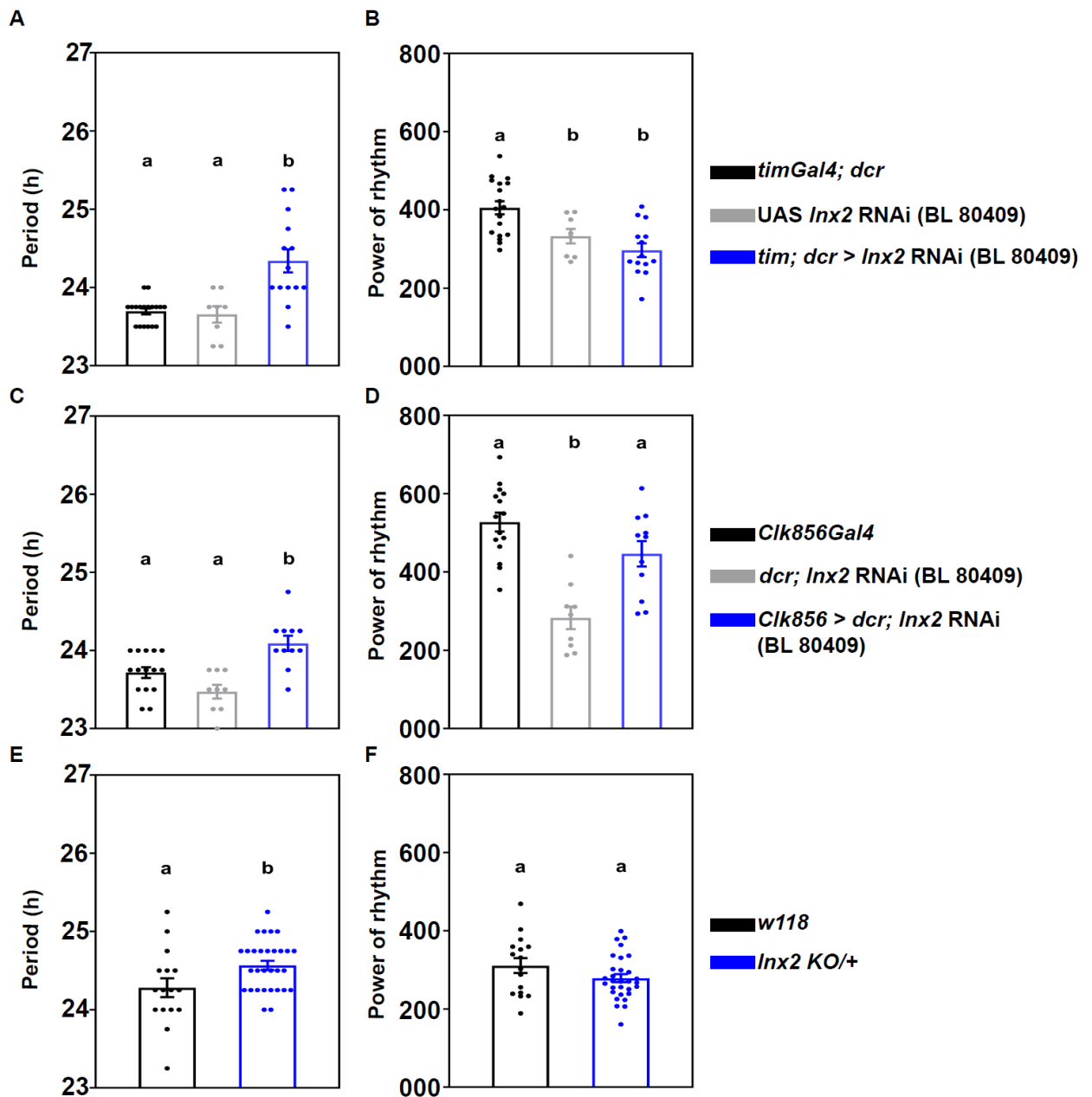
Figure 3.2: *Innexin2* **knockdown using alternate constructs lengthens the free-running period (A)** Free-running period (A) and power of rhythm **(B)** of experimental flies (*tim; dcr > Inx2* RNAi) (*n=16*) using an alternate construct (BL 80409) is plotted along with its Gal4 (*n=19*) and UAS control (*n=14*) flies. Free-running period **(C)** and power of rhythm **(D)** of experimental flies (*Clk856 > dcr; Inx2* RNAi) (*n=15*) using an alternate construct (BL 80409) is plotted along with its Gal4 (*n=15*) and UAS control (*n=14*) flies. Free-running period **(E)** and power of rhythm **(F)** of *Inx2* mutant flies (*Inx2 KO,* DGRC 111858) (*n=30*) is plotted along with its background control *w1118* (*n=19*) flies. Error bars are SEM, period and power values are determined using Chi-square periodogram for a period of 7 days.

3.3.2 Innexin2 functions in the adult brain to modulate the free-running period of locomotor activity rhythm.

Since several previous studies have shown that Innexin2 plays crucial roles during many developmental processes in *Drosophila* (Bauer et al., 2004, 2002; Holcroft et al., 2013), I wanted to examine if the period lengthening seen in our experiments is due to defects in development of the circadian pacemaker circuit or due to roles played by Innexin2 in the mature adult circuit. To distinguish between these two possibilities, I temporally restricted the *Innexin2* knockdown to the adult stages using the TARGET system (McGuire et al., 2004). The TARGET system allows for the temporal expression of a gene of interest under UAS control utilizing a temperature-sensitive Gal80ts, a repressor of Gal4. At a permissive temperature (19°C), *Gal80^{ts}* is active and represses Gal4; thus UAS *Innexin2* RNAi will not be expressed when flies are kept at this temperature. At restrictive temperatures (29°C), *Gal80^{ts}* will be inactive, hence Gal4 will drive the expression of UAS *Innexin2* RNAi in the cells of interest.
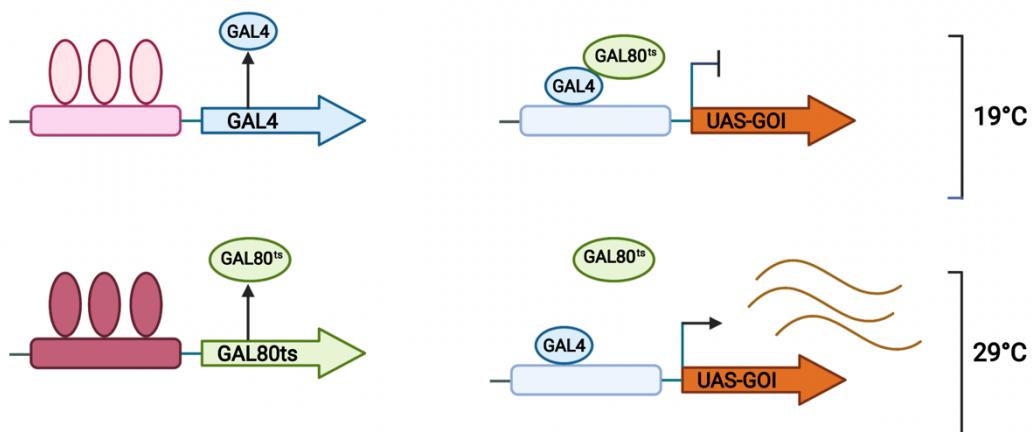
The efficiency of the system in repressing Gal4 was verified by expressing UAS-*eGFP* under the same driver, *timGal4*; *tubGal80^{ts}* and assessing GFP expression by

immunohistochemistry in the larval (L3) stage at 19°C and adult stages at 29°C (Fig. 3.3A and B). In the larval stages, I detect a faint trace of GFP in 1 out of 3-4 s-LNvs / hemisphere in a small fraction of brain samples (3/9 hemispheres), suggesting that *tubGal80^{ts}* may have been unable to completely repress the expression of the *Innexin2* RNAi construct during development. Significant lengthening of period of activity rhythm was observed in experimental flies as compared to controls even when *Innexin2* knockdown in clock neurons was restricted to the adult stages (Fig. 3.4A, Fig.3.4C, Table 3.1, Appendix 3.1), suggesting that Innexin2 has roles in the adult circadian circuit to determine the period of free-running rhythms, with the caveat that repression during the larval stages could have been incomplete. Under such adult-specific *Innexin2* knockdown, the power of the rhythm of experimental flies was found to be significantly lower only compared to its UAS control (Fig. 3.4B, Appendix 3.2). As a complementary experiment, I also restricted the knockdown of *Innexin2* to only the developmental stages using the TARGET system. In this case, significant lengthening of the free-running period was not observed in the experimental flies as compared to its parental control flies (Fig. 3.5A, Fig. 3.5C, Table 3.1, Appendix 3.1), with no change in the power of the rhythm (Fig. 3.5B, Appendix 3.2) thus strengthening the conclusion that Innexin2 functions only in the adult *Drosophila* circadian circuit to determine free-running period.

A *tim; tubGal80^{ts} > eGFP*; 19°C.

B *tim; tubGal80^{ts} > eGFP*; 29°C.
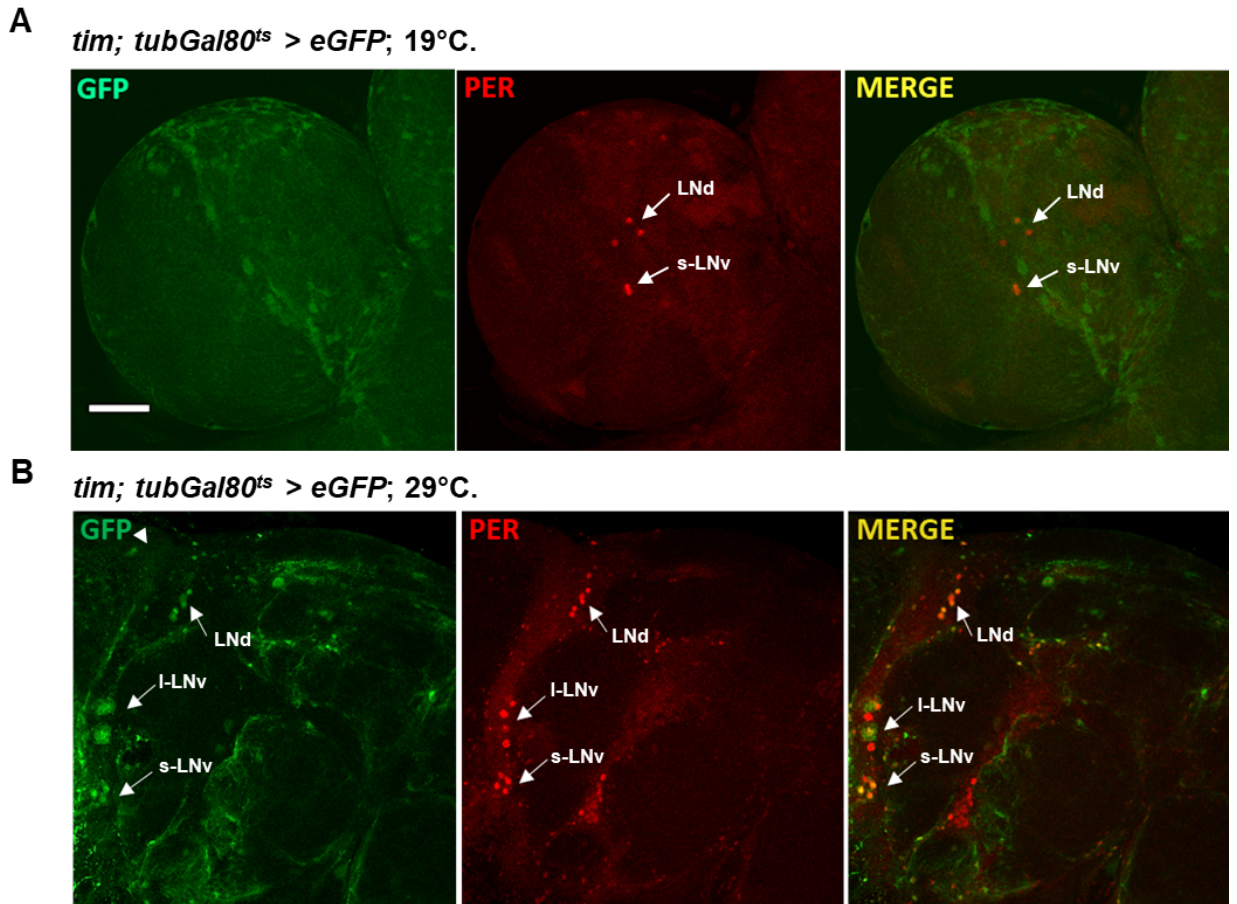
Figure 3.3: Verification of the efficiency of *tim; tubGal80^{ts}* construct The efficiency of the *tim; tubGal80^{ts}* construct was verified by crossing *tim; tubGal80^{ts}* with *eGFP* **(A)** The flies were reared at a permissive temperature of 19°C. Larvae (L3 stage) from the progeny were dissected and stained with anti-GFP and anti-PER antibodies. s-LNv do not express GFP at a permissive temperature (left), whereas strong PER staining was observed in these cells (middle panel). **(B)** Three days after eclosion, adult flies were transferred to high temperature of 29°C and dissected after another 4 days and stained with antibodies against GFP and PER. s-LNv, l-LNv and LNds show GFP expression under restrictive temperature of 29°C. Couple of l-LNv cells do not show GFP expression even under a restrictive temperature in a very small fraction of the brain samples, suggesting that the repression by *tubGal80^{ts}* may not have been completely reversed. *n=5* brain samples at each temperature. Scale bar = 55µm.
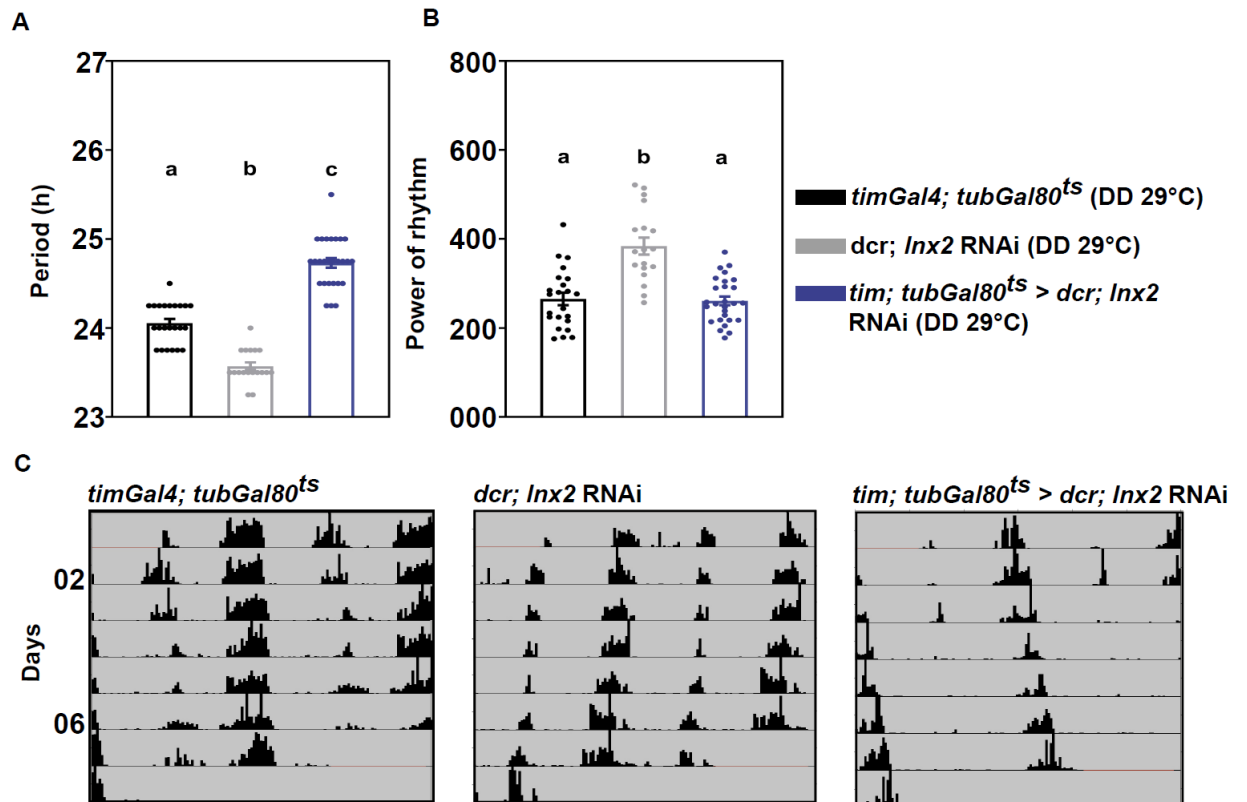
Figure 3.4: Adult-specific knockdown of *Innexin2* in clock neurons lengthens the free-running period (A) Free-running period **(A)** and power of rhythm **(B)** of experimental flies (*tim; tubGal80^{ts}> dcr ; Inx2* RNAi) (*n=27*) is plotted along with its Gal4 (*n=23*) and UAS control (*n=20*) flies **(C)** Representative double-plotted actograms of individual flies of each indicated genotype under constant darkness.

Error bars are SEM, period and power values are determined using Chi-square periodogram for a period of 7 days. All statistical comparisons were performed using one-way ANOVA with genotype as a fixed factor followed by post-hoc Tukey's HSD test. Data representative from 3 independent experiments. See Table 3.1 for more details.
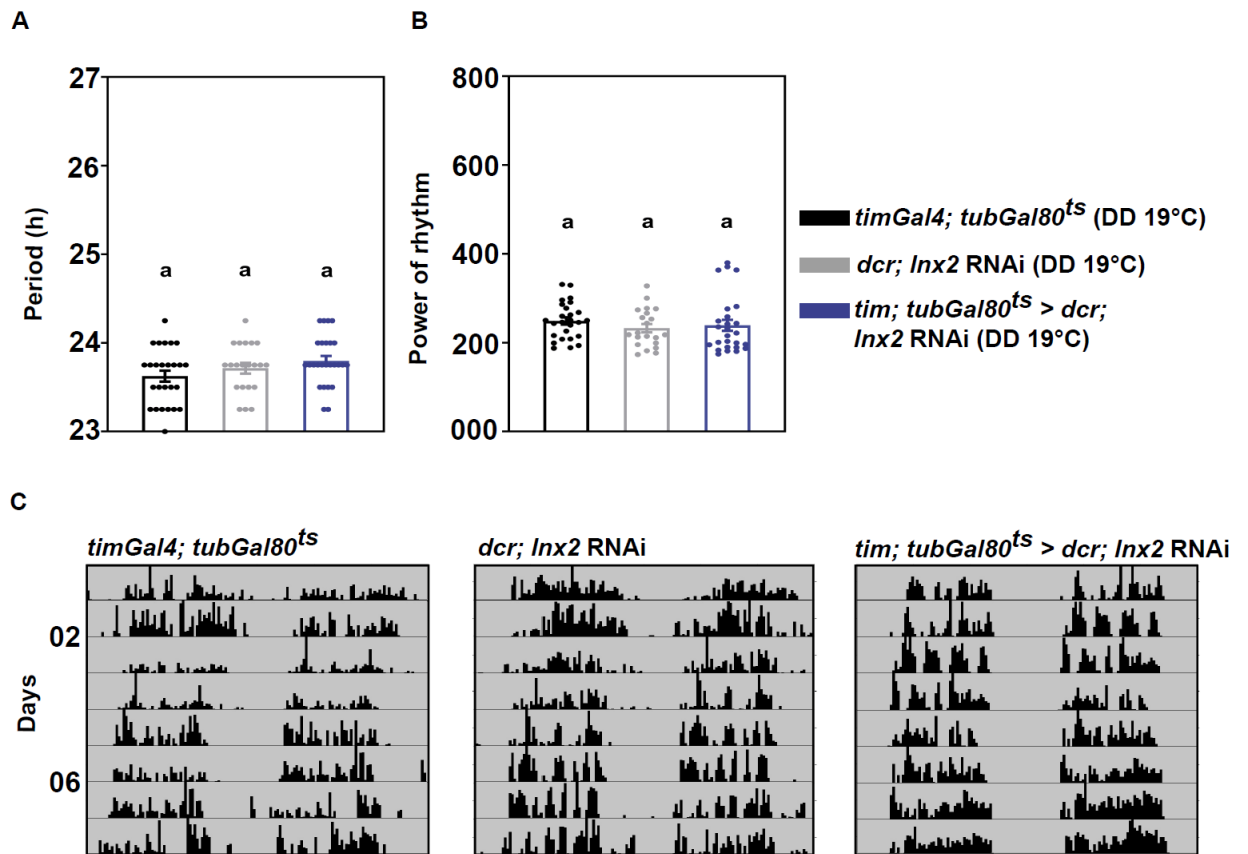
Figure 3.5: Development-specific knockdown of *Innexin2* in clock neurons does not affect the free-running period Free-running period **(A)** and power of rhythm **(B)** of experimental flies (*tim; tubGal80^{ts} > dcr; Inx2 RNAi*) (*n=26*) is plotted along with its Gal4 (*n=26*) and UAS control (*n=21*) flies **(C)** Representative double-plotted actograms of individual flies of each indicated genotype under constant darkness.

Error bars are SEM, period and power values are determined using Chi-square periodogram for a period of 7 days. All statistical analysis were performed using one-way ANOVA with genotype as a fixed factor followed by post-hoc Tukey's HSD test. Data representative from 2 independent experiments. See Table 3.1 for more details.

3.3.3 Adult-specific knockdown of *Innexin2* in ventral lateral neurons using the gene switch system

Additionally, as an alternate to the TARGET system for temporal control of gene expression, I have also used the inducible Gal4 system (Gene Switch system; Osterwalder et al., 2001) to downregulate *Innexin2* expression only in the adult stages. Due to the non-availability of an inducible form of the driver for all clock neurons (*timGal4(GS)*), I

downregulated *Innexin2* expression in the ventral lateral neurons in the adult stages using the *pdfGal4 (GS)* driver, which targets both the small and large ventral lateral neurons and has been verified in several previous reports (Depetris-Chauvin et al., 2011; Fernandez-Chiappe et al., 2020; Herrero et al., 2020). Experimental flies (*pdf (GS) > dcr; Inx2* RNAi) did not show a significantly lengthened free-running period as compared to both the parental control flies when they were maintained in food containing vehicle (80% Ethanol) throughout development and adulthood (Fig. 3.6A, Appendix 3.1). When flies were transferred to food containing the inducible agent, RU486 (mifepristone, an analog of the hormone progesterone), the free-running period of experimental flies after eclosion lengthened significantly as compared to its control flies maintained in vehicle food (Fig. 3.6C). However, I observed that the free-running period of the Gal4 control flies (*pdfGal4 GS*) also lengthened significantly and to comparable levels when transferred to RU-food (Fig. 3.6D), probably due to the non-specific effects of using the inducible system. This observation was also reported by several previous studies (Depetris-Chauvin et al., 2011; Fernandez-Chiappe et al., 2020; Frenkel et al., 2017). The period of experimental flies (*pdf GS > dcr; Inx2* RNAi*)* transferred to RU food after development was only significantly different from its UAS control and not different from its Gal4 control (Fig.3.6 B, Appendix 3.1). Statistically significant difference from both the parental controls was perhaps not detected because of the non-specific lengthening of the period seen in the Gal4 parental control flies. Since RU causes non-specific changes in the free-running period, which is the behaviour of my interest, it would be difficult to conclude if the period changes observed are because of the effects of RU or because of the downregulation of *Innexin2* in these neurons; hence TARGET would probably be a better method compared to gene switch for temporal downregulation of *Innexin2* in clock neurons.
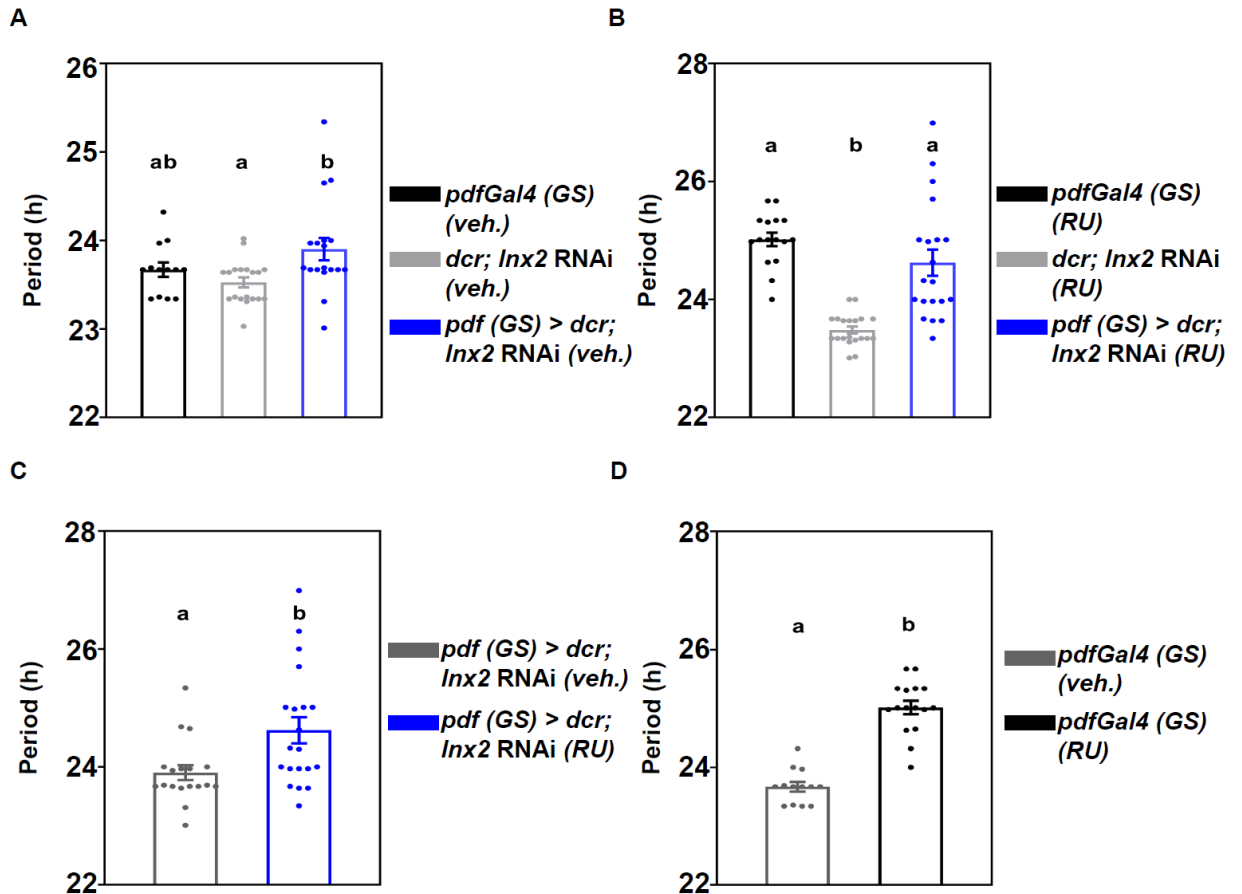
Figure 3.6: Adult-specific knockdown of _Innexin2_ using the gene-switch system: (A) Free-running period of experimental flies _pdf (GS) > dcr; Inx2_ RNAi (_n_=19) when they are fed food containing only vehicle (80% ethanol) in the adult stages is plotted along with its UAS (_n_=19) and Gal4 control (_n_=16) genotypes **(B)** Free-running period of experimental flies _pdf (GS) > dcr; Inx2_ RNAi (_n_=20) when they are fed food containing RU486 in the adult stages is plotted along with its UAS (_n_=20) and Gal4 control (_n_=17) genotype). **(C)** Free-running period of experimental flies _pdf (GS) > dcr; Inx2_ RNAi (_n_=20), when fed with RU486 food as adults is plotted along with the flies of the same genotype fed with vehicle (80% ethanol) (_n_=19) **(D)** Gal4 control flies (_pdf(GS)Gal4_), fed with RU486 (_n_=17) as adults plotted along with flies of the same genotype fed with vehicle (80% ethanol) (_n_=16).

Error bars represent SEM. All free-running period values are calculated using Chi-square periodogram for a period of 7 days. All statistical analysis were performed using one-way ANOVA with genotype as a fixed factor followed by post-hoc Tukey's HSD test.

3.3.4 Innexin2 in ventral lateral neurons is important for determining the period of free-running rhythms.

Since the knockdown of *Innexin2* in all clock neurons lengthens the period, I proceeded to downregulate its expression in smaller, distinct subsets of clock neurons to determine the functional role of Innexin2 in each of these subsets. First, I used *dvpdfGal4,* which targets the small and large ventral lateral neurons (s-LNv and l-LNv, respectively) and 4 dorsal lateral neurons (LNd). Knockdown of *Innexin2* with *dvpdfGal4* results in experimental flies having a significantly longer period than both its parental genotypes (Fig. 3.7A left, Table 3.1, Appendix 3.3). In this case, I also observed a significant decrease in the power of rhythm of the experimental flies (Fig. 3.7A right, Table 3.1, Appendix 3.4). Next, I used *pdfGal4,* which is only expressed in the ventral lateral neurons, to knockdown the levels of *Innexin2*. I found that the experimental flies have a significantly longer period than their parental controls (Fig. 3.7B left, Table 3.1, Appendix 3.3), suggesting that Innexin2 functions in the ventral lateral neurons in the circadian circuit. The period lengthening obtained in this case was similar to that observed with *Innexin2* knockdown using *timGal4*. To determine the contribution of Innexin2 in the LNd neurons to period lengthening, I downregulated the expression of *Innexin2* using *LNdGal4* (Bulthuis et al., 2019), which is strongly expressed in all 6 LNd cells but not in any ventral lateral neurons except for faint expression in some l-LNv (Bulthuis et al., 2019). Knockdown of *Innexin2* using *LNdGal4* did not significantly change the free-running period or power of rhythm as compared to both parental controls (Fig. 3.7C, Table 3.1, Appendix 3.3, Appendix 3.4), suggesting that, under free-running conditions, Innexin2 functions in the ventral neuronal subsets among the lateral neurons. I also downregulated *Innexin2* expression in the dorsal neuronal subsets (DN1p) using the *Clk4.1MGal4* and found no significant difference in

the period or power of rhythms from that of their respective parental controls (Fig. 3.7D, Table 3.1, Appendix 3.3, Appendix 3.4).
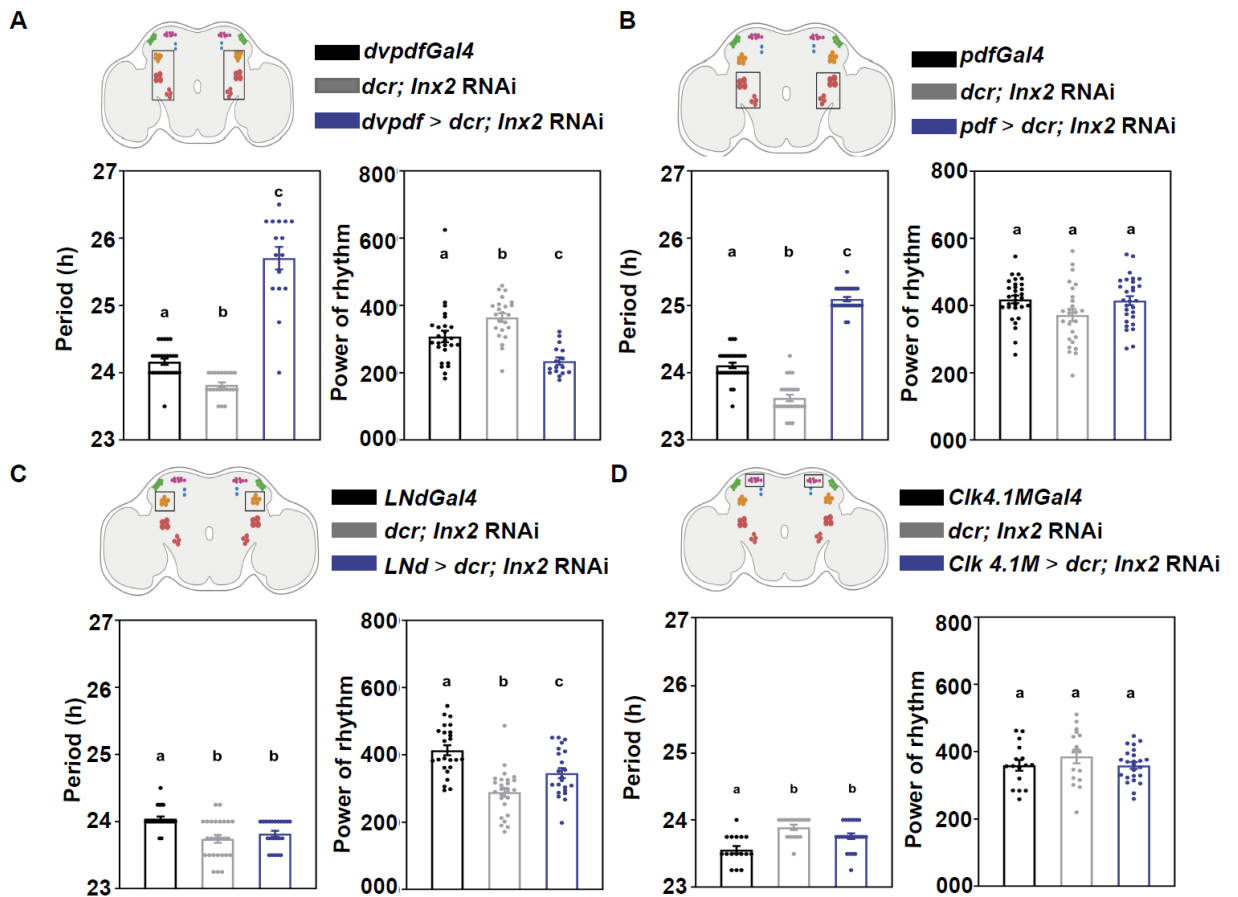
Figure 3.7: Knockdown of *Innexin2* in different clock neuronal subsets. Depiction of adult *Drosophila* brains with the box indicating the circadian neuronal subsets targeted (A) Free-running period (left) and power of rhythm (right) of experimental flies (*dvpdf > dcr; Inx2* RNAi*) (n=16) is plotted along with its Gal4 (n=26) and UAS control (n=23) genotypes **(B)** Free-running period (left) and power of rhythms (right) of experimental flies (*pdf > dcr; Inx2* RNAi) (n=29) is plotted along with its Gal4 control (n=30) and UAS control (n=26) genotypes, **(C)** Free-running period (left) and power of rhythm (right) of experimental flies (*LNd > dcr; Inx2* RNAi) (n=22) is plotted along with its Gal4 control (n=24) and UAS control (n=26) flies **(D)** Free-running period (left) and power of rhythm (right) of experimental flies (*Clk4.1M > dcr; Inx2* RNAi) (n=24) is plotted along with its Gal4 control (n=16) and UAS control (n=16) genotype.

Error bars are SEM. All period and power values are calculated using Chi-squared periodogram for a period of 7 days. All statistical comparisons are performed using one-way ANOVA with genotype as a fixed factor followed by post-hoc Tukey's HSD test. See Table 3.1 for more details.

Genotype	N	_n_	Period ± SEM	POR ± SEM
tim; dcr (Gal4 cont.)	3	30	23.6 ± 0.01	419.2 ± 13.1
		31	23.7 ± 0.03	276.8 ± 8.82
		29	23.7 ± 0.06	268 ± 7.1
UAS _Inx2_ RNAi	3	25	23.5 ± 0.02	424.2 ± 16.5
		29	23.7 ± 0.05	277.3 ± 10
		29	23.7 ± 0.04	292.7 ± 12.2
tim dcr > Inx2 RNAi	3	18	24.6 ± 0.07	377 ± 13.5
		27	24.7 ± 0.04	249.3 ± 10.52
		18	24.65 ± 0.07	271.7 ± 13.7
Clk856Gal4 (Gal4 cont.)	3	21	23.4 ± 0.05	337.8 ± 18.8
		29	23.6 ± 0.06	303.9 ± 11.7
		22	23.7 ± 0.06	244.1 ± 9.19
dcr: Inx2 RNAi (UAS cont.)	3	23	23.8 ± 0.05	348.1 ± 15.7
		29	23.3 ± 0.05	263.3 ± 11.7
		22	24 ± 0.05	273.5 ± 13.1
Clk856 > dcr; Inx2 RNAi	3	27	24.3 ± 0.05	347.9 ± 20.4
		26	24.5 ± 0.05	364.2 ± 14.5
		27	24.3 ± 0.04	272.5 ± 11.36
tim; tubGal80^{ts} (_Gal4_ cont.; DD 29°C)	3	18	24.2 ± 0.05	359.4 ± 24.9
		21	24 ± 0.05	430.4 ± 23.5
		23	24 ± 0.04	265.2 ± 13.9
dcr; Inx2 RNAi (UAS cont.;DD 29°C)	3	15	23.3 ± 0.09	302.7 ± 37.3
		14	23.3 ± 0.03	551 ± 21.4
		18	23.5 ± 0.04	384 ± 19.2
tim; tubGal80^{ts} > dcr; Inx2 RNAi (DD 29°C)	3	19	25.1 ± 0.09	533.9 ± 14.9
		27	24.9 ± 0.04	526.8 ± 15.1
		27	24.7 ± 0.05	260.9 ± 9.7
tim; tubGal80^{ts} (_Gal4_ cont.; DD 19°C)	2	22	23.7 ± 0.08	269.8 ± 13.6
		26	23.6 ± 0.06	248.8 ± 8
dcr; Inx2 RNAi (UAS cont.;DD 19°C)	2	22	24 ± 0.09	279.4 ± 11.5
		21	23.7 ± 0.06	232.7 ± 9.38
tim; tubGal80^{ts} > dcr; Inx2 RNAi (DD 19°C)	2	23	23.5 ± 0.05	231 ± 10.5
		26	23.7 ± 0.05	239 ± 12.5
dvpdfGal4 (Gal4 cont.)		26	24.1 ± 0.04	307.5 ± 17.2
dcr; Inx2 RNAi (UAS cont.)		23	23.8 ± 0.03	363.9 ± 12.9
dvpdf > dcr;Inx2 RNAi		16	25.7 ± 0.16	234.4 ± 11
pdfGal4 (Gal4 cont.)	2	30	24.1 ± 0.04	418.4 ± 11.35
		23	24.2 ± 0.06	244.5 ± 10.98
dcr: Inx2 RNAi _(UAS cont.)_	2	26	23.65 ± 0.04	371.6 ± 17.7
		22	24 ± 0.05	273.5 ± 13.1

Genotype	Replicates	No. of flies	Avg period (±SEM)	Avg power (±SEM)
pdf > dcr; Inx2 RNAi	2	29	25 ± 0.03	414.6 ± 13.3
		25	25.4 ± 0.05	287.4 ± 9.92
LNdGal4 (Gal4 cont.)	2	13	24 ± 0.06	524 ± 34.9
		24	24 ± 0.03	413.4 ± 14.9
dcr; Inx2 RNAi (UAS cont.)	2	28	23.8 ± 0.04	416.8 ± 17.8
		26	23.7 ± 0.04	288.9 ± 13.1
LNd > dcr; Inx2 RNAi	2	18	23.8 ± 0.05	450.2 ±26.1
		22	23.8 ± 0.04	345.5 ± 14.9
Clk4.1MGal4 (Gal4 cont.)		16	23.5 ± 0.05	359.2 ± 15.7
Clk4.5FGal4 (Gal4 cont.)		17	23.7 ± 0.06	294.6 ± 13.2
dcr; Inx2 RNAi (UAS cont.)		16	23.8 ± 0.04	385.9 ± 18.2
Clk4.1M > dcr; Inx2 RNAi		24	23.7 ± .04	358.8 ± 9.97
Clk4.5F > dcr; Inx2 RNAi		14	23.8 ± 0.04	372.9 ± 19.7
tim; pdfGal80 (Gal4 cont.)	2	23	23.9 ± 0.06	334.3 ± 17.5
		30	24.3 ± 0.06	328.2 ± 16.5
dcr; Inx2 RNAi (UAS cont.)	2	29	23.3 ± 0.05	263.3 ± 11.7
		27	23.8 ± 0.08	317.4 ± 15.9
tim; pdfGal80 > dcr; Inx2 RNAi	2	25	24 ± 0.04	310.2 ± 12.4
		29	24.25 ± 0.07	275.2 ± 14.25
timGal4 (Gal4 cont.)		28	24 ± 0.05	362.9 ± 13.3
pdfGal4 (Gal4 cont.)		29	24.3 ± 0.03	393.7 ± 8.79
UAS *RFP-Inx2* (UAS cont.)		27	23.9 ± 0.05	385.5 ± 14.2
tim > RFP-Inx2		30	24.5 ± 0.05	429.1 ± 11.7
pdf > RFP-Inx2		31	24.6 ± 0.05	427.8 ± 13.6

Table 3.1: Table representing the genotype, no. of replicates, no. of flies, average period (±SEM), and average power of the periodogram (± SEM) values in case of knockdown of *Innexin2* in different subsets of clock neurons.

3.3.5 Distribution of Innexin2 in the circadian pacemaker circuit

To investigate the distribution of Innexin2 protein in the adult *Drosophila* circadian circuit, I performed immunohistochemistry using a previously characterized anti-Innexin2 antibody (Bohrmann and Zimmermann, 2008). To examine the co-localization of Innexin2 with the clock neurons, I dissected the brains of wild-type flies and stained them with antibodies against Period (PER), Innexin2, and PDF. In accordance with my

behavioural results, I find that among clock neurons, Innexin2 is expressed only in the ventral lateral neuronal subset i.e., the small and large ventral neurons (Fig. 3.8, top panel). Additionally, I also consistently observe Innexin2 in optic lobes co-localized with PDF marking the varicosities of l-LNv projections. Multiple such points of co-localization are marked in the image (Fig. 3.8, lower panel, arrowheads). Surprisingly, in my IHC experiments, I never observed Innexin2 to be co-localized with PDF projections either in the dorsal or contralateral region of the brain (Fig. 3.9A). Innexin2 was also not observed to be co-localized with PER in the dorsal lateral subset (LNd) of neurons or any of the dorsal neuronal subsets (DNs) (Fig. 3.9B and C).
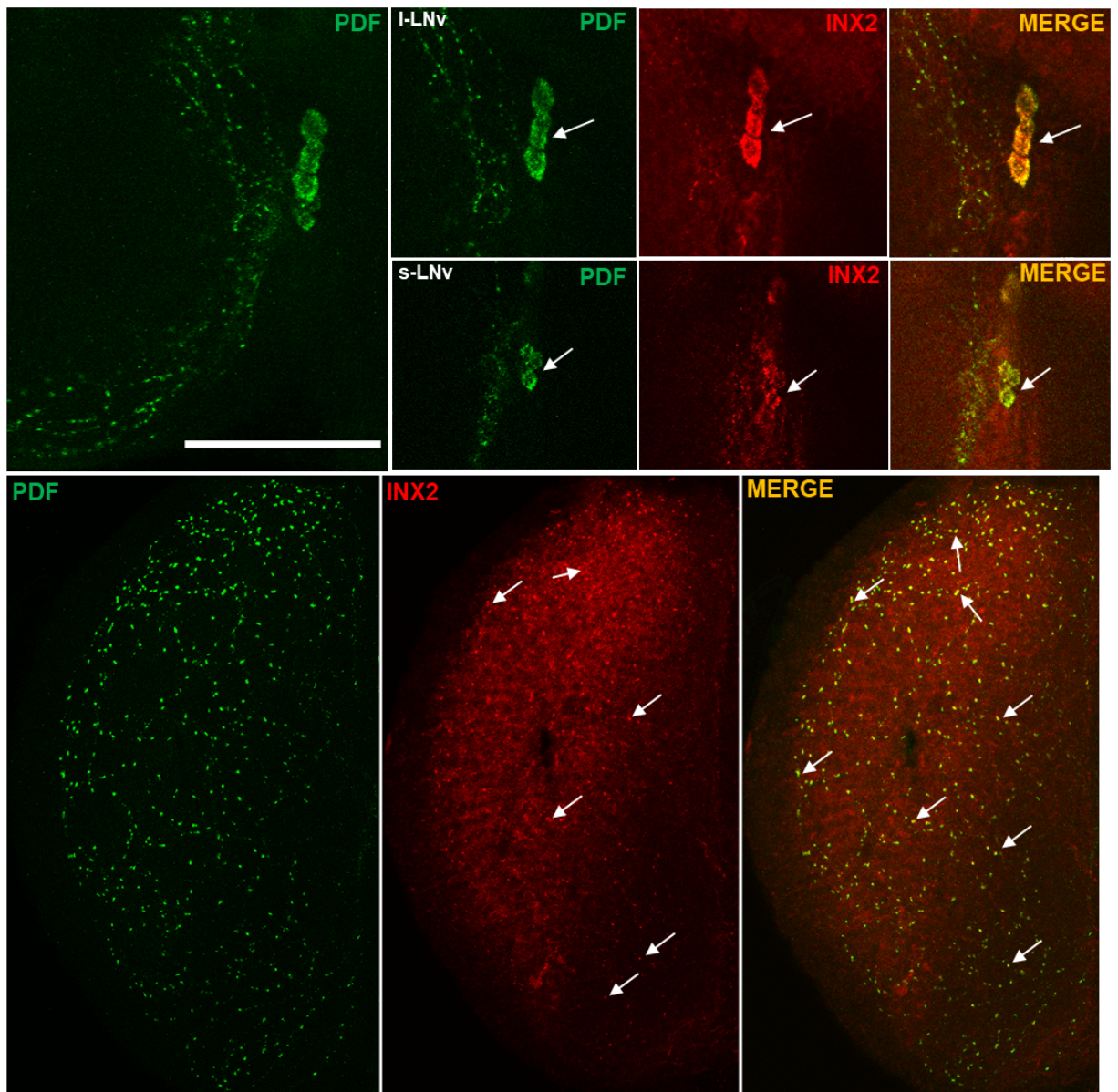
Figure 3.8: Innexin2 is expressed in the small and large ventral lateral neurons in the circadian pacemaker circuit Representative images of adult *Drosophila* brains showing the distribution of Inx2 protein among the clock cells. Flies were dissected at ZT12 and stained with anti-Inx2 antibody and co-stained with anti-PDF antibody for identification and co-localization with ventral lateral neurons. Inx2 was found to be predominantly localized to the small and large ventral lateral neurons (s-LNv and l-LNv) among the clock neurons (arrows, top panel). Inx2 was also found to be present in the varicosities of l-LNv projections in the optic lobes (arrows, bottom panel). Brightness and contrast of representative images were adjusted to facilitate better visualization. Scale-bar represents 55 μm, *n* = 12 brain samples were imaged.
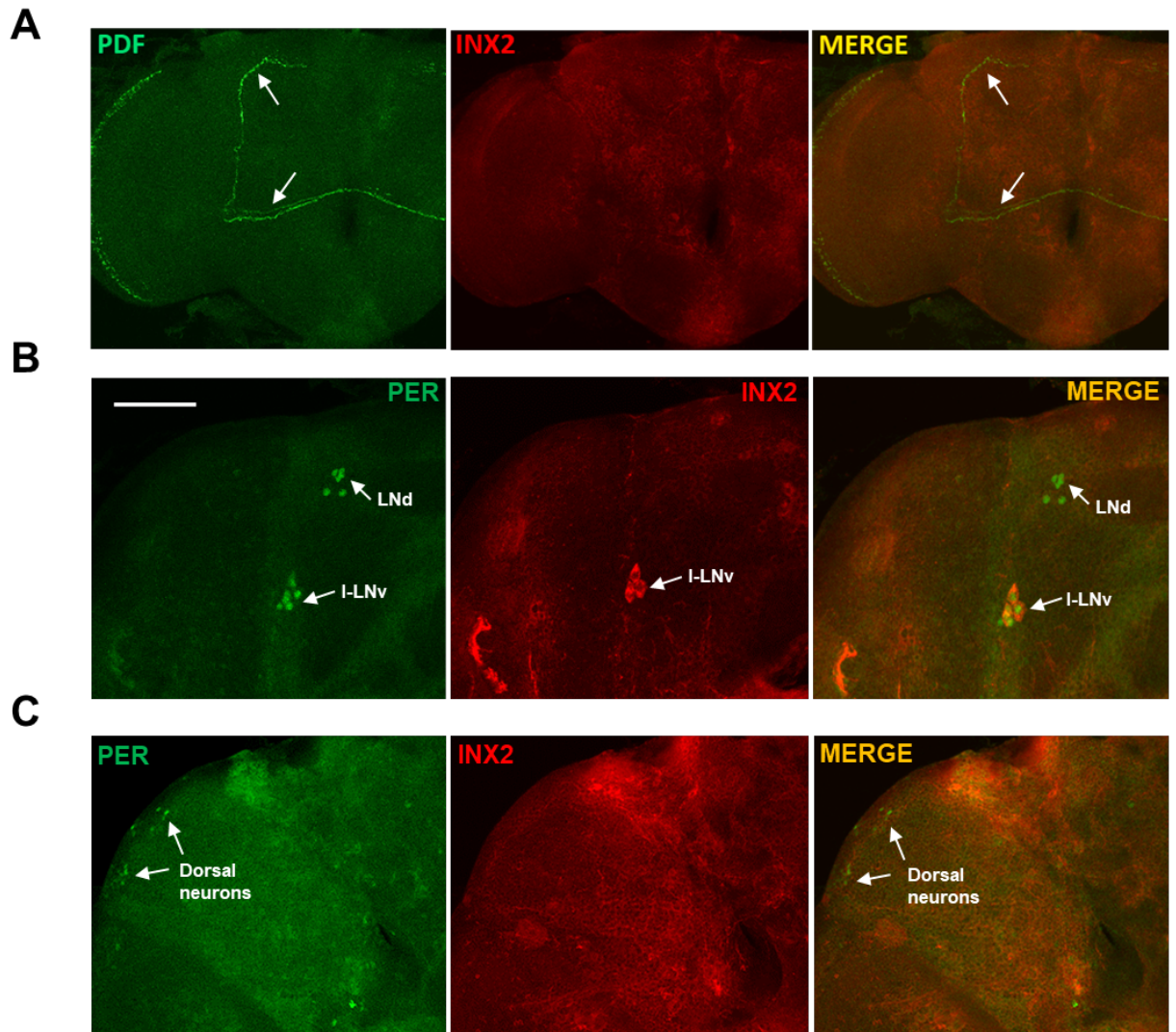
Figure 3.9: Innexin2 is only expressed in the small and large ventral lateral neurons in the circadian pacemaker circuit (A) Representative images of wild-type *Drosophila* adult brains stained with antibodies against neuropeptide PDF and Innexin2. Innexin2 does not co-localize with PDF projections both in the dorsal and contralateral regions. **(B and C)** Representative images from wild-type *Drosophila* adult brains stained with anti-Inx2 antibody and co-stained with anti-PER for identification and co-localization with clock neurons. Inx2 did not co-localize with the LNd (middle panel) or the DN subsets (bottom panel). Brightness and contrast of representative images were adjusted in Fiji to facilitate better visualization. Arrows are used to indicate PDF projections, l-LNv, LNd and DN. Scale-bar represents 55 μm, $n = 8$ brain samples. All dissections were performed at ZT4.

Finally, to eliminate the contribution of Innexin2 in other clock neurons apart from the ventral lateral neurons, I downregulated *Innexin2* expression in all clock neurons except the LNv using *timGal4; pdfGal80* and *Clk856Gal4; pdfGal80*. The efficiency of the *pdfGal80* construct in suppressing Gal4 expression in the ventral lateral neurons was verified via immunohistochemistry using a GFP marker (Fig. 3.10A). *tim; pdfGal80 > Inx2* RNAi flies do not show a significantly lengthened free-running period compared to both the parental controls (Fig. 3.10B left, Table 3.1, Appendix 3.3) and there was no significant change in the power of the rhythm compared to both parental controls (Fig. 3.10B right, Table 3.1, Appendix 3.4). Similarly, *Clk856; pdfGal80 > Inx2* RNAi flies do not have a significantly lengthened free-running period compared to its respective parental control genotypes (Fig. 3.10C, Appendix 3.3), suggesting that Innexin2 functions in the ventral lateral subset among the clock neurons. Thus, taken together, my results from behavioural and immunohistochemistry experiments suggest that Innexin2 protein expressed in the ventral lateral neuronal subsets of the circadian pacemaker circuit is critical for determining the period of free-running rhythms.

The efficiency of the RNAi construct used for knockdown was examined in the s-LNv and l-LNv cells using immunohistochemistry. I find that Innexin2 levels were significantly reduced in the experimental flies in the s-LNv, whereas I could only observe a trend in the case of l-LNv neurons (Fig. 3.11, Appendix 3.7). This could be because of my inability to detect a significant decrease in the levels at this given antibody concentration as Innexin2 levels are much higher in the l-LNv cells. Perhaps, a lower antibody concentration can be used for detecting differences in this case.

A *tim;pdfGal80 > eGFP*, co-localized with PER antibody

GFP — LNd

PER — LNd, l-LNv, s-LNv

GFP PER — LNd, l-LNv, s-LNv

55 µm

B

Period (h)

a   b   a

Power of rhythm

a   ab   b

■ *timGal4; pdfGal80*
■ *dcr; Inx2* RNAi
■ *tim; pdfGal80 > dcr; Inx2* RNAi

C

Period (h)

a   b   a

■ *Clk856Gal4; pdfGal80*
■ *dcr; Inx2* RNAi
■ *Clk856; pdfGal80 > dcr; Inx2* RNAi
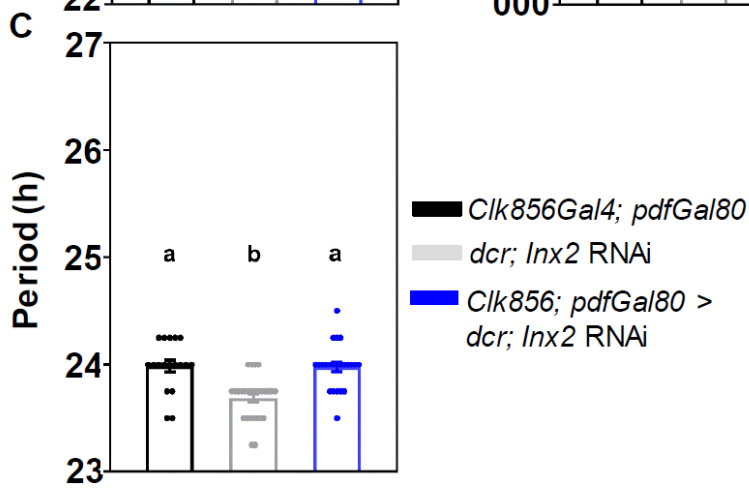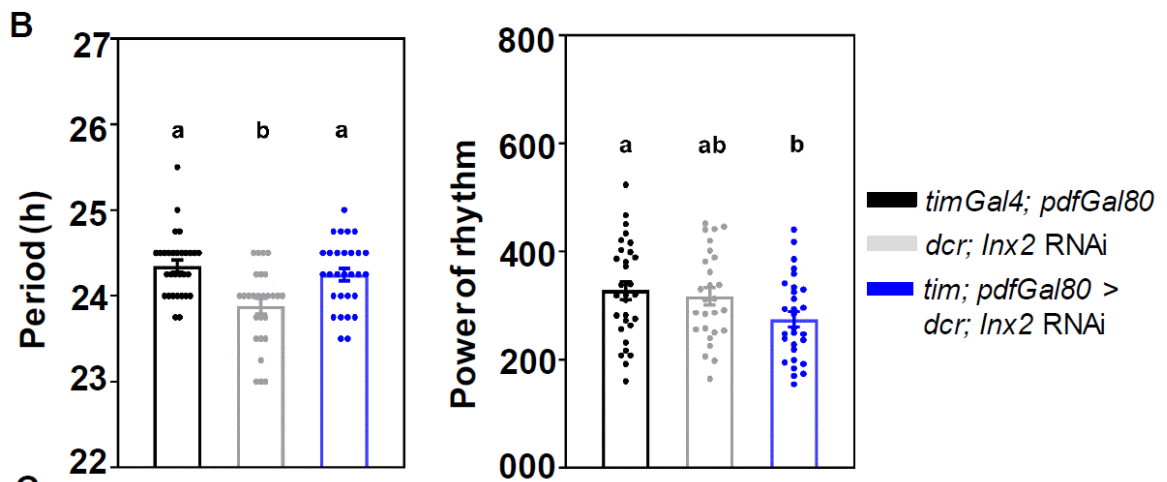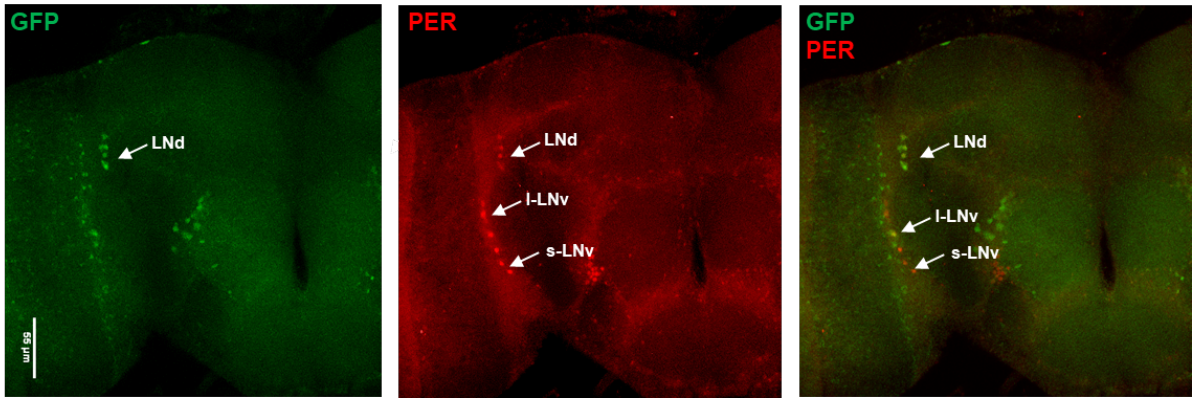
Figure 3.10: Innexin2 functions only in the ventral lateral subsets among the clock neurons (A) The efficiency of *pdfGal80* construct in suppressing Gal4 driven UAS expression was verified by crossing *timGal4*; *pdfGal80* with GFP, dissecting the brains at ZT22 and staining with GFP and PER. Both s-LNv and l-LNv did not show any GFP staining (left), whereas PER staining was observed in all lateral clock neurons (middle). *n=6* brain samples. Scale bars represent 55μm. **(B)** Free-running period (left) and power of rhythm (right) of experimental flies (*tim; pdfGal80 > dcr*; *Inx2* RNAi) (*n=29*) is plotted along with its UAS control (*n=27*) and Gal4 control (*n=30*) flies. **(C)** Free-running period of experimental flies (*Clk856; pdfGal80 > dcr; Inx2* RNAi) (*n=25*) is plotted along with its UAS control (*n=21*) and Gal4 control (*n=20*) genotype.

Error bars are SEM, period values are determined using Chi-square periodogram for a period of 8 days. All comparisons between genotypes are done using one-way ANOVA followed by post-hoc Tukey's HSD test.
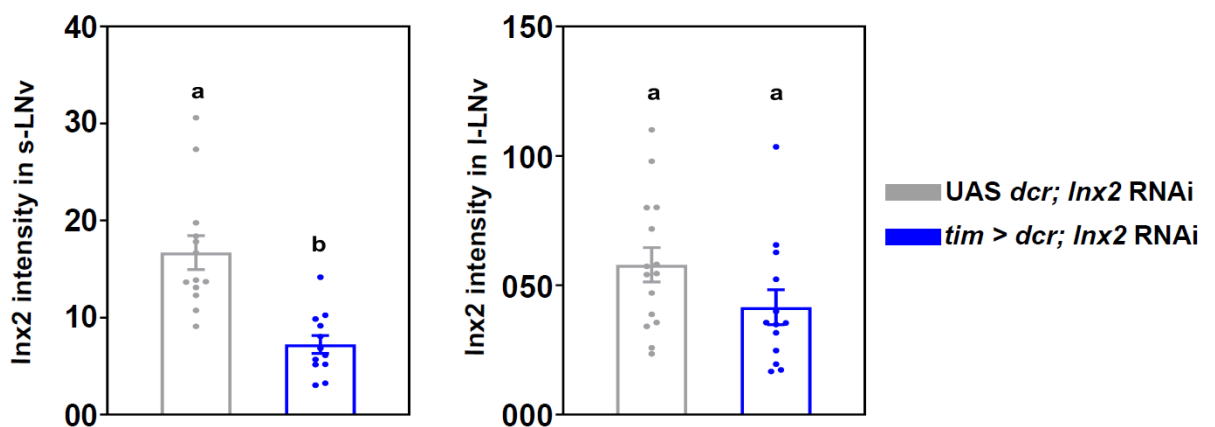
Figure 3.11: Verification of *Innexin2* RNAi construct *Innexin2* RNAi construct was verified by dissecting adult brains of both control (*dcr; Inx2* RNAi) and experimental flies (*tim > dcr; Inx2* RNAi) at ZT12 and staining them with anti-Inx2 antibody. Inx2 intensity was quantified in both s-LNvs and l-LNvs and compared between control and experimental flies. Inx2 levels were significantly lower in s-LNvs (left) in case of experimental flies (*n=12* brains, Mann Whitney U test, *p < 0.001*). In case of l-LNvs, (right) although we see a trend, there was no statistically significant difference in Inx2 intensity between the experimental and control flies. (*n=13* brains, Mann Whitney U test, *p > 0.05*). Error bars are SEM. Statistical comparisons between control and experimental genotypes were performed using the Mann Whitney U test.

3.3.6 Innexin2 protein levels oscillate in the ventral lateral neurons under Light: Dark cycles (LD 25°C).

A previous study shows that *Innexin2* mRNA levels oscillate in the wild-type adult *Drosophila* heads with a peak phase around Zeitgeber time (ZT) 22 - ZT 2, which is absent in *per* null mutants (Zhang et al., 2018), suggesting that the circadian clock plays a role in the oscillation of this gene. Since mRNA was isolated from the whole heads of *Drosophila*, and Innexin2 is abundant in glial cells, it could be possible that this peak phase reflects the peak expression of *Innexin2* transcript in these cells. To determine if Innexin2 protein expression levels oscillate in the ventral lateral clock neurons, I dissected wild-type adult *Drosophila* brains and measured the intensity of Innexin2 protein in both the s-LNv and l-LNv cell types under Light: Dark cycles (LD 25°C) over a 24-hour time period. Innexin2 protein levels show a significant 24-hour oscillation in both the cell types with peak phase at ZT12 around Lights-Off transition (Fig. 3.12 A and B, Appendix 3.8).
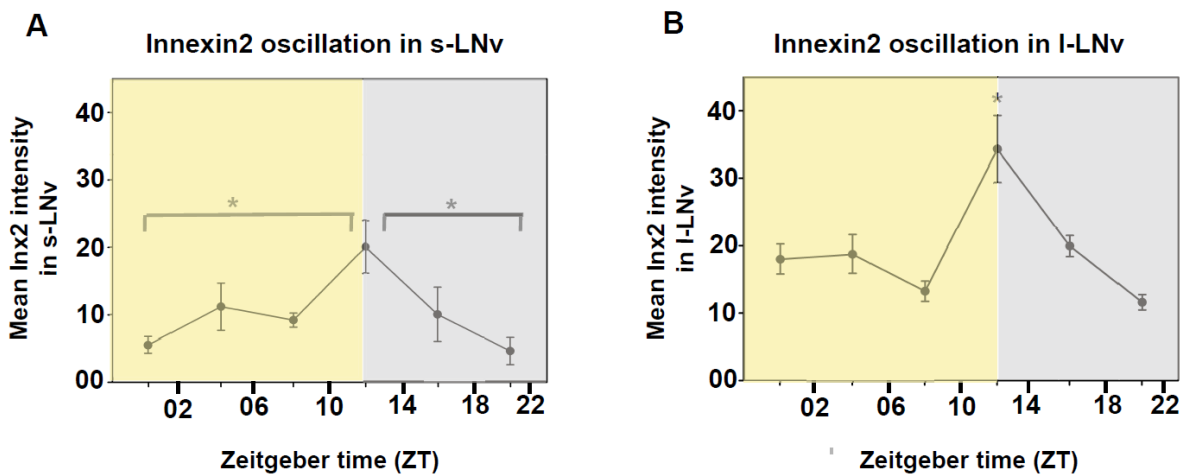
Figure 3.12: Innexin2 protein levels oscillate in the LNv neurons under LD 25°C (A) Plot represents the mean intensity values of Innexin2 protein in s-LNv neurons at 6 timepoints over a 24-hour period under Light: Dark (LD) cycles. Innexin2 oscillates in the s-LNv with a peak at LIGHTS-OFF transition (ZT12). Each point in the plot is obtained by averaging across at least 6-7 brain hemispheres for each timepoint. **(B)** Plot represents the mean intensity values of Innexin2 protein in l-LNv neurons at 6 timepoints over a 24-hour period under Light: Dark (LD) cycles. Innexin2 oscillates in the l-LNv with a peak at LIGHTS-OFF transition (ZT12). Each point in the plot is obtained by averaging across at least 8 brain hemispheres for each timepoint. Asterisks indicate significant effect obtained from one-way ANOVA performed on the log transformed values with timepoint as the main factor, post-hoc Tukey's test *p < 0.05,* error bars are SEM.

3.3.7 Knockdown of *Innexin2* delays the phase of Period (PER) protein oscillation in the circadian clock network.

To examine the mechanism by which Innexin2 influences the period of free-running rhythms in *Drosophila*, I tracked the phase of oscillation of the core molecular clock protein Period (PER) in 6 circadian pacemaker cell clusters over a 24-hour cycle on the third day after introducing both control (*dcr*; *Inx2* RNAi) and experimental (*Clk856 > dcr*; *Inx2* RNAi) flies into constant darkness (DD). Using a COSINOR-based curve-fitting method, (Lee Gierke and Cornelissen, 2016), I found a significant 24-hour rhythm in PER oscillation in s-LNv in the case of both control and experimental flies (Fig. 3.13A, Fig. 3.14A and B, Table 3.2). The phase of PER oscillation in the case of experimental flies was significantly delayed compared to control flies (Fig. 3.13A, Fig. 3.14 A and B, Table 3.2), suggesting that *Innexin2* knockdown results in a delay in the core molecular clock protein oscillation in the s-LNv. The amplitude of oscillation upon *Innexin2* downregulation was not different from the controls (Fig. 3.13B). In the case of l-LNv, I could detect a significant 24-hour period of oscillation for both the control and experimental flies (Fig. 3.13A, Table 3.2). The phase of oscillation was also significantly delayed in experimental flies as compared to controls (Fig. 3.13A). The amplitude of PER oscillation in the l-LNv of experimental flies was not found to be different from the

controls (Fig. 3.13B). However, in control flies, consistent with previous reports, the amplitude of oscillation in the l-LNv was significantly lower than that of the s-LNv (Fig. 3.14C). In the case of 5th s-LNv, I was unable to detect cells at certain timepoints of lower intensities. Hence a COSINOR-based analysis was not performed for this cell type. Nevertheless, a scatter plot of control and experimental intensities is represented (Fig. 3.13A). In the case of LNd, both the control and experimental flies show a significant 24-hour rhythm in PER oscillation (Fig. 3.13A, Table 3.2). The phase of oscillation of PER in experimental flies was significantly delayed compared to controls (Fig. 3.13A). The amplitude of oscillation in LNd was not different between the control and experimental flies (Fig. 3.13B). In the case of DN1, although I could detect a significant 24-hour period in control flies, the amplitude of oscillation was highly dampened (Fig. 3.13A, Fig. 3.14C, Table 3.2). However, DN1 does not show significant rhythmicity in PER oscillation in experimental flies and had overall low amplitude values (Fig. 3.13A, Table 3.2). PER levels in DN2 do not show significant 24-hour rhythmicity and are highly dampened in both control and experimental flies (Fig. 3.13A, Table 3.2).

A

● *dcr; Inx2* RNAi (UAS control)   ● *Clk856 > dcr; Inx2* RNAi

s-LNv   s-LNv   DN1

l-LNv   l-LNv   DN2

LNd   LNd   5th s-LNv

PER intensity (a.u)

Circadian time (hours)

B

Amplitude of PER oscillation (a.u)

■ *dcr; Inx2* RNAi (UAS control)

■ *Clk856 > dcr; Inx2* RNAi

s-LNv   l-LNv   LNd
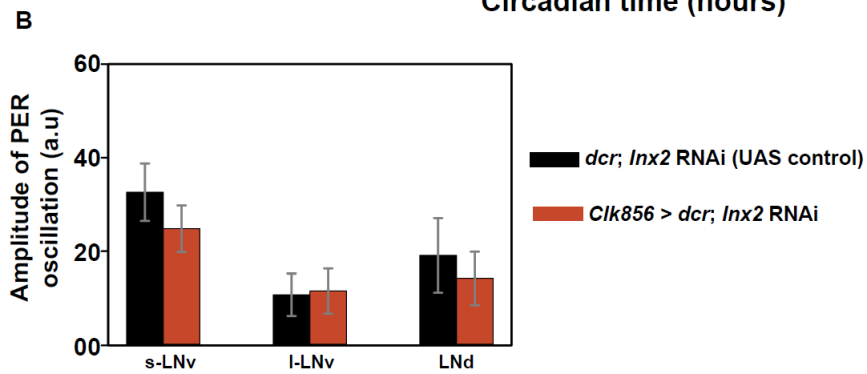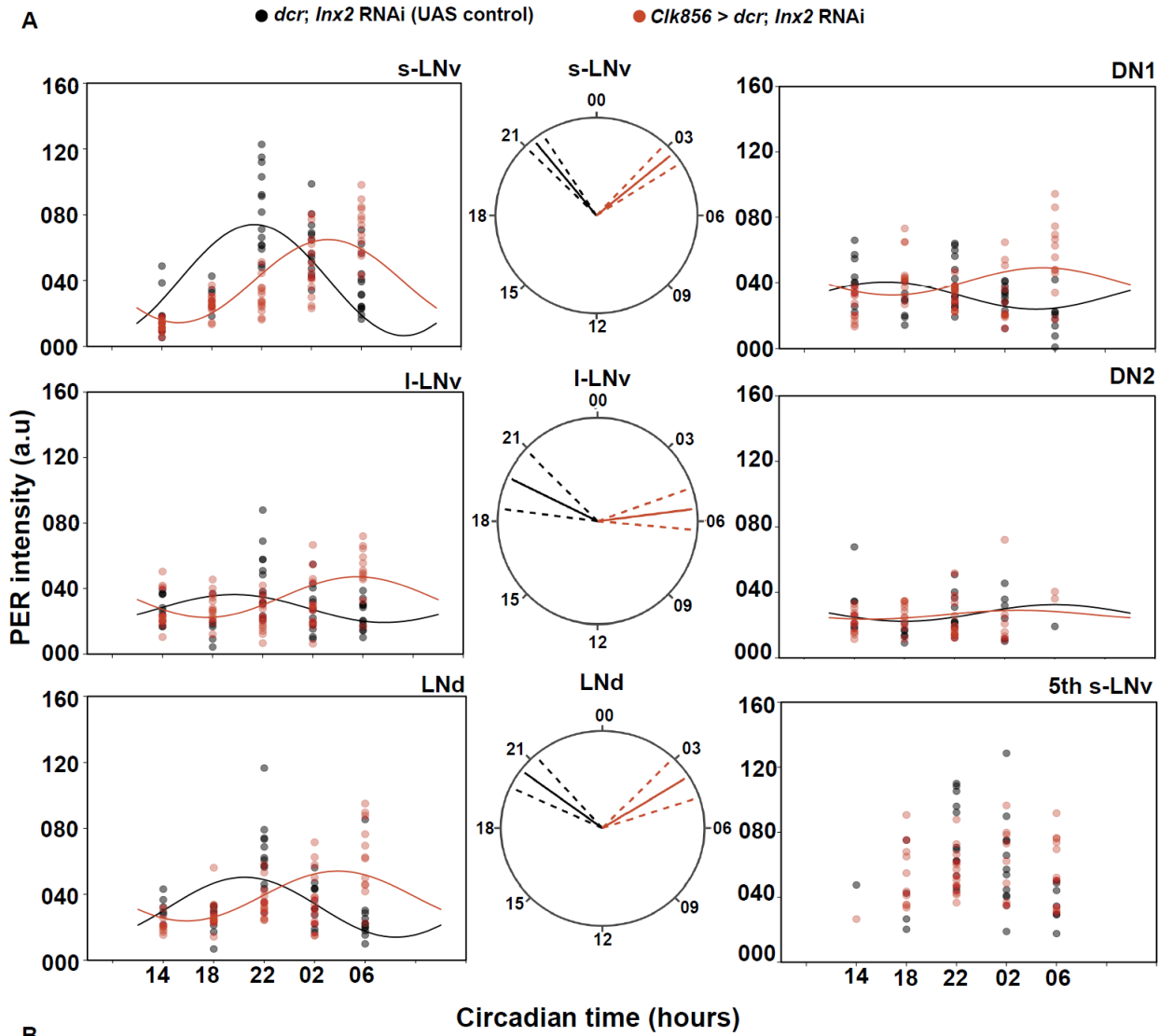
Figure 3.13: Knockdown of *Innexin2* delays the oscillation of PER protein in clock neuronal subsets (A) Scatter plots of PER staining intensities in each of the bilaterally located six distinct neuronal clusters of the circadian pacemaker network of both the control (*dcr*; *Inx2* RNAi) and experimental (*Clk856 > dcr*; *Inx2* RNAi) flies plotted at different time-points over a 24-hour cycle on the third day of DD. Each dot represents the mean PER intensity value averaged over both the hemispheres of one brain. The black and red lines are the best fit COSINE curve from the parameters that were extracted from the COSINOR analysis. Polar-plots are depicting the acrophase of PER oscillation in control (*dcr*; *Inx2* RNAi) (black lines) and experimental flies (*Clk856 > dcr*; *Inx2* RNAi) (red lines) in 3 distinct neuronal clusters of the circadian pacemaker network where both control and experimental genotypes show a significant 24-hour rhythm in COSINOR analysis. The acrophase values obtained after COSINOR curve fitting are shown as solid lines and the error (95% CI values) is depicted as dashed lines around the mean for all the cell types. Non-overlapping error values indicate that phase values of experimental flies are significantly different from controls as seen in the case of s-LNv, l-LNv, and LNd. **(B)** Amplitude values obtained from COSINOR curve fits are plotted for control and experimental flies for those cell groups which show significant 24-hour rhythms (s-LNv, l-LNv and LNd). Error bars are 95% CI values calculated from the standard error obtained from COSINOR analysis. Overlapping error bars indicate that amplitude values of experimental flies are not significantly different from controls, See Table 3.2 for more details. *n* > 7 brain samples both in case of control and experimental flies in most cell types (s-LNv, l-LNv, LNd, DN1) and all time points except for DN2.

A *dcr; Inx2* RNAi (UAS cont.)

CT14 | CT18 | CT22 | CT02 | CT06

B *Clk856 > dcr; Inx2* RNAi

CT14 | CT18 | CT22 | CT02 | CT06

C

UAS *dcr; Inx2* RNAi
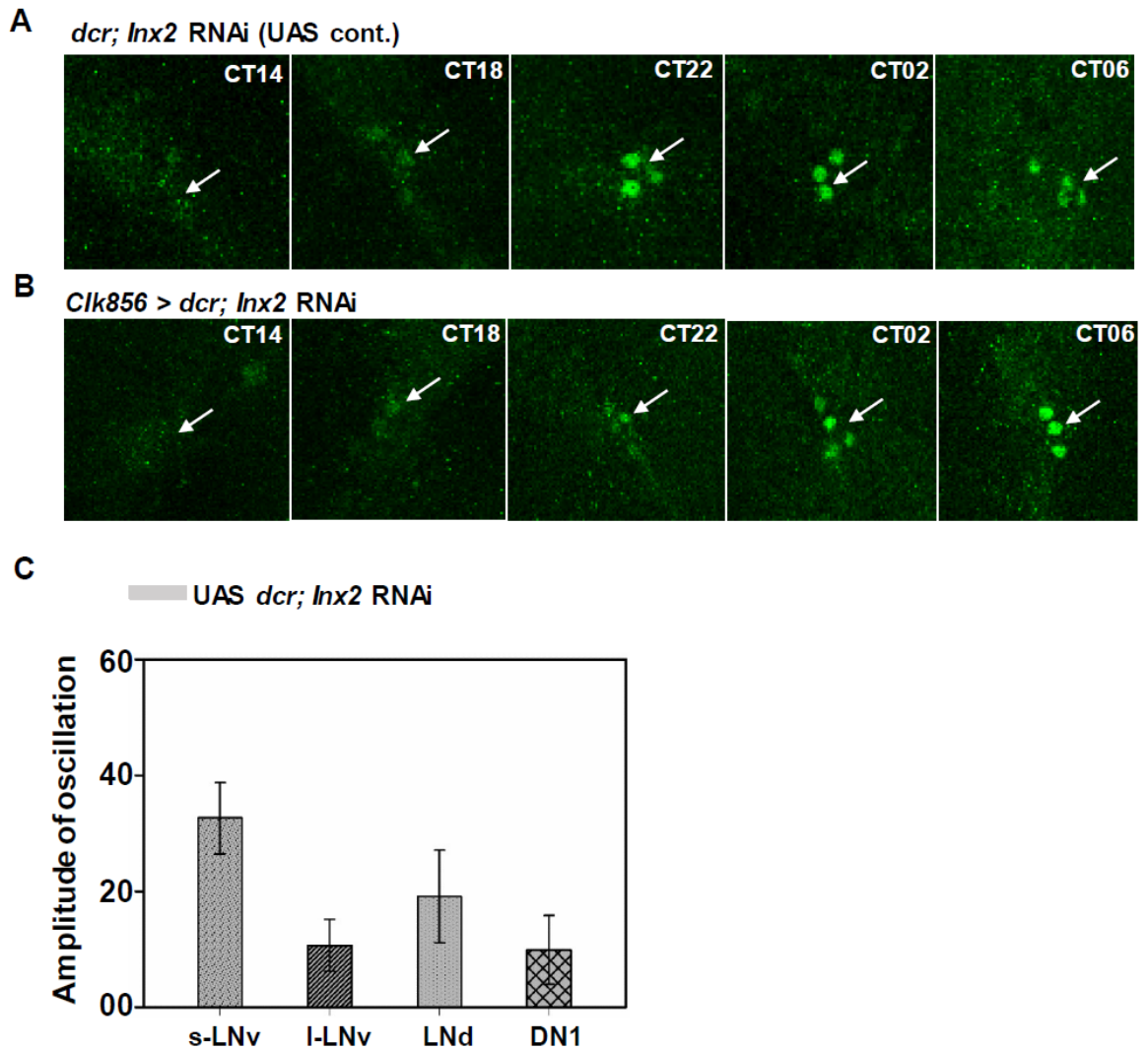
Figure 3.14: Knockdown of *Innexin2* delays the phase of oscillation of PER protein in clock neurons Representative images of PER intensity in s-LNv at five different time points of a 24-hour cycle on the third day of DD 25°C in both control (UAS *dcr Inx2* RNAi) **(A)** and experimental (*Clk856 > dcr;Inx2* RNAi) **(B)** flies. Phase of PER oscillations is delayed in brain samples of experimental flies as compared to the control flies. Scale bar represents 55μm. **(C)** Amplitude values of PER oscillation in circadian neuronal subsets, obtained from COSINOR curve fits are plotted for control (UAS *dcr; Inx2* RNAi) flies. Error bars are 95% CI values calculated from the standard error obtained from COSINOR analysis. Non-overlapping error bars in case of l-LNv, and DN1 compared to s-LNv indicate that these amplitude values are different from s-LNv.

3.3.8 Knockdown of *Innexin2* leads to higher levels of PDF accumulation and higher amplitude of PDF oscillation in the s-LNv dorsal terminals.

Since PDF is an important neuropeptide in the circadian pacemaker circuit for synchronisation of clock neurons and acts as an output signal, I examined whether *Innexin2* knockdown affects the PDF levels or oscillations in the s-LNv dorsal terminal. I found that both control and experimental flies show a robust 24-hour oscillation in PDF levels in the dorsal projections (Fig. 3.15A, Fig. 3.16A, and B, Table 3.2). In contrast to PER oscillation, there was no significant difference in the phase of PDF oscillation in experimental flies compared to the control flies (Fig. 3.15B, Fig. 3.16A and B, Table 3.2). However, I observed that PDF levels and amplitude were significantly higher in experimental flies than the control flies (Fig. 3.15C, Fig.3.15D, Fig. 3.16A and B, Table 3.2), suggesting that Innexin2 levels could possibly affect neuropeptide release from the s-LNv.
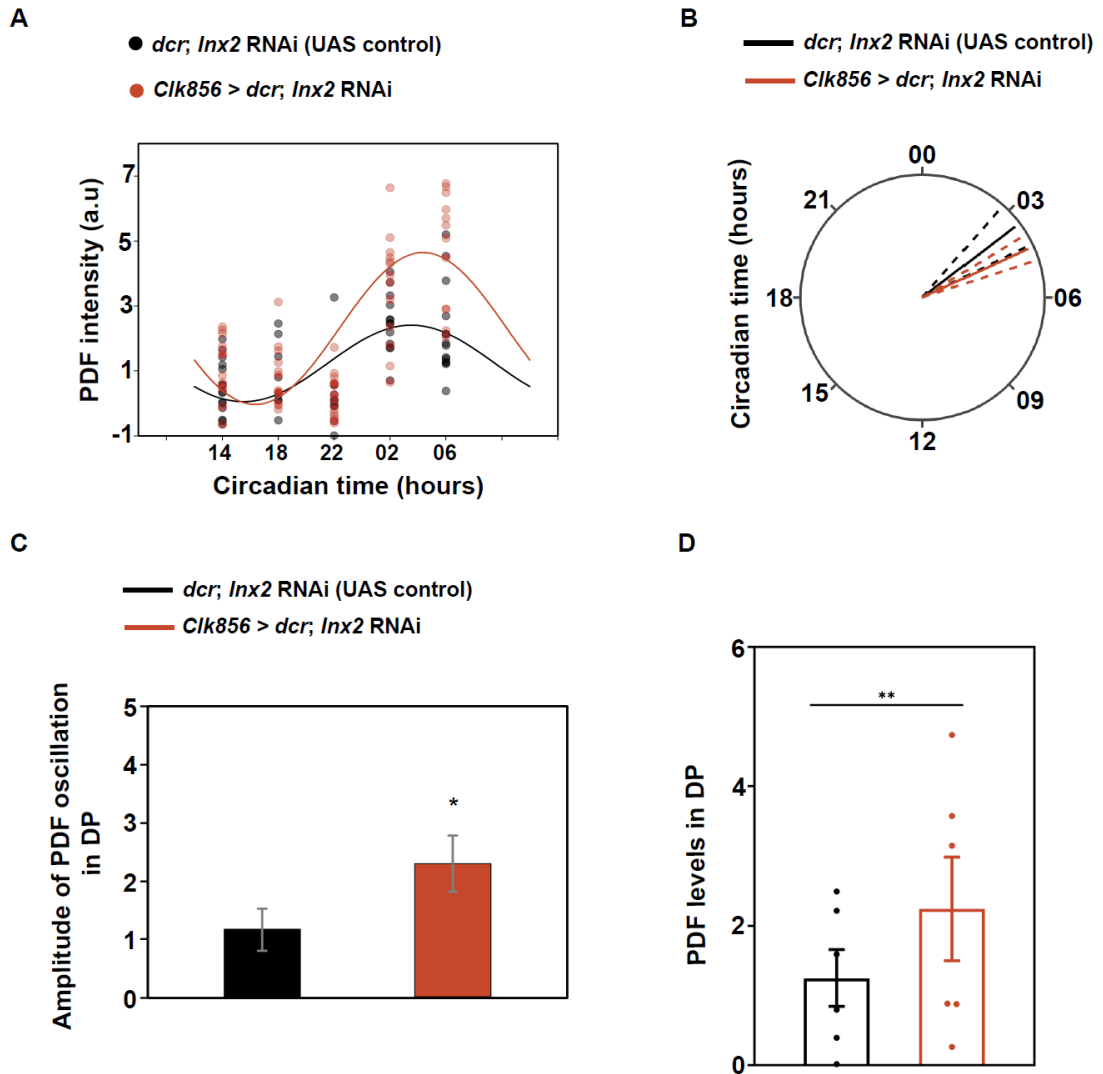
Figure 3.15: *Innexin2* **knockdown affects the amplitude of oscillation and levels of PDF in the s-LNv dorsal projection (A)** Scatter plots of PDF intensity in the s-LNv dorsal projection of both the control (*dcr; Inx2* RNAi) and experimental (*Clk856 > dcr; Inx2* RNAi) flies plotted at different time-points over a 24-hour cycle on the third day of DD. Each dot represents the mean PDF intensity value averaged over both the hemispheres of one brain. The black and red lines are the best-fit COSINE curve from the parameters that were extracted from the COSINOR analysis. **(B)** Polar-plots depicting the acrophase of PDF oscillation in control (*dcr; Inx2* RNAi) and experimental flies (*Clk856 > dcr; Inx2* RNAi). The phase values obtained after COSINOR curve fitting are shown as solid lines and the error values (95% CI) are depicted as dashed lines around the mean. Overlapping error bands indicate that the experimental phases are not significantly different from controls. **(C)** Amplitude values obtained from COSINOR curve fits are plotted for control and experimental flies. Error bars are 95% CI values calculated from the standard error obtained from COSINOR analysis. **(D)** The overall levels of PDF in DP are significantly higher in experimental flies as compared to control flies (Wilcoxon matched pair test, *p = 0.0022*). Each point represents the average value of PDF intensity averaged across brains for each time point. Error bars are SEM. n > 9 brain samples both in case of control and experimental flies for all time points. See Table 3.2 for more details.

A *dcr; Inx2* RNAi (UAS cont.)

CT14 CT18 CT22 CT02 CT06

B *Clk856 > dcr; Inx2* RNAi

CT14 CT18 CT22 CT02 CT06
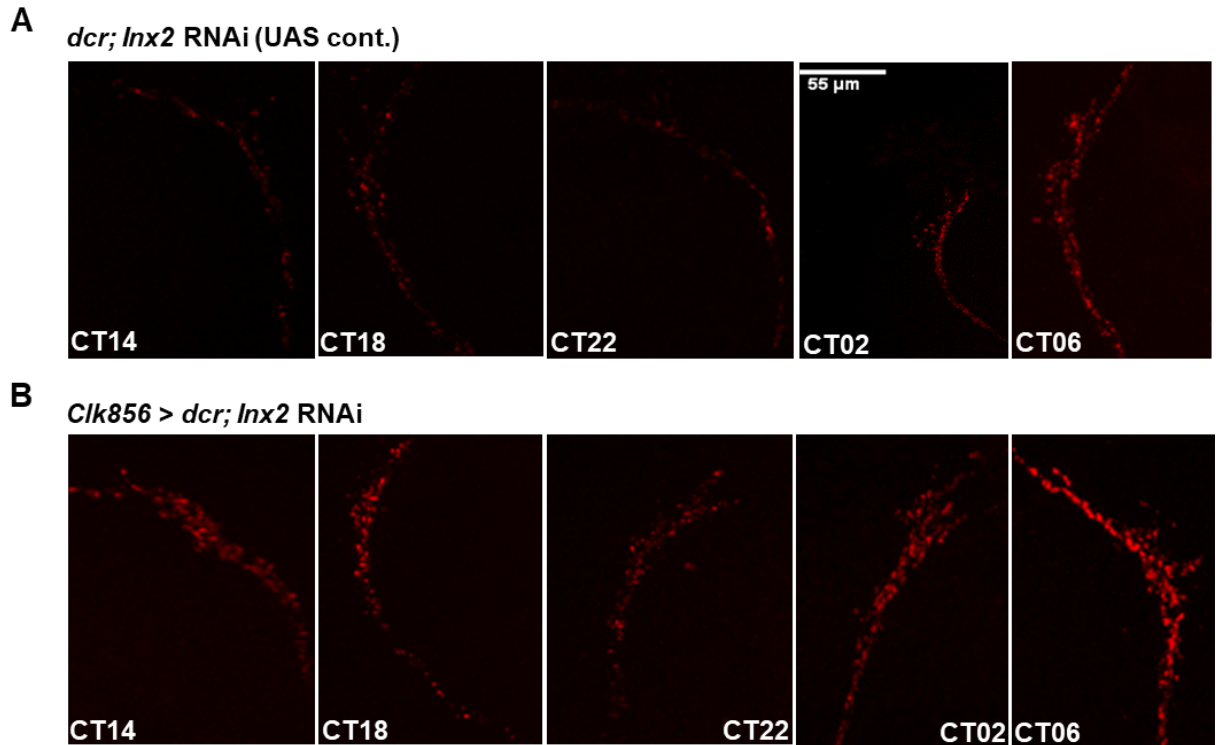
Figure 3.16: Knockdown of *Innexin2* increases the amplitude of PDF cycling in the s-LNv dorsal projections Representative images of PDF intensity in s-LNv dorsal projections at five different time points of a 24-hour cycle on third day of DD 25°C in both control (UAS *dcr;Inx2* RNAi) **(A)** and experimental (*Clk856 > dcr*;*Inx2* RNAi) **(B)** flies. Amplitude of PDF oscillation is higher in experimental flies as compared to control flies. Scale bar represents 55µm.

Cell type	p value	PR	Amplitude ± SE	Phase ± SE
s-LNv (control)	< 0.05	53.7	33.82 ± 4.28	-321.1 ± 6.15
s-LNv (experimental)	< 0.05	62.8	25.3 ± 2.59	-50.12 ± 7.13
l-LNv (control)	< 0.05	11.8	8.52 ± 3.19	-295.46 ± 18.38
l-LNv (experimental)	< 0.05	28.7	12.41 ± 2.64	-82.94 ± 12.05
LNd (control)	< 0.05	23.8	18.16 ± 4.77	-306.69 ± 11.78
LNd (experimental)	< 0.05	32.9	15.11 ± 2.94	-57.67 ± 13.89
DN1 (control)	< 0.05	13.88	8.19 ± 3.01	-247.28 ± 20

DN1 (experimental)	> 0.05	9.88	8.3 ± 3.48	−75.34 ± 25.3
DN2 (control)	> 0.05	3.58	5.07 ± 4.99	−89.82 ± 36.5
DN2 (experimental)	> 0.05	1.94	2.72 ± 3.38	-47.2 ± 67.5
PDF in DP (control)	< 0.05	35.36	1.17 ± 0.2	−52.71 ± 11.39
PDF in DP (experimental)	< 0.05	58.73	2.34 ± 0.25	−65.41 ± 6.63

Table 3.2: Table representing the parameters obtained after fitting a COSINE curve on the PER and PDF intensity data obtained over a 24-hour period for all the circadian neuronal subsets on third day of constant darkness. The parameters represented are *p*-values and percent rhythm (PR) to test for significant 24-hour periodicity, and the amplitude and phase values along with their respective standard errors (SE).

3.3.9 Overexpression of *Innexin2* in clock neurons does not affect the free-running period.

Since knockdown of *Innexin2* in clock neurons lengthens the free-running period, I wanted to examine the effect of overexpression of *Innexin2* in clock neurons. I used a previously verified construct of Innexin2 (*Inx2-GFP*) (Bauer et al., 2004) and overexpressed it in all clock neurons using *timGal4* and *pdfGal4* drivers. Surprisingly, overexpression of *Inx2-GFP* using *timGal4* does not affect the free-running period of experimental flies as compared to both the parental controls (Fig. 3.17A left, Appendix 3.5), and there is no change in the power of rhythm in experimental flies as compared to both the parental control genotypes (Fig. 3.17A right, Appendix 3.6). Similarly, overexpression of *Inx2-GFP* using *pdfGal4* also did not significantly alter the free-running period of experimental flies as compared to both its parental control genotypes (Fig. 3.17B left, Appendix 3.5) and also did not significantly alter the power of rhythm of the experimental flies (Fig. 3.17B right, Appendix 3.6).
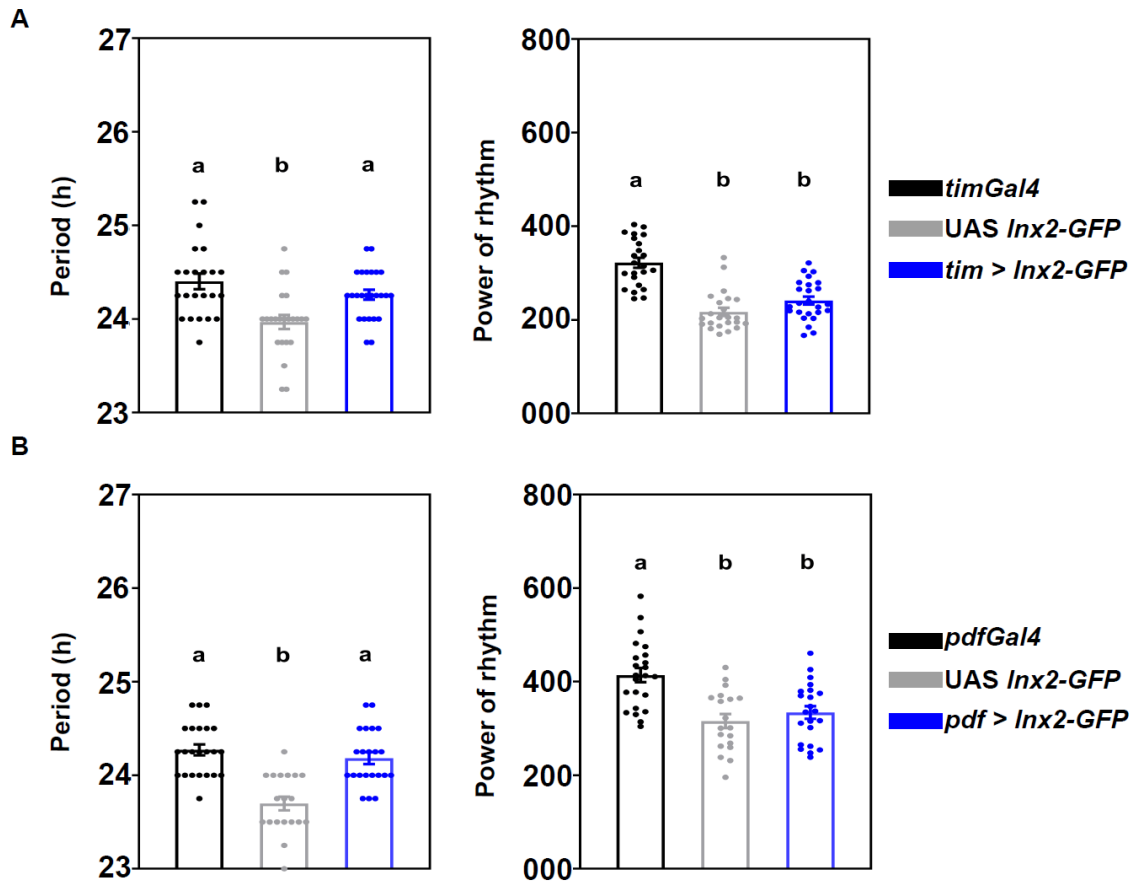
Figure 3.17: Overexpression of *Innexin2* in clock neurons does not affect the free-running period (A) Free-running period (left) and power of rhythm (right) of experimental flies (*tim > Inx2-GFP*) (*n=25*) is plotted along with its Gal4 control (*n=23*) and UAS control (*n=23*) flies **(B)** Free-running period (left) and power of rhythm (right) of experimental flies (*pdf > Inx2-GFP*) (*n=22*) is plotted along with its Gal4 control (*n=23*) and UAS control (*n=20*) flies.

Error bars are SEM, period and power values are determined using Chi-square periodogram for a period of 7 days. All statistical comparisons are performed using one-way ANOVA with genotype as a fixed factor followed by post-hoc Tukey's HSD test.

3.3.10 Innexin2 functions as gap junctions or hemichannels in the ventral lateral neurons

Innexin2, being a gap junction protein, can function in cells either as intercellular channels or hemichannels (Holcroft et al., 2013). Alternatively, many gap junction proteins, including Innexin2, have been shown to have channel-independent functions like cell

adhesion and signalling roles in gene regulation (Dbouk et al., 2009; Elias and Kriegstein, 2008; Richard and Hoch, 2015). To distinguish between these two roles of Innexin2 in clock neurons, I used a previously characterised mutant, where a reporter gene is fused with Innexin2 (UAS *RFP-Inx2*) such that it interferes with the folding of the N-terminal domain, which is essential for channel formation, thus affecting only the channel-based functions of Innexin2 (Nakagawa et al 2010; Spéder and Brand, 2014). Expression of *RFP-Inx2* with *timGal4* lengthens the period of free-running rhythms in experimental flies compared to controls without a significant change in the power of the rhythm (Fig. 3.18A, Table 3.1, Appendix 3.5, and Appendix 3.6). Similarly, expression of *RFP-Inx2* under *pdfGal4* driver also lengthens the free-running period without any change in the power of the rhythm (Fig. 3.18B, Table 3.1, Appendix 3.5, and Appendix 3.6). Taken together, these results suggest that Innexin2 could function as gap junctions or hemichannels in the ventral lateral neurons, and a disruption of its channel-forming domain lengthens the free-running period.
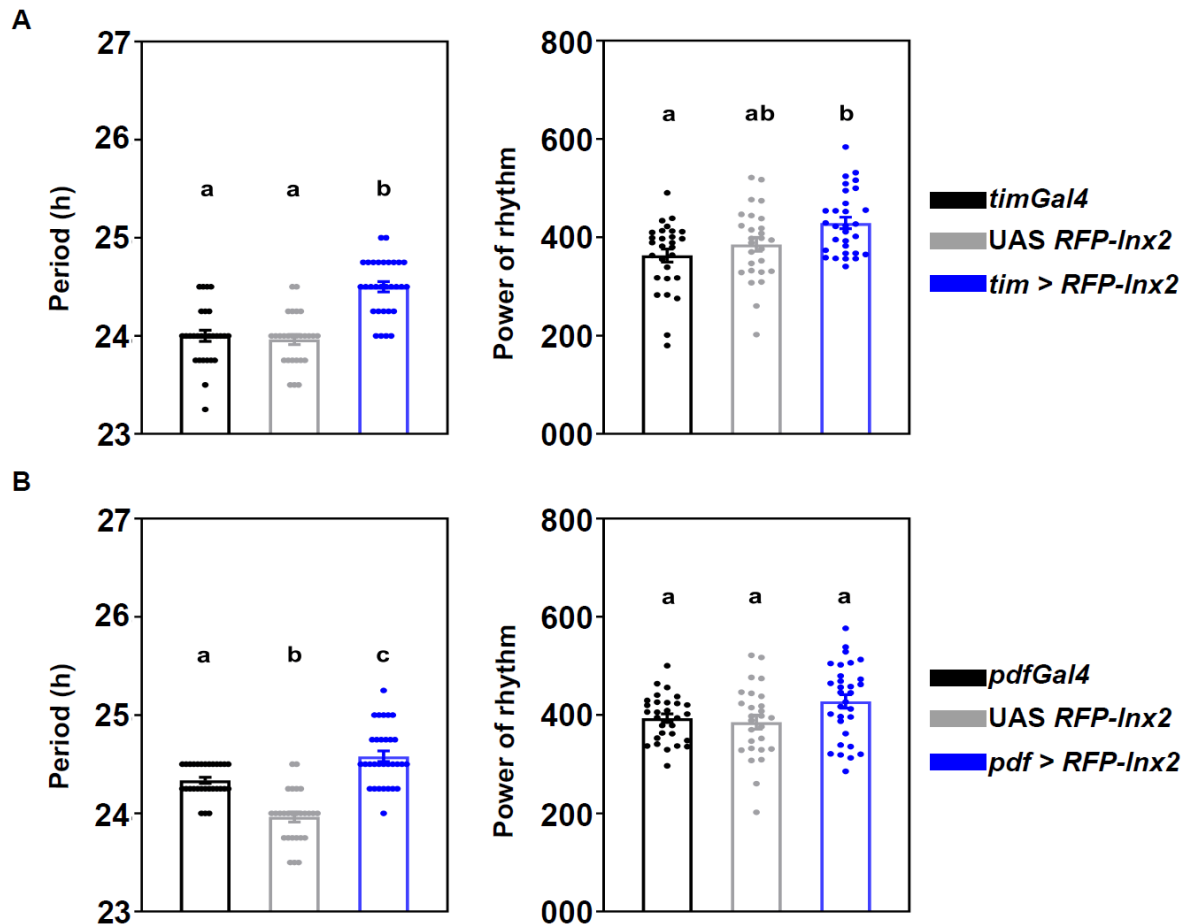
Figure 3.18: Altering the gap junction forming domain of Innexin2 lengthens the free-running period (A) Free-running period (left) and power of rhythm (right) of experimental flies (*tim > RFP-Inx2*) (*n*=30) is plotted along with its Gal4 (*n*=28) and UAS (*n*=27) parental control flies (**(B)** Free-running period (left) and power of rhythm (right) of experimental flies (*pdf > RFP-Inx2*) (*n*=31) is plotted along with its Gal4 (*n*=29) and UAS (*n*=27) parental control flies.

Error bars are SEM, period and power values are determined using Chi-square periodogram for a period of 8 days. All statistical comparisons were made using one-way ANOVA with genotype as a fixed factor followed by post-hoc Tukey's HSD test.

3.4 Discussion

3.4.1 Innexin2 functions in the ventral lateral clock neurons

In this chapter, I show that gap junction protein Innexin2 plays an important role in the

Drosophila circadian pacemaker circuit to influence the period of free-running rhythms.

To shed light on the mechanism of action of Innexin2 in the LNvs, I examined if Innexin2

protein levels oscillate in these cells. My experiments reveal that Innexin2 protein levels oscillate in both s-LNv and l-LNv cell types under Light: Dark cycles with a peak around the Light-Dark transition (ZT 12). However, further experiments are required to comment on the relationship between the levels of Innexin2 in these cells and its role in modulating the free-running period. The first step would be to perform an experiment to find out if Innexin2 levels also cycle under constant darkness (DD) and in core clock mutants like *per* null or *tim* null flies. This will establish if the cycling of Innexin2 is under the control of the circadian clock. There is evidence from previous studies to show reciprocal regulation of membrane properties and core clock protein oscillations. Disruption of membrane firing properties by constitutively expressing ion channels can affect the core circadian clock by either disrupting the oscillations of these proteins (Nitabach et al., 2006, 2002) or by phase-shifting them (Mizrak et al., 2012). Similarly, core clock protein oscillations are required to sustain the rhythm in the clock neurons' membrane firing properties (Cao and Nitabach, 2008; Sheeba et al., 2008b). Since my experiments indicate that a lack of *Innexin2* can phase-shift the molecular clocks in the clock neurons, it would be interesting to see if the absence of a core clock can reciprocally regulate the levels and oscillation of Innexin2. Finally, the peak phase of Innexin2 oscillations happens around the time of lights-Off transition, which coincides with the evening activity of *Drosophila*. In the previous chapter, I observe that a lack of *Innexin2* delays the onset of evening activity (See Chapter 2, Figure 2.5). It would be interesting to examine the relationship between the levels of Innexin2 and its effect on the phasing of the evening activity bout in *Drosophila*.

Apart from their roles in forming gap junctions, Innexin2 can also function as an intercellular signalling molecule in the circadian neurons. Do Innexin2 form gap junctions/ hemichannels in the LNv? From my experiments with the *Innexin2* mutant,

which selectively abolishes channel-based functions (Spéder and Brand, 2014), I can infer that Innexin2 probably works as gap junctions or hemichannels in these cells. However, their other cellular roles cannot be entirely excluded.

3.4.2 Innexin2 functions in the mature, adult circadian circuit to influence the free-running periodicity

Most of the studies which focus on the role of Innexins in *Drosophila* have described it to be essential during development (Güiza et al., 2018); however, in the recent past, several reports have implicated their roles in mature, adult nervous systems to modulate complex behaviours like learning, memory, and sleep (Liu et al., 2016; Troup et al., 2018; Wu et al., 2011). I find that Innexin2 plays a predominant role in the adult circadian circuit to modulate the period of free-running rhythms. I also show that loss of *Innexin2* during development in clock neurons does not affect the free-running period as adults. While previous studies have demonstrated critical roles for Innexin2 in various aspects of nervous system development (Holcroft et al., 2013), my studies do not detect any defects in the pace-making function of clock neurons due to the absence of Innexin2 in most clock neurons during the developmental stages. Interestingly, *Innexin2* knockdown with *dvpdfGal4* (Fig.3.8A) gives a greater period lengthening compared to other drivers. Since the only difference between *dvpdf* and *pdfGal4* driver expression in the adult brain is that the former also targets the LNd neuronal subset (Bahn et al., 2009), I used *LNdGal4* (Bulthuis et al., 2019) to target all 6 LNds, which did not result in significant period lengthening as compared to controls. Furthermore, I do not observe any Innexin2 expression in the LNd neurons. Therefore I speculate that the difference in period lengthening seen here is due to the difference in the strength of RNAi mediated knockdown by the drivers.

3.4.3 Innexin2 phase-shifts the molecular clocks in circadian neurons

I found that, among clock neurons, Innexin2 is present and functions solely in the small and large ventral lateral neuronal subsets. Several previous studies have shown the importance of s-LNv and PDF in the circadian network under constant darkness to generate free-running rhythms of near 24-hour periodicity (Delventhal et al., 2019; Dissel et al., 2014; Grima et al., 2004; Park et al., 2000; Renn et al., 1999; Schlichting et al., 2019; Sheeba et al., 2008c; Stoleru et al., 2004; Yao and Shafer, 2014; Yoshii et al., 2009). Since Innexin2 is present in the s-LNv and influences the free-running period, I investigated the underlying mechanism. As a first step towards the same, I examined the phase of oscillation of molecular clock protein PERIOD on the third day of DD in both control and experimental flies in which *Innexin2* was knocked down in all clock neurons. I found that the phase of the molecular clock is delayed in most clock neurons even though Innexin2 was only found to be present in the LNv. This is similar to what has been observed in the case of *Cx36* mutants in SCN, where lack of *Cx36* affects the period of behavioural rhythms, but does not affect the amplitude or synchrony among molecular clocks in SCN slices (Diemer et al., 2017; Long et al., 2005). The phase of PER oscillations in the case of s-LNv, l-LNv, and LNd cell types in experimental flies were found to be significantly delayed as compared to control flies. Although the amplitude of PER oscillations was not different between the experimental and control flies in each of these cell types, the amplitude of oscillations in l-LNv in control flies was significantly lower than the s-LNv. It has been observed in several previous studies that the amplitude of PER oscillation in l-LNv dampens under constant darkness (Peng et al., 2003; Roberts et al., 2015; Shafer et al., 2002; Yang and Sehgal, 2001), similar to my experiment. In the case of LNd, I find that the molecular clock in *Innexin2* knockdown flies is delayed compared to controls. Although the amplitude of oscillations in LNds in control flies is not significantly different

from s-LNvs, I observe lower amplitude values. This could be because LNd cells are a heterogeneous cell group that are differentially coupled to the s-LNv (Yao and Shafer, 2014) and the low amplitude values could be the result of averaging PER intensity across these different cell types. In the case of DN1, I observe highly dampened rhythms in control flies, similar to previous studies which have reported less robust rhythms, with patterns of dampening amplitude and loss of coherent rhythmicity in DN1 over 6 days in DD (Roberts et al., 2015; Yoshii et al., 2009). Lack of rhythmicity in DN1 in the case of experimental flies could be explained by the fact that these cells receive conflicting signals from s-LNv and LNd with different periodicities (Zhang et al., 2010). In the case of DN2, neither the control nor the experimental flies show significant 24-hour rhythmicity but have highly dampened rhythms. Although PDFR is expressed in DN2, the molecular clock in DN2 was found to be independent of the control of s-LNv and does not seem to have profound effects on rhythmic activity-rest behaviour in DD (Stoleru et al., 2005). Thus, overall our results indicate that Innexin2 influences the free-running period via the molecular clock and reduced Innexin2 levels result in a delay in clock protein oscillations across the circuit.

In my experiments, I also find that apart from the changes in the phase of oscillation of the molecular clock protein Period, the amplitude of oscillation and the levels of the circadian neuropeptide PDF in the s-LNv dorsal projections is significantly higher when *Innexin2* is downregulated. Several previous studies have shown that PDF acts to lengthen the period of the circadian network and that overexpression or ectopic expression of PDF in the dorsal protocerebrum lengthens the period of activity rhythms, leads to desynchronization of activity-rest behaviour and molecular clocks in the circadian neurons (Helfrich-Förster et al., 2000; Shafer and Yao, 2014; Wülbeck et al., 2008). I hypothesize that the knockdown of *Innexin2* phase-shifts the molecular clocks of LNv cells, and this information is then

transmitted to other cells in the network, possibly via PDF. Knockdown of *Innexin2* affects the levels and amplitude of PDF cycling in the s-LNv dorsal terminals, and it is also associated with changes in the phase of downstream neurons. While I speculate that altered PDF cycling in s-LNv results in the changes seen downstream, whether it is causal is yet unknown. An experiment supporting this hypothesis would be to downregulate the expression of Innexin2 in a *pdf/pdfR* null background to examine if there are phase differences in the molecular clock oscillations between the LNv and non-LNv cells.

Chapter 4: Role of Innexin1 in modulating the free-running period of activity-rest rhythms.

4.1 Introduction:

Genetic screens using EMS mutagenesis in the fly *Drosophila melanogaster* identified a locus on the X-chromosome giving rise to multiple lethal and viable alleles of a gene, where the (Cline, 1983; Lipshitz and Kankel, 1985) lethal mutants were unable to survive beyond the third instar larval stages. Most viable alleles showed a defect in the central nervous system, especially in the development of the optic lobes. Optic lobes of mutant animals were drastically reduced in volume. The regular, repeating architecture of the optic lobes characteristic of the wild type was nearly absent; the external and internal chiasmata are missing or highly disarrayed, and a clear division into lamina, medulla, and lobula complex was not detectable; hence the mutant derived its name as *optic ganglion reduced* (*ogre*), now also known as *Innexin1* (Lipshitz and Kankel, 1985). An interesting observation in this study was that the viable mutants of *ogre* showed a developmental delay of about 24 hours from the larval stages till eclosion compared to wild-type flies, suggesting that this locus probably has some role to play in the timing of various stages of development. Molecular analysis of this locus revealed that it encodes a transcript of 2.9kb and a functional protein of 362 amino acids (Watanabe and Kankel, 1990). Characterization of the *ogre* gene locus then led to an investigation of its roles in a multitude of processes during development.

Ogre is required for normal signal transduction from the photoreceptor cells in the retina to the lamina monopolar neurons in the optic lobe. Ogre in the lamina monopolar neurons forms functional heterotypic channels with shakB/Innexin8 in the photoreceptor cells, and this combination is required for proper visual transduction (Curtin et al., 2002) and essential for ON/OFF transients in response to light pulses in electroretinogram (Han et al., 2017). Several studies have also shown *ogre* expression outside the optic lobes and the central nervous system. ogre mRNA and protein expression were detected in the

basolateral domain of ovarian follicle cells, where it forms heteromeric gap junction channels with Innexin3 and is required for intercellular coupling among the follicle cells (Bohrmann and Zimmermann, 2008; Schotthöfer and Bohrmann, 2020). It is also detected in the embryonic ectoderm and, along with Innexin2 and Innexin3, is required for dorsal closure events during embryogenesis (Giuliani et al., 2013). Three independent studies show the importance of heteromeric channels of Inexin1 and 2 in glial cells. Innexin1 and 2 are required in glial cells for proper postembryonic development of the central nervous system, and RNAi-mediated knockdown of these proteins in glia leads to a drastic reduction in the size of the larval CNS (Holcroft et al., 2013). Similarly, gap junctions made up of Innexins 1 and 2 mediate calcium oscillations in glial cells of the blood-brain barrier to reactivate neural stem cells via insulin signalling at the end of embryogenesis, an essential step in the development of CNS (Spéder and Brand, 2014). Likewise, channels made up of Innexin1 and 2 are also required for differentiation of wrapping glial cells in larval stages- an absence of these proteins leads to defects in axonal diameter, conductance velocity and, locomotor behavioural deficits (Kottmeier et al., 2020). Innexin1 is required extensively during development in *Drosophila*, but there are very few reports suggesting a role for this gene in the modulation of adult behaviours. Although *Innexin1* mRNA is expressed in the adult *Drosophila* brain (Liu et al., 2016; Wu et al., 2011), till now, very few of the knockdown screens performed for the downregulation of *Innexins* (Liu et al., 2016; Wu et al., 2011) identify a role for Innexin1 in mediating adult-specific behaviours such as learning and memory. Only one study suggests roles for Innexin1 in adult behaviour in *Drosophila.* This study reports that channels made up of Ogre and ShakB / Innexin8 are required for information transfer between the Johnston's organ neurons and giant fiber neurons to mediate escape response in flies (Pézier et al., 2016). My RNAi knockdown screen identifies *Innexin1* along with *Innexin2* as a potential

candidate for modulating clock properties under free-running conditions (See Chapter 2). Our study will be the first of its kind, which provides evidence for the role of Innexin1 in adult-specific behaviours in *Drosophila*. In this chapter, I will describe in detail the experiments performed to understand the roles played by Innexin1 in modulating the free-running period of activity-rest rhythms.

4.2 Materials and Methods:

4.2.1 Fly lines and rearing conditions:

All genotypes were reared on standard cornmeal medium under LD (12 hr **L**ight: 12 hr **D**ark) cycles and 25°C unless specified otherwise. The following fly lines were used in this study; UAS *Innexin1* RNAi (BL 44048), UAS *Innexin1* RNAi (BL 27283), *ogre KO* (BL 53719), UAS *dicer-2* (II chromosome) (BL 24650), UAS *dicer-2* (III chromosome) (BL 24651), UAS *eGFP* (BL 6874)*,* UAS *tub*Gal80^{ts} (BL 7017), *Clk4.1MGal4* (BL 36316), *Clk4.5FGal4* (BL 37526), *R77H08Gal4* (BL 39981), *R51H05Gal4* (BL 41275), *R64A07Gal4* (BL 39288), *Kurs58Gal4* (BL 80985), *alrmGal4* (BL 67032) were obtained from Bloomington *Drosophila* Stock Centre, Indiana. *NP2222Gal4* (DGRC 112830) and *NP0076Gal4* (DGRC 103516) were obtained from Kyoto Stock Centre. *pdfGal4* and *timGal4* (obtained from Todd Holmes, UC Irvine), *pdfGal4(GS)* (received from Fernanda Ceriani, Leloir Institute Foundation, Argentina), *Clk856Gal4* (provided by Orie Shafer, ASRC, CUNY), *pdf*Gal80 (obtained from Helfrich-Forster, University of Wurzburg), *dvpdfGal4* (obtained from Michael Rosbash, Brandeis University), *LNdGal4* (obtained from Daniel Cavanaugh, Loyola University), *Dilp2Gal4* (provided by Amita Sehgal, University of Pennsylvania), *Mai301Gal4* (provided by Gunter Korge, Freie University of Berlin), UAS *Inx1-GFP* and UAS *GFP-Inx1* (obtained from Andrea Brand, University of Cambridge), UAS *Inx1-myc* and UAS *Inx2-GFP* (provided by Michael Hoch and Reinhard Bauer, University of Bonn).

Refer to Chapter 3 (Materials and Methods, sections 3.2.1 and 3.2.2) for detailed methodology describing the temporal knockdown using the TARGET and gene switch systems.

4.2.2 Locomotor activity rhythm assay and analysis

Please refer to Chapter 3 (Materials and Methods, sections 3.2.3 and 3.2.5.1) for detailed methodology on activity-rest assay set-up and analysis.

4.2.3 Immunohistochemistry

Please refer to Chapter 3 (Materials and Methods, section 3.2.4) for detailed methodology on Immunohistochemistry of Drosophila larval and adult brains. The following primary and secondary antibodies were used,anti-PER (rabbit, 1:20,000, kind gift from Jeffrey Hall, Brandeis University), anti-PDF (mouse, 1:5000, C7, DSHB), anti-GFP (chicken, 1:2000, Invitrogen), anti-repo (mouse, 1:1000, DSHB),goat anti-chicken 488 (1:3000, Invitrogen), goat anti-rabbit 488 (1:3000, Invitrogen), goat anti-mouse 546 (1:3000, Invitrogen), goat anti-mouse 647 (1:3000, Invitrogen).

4.2.4 Image acquisition and analysis

The slides prepared for immunohistochemistry were imaged using confocal microscopy in a Zeiss LSM880 microscope with 20X, 40X (oil immersion), or 63X (oil immersion) objectives. Image analysis was performed using Fiji software (Schindelin et al., 2012). In the samples, ventral lateral clock neurons were classified based on their size and anatomical locations. PER intensity in these neurons was measured by selecting the slice of the Z-stack, which shows maximum intensity, drawing a Region of Interest (ROI) around the cells, and measuring their intensities. 3-6 different background values were measured around each cell, and the final intensity was taken as the difference between the cell intensity and the background. For PDF quantification in the dorsal projections, a

rectangular box was drawn as ROI starting from the point where the PDF projection turns into the dorsal brain, and intensity was measured. 3-6 background values were also measured around the projection. The intensity values obtained from both the hemispheres for each cell type for each brain were averaged and used for statistical analysis. A non-parametric method called RAIN (Rhythmicity Analysis Incorporating Non-parametric methods) (Thaben and Westermark, 2014) was used to test for rhythmicity and extract phase information from the underlying waveforms in both the experiments involving PER and PDF cycling. RAIN package was implemented using R studio.

4.2.5 Western blotting

4.2.5.1 Protein extraction

Adult flies of both control (w^{1118}) and *Innexin1* mutant flies (*ogre KO*; BL 53719) were entrained to light: dark cycles (LD 12:12) for 4-5 days. Thirty flies (males and females) of each genotype were frozen at ZT12 and used for extraction. For decapitation, the frozen flies were subjected to liquid nitrogen and vigorous vortexing, thrice for 15secs each. Whole heads were then transferred to Eppendorf tubes and kept on ice. 30µl of extraction buffer (20 mM HEPES, pH 7.5, 100mM KCl, 5% glycerol, 10mM EDTA, 0.1% Triton, 1mM dithiothreitol, and protease inhibitor cocktail (0.5mM phenylmethylsulfonyl fluoride, 20 mg/mL aprotinin, 5 mg/mL leupeptin, 5mg/mL pepstatin A) was added to each Eppendorf tube. The heads were ground three times for 30 seconds each using a homogenizer, followed by centrifugation at 12000 rpm for 10 minutes at 4ºC. After centrifugation, the supernatant was transferred to a fresh tube and stored at -80 ºC.

4.2.5.2 SDS-PAGE and Western blotting

The total protein concentration in the cell lysate was estimated using the bicinchoninic acid (BCA) assay. 50µg of protein were boiled in 6X SDS loading dye for 5 minutes and

loaded and resolved in 12% SDS-polyacrylamide gel. The proteins were then transferred onto a nitrocellulose membrane (GE Healthcare, USA) using a semi-dry transfer apparatus (Amersham biosciences, UK) at 20V for 1 hour. The blot was washed with 1X PBS and then kept in the blocking solution (5% skim milk in 1X PBS) overnight at 4°C with constant shaking. It was then incubated overnight in the primary Ab solution (anti-Innexin1 antisera obtained from immunization of 4 different mice, M1 (2nd bleed), M2-M4 (4th bleed) at 1:500 concentration) at 4°C, followed by washes with 0.1 % PBST twice for 10 minutes each. The blot was then incubated in a secondary antibody solution conjugated with HRP substrate (1:5000 dilution) for 4 hours at 4°C. The blot was again washed with 0.1 % PBST twice for 10 minutes each. The protein bands were detected using enhanced chemiluminescence substrate (West pico, Pierce, USA).

4.2.7 Peptide synthesis and immunization of mice for anti-Innexin1 Ab production

A polyclonal, peptide-based antibody against Innexin1 protein was raised *de novo* in collaboration with Dr.Rajeshwari, Bioklone Biotech Pvt. Limited. Since most *Drosophila* Innexin proteins share very similar structures, a unique peptide sequence of 31-mer **(REEKEAKRDALLDYLIKHVKRHKLYAIRYWA)** in the cytoplasmic loop of Innexin1 protein was chosen as a unique epitope for raising an antibody. The 31-mer peptide was coupled to ovalbumin using glutaraldehyde. Two hundred micrograms of the peptide-ovalbumin conjugate in aluminium phosphate were administered intraperitoneally into six-week-old female BALB/c mice. The mice were boosted at an interval of two weeks. A total of ten injections were given to the mice. Bleeds were collected on the tenth day after the boosters, and the antisera were used for immunostaining.

4.3 Results

4.3.1 Knockdown of *Innexin1* in all clock neurons lengthens the free-running period.

Our genetic knockdown screen of *Innexins* in all clock neurons identifies *Innexin1* as a potential candidate in regulating free-running period of activity-rest rhythms (Fig. 2.1). Next, I used a narrower driver (*Clk856Gal4,* (Gummadova et al., 2009) to downregulate the expression of *Innexin1*. Knockdown of *Innexin1* using *Clk856Gal4* also lengthens the free-running period as compared to both its parental controls (Fig. 4.1A, Fig. 4.1C, Table 4.1, Appendix 4.1) with no change in power of rhythms (Fig. 4.1B, Fig. 4.1C, Table 4.1, Appendix 4.2), suggesting that Innexin1 in clock neurons are essential to determine the free-running period with no effect on activity consolidation. To avoid the confounding factor of positional effect of transgene insertion on the period lengthening phenotype observed, I used an alternate RNAi construct (BL 27283) which targets a different sequence of the *Innexin1* transcript to downregulate its expression in all clock neurons. Knockdown of *Innexin1* using this alternate construct in all clock neurons also lengthened the free-running period similar to the previous construct used, with no change in power of rhythms, suggesting that the period lengthening observed was not due to off-target effects (Fig. 4.2A and B). Additionally, I also used a previously characterized mutant of *Innexin1* (*ogre KO*; (Giuliani et al., 2013) to verify the phenotype obtained using the RNAi method. *ogre KO* flies show a lengthened period of free-running rhythms compared to its background control (Fig. 4.2C). In this case, however, I observe that the power of rhythm of mutant flies is slightly but significantly lower than the control flies (Fig. 4.2D).

Figure 4.1: Knockdown of *Innexin1* in all clock neurons lengthens the free-running period Free-running period **(A)** and power of rhythm **(B)** of experimental flies (*Clk856 > dcr; Inx1* RNAi) (*n=24*) is plotted along with its Gal4 (*n=29*) and UAS control (*n=26*) genotypes **(C)** Representative double-plotted actograms of individual flies of each indicated genotype under constant darkness.

Error bars are SEM, period and power values are determined using Chi-square periodogram for a period of 7 days, all statistical comparisons are performed using one-way ANOVA with genotype as a fixed factor followed by post-hoc Tukey's HSD test. Data representative from 3 independent experiments. See Table 4.1 for more details.
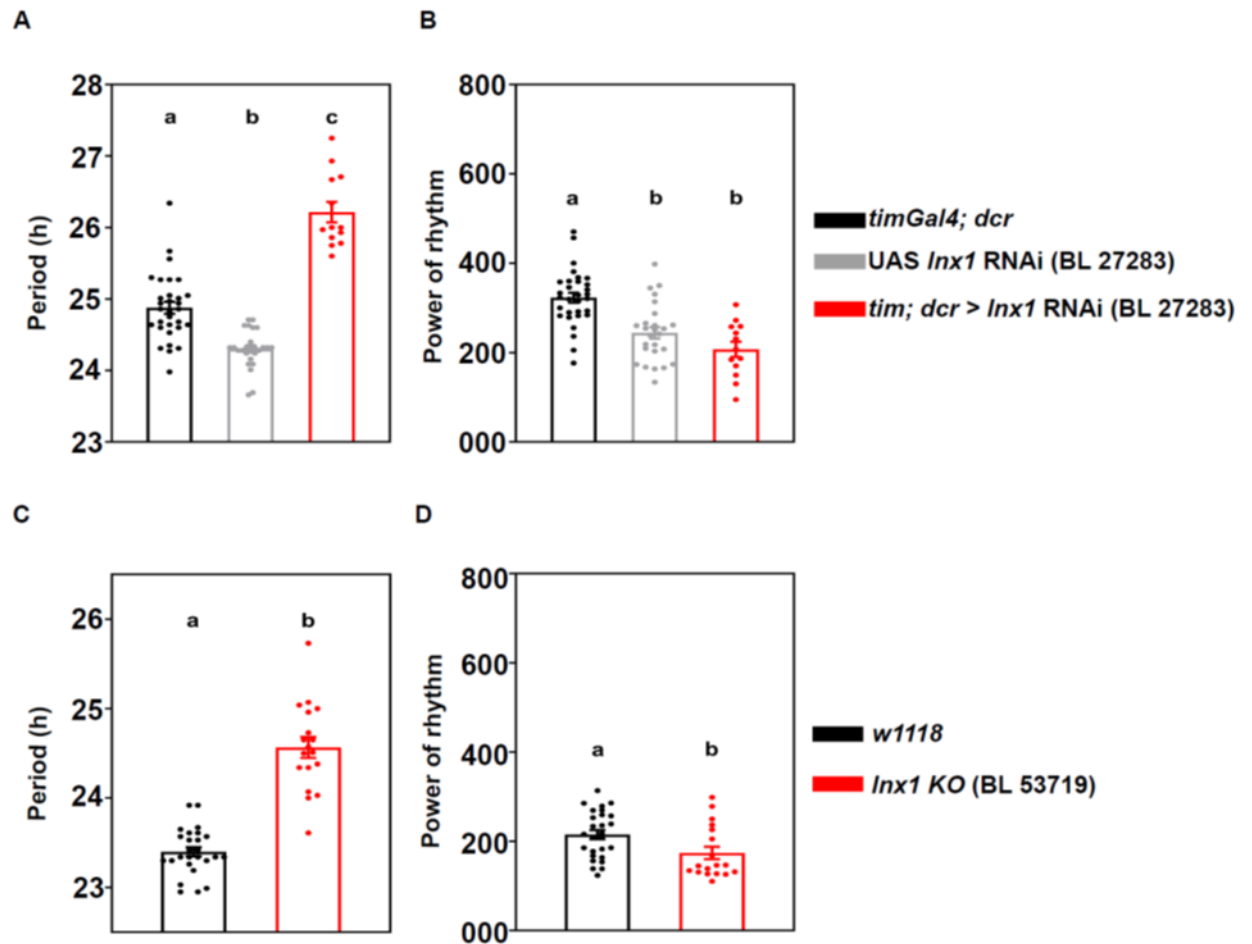
Figure 4.2: Knockdown of *Innexin1* using alternate constructs lengthens the free-running period Free-running period **(A)** and power of rhythm **(B)** of experimental flies (*tim; dcr > Inx1* RNAi) (*n=16*) using an alternate construct (BL 27283) is significantly plotted along with its Gal4 control (*n=25*) and UAS control (*n=26*) flies. Free-running period **(C)** and power of rhythm **(D)** of *Innexin1* mutant flies (BL 53719) (*n=18*) is plotted along with its background control flies (*n=27*).

Error bars are SEM, period and power values are determined using Chi-square periodogram for a period of 7 days, all statistical comparisons are performed using one-way ANOVA with genotype as a fixed factor followed by post-hoc Tukey's HSD test.

4.3.2 Development and adult-specific knockdown of *Innexin1* in the circadian circuit lengthens the free-running period.

Innexin1 is extensively involved in several processes during development in *Drosophila,* including central nervous system development (Curtin et al., 2002; Güiza et al., 2018;

Hasegawa and Turnbull, 2014; Holcroft et al., 2013; Lipshitz and Kankel, 1985). To distinguish between the developmental versus adult-specific roles of Innexin1 in modulating free-running period, I did a stage-specific knockdown of *Innexin1* in clock neurons using the TARGET system (McGuire et al., 2004); (see Chapter 3 for detailed methodology and verification of the efficiency of *tubGal80^{ts}*) and examined its effect on the free-running period. Knockdown of *Innexin1* in all clock neurons using *timGal4* only in the adult stages led to lengthening of the free-running period of experimental flies as compared to both the parental genotypes (Fig. 4.3A, Fig. 4.3C, Table 4.1, Appendix 4.1), suggesting that Innexin1 plays a role in the mature, adult circuit to determine the period of free-running rhythms. Although the power of rhythms of experimental flies was significantly different from both the parental control genotypes, it was higher than the driver control while being lower than the UAS parental control, thus suggesting that downregulating *Innexin1* in adult stages does not particularly affect the power of rhythms (Fig. 4.3B, Fig. 4.3C, Table 4.1, and Appendix 4.2). As a complementary experiment, I also restricted the knockdown of *Innexin1* to the developmental stages using the TARGET system by rearing the flies at a restrictive temperature of 29°C and assaying them at a permissive temperature of 19°C and examined the free-running period as adults. Similar to the adult-restricted manipulation, knockdown of *Innexin1* expression only during the developmental stages also lengthened the free-running period (Fig. 4.4A, Fig. 4.4C, Table 4.1, Appendix 4.1), suggesting that Innexin1 is required in the cells targeted by *timGal4* even during the developmental stages, the absence of which possibly affects the speed of the clock in these cells during the adult stages. The power of rhythm, in this case, was not different between the experimental and control flies (Fig. 4.4B, Fig. 4.4C, Table 4.1, and Appendix 4.2).
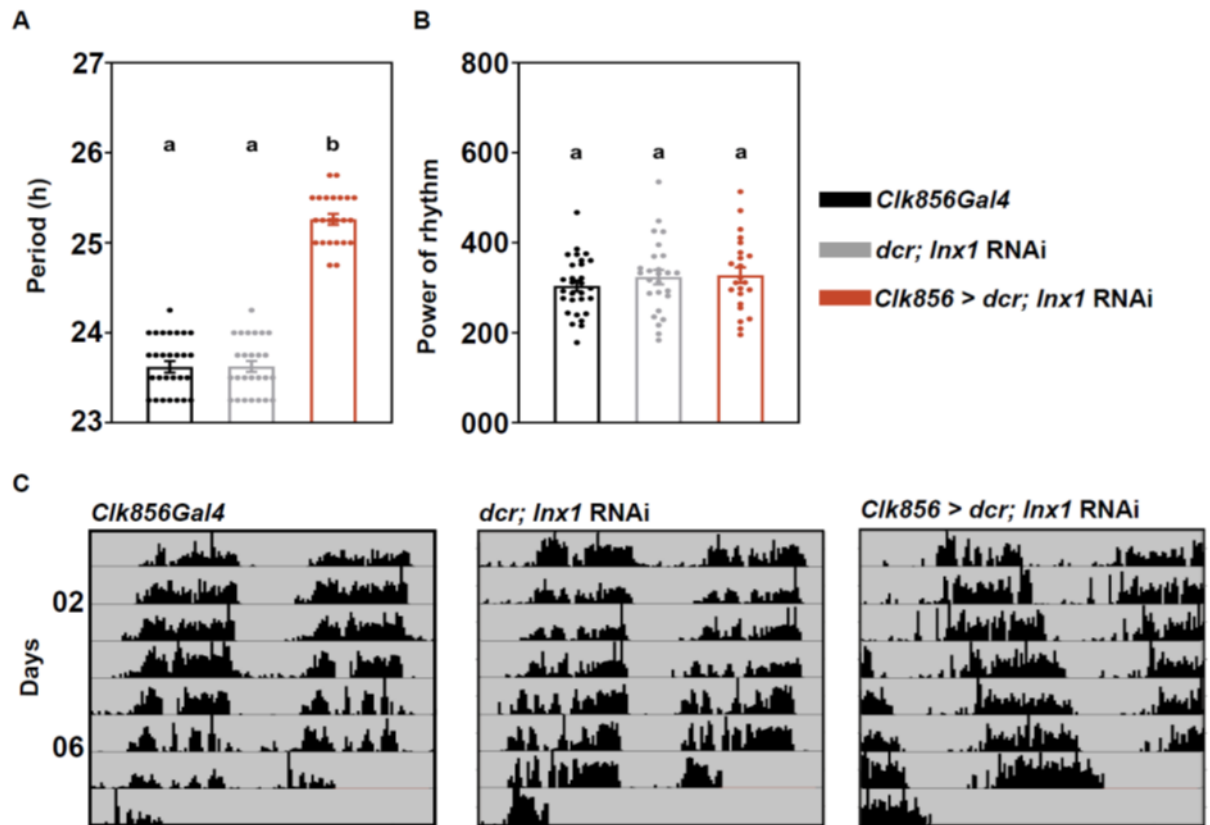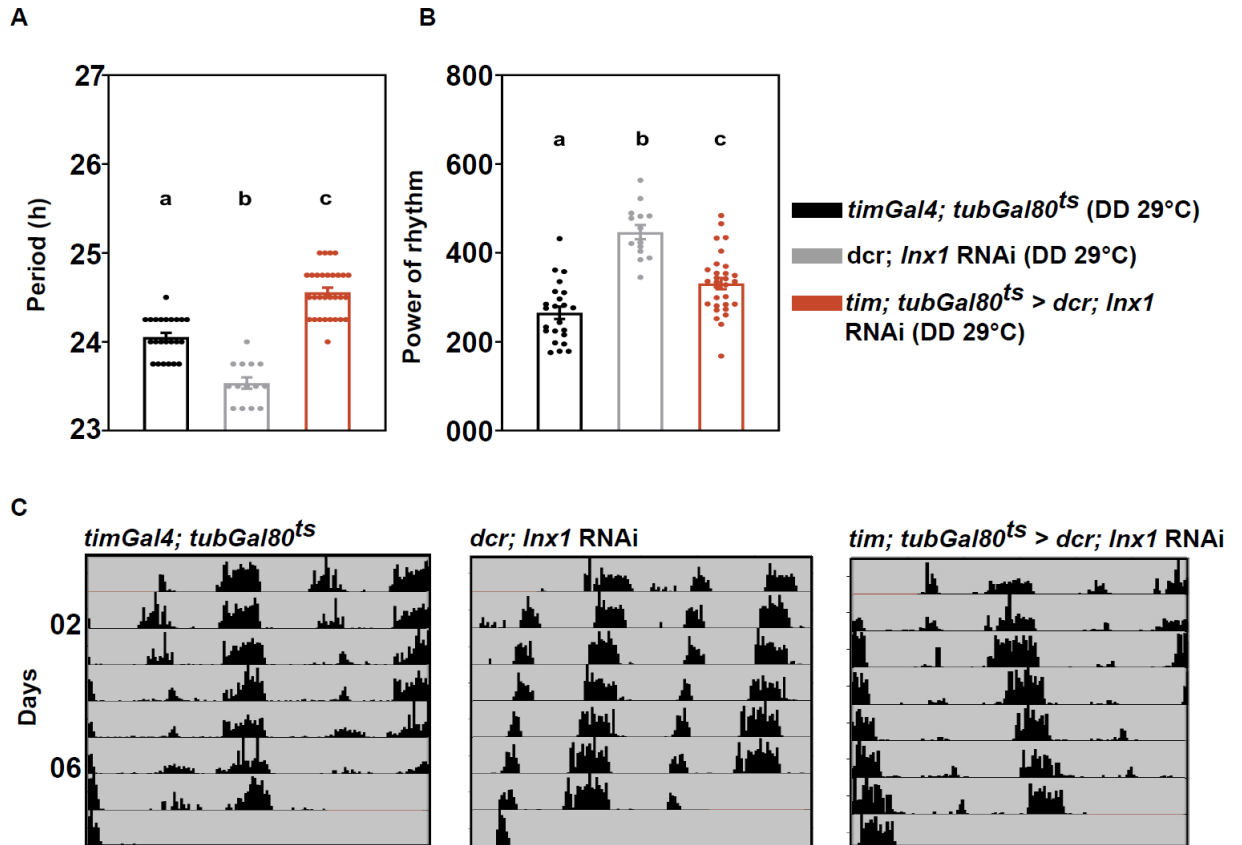
Figure 4.3: Adult-specific knockdown of *Innexin1* in clock neurons lengthens the free-running period Free-running period **(A)** and power of rhythm **(B)** of experimental flies (*tim; tubGal80ts > dcr ;Inx1 RNAi*) (*n=30*) is plotted along with its Gal4 control (*n=23*) and UAS control (*n=24*) flies **(C)** Representative double-plotted actograms of individual flies of each indicated genotype under constant darkness..

Error bars are SEM, period and power values are determined using Chi-square periodogram for a period of 7 days, all statistical comparisons were performed using one-way ANOVA with genotype as a fixed factor followed by post-hoc Tukey's HSD test. Data representative from 3 independent experiments. See Table 4.1 for more details.
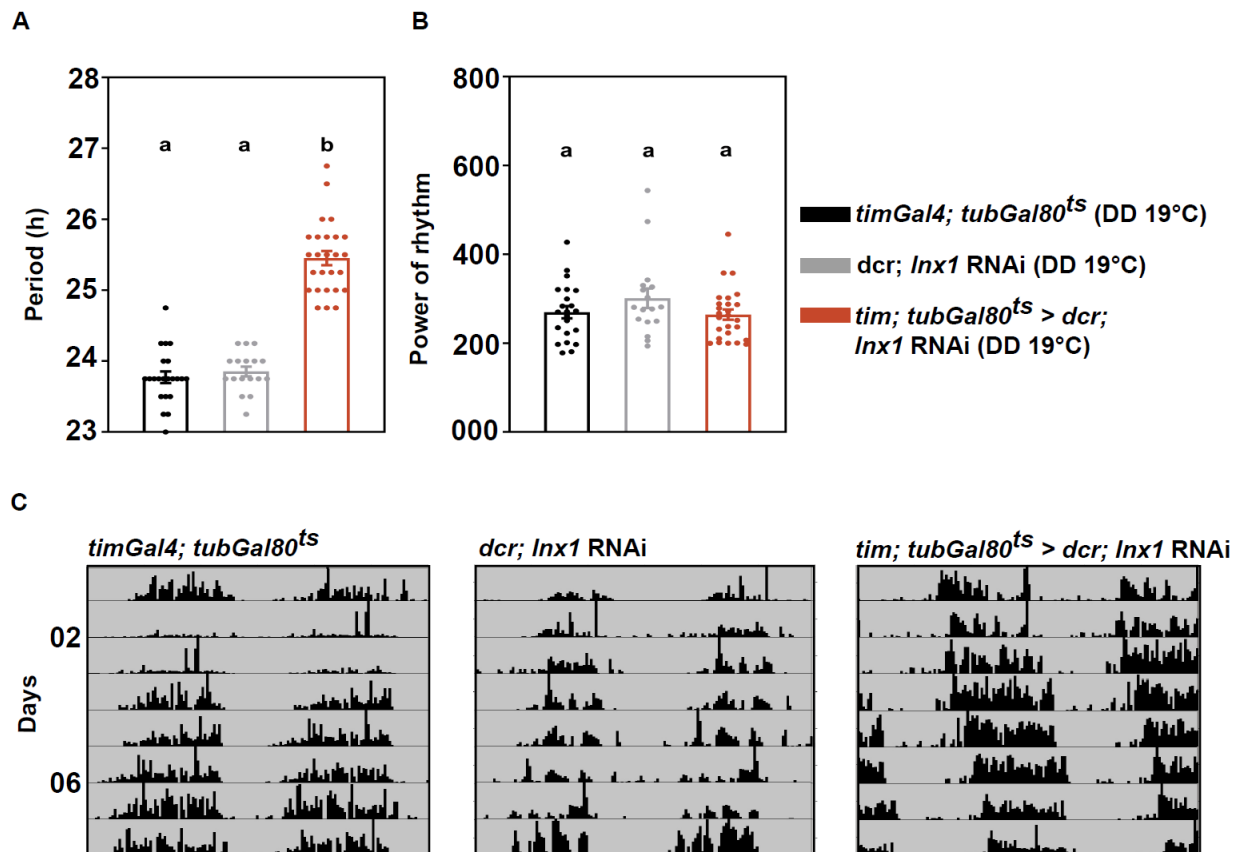
Figure 4.4: Development-specific knockdown of *Innexin1* in clock neurons lengthens the free-running period Free-running period **(A)** and power of rhythm **(B)** of experimental flies (*tim; tubGal80ts > dcr; Inx1 RNAi*) (*n=26*) is plotted along with its Gal4 control (*n=22*) and UAS control (*n=18*) flies **(C)** Representative double-plotted actograms of individual flies of each indicated genotype under constant darkness.

Error bars are SEM, period and power values are determined using Chi-square periodogram for a period of 7 days, all statistical comparisons are performed using one-way ANOVA with genotype as a fixed factor followed by post-hoc Tukey's HSD test. Data representative from 2 independent experiments. See Table 4.1 for more details.

4.3.3 Adult-specific knockdown of *Innexin1* in the ventral lateral neurons using the gene-switch system.

Additionally, as an alternate to the TARGET system for temporal control of gene expression, I have also used the inducible Gal4 system (Gene Switch system; (Osterwalder et al., 2001) to downregulate *Innexin1* expression only in the adult stages (methodology

described in detail in the Materials and Methods section of Chapter 3). I downregulated *Innexin1* expression in the ventral lateral neurons in the adult stages using the *pdfGal4(GS)* driver, which has been verified in several previous reports (Depetris-Chauvin et al., 2011; Fernandez-Chiappe et al., 2020; Herrero et al., 2020). No significant lengthening of the free-running period was obtained in experimental flies compared to control flies when these flies were transferred after eclosion to food containing the vehicle (80% ethanol) (Fig. 4.5A, Appendix 4.1). When flies were transferred to food containing the inducible agent, RU486 (mifepristone, an analog of the hormone progesterone), after eclosion, the free-running period of experimental flies lengthened significantly as compared to its control flies maintained in vehicle food (Fig. 4.5C). However, I observed that the free-running period of the Gal4 control flies, *pdfGal4 (GS)*, also lengthened significantly and to a comparable level when transferred to RU-food (Fig. 4.5D), probably due to the non-specific effects of using the inducible system. The period of experimental flies (*pdf GS > dcr; Inx1* RNAi*)* transferred to RU food after development was only significantly different from its UAS control and not different from its Gal4 control (Fig. 4.5B, Appendix 4.1). Statistically significant difference from both the parental controls was perhaps not detected because of the non-specific lengthening of period seen in Gal4 control flies.
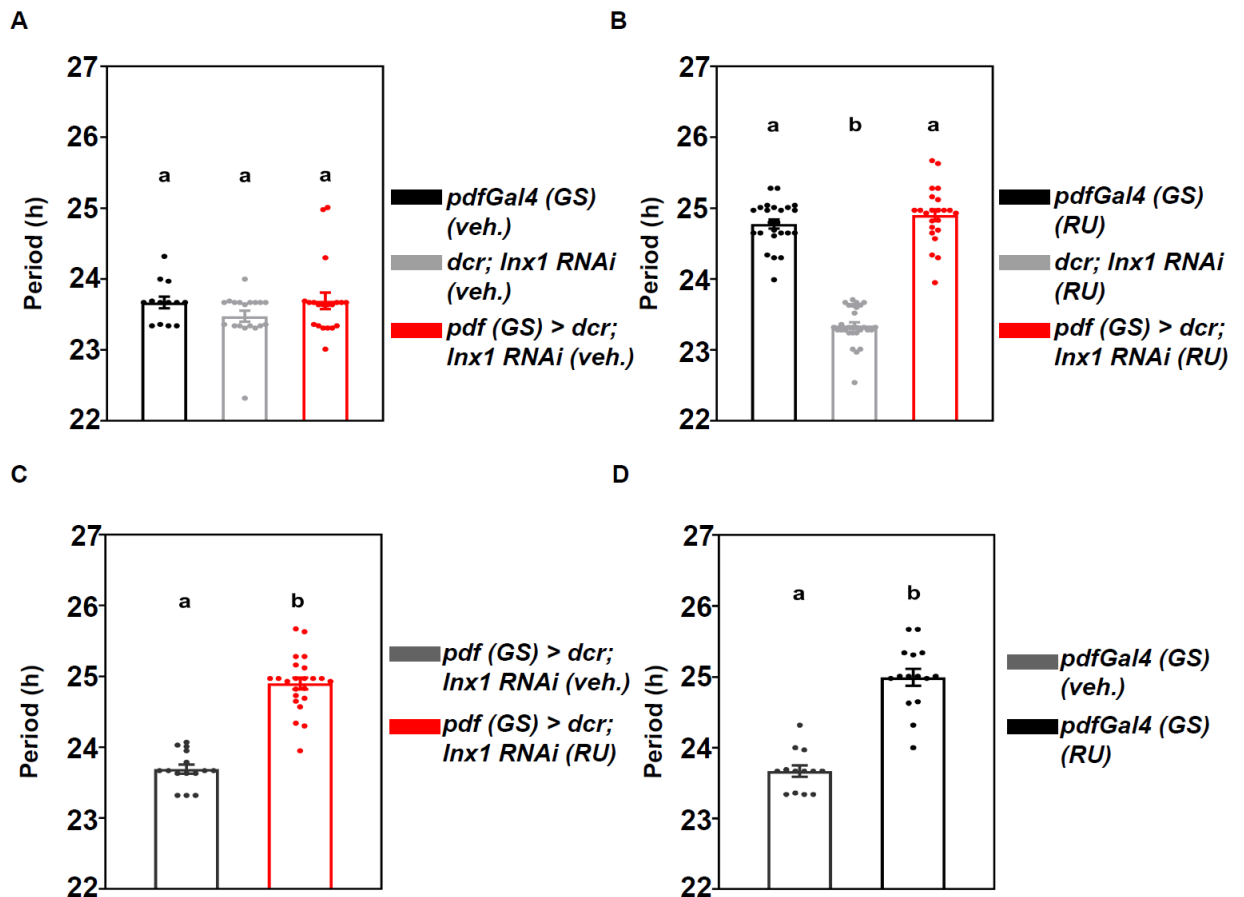
Figure 4.5: Adult-specific knockdown of *Innexin1* using the gene-switch system: (A) Free-running period of experimental flies *pdf (GS) > dcr; Inx1* RNAi (*n=22*) when they are fed food containing only vehicle (80% ethanol) in the adult stages is plotted along with its Gal4 control (*n=16*) or its UAS control (*n=19*) genotypes. **(B)** Free-running period of experimental flies *pdf (GS) > dcr; Inx1* RNAi (*n=23*) when they are fed food containing only RU486 in the adult stages is plotted along with its UAS control (*n=29*) and not from its Gal4 control (*n=24*) genotypes **(C)** Free-running period of experimental flies *pdf (GS) > dcr; Inx1* RNAi (*n=23*), when fed with RU486 food as adults is plotted along with the flies of the same genotype fed with vehicle (80% ethanol) (*n=15*) (one-way ANOVA, post-hoc Tukey's HSD, *p < 0.001*). **(D)** Gal4 control flies *pdf (GS) Gal4*, fed with RU486 (*n=16*) as adults is plotted along with the flies of the same genotype fed with vehicle (80% ethanol) (*n=15*).

Error bars represent SEM. All free-running period values are calculated using Chi-squared periodogram for a period of 7 days. All comparisons were made using one-way ANOVA with genotype as a fixed factor, followed by post-hoc Tukey's HSD test.

4.3.4 Knockdown of *Innexin1* in ventral lateral neurons lengthens the free-running period.

To identify critical subsets among the circadian pacemaker neurons where Innexin1 mediates the clock speed, I restricted the downregulation of *Innexin1* to smaller subsets of neurons in the clock network using specific drivers which target smaller cell groups. Knockdown of *Innexin1* using *dvpdfGal4* driver, which targets most of the lateral neuron subsets (Bahn et al., 2009) significantly lengthens the free-running period of the experimental flies as compared to control flies suggesting that Innexin1 functions in the lateral neuronal subset to determine free-running period (Fig. 4.6A left, Table 4.1, Appendix 4.3). The power of rhythm of experimental flies, in this case, was observed to be significantly lower compared to control flies (Fig. 4.6A right, Table 4.1, Appendix 4.4). Knockdown of *Innexin1* using *pdfGal4* significantly lengthens the free-running period compared to control flies, suggesting that Innexin1 expression in the ventral lateral neurons is vital to modulate the free-running period (Fig. 4.6B left, Table 4.1, Appendix 4.3). The power of the rhythm, in this case, was not found to be different between the control and experimental genotypes (Fig. 4.6B right, Table 4.1, Appendix 4.4).

Knockdown of *Innexin1* using *LNdGal4* does not lengthen the free-running period compared to its controls. No difference in the power of rhythms was observed between the experimental and control genotypes (Fig. 4.6C, Table 4.1, Appendix 4.3, Appendix 4.4), suggesting that Innexin1 function in LNd and 5th s-LNv neurons are not required to modulate the free-running period. To assess the contribution of *Innexin1* in other neurons in the circuit apart from the ventral lateral neurons in modulating the free-running period, I used a *timGal4; pdfGal80* construct to downregulate the expression of *Innexin1* (the efficiency of the construct in restricting the expression to non-LNv cells was verified and the data is shown in Chapter 3, Figure 3.10). Knockdown of *Innexin1* using *timGal4; pdfGal80* shows a significant lengthening of the free-running period of experimental flies compared to its parental controls (Fig. 4.6D left, Table 4.1, Appendix 4.3), suggesting that

Innexin1 probably also functions in other neurons apart from the ventral lateral subset in modulating free-running period. The power of the rhythm was not different between the experimental and control genotypes (Fig. 4.6D right, Table 4.1, Appendix 4.4).
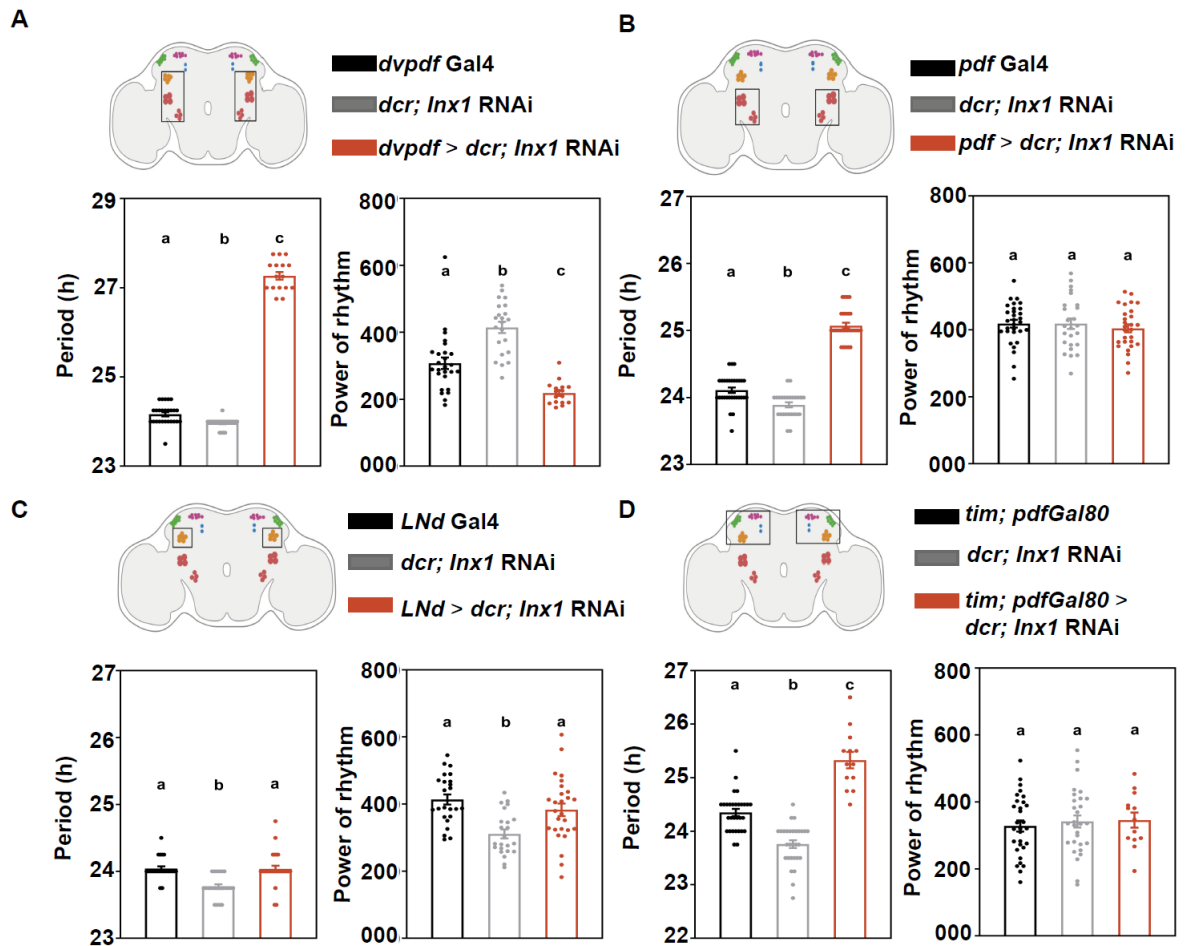
Figure 4.6: Knockdown of *Innexin1* in different subsets of clock neurons (A) Free-running period (left) and power of rhythm (right) of experimental flies (left) (*dvpdf > dcr; Inx1 RNAi*) (*n=20*) is plotted along with its Gal4 control (*n=26*) and UAS control (*n=22*) flies (**(B)** Free-running period (left) and power of rhythm (right) of experimental flies (*pdf > dcr; Inx1 RNAi*) (*n=28*) is plotted along with its Gal4 control (*n=30*) and UAS control (*n=25*) flies **(C)** Free-running period (left) and power of rhythm (right) of experimental flies (left) (*LNd > dcr; Inx1 RNAi*) (*n=27*) is plotted along with its Gal4 control (*n=24*) and UAS control (*n=23*) flies **(D)** Free-running period (left) and power of rhythm (right) of experimental flies (left) (*tim; pdfGal80 > dcr; Inx1 RNAi*) (*n=17*) is plotted along with its Gal4 control (*n=25*) and UAS control (*n=24*) flies. Error bars are SEM, period and power values are determined using Chi-square periodogram for a period of 7 days. See Table 4.1 for more details.

4.3.5 Knockdown screen of *Innexin1* in the adult brain

My results thus far suggests that Innexin1 is necessary in the ventral lateral neurons to modulate the free-running period. To investigate the role of Innexin1 in other cells apart from ventral lateral neurons in modulating the free-running period, I did a systematic knockdown screen of *Innexin1* in all the cell groups that have been previously shown to affect circadian properties in *Drosophila*. Since I have already targeted all the lateral neurons, I now used drivers specifically targeting the dorsal group of neurons in the circadian clock circuit. Previous studies have shown that clocks in the dorsal subset of neurons largely do not contribute to rhythm properties like rhythmicity and free-running period under constant conditions (Chatterjee et al., 2018; Delventhal et al., 2019), although membrane properties of the non-LNv neurons are important for robust rhythms in DD (Bulthuis et al., 2019), and clocks in some subsets of evening cells including the DN1p modulate free-running period to a small extent (Schlichting et al., 2019). I used two drivers previously reported to be expressed in the DN1p (*Clk 4.1MGal4* and *Clk 4.5FGal4*, which target 8-10 and 4 DN1p respectively) (Zhang et al., 2010) to downregulate the expression of *Innexin1*. Knockdown of *Innexin1* using *Clk 4.1M* or *Clk 4.5FGal4* did not alter the free-running period of experimental flies compared to control flies (Fig. 4.7A, Appendix 4.5). The power of rhythm was also not different in each of these cases (Fig. 4.7B, Appendix 4.6). A recent study screened the enhancer trap lines established in the Janelia Research Campus to identify Gal4 lines with an expression in clock neurons (Sekiguchi et al., 2020). I used some of these Gal4 lines to target the knockdown of *Innexin1* to the other dorsal neuronal sub-groups. Knockdown of *Innexin1* using *R77H08Gal4,* which targets ~7 DN3s, did not significantly alter the free-running period or power of rhythms (Fig. 4.7A, Fig. 4.7B, Appendix 4.5, and Appendix 4.6). Knockdown of *Innexin1* using the *R51H05Gal4* that targets about 10 DN1p neurons did not alter the free-running period

of experimental flies compared to the control flies, and there was no change in the power of rhythm (Fig. 4.7A, Fig. 4.7B, Appendix 4.5, Appendix 4.6). Next, I downregulated *Innexin1* expression in DN2 neurons using the *R64A07Gal4,* which also did not significantly alter the period and power of rhythms compared to its parental control genotypes (Fig. 4.7A, Fig. 4.7B, Appendix 4.5, Appendix 4.6). Knockdown of *Innexin1* in most clock neurons, excluding the ventral lateral neurons, did not alter the free-running period. Hence, I focused on targeting the downregulation of *Innexin1* to subsets of neurons outside the canonical clock cells but still known to affect clock properties. The Pars Intercerebralis (PI) in *Drosophila* is the equivalent of the mammalian hypothalamus. It controls various processes like sleep (Crocker et al., 2010), rhythmic locomotor activity-rest behaviour (Cavanaugh et al., 2014; Cavey et al., 2016; King et al., 2017), and feeding and metabolism (Barber et al., 2016; Broughton et al., 2005; Rulifson et al., 2002). Since PI is a known output region of circadian activity-rest behaviour and affects clock properties, I used drivers that target subsets of PI neurons to downregulate *Innexin1* expression and examine its effect on activity-rest rhythms. I used *Kurs58Gal4* (Siegmund, 2001), expressed in about 16-18 DH44 neuropeptide expressing PI neurons and essential for rhythmic activity-rest behaviour(Cavanaugh et al., 2014). Knockdown of *Innexin1* using *Kurs58Gal4* did not lengthen the period of activity-rest rhythms in experimental flies. There was no difference in the power of rhythms in experimental flies compared to control flies (Fig. 4.8A, Fig. 4.8B, Appendix 4.5, and Appendix 4.6). Next, I used *Dilp2Gal4*, which targets about 14 Insulin-producing cells (IPC) of the PI and shows almost no overlap with the cells targeted by Kurs58*Gal4* (Cavanaugh et al., 2014). PI subsets targeted by the *Dilp2* driver form part of the circadian output centre, where the central clock neurons regulate the firing rates of IPCs. Dilp2 neurons also directly modulate feeding rhythms and sleep, which are thought to be major circadian clock outputs

(Barber et al., 2016; Crocker et al., 2010). Knockdown of *Innexin1* using *Dilp2Gal4* does not affect the period or power of rhythms in experimental flies compared to control flies suggesting that *Innexin1* does not function in this subset of PI neurons (Fig. 4.8A, Fig. 4.8B, Appendix 4.5, Appendix 4.6). Finally, I used an alternate driver, *Mai301Gal4,* to target a subset of DH44 +ve neurons; the cells targeted by this driver have previously been shown to modulate sleep in *Drosophila* (Stavropoulos and Young, 2011). Knockdown of *Innexin1* using *Mai301Gal4* also did not alter the free-running period and power of rhythms in experimental flies compared to control flies (Fig. 4.8A, Fig. 4.8B, Appendix 4.5, Appendix 4.6), suggesting that *Innexin1* in this subset of PI neurons is also not involved in modulating the free-running period.
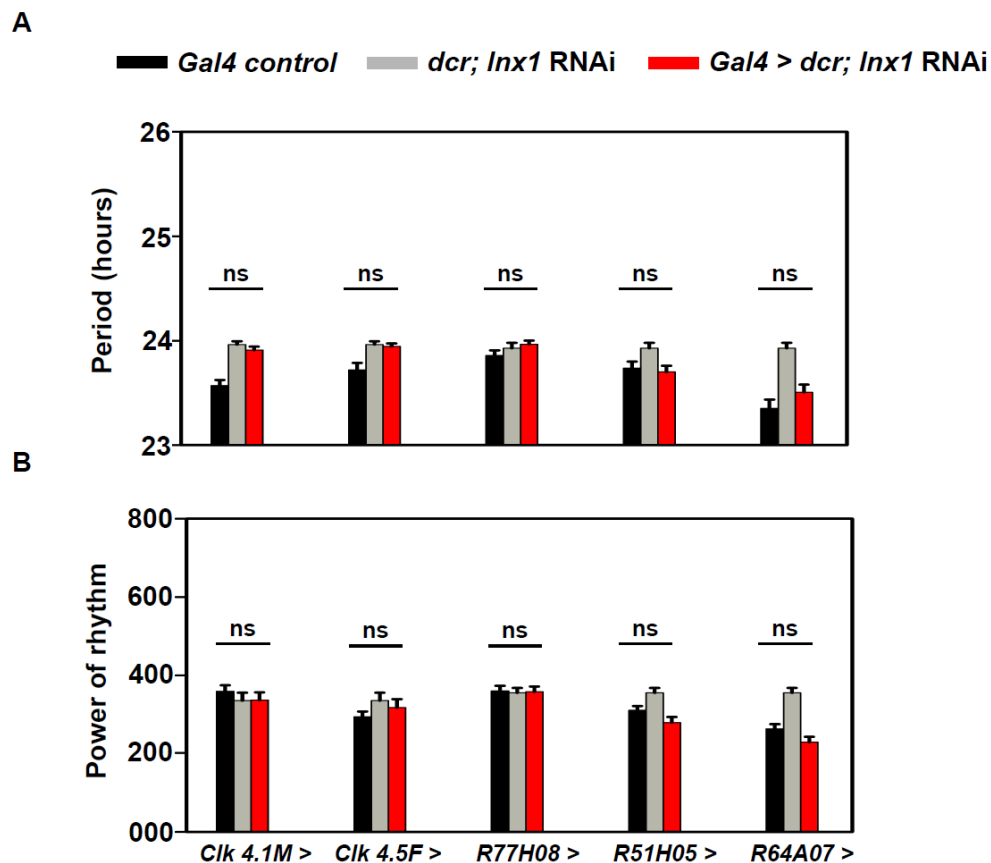
Figure 4.7: Knockdown of *Innexin1* in dorsal subsets of clock neurons does not affect the free-running period (A) Mean free-running period of flies with *Innexin1* gene downregulated in different subsets of dorsal clock neurons targeted by the different drivers are being plotted. No significant difference in free-running period was observed in any of the experimental flies as compared to both its parental controls. **(B)** Power of the Chi-square periodogram of experimental flies was also not found to be significantly different from both the parental controls in case of *Innexin1* knockdown in any of the dorsal neuronal subsets. Error bars are SEM. Period and power values were calculated using Chi-squared periodogram for a period of 7 days. One-way ANOVA with a post-hoc Tukey's HSD was performed in each case. ns (not significant) indicates that the experimental genotypes are not significantly different from both its parental control flies, $n > 25$ flies for each genotype.
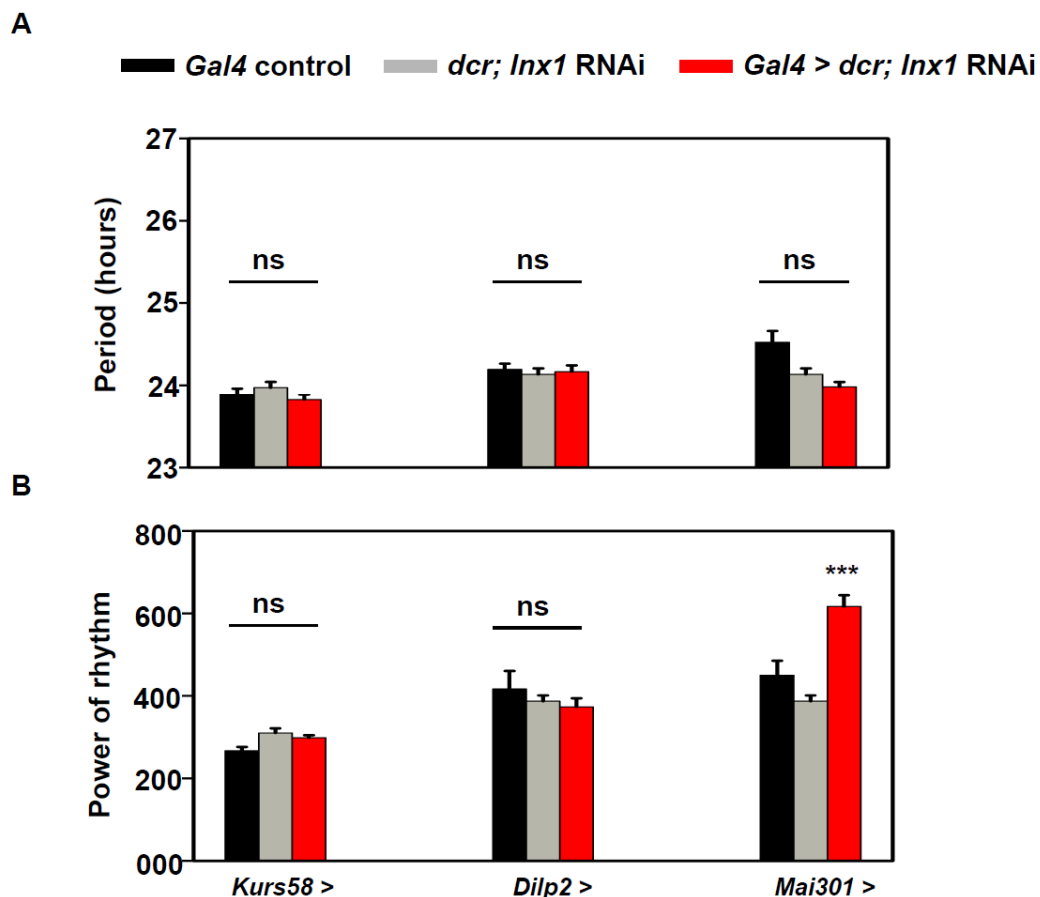
Figure 4.8: Knockdown of *Innexin1* in subsets of Pars Intercerebralis (PI) neurons does not affect the free-running period (A) Mean free-running period of flies with *Innexin1* gene downregulated in different subsets of Pars Intercerebralis neurons targeted by the different drivers are being plotted. No significant difference in free-running period was observed in any of the experimental flies as compared to both their parental controls. **(B)** Power of rhythm of experimental flies was found to be significantly greater in case of knockdown of *Innexin1* using *Mai301Gal4* as compared to its respective parental controls (One-way ANOVA followed by Tukey's HSD, $p < 0.001$). There was no difference in power of rhythm observed in case of *Innexin1* knockdown using the drivers that target the other two subsets of PI neurons (*Kurs58Gal4* and *Dilp2Gal4*). Error bars are SEM. Period

and power values were calculated using Chi-Squared periodogram for a period of 7 days. One-way ANOVA with a post-hoc Tukey's HSD was performed in each case. ns (not significant) indicates that the experimental flies are not different from both the Gal4 and UAS parental control genotypes. *n > 28* flies for each genotype.

Innexin1 function does not seem to be important in dorsal subsets of clock neurons and PI neurons for modulating the free-running period. To rule out the contribution of Innexin1 in other neuronal cells apart from the ventral lateral neurons in the regulation of the free-running period, I downregulated its expression using the *elavGal4; pdfGal80* construct. *elav; pdfGal80 > dcr; Inx1* RNAi flies do not show a significantly lengthened period compared to both its parental controls (Fig. 4.9A, Appendix 4.7), suggesting that among neurons, Innexin1 probably only functions in the ventral lateral circadian cells. The power of the rhythm in the case of experimental flies was not found to be significantly different from both its parental controls (Fig. 4.9B, Appendix 4.8). Hence, I next proceeded to ask if the function of Innexin1 is important in glial cells to modulate the free-running rhythms. Glial cells in *Drosophila* have been shown to play important roles in sleep and rhythmic locomotor activity (reviewed in Jackson, 2015). Although clocks in glial cells are not known to modulate activity-rest rhythms, genetic manipulations that affect exocytosis, membrane ionic gradients, and calcium levels, of astrocytes-, a subset of glial cells, lead to disruption of rhythmic activity-rest behaviour (Ng et al., 2011). This suggests that glia-neuron communication and proper release of gliotransmitters are probably crucial for rhythmic activity-rest behaviour. Glial cells and glia-neuron communication have been shown to affect sleep, a critical output behaviour governed by the circadian clock (Chen et al., 2014; Farca Luna et al., 2017; Seugnet et al., 2011). Innexins are widely present in various subsets of glial cells in *Drosophila* and are shown to affect multiple processes from development to behaviour (Chaturvedi et al., 2014; Farca Luna et al., 2017; Holcroft et al., 2013; Spéder and Brand, 2014; Zhang et al., 2018). To examine the importance of

Innexin1 in glial cells in modulating the free-running period, I downregulated *Innexin1* expression using *repoGal4*, a pan-glial driver targeting about 99% of glial cell populations (Sepp et al., 2001; Stork et al., 2012). Knockdown of *Innexin1* using *repoGal4* resulted in the lethality of experimental flies of the desired genotype, with only a small number of flies eclosing, which die within a few days of their emergence. This suggests that perhaps Innexin1 in glial cells is necessary for some essential developmental processes, a phenomenon that has been previously reported in another study (Holcroft et al., 2013). Therefore, I targeted the knockdown of *Innexin1* to a smaller subset of glial cells, the astrocyte-like glia using a specific driver, *alrm-Gal4* (Doherty et al., 2009). Knockdown of *Innexin1* using *alrm-Gal4* resulted in significant lengthening of the free-running period in experimental flies compared to both the parental controls, suggesting that *Innexin1* probably also functions in astrocytes apart from the ventral lateral clock neurons in modulating the free-running period (Fig. 4.10A left, Appendix 4.7). The power of rhythm in experimental flies was not different from the control flies (Fig. 4.10A right, Appendix 4.8). I also used a driver to specifically target another subset of glial cells, the cortical glia (*NP2222Gal4*, Edwards and Meinertzhagen, 2010). Knockdown of *Innexin1* in cortical glial cells did not affect the free-running period or the power of rhythm in experimental flies compared to their parental controls (Fig. 4.10B, Appendix 4.7, Appendix 4.8).
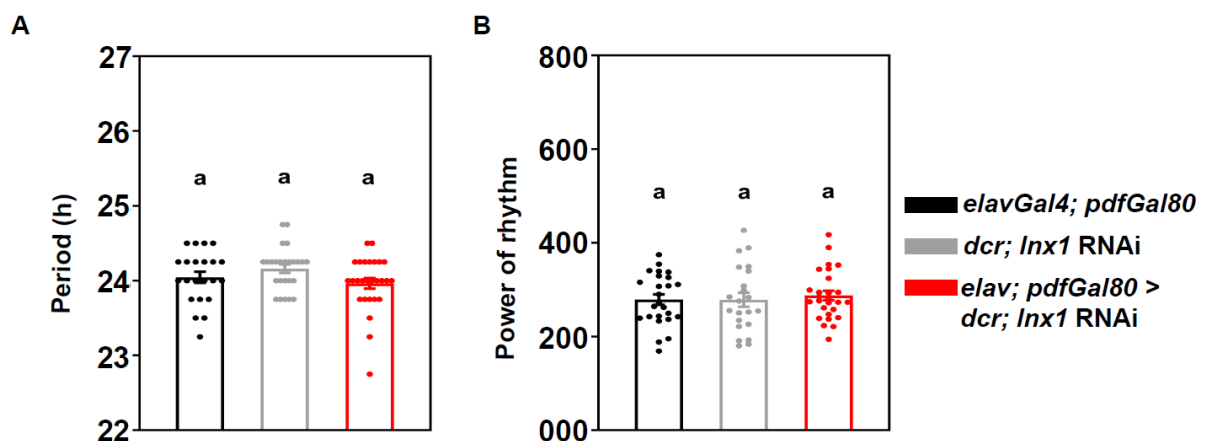
Figure 4.9: Knockdown of *Innexin1* in all neurons apart from the ventral lateral neurons does not lengthen the free-running period Free-running period **(A)** and power of rhythm **(B)** of experimental flies (*elav; pdfGal80 > dcr; Inx1* RNAi) (*n=28*) is plotted along with its Gal4 control (*n=22*) and UAS control (*n=24*) flies. Error bars are SEM, period and power values are determined using Chi-square periodogram for a period of 7 days, all statistical comparisons are performed using one-way ANOVA with genotype as a fixed factor followed by a post-hoc Tukey's HSD test.
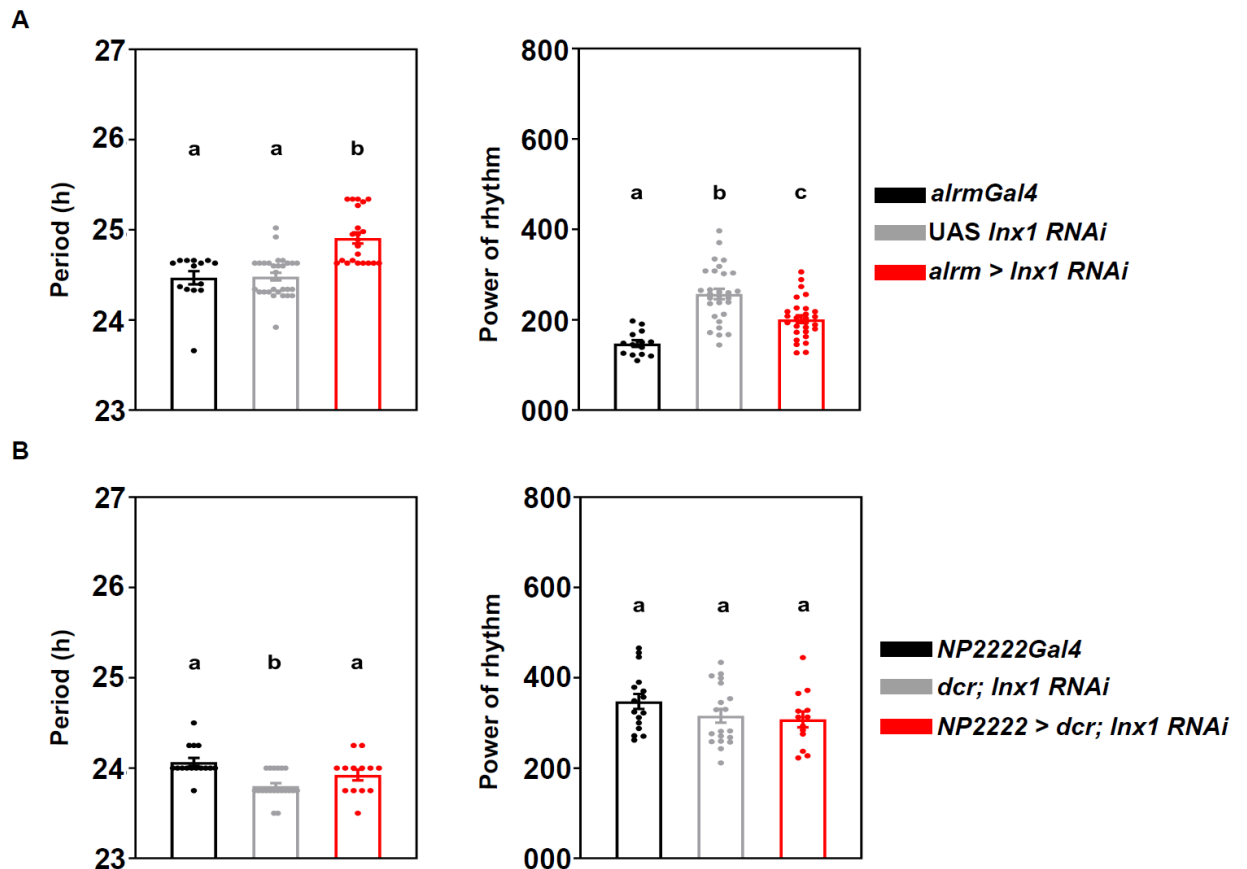
Figure 4.10: Knockdown of *Innexin1* in astrocyte-like glia lengthens the free-running period (A) Free-running period (left) and power of rhythm (right) of experimental flies (*alrm > Inx1 RNAi*) (*n=25*) is significantly longer than both the Gal4 control (*n=16*) and UAS control (*n=26*) flies **(B)** Free-running period (left) and power of rhythm (R) of experimental flies (left) (*NP2222 > dcr; Inx1 RNAi*) (*n=16*) is plotted along with its UAS control (*n=23*) and Gal4 control (*n=21*) flies. Error bars are SEM, period and power values are determined using Chi-square periodogram for a period of 7 days, all statistical analysis are performed using one-way ANOVA with genotype as a fixed factor followed by Tukey's post-hoc HSD test.

Genotype	N	*n*	Period ± SEM	POR ± SEM
tim; dcr (Gal4 cont.)	4	30 31 29 22	23.6 ± 0.01 23.7 ± 0.03 23.7 ± 0.06 23.9 ± 0.03	419.2 ± 13.1 276.8 ± 8.82 268 ± 7.1 492 ± 16.9
UAS *Inx1* RNAi	4	24 30 30 20	23.5 ± 0.03 23.79 ± 0.07 23.3 ± 0.04 24.01 ± 0.04	393.8 ± 13.24 255.3 ± 10.1 284.7 ± 12.61 517.2 ± 25.01
tim dcr > Inx1 RNAi	4	20 26 31 17	25.7 ± 0.07 25.6 ± 0.13 26 ± 0.06 25.7 ± 0.1	385.3 ± 14.55 238.1 ± 10.65 275.1 ± 11.64 444.8 ± 25.47
Clk856Gal4 (Gal4 cont.)	3	21 29 17	23.4 ± 0.05 23.6 ± 0.06 23.9 ± 0.03	337.8 ± 18.8 303.9 ± 11.7 362.5 ± 20.02
dcr: Inx1 RNAi (UAS cont.)	3	21 26 22	23.9 ± 0.07 23.6 ± 0.06 23.9 ± 0.02	343.2 ± 14.4 323.6 ± 16 414.5 ± 16.83
Clk856 > dcr; Inx1 RNAi	3	29 23 20	25.31 ± 0.04 25.2 ± 0.05 24.6 ± 0.013	408.5 ± 19.89 327.9 ± 17.26 294.3 ± 12.84
tim; tubGal80^{ts} (Gal4 cont.; DD 29°C)	3	18 21 23	24.2 ± 0.05 24 ± 0.05 24 ± 0.04	359.4 ± 24.9 430.4 ± 23.5 265.2 ± 13.9
dcr; Inx1 RNAi (UAS cont.;DD 29°C)	3	18 15 17	23.3 ± 0.06 23.29 ± 0.05 23.5 ± 0.06	368.5 ± 22.5 505.2 ± 37.26 446.8 ± 15.9
tim; tubGal80^{ts} > dcr; Inx1 RNAi (DD 29°C)	3	25 29 26	24.6 ± 0.03 24.5 ± 0.03 24.5 ± 0.05	570.2 ± 18.6 567.6 ± 23.2 331 ± 12.6
tim; tubGal80^{ts} (Gal4 cont.; DD 19°C)	2	22 18	23.7 ± 0.08 24.09 ± 0.1	269.8 ± 13.6 183.7 ± 6.22
dcr; Inx1 RNAi (UAS cont.;DD 19°C)	2	17 15	23.85 ± 0.06 24.35 ± 0.18	301.1 ± 21.86 175.7 ± 6.36
tim; tubGal80^{ts} > dcr; Inx1 RNAi (DD 19°C)	2	26 19	25.4 ± 0.1 25.7 ± 0.11	264.3 ± 11.67 195 ± 6.48
dvpdfGal4 (Gal4 *cont.*)		26	24.1 ± 0.04	307.5 ± 17.2
dcr; Inx1 RNAi (UAS cont.)		22	23.9 ± 0.02	414.5 ± 16.83
dvpdf > dcr; Inx1 RNAi		17	27.2 ± 0.08	218.6 ± 8.73
pdfGal4 (Gal4 *cont.*)	2	30 20	24.1 ± 0.04 24.2 ± 0.04	418.4 ± 11.35 400 ± 16.4
dcr: Inx1 RNAi *(UAS cont.)*	2	25 23	23.89 ± 0.03 23.9 ± 0.06	418.3 ± 15.74 339.7 ± 13.49
pdf > dcr; Inx1 RNAi	2	28 30	25.07 ± 0.04 25.19 ± 0.05	404.4 ± 11.82 378.7 ± 14.03
*LNd*Gal4 (Gal4 cont.)		13	24 ± 0.06	524 ± 34.9

	2	24	24 ± 0.03	413.4 ± 14.9
dcr; Inx1 RNAi (UAS cont.)	2	24	24.1 ± 0.06	387 ± 14.0
		23	23.7 ± 0.03	311 ± 13.3
LNd > dcr; Inx1 RNAi	2	20	24.1 ± 0.06	481.5 ± 23.3
		27	24.0 ± 0.07	382.7 ± 18.59
Clk4.1MGal4 (Gal4 cont.)		16	23.5 ± 0.05	359.2 ± 15.7
Clk4.5FGal4 (Gal4 cont.)		17	23.7 ± 0.06	294.6 ± 13.2
dcr; Inx1 RNAi (UAS cont.)		21	23.9 ± 0.03	335.8 ± 20
Clk4.1M > dcr; Inx1 RNAi		15	23.9 ± 0.03	337.3 ± 19.3
Clk4.5F > dcr; Inx1 RNAi		16	23.9 ± 0.02	317.8 ± 21.7
tim; pdfGal80 (Gal4 *cont.*)		30	24.3 ± 0.06	328.2 ± 16.5
dcr; Inx1 RNAi (UAS cont.)		29	23.75 ± 0.07	341.8 ± 18.1
tim; pdfGal80 > dcr; Inx1 RNAi		17	25.3 ± 0.15	345.8 ± 22.5
R77H08Gal4 (Gal4 *cont*)		25	23.86 ± 0.04	360.2 ± 13.4
R51H05Gal4 (Gal4 *cont.*)		23	23.7 ± 0.06	311 ± 10.5
R64A07Gal4 (Gal4 *cont.*)		18	23.3 ± 0.08	263.8 ± 11.8
dcr; Inx1 RNAi (UAS cont.)		27	23.9 ± 0.05	355.6 ± 12.4
R77H08 > dcr; Inx1 RNAi		31	23.9 ± 0.03	358.2 ± 13.47
R51H05 > dcr; Inx1 RNAi		21	23.7 ± 0.05	279.3 ± 14.6
R64A07 > dcr; Inx1 RNAi		20	23.5 ± 0.07	229.6 ± 13.5
timGal4 (Gal4 cont.)		28	24 ± 0.05	362.9 ± 13.3
UAS *GFP-Inx1* (UAS cont.)		24	24.05 ± 0.06	296.2 ± 15.05
tim > GFP-Inx1		31	24.5 ± 0.04	355.1 ± 11.6
pdfGal4 (Gal4 cont.)		20	24.2 ± 0.04	400 ± 16.42
UAS *GFP-Inx1* (UAS cont.)		19	23.8 ± 0.06	296 ± 19.83
pdf > GFP-Inx1		23	24.5 ± 0.04	406.8 ± 15.25
timGal4 (Gal4 *cont.*)		23	24.4 ± 0.08	321.8 ± 10.6
pdfGal4 (Gal4 *cont.*)		21	24.4 ± 0.06	280.9 ± 14.1
UAS Inx1-GFP (UAS cont.)		21	23.9 ± 0.06	280.8 ± 13.7
tim > Inx1-GFP		25	24.1 ± 0.07	282.4 ± 13.28
pdf > Inx1-GFP		26	24.4 ± 0.05	314.6 ± 11.5
pdfGal4 (Gal4 *cont.*)		28	23.7 ± 0.03	260.1 ± 9.97
UAS Inx1-myc (UAS cont.)		30	23.2 ± 0.04	250 ± 10.1
pdf > Inx1-myc		32	23.8 ± 0.04	263.6 ± 7.61
Pdf; Inx1-myc (Gal4 *cont.*)		30	23.6 ± 0.06	325.7 ± 12.6
UAS Inx2GFP;; (UAS cont.)		28	24.1 ± 0.05	266.6 ± 9.24
pdf > Inx1-myc; Inx2-GFP		24	24.1 ± 0.09	263.7 ± 14.7

Table 4.1: Table representing the genotype, no. of replicates, no. of flies, average period (±SEM), average power of the periodogram (± SEM) values in case of knockdown and overexpression of *Innexin1* in different subsets of clock neurons.

4.3.6 Expression pattern of *Innexin1* in adult *Drosophila* brain and clock neurons

To examine the distribution of *Innexin1* in the adult *Drosophila* brain and among the clock circuit, I used a previously characterized enhancer trap line (*NP0076Gal4*, Spéder and Brand, 2014), expressed an *eGFP* reporter gene, and co-stained with PER and PDF proteins to visualize co-localization with the circadian clock neurons. I observe GFP expression in the large ventral lateral neurons among the clock neurons (Fig .4.11A, top left and middle panels). Additionally, I also observed GFP expression very close to the lateral dorsal neurons (LNd) and the dorsal neuronal subsets (DN) (Fig. 4.11A extreme right, Fig. 4.11B), which could be glial cells surrounding these neurons. To examine if *Innexin1* is expressed in glial cell groups, I co-stained the brains with an anti-Repo antibody, a glial cell marker. I observed that GFP and Repo expression co-localize at multiple regions in the lateral and dorsal areas of the brain (Fig. 4.11C right, arrows), suggesting that *Innexin1* is expressed both in clock neurons and glial cells in the adult *Drosophila* brain. To examine if Innexin1 protein is expressed in clock neurons, I used a previously characterized peptide antibody against the C-terminus region of the protein (Bauer et al., 2003). However, I did not observe staining of any specific cells and structures, but non-specific patches, which were observed in the adult brains of both control and *ogre KO* flies, suggesting that the antibody does not work very efficiently and specifically in the tissue of our interest. Therefore, I proceeded to raise a polyclonal peptide-based antibody against the Innexin1 protein *de novo*. Since most *Drosophila* Innexin proteins share very similar structures, only a few regions in the protein can be selected as a unique site for antibody synthesis (Bauer et al., 2005). After carefully evaluating the sequence similarities, I chose a unique peptide sequence of 31-mer (REEKEAKRDALLDYLIKHVKRHKLYAIRYWA) in the cytoplasmic loop of Innexin1 protein as a unique epitope for raising an antibody (in collaboration with Dr. Rajeshwari,

Bioklone Biotech). After peptide synthesis and immunization of mice (see Materials and methods for detailed description), Innexin1 anti-sera (4th bleed after immunization for 28M2 and M4 mice and 2nd bleed after immunization for 28M1) was collected and examined for specificity using Western blot with protein extracts from whole heads of both control *(w1118)* and *ogre KO* flies. Protein bands of the desired size corresponding to the molecular weight of *Innexin1* (~37 kDa) (Holcroft et al., 2013) was observed in extracts from control flies and absent in extracts from mutant flies (Fig. 4.12A), which shows that the anti-sera has reasonable specificity even after the first couple of rounds of immunizations. Multiple non-specific bands were also detected in western blots, which is not surprising given that the complete anti-sera and not the purified antibody was used for staining. I also examined Innexin1 expression using the anti-sera in adult brain tissues of *pdf > GFP* flies as a preliminary experiment. I observed Innexin-like structures co-localizing with GFP cells in some brain samples (Fig. 4.12B). However, it seems like the anti-sera was also binding non-specifically to many proteins in the tissue. More rounds of immunizations and purification processes are necessary to conclude about the expression of Innexin1 protein in the adult *Drosophila* brain.
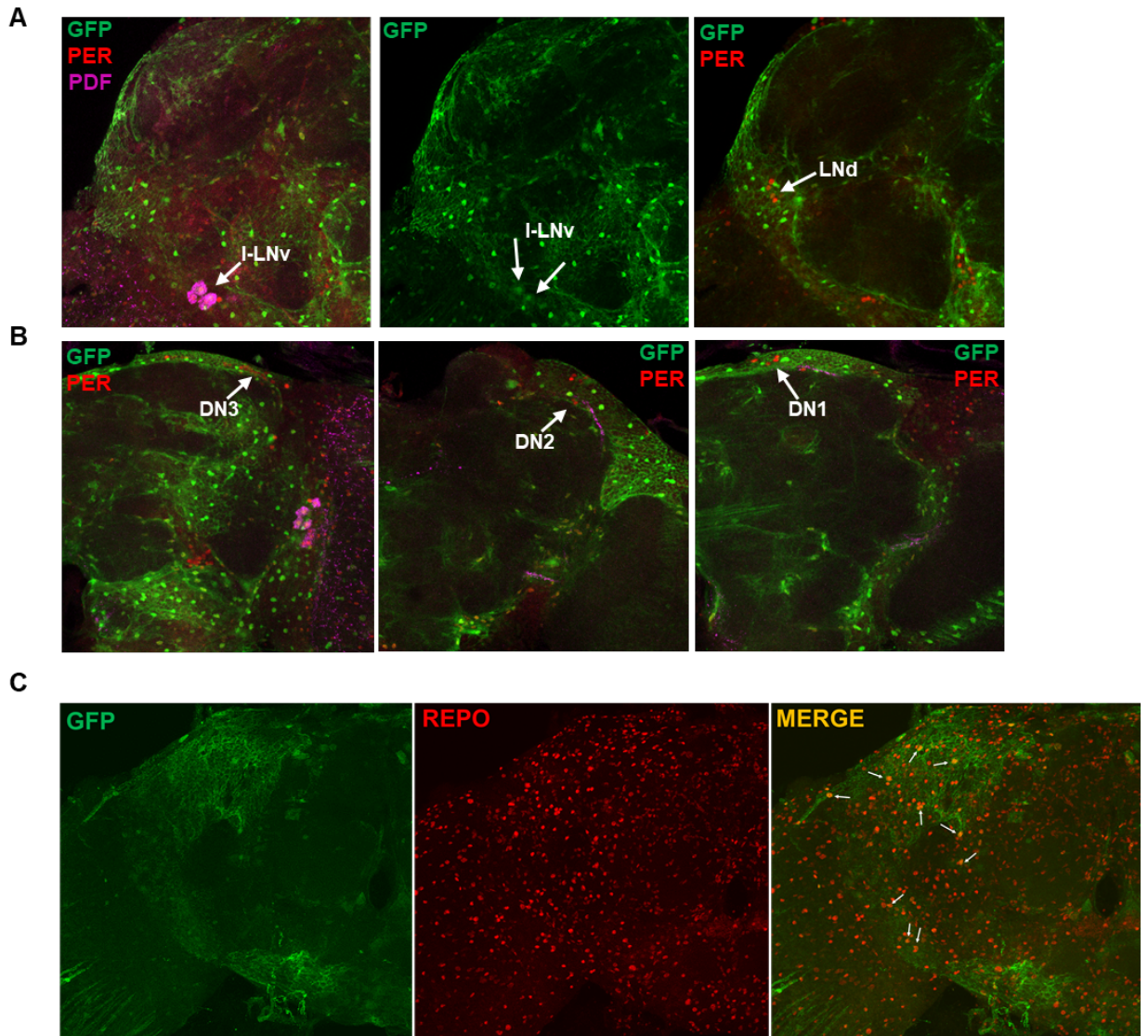
Figure 4.11: Expression pattern of *Innexin1Gal4* indicates its presence in the ventral lateral neurons and glial cells: (A and B) Representative images of adult *Drosophila* adult showing the co-localization of *Inx1 > GFP* with clock proteins, PER and PDF. GFP expression was seen in the large ventral lateral neurons (l-LNv), in close proximity to the dorsal lateral neurons (LNd), and the dorsal neurons (DN1, DN2 and DN3) which are marked by arrows in each panel. **(C)** Innexin1 expression in the adult *Drosophila* brain co-localized with a pan-glial marker, repo. Co-localization was observed both in the lateral and dorsal regions of the brain (areas of co-localization are marked by arrows). Brightness and contrast of representative images were adjusted to facilitate better visualization. *n* > 8 brain samples were imaged in each case.
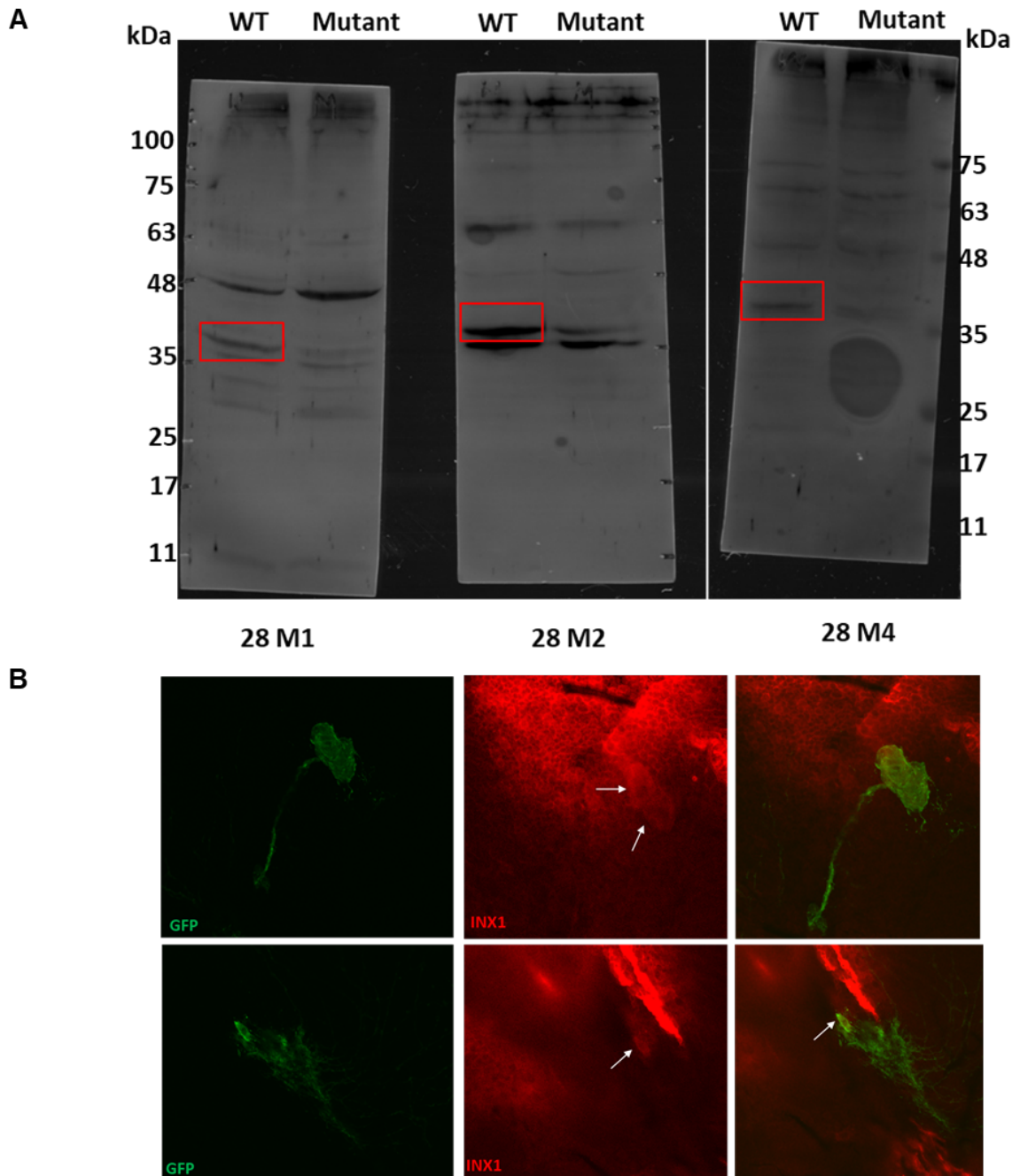
Figure 4.12: Preliminary assessment of anti-Innexin1 anti-sera (A) Western blots of *Drosophila* whole head extracts of wild-type and *ogre KO* flies with anti-Innexin1 anti-sera (2nd bleed) shows a band around the predicted size of Innexin1 protein (~37 kDa), which is diminished in the mutant lane. 28M1, M2 and M4 are the identities of the mice immunized with the peptide. **(B)** Representative images of adult *Drosophila* brain of *pdf > GFP* flies, co-stained with anti-Innexin1 antisera, co-localization of GFP and Inx1 in the ventral lateral neurons was observed in some brain samples. The anti-sera was obtained from 28M1 mouse. Brightness and contrast of representative images were adjusted to facilitate better visualization.

4.3.7 Over-expression of *Innexin1* does not affect the free-running period of activity-rest rhythms.

Further, I wanted to examine the effect of over-expression of *Innexin1* in clock neurons. I used a UAS *Inx1-GFP* construct (Spéder and Brand, 2014) and expressed it in clock neurons using the *timGal4* driver. Surprisingly, over-expression of the *Inx1-GFP* construct did not alter the free-running period of experimental flies compared to control flies (Fig. 4.13A left, Appendix 4.9). The power of the rhythm was not different between the control and experimental genotypes (Fig. 4.13A right, Appendix 4.10). Since knockdown of *Innexin1* only in the ventral lateral neurons also lengthened the free-running period, I over-expressed *Inx1-GFP* using *pdfGal4*. However, even in this case, I observed that the period of experimental flies was not significantly different from the control flies (Fig. 4.13B left, Appendix 4.9). The power of rhythms was also not significantly different in the experimental flies (Fig. 4.13B right, Appendix 4.10).

I also used an alternate UAS construct of *Innexin1*, *Inx1-myc* (Richard et al., 2017) for over-expression in clock neurons. Over-expression of *Inx1-myc* with *pdfGal4* does not alter the free-running period of experimental flies compared to controls (Fig. 4.14A left, Appendix 4.9). The power of rhythms of experimental flies is not significantly different compared to control flies (Fig. 4.14A right, Appendix 4.10).

Since downregulation of *Innexin1* and *Innexin2* individually in ventral lateral neurons lengthens the free-running period (refer to Chapter 3), and Innexins 1 and 2 have been shown previously to form heteromeric gap junction channels (Holcroft et al., 2013), I hypothesized that lack of change in the free-running period observed in case of over-expression of *Innexin1* and *2* individually could be because of the partner subunit not being simultaneously overexpressed. Hence, I carried out a simultaneous over-expression of

both *Inx1-myc* and *Inx2-GFP* constructs in ventral lateral clock neurons. Over-expression of both *Inx1-myc* and *Inx2-GFP* using *pdfGal4* also did not significantly alter the free-running period of experimental flies compared to control flies (Fig .4.14 B left, Appendix 4.9). The power of rhythm, in this case, was also not significantly different from the parental controls (Fig. 4.14B right, Appendix 4.10).
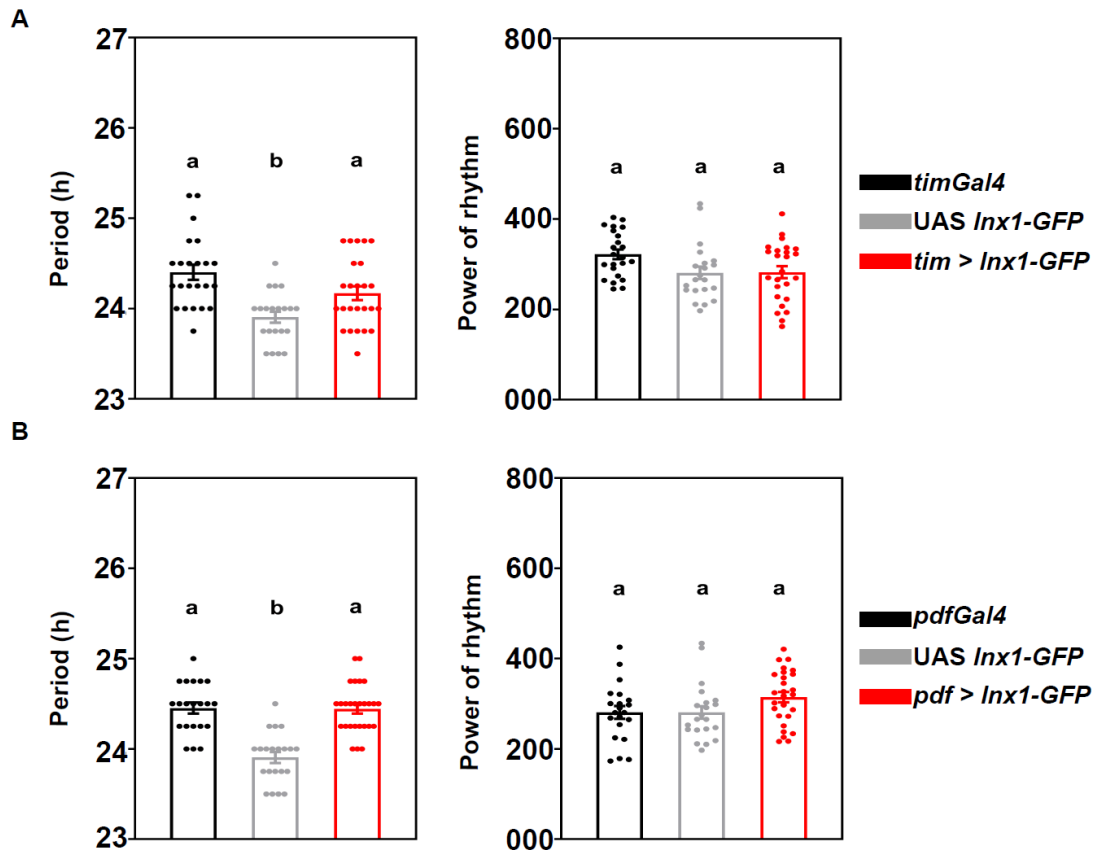
Figure 4.13: Overexpression of *Innexin1* in clock neurons does not affect the free-running period (A) Free-running period (left) and power of rhythm (right) of experimental flies (*tim > Inx1-GFP*) (*n=25*) is plotted along with its Gal4 control (*n=23*) and UAS control (*n=21*) flies **(B)** Free-running period (left) and power of rhythm (right) of experimental flies (*pdf > Inx1-GFP*) (*n=26*) is plotted along with its Gal4 control (*n=21*) and UAS control (*n=21*) flies. Error bars are SEM, period and power values are determined using Chi-square periodogram for a period of 7 days, all statistical analysis were performed using one-way ANOVA with genotype as a fixed factor, followed by post-hoc Tukey's HSD test.
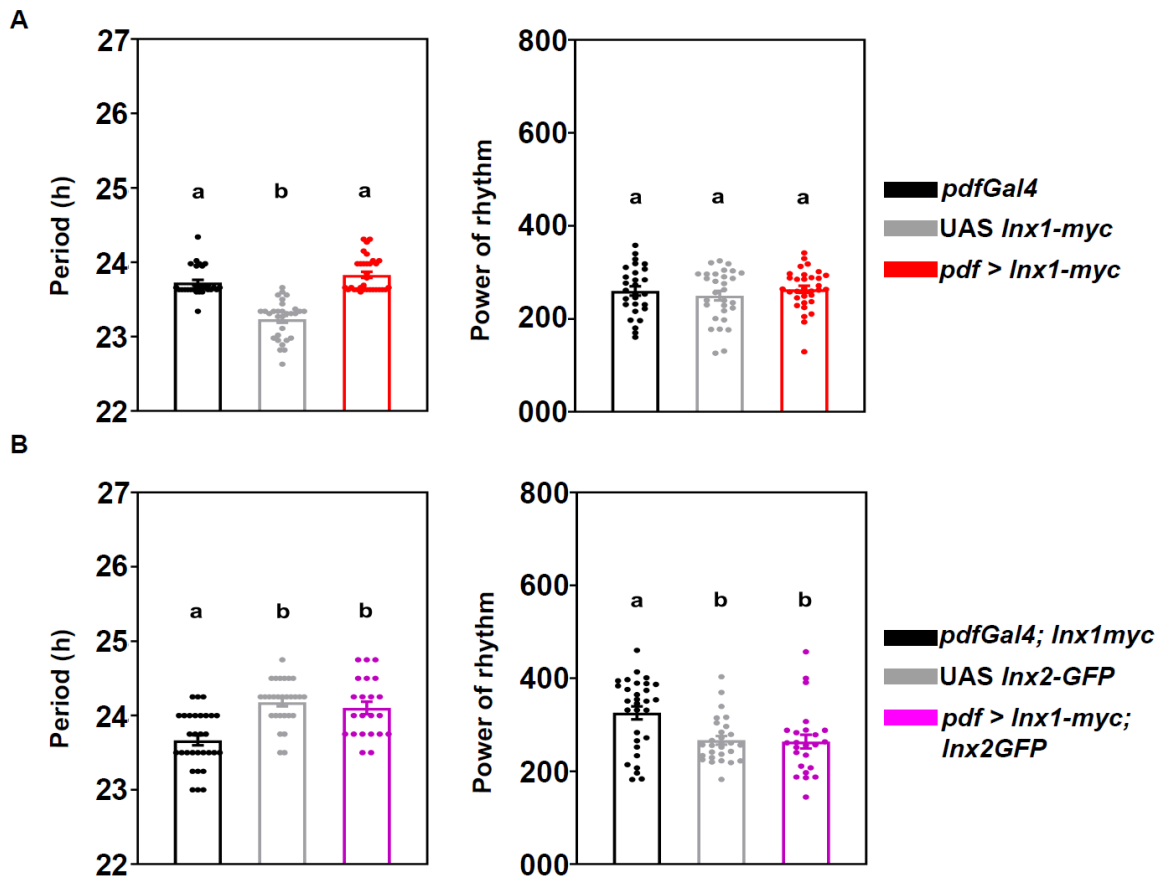
Figure 4.14: Overexpression of *Innexin1* and *Innexin2* in clock neurons does not affect the free-running period (A) Free-running period (left) and power of rhythm (right) of experimental flies (*pdf > Inx1*-myc) (*n=32*) is plotted along with its Gal4 control (*n=28*) and UAS control (*n=30*) flies **(B)** Free-running period (left) and power of rhythm (right) of experimental flies (*pdf > Inx1*myc; *Inx2GFP*) (*n=24*) is plotted along with its Gal4 control (*n=30*) and UAS control (*n=28*) flies. Error bars are SEM, period and power values are determined using Chi-square periodogram for a period of 7 days, all statistical analysis are performed using one-way ANOVA with genotype as a fixed factor followed by post-hoc Tukey's HSD test.

4.3.8 Disruption of the gap-junction forming domain of Innexin1 lengthens the free-running period

To distinguish between the gap junction versus non-channel based functions of Innexin1 in clock neurons, I used a previously characterized construct of Innexin1, *GFP-Inx1*, where the reporter gene, GFP is fused with the N-terminal region of the protein (Spéder

and Brand, 2014). Previous studies have shown that the N-terminal regions of both Connexins and Innexins are required to form gap junctions or hemichannels in cell membranes (Nakagawa et al 2010). Therefore, this construct is made such that the gap-junction and hemichannel-forming domains of Innexin1 are disrupted, but its other non-junction-based cellular functions are unaffected. Expression of *GFP-Inx1* in all clock neurons using *timGal4* lengthens the free-running period of experimental flies compared to control flies (Fig. 4.15A left, Appendix 4.9), suggesting that Innexin1 functions as gap junctions or hemichannels in these neurons. The power of rhythm of experimental flies was not found to be different from the control flies (Fig. 4.15A right, Appendix 4.10). Expression of *GFP-Inx1* in ventral lateral neurons using *pdfGal4* also lengthened the period of experimental flies as compared to controls (Fig. 4.15B left, Appendix 4.9), with no change in the power of rhythms (Fig. 4.15B right, Appendix 4.10), suggesting that Innexin1 functions as gap junctions in the ventral lateral clock neurons.
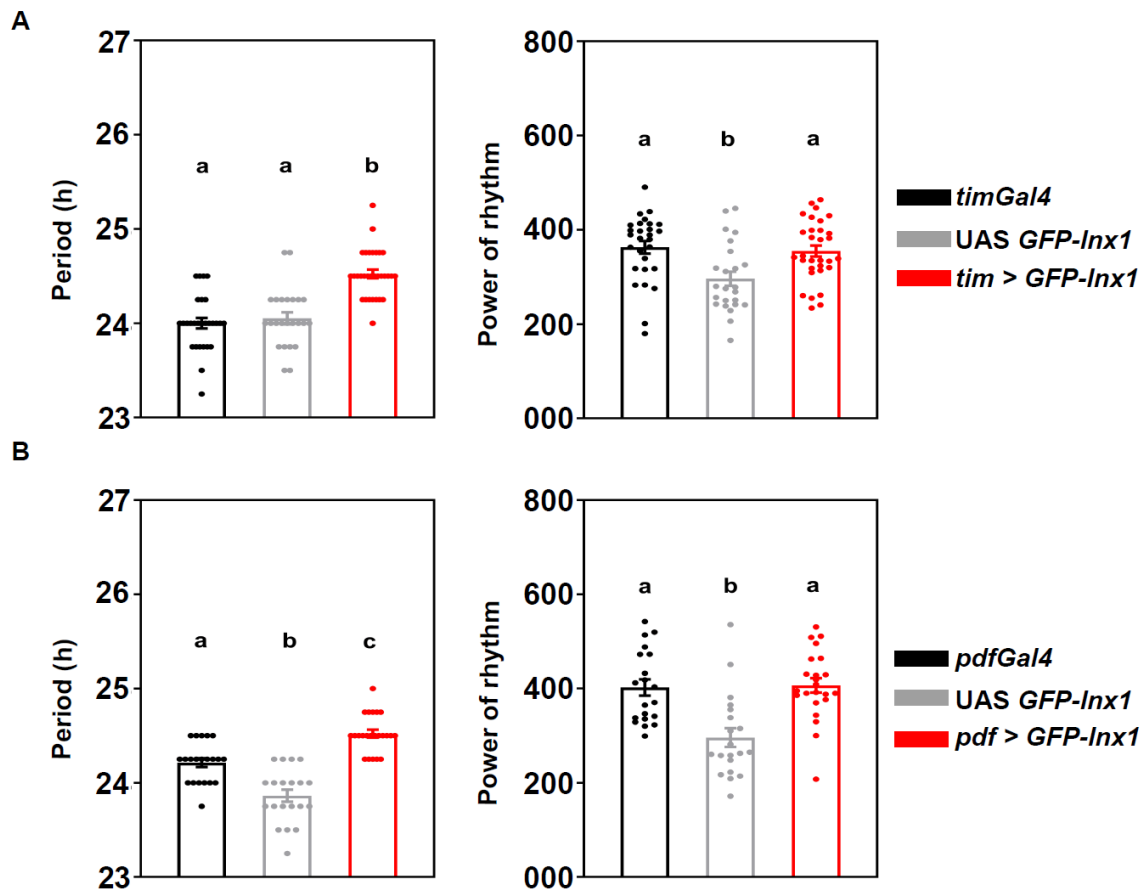
Figure 4.15: Altering the gap-junction forming domain of Innexin1 lengthens the free-running period (A) Free-running period (left) and power of rhythm (right) of experimental flies (*tim > GFP-Inx1*) (*n=31*) is plotted along with its Gal4 control (*n=28*) and the UAS control (*n=24*) flies **(B)** Free-running period (left) and power of rhythm (right) of experimental flies (*pdf > GFP-Inx1*) (*n=23*) is plotted along with its Gal4 control (*n=22*) and UAS control (*n=21*) flies. Error bars are SEM, period and power values are determined using Chi-square periodogram for a period of 7 days, all statistical comparisons are performed using one-way ANOVA with genotype as a fixed factor followed by post-hoc Tukey's HSD test.

4.3.9 Effect of *Innexin1* knockdown on the molecular clock protein oscillation in circadian clock neurons.

To examine the effect of *Innexin1* knockdown on the oscillation of molecular clock protein in clock neurons, I dissected the brains of control (*dcr; Inx1* RNAi) and experimental (*Clk856 > dcr; Inx1* RNAi) flies on day 3 of constant darkness (DD day3), every 4 hours for a period of 24-hours and examined the levels of clock protein Period (PER). I plotted

the values of PER intensity over time for the two groups of ventral lateral neurons and proceeded to fit a COSINOR wave of a specific periodicity to estimate the phase and amplitude of the oscillation. Since the conventional methods of phase estimation from oscillatory waveforms, which assume the underlying waveform to be sinusoidal, including COSINOR, did not fit well with this data, I used a non-parametric method called RAIN (Rhythmicity Analysis Incorporating Non-parametric methods) (Thaben and Westermark, 2014) to test for rhythmicity and to extract phase information from the underlying waveform. In the case of the small ventral lateral neurons (s-LNv), RAIN analysis revealed the presence of significant 24-hour rhythms in PER oscillations of both control ($p = 4.01E-18$) and experimental flies ($p = 1.02E-16$) (Fig. 4.16A and B, Fig. 4.16C, left, Appendix 4.11). The predicted acrophase of oscillation for experimental flies (CT 8) was found to be delayed as compared to the control flies (CT 4) (Appendix 4.11), suggesting that knockdown of *Innexin1* delays the molecular clock in the s-LNv. I also performed a pairwise comparison among genotypes at each of the time points. I found that PER intensities are significantly different in experimental flies as compared to control flies at time points where the PER intensity curve is rising (CT19 and CT23) and falling (CT7 and CT11) (Mann-Whitney U test, $p < 0.05$) and not different at other time points (CT3 and CT15) (Mann-Whitney U test, $p > 0.05$) (Appendix 4.14). This suggests that PER protein intensities are rising and falling slower in experimental flies as compared to control flies, which results in an overall phase delay in the molecular clock oscillation. Thus, lack of *Innexin1* possibly affects the free-running period via the molecular clocks. In the case of the large ventral lateral neurons (l-LNv), RAIN analysis could not detect the presence of 24-hour rhythmic oscillations in control flies ($p = 0.1124$). In contrast, experimental flies showed significant 24-hour rhythmic oscillations ($5.62E-06$) (Fig. 4.16C right, Appendix 4.12). This is not surprising as several previous studies have observed PER oscillations to

dampen in l-LNv around 2-6 days in constant darkness (Shafer et al., 2002; Yang and Sehgal, 2001). Since the control flies did not show significant 24-hour oscillations, I could not estimate and compare the phase of PER oscillations among the control and experimental genotypes in the l-LNvs.
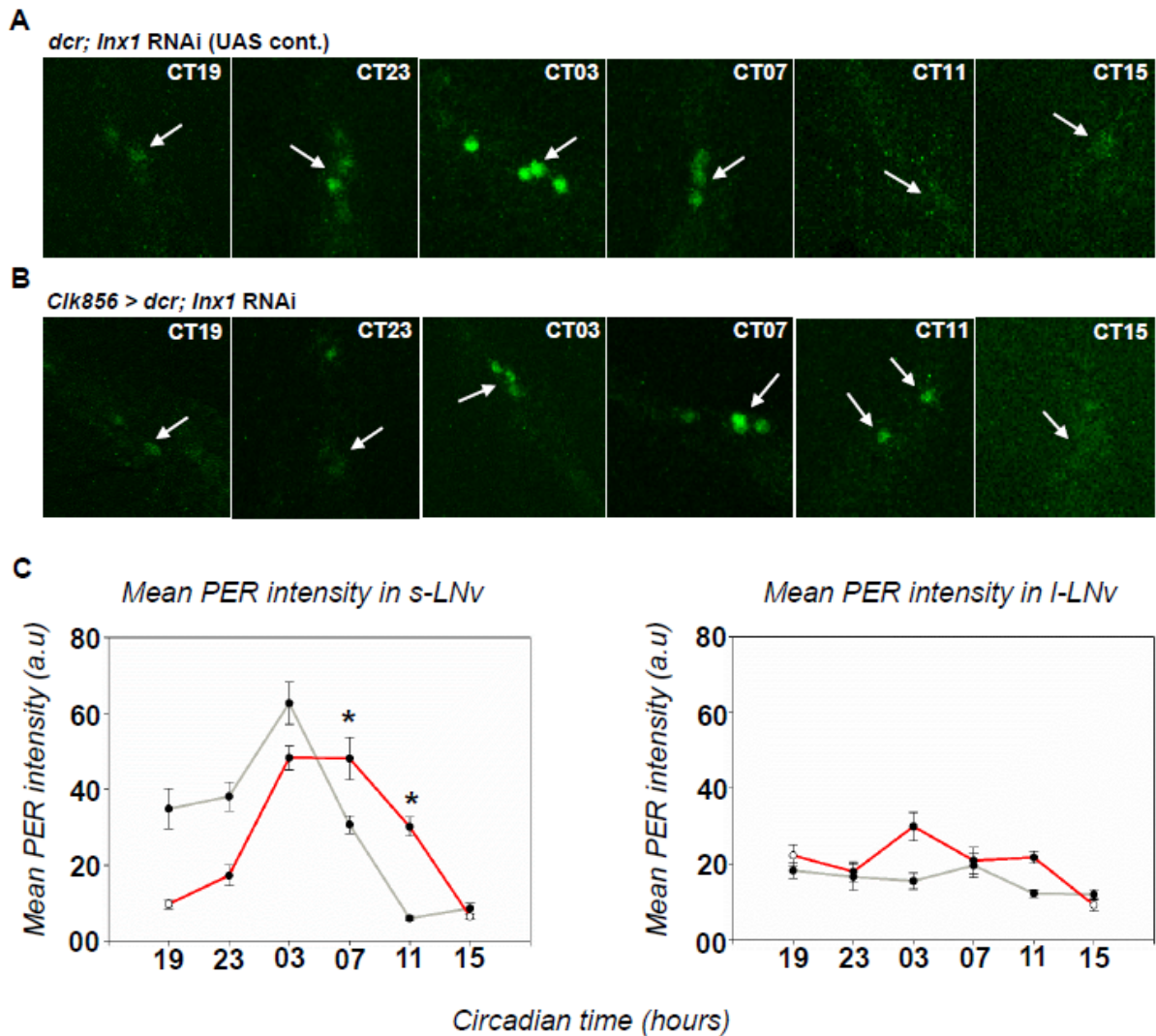
Figure 4.16: Effect of *Innexin1* knockdown on molecular clock protein oscillation in the ventral lateral neurons Representative images of PER intensity in s-LNv at six different time points of a 24-hour cycle on the third day of DD 25°C in both control (UAS *dcr Inx1* RNAi) **(A)** and experimental (*Clk856 > dcr;Inx1* RNAi) **(B)** flies. **(C)** Mean intensity of Period (PER) protein oscillation in small ventral lateral neurons (s-LNv) **(left)** and large ventral lateral neurons (l-LNv) **(right)** plotted at each of the time points over a 24-hour cycle in both control (*dcr; Inx1 RNAi*) and experimental (*Clk856 > dcr; Inx1 RNAi*) flies on day 3 of constant darkness (DD day3). Rhythmicity of oscillations and phase estimations are done using RAIN (see appendix table 4.11 and 4.12 for more details). The value at each timepoint is obtained by averaging across at least 11 brain

samples for both control and experimental genotypes and for both cell types. Error bars are SEM.

4.3.10 Effect of knockdown of *Innexin1* on the oscillation of Pigment Dispersing Factor (PDF) in the s-LNv dorsal projection.

s-LNv release the neuropeptide Pigment Dispersing Factor (PDF), which rhythmically accumulates in its dorsal terminals in a time-of-day dependent manner (Park et al., 2000). PDF is required to maintain rhythmicity under constant darkness, synchronize clocks of non-LNv cells, and acts as a major output factor in the clock network (reviewed in Shafer and Yao, 2014). PDF cycling in dorsal terminals is abolished in clock mutants, but it could also be independently affected by other factors like light and membrane excitability states of the ventral lateral neurons (Abhilash et al., 2020; Mezan et al., 2016; Nitabach et al., 2006; Prakash et al., 2017). Since gap junctions are known to affect the synchronous release of neuropeptides and neurotransmitters, I wanted to examine the effect of *Innexin1* knockdown on the levels and oscillation of PDF in dorsal terminals. Similar to the previous experiment, I dissected the brains of control (*dcr; Inx1* RNAi) and experimental (*Clk856 > dcr; Inx1* RNAi) flies on day 3 of constant darkness (DD day 3), every 4 hours for a period of 24 hours and stained to check the levels of PDF in s-LNv dorsal terminals. I plotted the values of PDF intensity over time for both the genotypes and estimated rhythmicity and phase using RAIN. RAIN analysis indicates the presence of significant 24-hour rhythms in PDF oscillations in control flies (p = 7.07E-09) and experimental flies (p = 0.00018) (Fig. 4.17A and B, Fig. 4.17C, Appendix 4.13). The predicted phase of oscillation of PDF in experimental flies (CT 8) was found to be delayed as compared to control flies (CT 4), suggesting that knockdown of *Innexin1* delayed the oscillation of PDF, probably via the s-LNv molecular clock (Fig. 4.17C, Appendix 4.13). Similar to

Innexin2 knockdown (described in Chapter 3, Fig. 3.15), even in this case, I observe that the PDF levels in dorsal projections are significantly higher in experimental flies than control flies (Fig. 4.17D), suggesting that lack of *Innexin1* could affect neuropeptide release in the s-LNv dorsal terminal.
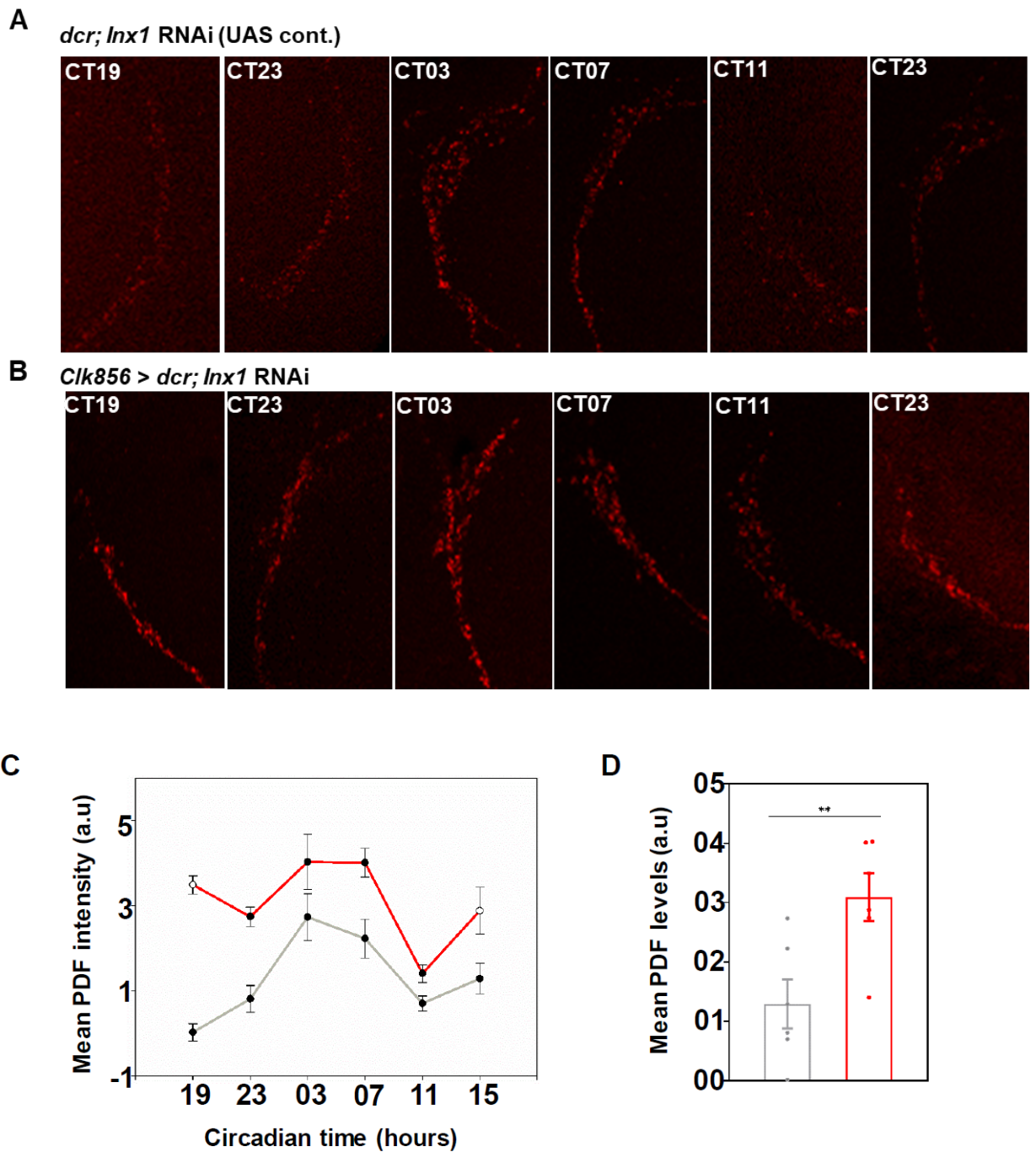
Figure 4.17: Knockdown of *Innexin1* affects the levels of PDF in the s-LNv dorsal projections Representative images of PDF intensity in the s-LNv dorsal projections at six different time points of a 24-hour cycle on third day of DD 25°C in both control (UAS *dcr;Inx1* RNAi) **(A)** and experimental (*Clk856 > dcr;Inx1* RNAi) **(B)** flies. **(C)** Mean intensity of PDF in the dorsal projection of small ventral lateral neurons (s-LNv) plotted at each time point over a 24-hour cycle in both control (*dcr; Inx1 RNAi*) and experimental (*Clk856 > dcr; Inx1 RNAi*) flies on day 3 of constant darkness (DD day3). Rhythmicity of oscillations and phase estimations are done using RAIN (see appendix table 4.13 for more details). The value at each time point is obtained by averaging across at least 13 brain samples for both control and experimental genotypes. Error bars are SEM. **(D)** The overall levels of PDF in the dorsal projections are significantly higher in experimental flies as compared to control flies (Wilcoxon matched pair test, *p = 0.002*). Error bars are SEM.

4.4 Discussion

4.4.1 Innexin1 in clock neurons and astrocytes modulates the free-running period

While Innexin1 has been extensively studied during the development of nervous systems, there are very few reports which show a role for Innexin1 in adult behaviours. My RNAi-based knockdown screen for gap junction genes that modulate circadian rhythm properties identified Innexin1 as a potential candidate (See chapter 2). Using two independent RNAi constructs and a whole-body mutant of *Innexin1*, I establish that Innexin1 is required in clock neurons to modulate the circadian clock's critical and core property, its free-running period. I further restricted the knockdown of *Innexin1* to specific subsets of clock neurons and found it to be important in the ventral lateral neurons, a subset of which are crucial to regulate clock properties like rhythmicity and free-running period under constant conditions (DD 25°C), as shown by several previous studies (Delventhal et al., 2019; Grima et al., 2004; Helfrich-Förster, 1998; Renn et al., 1999; Schlichting et al., 2019; Stoleru et al., 2004; Yao and Shafer, 2014). The power of the rhythm, in experimental flies, in the case of *Innexin1* knockdown, however, was not found to be significantly different from the control flies, in most cases except when *Innexin1* was downregulated

using *dvpdfGal4*. While the power of rhythm in the case of *ogre KO* was slightly but significantly lower than the controls, the difference seen with *dvpdfGal4* was much higher. This inconsistency of an RNAi construct showing a better reduction in rhythm power compared to controls could be because knockdown of *Innexin1* affects rhythm power, and the *Innexin1* mutant used is not a true null, but a hypomorph, as suggested by previous studies (Curtin et al., 2002; Watanabe and Kankel, 1992, 1990). Apart from the ventral lateral neurons, our behavioural studies indicate that Innexin1 functions in a subset of glial cells- astrocytes to modulate the free-running rhythms. Astrocytes are a major type of glial cells (~ 4600) present in the adult *Drosophila* brain (Bittern et al., 2021). They have been shown to play roles in sleep and circadian behaviour in *Drosophila* (Chaturvedi et al., 2021; Davla et al., 2020; Farca Luna et al., 2017; Gerstner et al., 2017; Vanderheyden et al., 2018; Ng et al., 2011). While the clocks in astrocytes do not seem to play a role in modulating activity-rest under constant conditions (DD 25°C), the membrane properties, calcium levels, and communication between astrocytes and neurons are necessary to sustain rhythmic activity-rest behaviour (Ng et al., 2011). Astrocytes in *Drosophila* and mammals are known to express gap junction proteins that are involved in coupling among astrocytes, the release of gliotransmitters, and regulation of neurotransmitter homeostasis (Bittern et al., 2021). Recently, a study in mice revealed the importance of Connexin43; a major gap junction expressed in astrocytes, in regulating molecular oscillations and period of behavioural rhythms in the SCN (Brancaccio et al., 2019). While the mechanism of action by which Innexin1 in astrocytes affects the free-running period is currently unknown, there are possible hypotheses that could be tested in the future. Innexin1 in astrocytes may be important in glia-neuron communication and release of gliotransmitters, modulating the clock neurons to affect the free-running period. While the identity of gliotransmitters in *Drosophila* is still unknown, some small secretory molecules like

Noktochor (Nkt) and TNF-alpha homologue, Eiger, could be the possible candidates (Vanderheyden et al., 2018; Sengupta et al., 2019). In support of our findings, a recent report showed that blocking Nitric Oxide (NO) signalling in astrocytes lengthens the free-running period (Kozlov et al., 2020), suggesting that astrocyte-neuron communication is an important modulator of free-running rhythms and Innexin1 could be a potential candidate in this communication axis. While Innexin1 in astrocytes may modulate the free-running period via the molecular clocks, an alternate hypothesis could be that they directly and independently affect the levels and oscillation of PDF in the dorsal terminals. Evidence for this hypothesis has been previously reported by two other studies which show that disrupting the communication between astrocytes and neurons could directly affect PDF levels and oscillations in the dorsal terminals (Kozlov et al., 2020; Ng et al., 2011).

4.4.2 Adult versus developmental roles of Innexin1 in the clock circuit

Both adult-specific and development-specific knockdown of *Innexin1* in the clock neurons leads to lengthening of the free-running period, suggesting that Innexin1 has roles in both the life stages of the fly in modulating the free-running period. The mechanisms by which period modulation is brought about at each stage could be similar or different. Several studies, both in vertebrates and invertebrates, implicate a role for electrical synapses in the proper development of nervous systems and placement of chemical synapses (reviewed in Pereda, 2014). Innexin1 is widely expressed in *Drosophila* glial cells during the development of the entire nervous system and is required for their proper functioning (Holcroft et al., 2013; Kottmeier et al., 2020; Lipshitz and Kankel, 1985; Spéder and Brand, 2014). While currently it is unclear whether the function of Innexin1in the ventral lateral neurons or astrocytes are essential during development or adult-specific stages, systematic and stage-specific knockdown of *Innexin1* in these sets of cells will be able to distinguish these roles. I did not observe gross morphological changes in the anatomy,

number, and position of the clock cells or the projection pattern of PDF projections upon knockdown of *Innexin1* in the developmental stages. However, one cannot rule out the micro-anatomical changes in the clock circuit, which could eventually affect clock properties. Both in vertebrates and invertebrates, it has been well-established that there is a network of electrical synapses formed during development which lays down the blueprint of the nervous system organization for the animal by regulating several processes like cell differentiation, cell migration, placement of chemical synapses, and formation of neuronal circuits (reviewed in Pereda, 2014). Currently, it is unknown whether gap junctions made up of Innexin1 may regulate any of these processes in the development of clock circuitry, but future experiments where Innexin1 is rescued at various stages of development in an *Innexin1* null background could shed some light on its functions during these processes.

4.4.3 Overexpression of Innexin1 and Innexin2 in clock neurons

Since knockdown of *Innexin1* leads to lengthening of the free-running period by about 1.5 hours, it was surprising to me that overexpression of *Innexin1* did not affect the free-running period. I used two different, full-length protein constructs of Innexin1, *Inx1-GFP*, and *Inx1-myc* but did not observe any change in period upon their overexpression. I also overexpressed Innexin1 and Innexin2 simultaneously, as it is known that these two proteins interact to form heteromeric channels together (Holcroft et al., 2013) and knockdown of each of them individually leads to period lengthening. Surprisingly, overexpression of *Innexin1* and *Innexin2* simultaneously also did not affect the free-running period. A possible explanation for this phenomenon could be a regulation imposed by the cell in the number of gap junction units that can be positioned in the membrane as a part of a functional gap junction plaque. While I did not come across such studies in the case of Innexins, many reports investigate the dynamics of assembly of Connexin proteins and their insertion into the plasma membrane. Studies in cell lines that

use fluorescently tagged Connexin proteins reveal that the size and number of gap junction plaques on the membrane is highly regulated, such that the addition of newly synthesized channels is always accompanied by the removal of an older one such that steady-state is maintained, a phenomenon consistently observed with Connexin plaques (Gaietta et al., 2002; Lauf et al., 2002). Hence it is possible that Innexin1 and Innexin2 levels are overexpressed in the cells, but their entry into the membrane is highly regulated. Thus I do not see any effect of overexpression at the level of behaviour. This hypothesis needs experimental validation. A possible experiment would be to fluorescently tag Innexin1 and Innexin2 proteins and overexpress them in a *Drosophila* neuronal cell line to study the dynamics of entry, stabilization, and destabilization of these proteins on the membrane.

4.4.4 Mechanism of action of Innexin1 in the clock network

My genetic and behavioural screen revealed that Innexin1 functions in the ventral lateral clock neurons to modulate the free-running period. To further investigate the underlying mechanism of action of Innexin1 in the clock circuit, I examined the effect of *Innexin1* knockdown on the phase of oscillation of the molecular clock protein, PERIOD in these cells. In the case of s-LNv, I found that both the control and experimental flies exhibit robust, 24-hour rhythms in the oscillation of PER protein, thus suggesting that knockdown of *Innexin1* does not affect the rhythmicity of oscillation of the molecular clock. However, I observe that the phase of oscillation of PER in s-LNv is phase-delayed in experimental flies exhibiting long free-running periods as compared to control flies. Further, I also found that PER protein levels rise and fall slowly in experimental flies compared to control flies. These results suggest that Innexin1 modulates the free-running period, possibly via the molecular clocks. In case of the l-LNvs, I do not detect a significant 24-hour rhythm even in the case of control flies. This phenomenon has been observed previously by several other groups, which report that the molecular clock protein oscillations in the l-

LNv dampen fast when flies are introduced to DD conditions (Roberts et al., 2015; Shafer et al., 2002; Yang and Sehgal, 2001). When the cells of control flies do not show robustly rhythmic oscillations, it is futile to compare the phases of oscillations between control and experimental flies.

How does Innexin1 affect the phase of oscillation of molecular clock protein in the s-LNv? Innexin1 could determine membrane properties such as firing rate and synchronous firing among the s-LNv clock neurons, translating into a change in clock gene expression patterns. Several previous studies have shown the influence of membrane properties on the molecular clock. A disruption in firing pattern and properties leads to disruption of molecular clock protein oscillations (Depetris-Chauvin et al., 2011; Mizrak et al., 2012; Nitabach et al., 2006, 2002). Alternatively, it is possible that the gap junctions made up of Innexin1 protein are necessary for the passage of small, secondary messengers, which could be essential for the proper functioning of the clock machinery. Lack of these molecule/s could then delay the TTFL machinery, which is reflected in the phase of molecular protein oscillations and eventually as lengthening of the free-running period.

Apart from the molecular clocks, I also examined the status of oscillation of a major output neuropeptide secreted by the clock neurons, PDF, in the s-LNv dorsal projection. PDF oscillations showed robust and significant 24-hour rhythms both in the case of control and experimental flies, thus suggesting that knockdown of *Innexin1* does not affect the rhythmicity of PDF oscillations in the dorsal terminals. The phase of oscillation of PDF in experimental flies was found to be delayed as compared to control flies. This suggests that Innexin1 affects the phase of PDF oscillations, either directly or via the s-LNv molecular clock. I also observe that PDF levels in the dorsal projections are significantly higher in experimental flies compared to control flies. Higher PDF levels in the dorsal termini are associated with a delay in the clocks in the other cells of the clock circuit,

170

leading to period lengthening (reviewed in Shafer and Yao, 2014). I hypothesize that gap junctions made up of Innexin1 could be involved in the efficient release of neuropeptide PDF in the dorsal terminals and a lack of Innexin1 leads to its accumulation in the termini. Synchronized firing of neurons for the efficient release of neuropeptides is an important function of gap junction proteins observed in Connexins (Pereda, 2014). Alternatively, lack of Innexin1 in the membrane could result in overall higher transcription of PDF, leading to its higher accumulation in the dorsal terminals, as membrane properties could also affect PDF levels independently of the molecular clock (Mezan et al., 2016). It would be interesting to see whether the secretion of PDF from the dorsal terminals is itself affected in the case of Innexin1 mutants.

Chapter 5: Conclusions

The neuronal and molecular mechanisms underlying circadian rhythms have been extensively studied in *Drosophila melanogaster* for many years. Yet, we do not have a complete understanding of how free-running behavioural rhythms with a near 24-hour periodicity are generated by the network. Coherent rhythms in behaviour and physiology are generated only when the underlying neuronal oscillators function as a network. Both mathematical modelling and experimental studies have shown this phenomenon to be true in multiple model systems ranging from plants to *Drosophila* to mammalian circadian clocks (Beckwith and Ceriani, 2015; Gu et al., 2021; Herzog et al., 2017; Micklem and Locke, 2021). Circadian neurons are known to communicate extensively amongst themselves and with the downstream output centres using chemical modes of communication mediated by neurotransmitters and neuropeptides. However, very few reports examine a role for electrical synapses in communication among circadian neurons. Although studies in mammals indicate that gap junctions play a role in regulating some aspects of circadian rhythms (Diemer et al., 2017; Long et al., 2005; Wang et al., 2014), there has been no systematic investigation of the roles of each of these gap junction genes and the mechanisms by which they regulate rhythm properties. This motivated me to ask if gap junctions contribute to regulating circadian rhythms in *Drosophila melanogaster* by downregulating each of the eight gap junction genes and examining circadian locomotion under both constant conditions and different cyclic environments.

I found that gap junction genes *Innexin1* and *Innexin2* function in circadian neurons to determine a near 24-hour free-running period in locomotor activity rhythm, and that downregulation of the levels of these *Innexins* lengthen the free-running period. Knockdown of *Innexin1* and *Innexin2* delays the phase of oscillations of the core clock protein Period in clock neurons. This suggests that Innexins affect the free-running period via the molecular clock machinery. Although Innexin2 is present and functions only in

the ventral lateral neurons, molecular clocks are delayed in most other neuronal subsets in the clock network, suggesting that network synchrony of molecular clock oscillations is perhaps not affected. In the case of mammals, *Connexin36* knockout mice show a lengthened period of free-running rhythms in wheel-running activity, as well as a lengthening of the period of molecular clocks, but the phase dispersion of molecular clock protein oscillations across SCN cells is not affected in experimental mice (Diemer et al., 2017). Thus, my studies with *Innexin* downregulation in flies show similarities to the behavioural and molecular phenotypes seen in *Connexin36* knockout mice. This suggests that gap junctions possibly have conserved functions and mechanisms in both invertebrates and vertebrates in modulating circadian rhythm properties. My RNAi-mediated knockdown screen of *Innexins* and downregulation of *Innexin1* and *Innexin2* in most clock and non-clock neuronal subsets did not significantly affect the power of rhythm or consolidation of activity. Similarly, knockdown of *Innexin1* and *Innexin2* also did not affect the precision of activity-rest rhythms. Overall, all the above results put together suggest that Innexin1 and Innexin2 function in the circadian network to determine the free-running period, but they possibly do not affect the synchrony of the network as seen with the synchronous phase of PER oscillations across most clock neurons as well as lack of an effect on the power and precision of rhythms upon their downregulation.

How do Innexin1 and Innexin2 affect the free-running period? My experiments using constructs that selectively affect the channel-forming domain of Innexins suggest that these proteins function as hemichannels or gap junctions in clock neurons. There could be two possible hypotheses for the mechanism by which Innexin1 and 2 in the LNv membrane could affect the free-running period. The first possibility is that these Innexins could be involved in electrical coupling and synchronous neuronal firing among the LNv cells, and its absence results in desynchronized firing, which affects the release of PDF

from s-LNv dorsal terminals (Fig. 5.1). This hypothesis is supported by previous studies in mammals which show that SCN neurons in gap junction mutant mice fire action potentials in a desynchronized manner (Long et al., 2005). Similar desynchronization of clock neuronal firing was also reported in invertebrates when gap junction blockers were applied to the bath while recording from the accessory medulla region (Schneider and Stengl, 2006). While the significance of synchronized firing of circadian neurons for rhythmic behaviour is unclear, examples from other instances have suggested that a pre-synaptic group of neurons are most efficient in driving post-synaptic sites when their firing is synchronized (Long et al., 2005). In my experiments, I find that the amplitude of PDF oscillation and level of PDF in the s-LNv dorsal projections is significantly higher in each of the cases where *Innexin1* and *Innexin2* are downregulated. Several previous studies have shown that PDF acts to lengthen the period of the circadian network and that overexpression or ectopic expression of PDF in the dorsal protocerebrum lengthens the period of activity rhythms, leads to desynchronization of activity-rest behaviour and molecular clocks in the circadian neurons (Helfrich-Förster et al., 2000; Shafer and Yao, 2014; Wülbeck et al., 2008b). While higher levels of PDF observed in termini of experimental flies does not necessarily imply a defect in the release of the neuropeptide, it would be worthwhile to assess if the release of neuropeptide from LNv termini is actually affected upon *Innexin* downregulation. A recent study examines the dynamics of release of neuropeptide from the LNv cells using a fluorescent neuropeptide release indicator, Dilp2-FAP (Klose et al., 2021). Blocking neuropeptide release from LNv soma and termini adversely affects circadian behaviour indicating the importance of neuropeptide release from these cells. It would be interesting to examine the effect of knockdown of *Innexin1* and *Innexin2* on the dynamics of neuropeptide release from LNv cells and termini.

An alternate possibility could be that Innexin1 and 2 are necessary to maintain the appropriate membrane potential of the LNv at specific times of the day or to regulate the number, frequency or pattern of action potential firing in these cells. Disruption of this temporal pattern of firing in case of knockdown of *Innexins* could translate into a delay in the molecular clocks in LNvs, which in turn could be transmitted to other neurons in the circuit via PDF (Fig. 5.1). Previous studies have shown that membrane excitability states of the LNv can affect both the core molecular clock and properties of activity-rest rhythms (Mizrak et al., 2012; Nitabach et al., 2006, 2002). Indeed, there is some evidence to suggest that gap junctions affect the frequency of firing of action potentials in the l-LNv membrane. A study by Cao and Nitabach using gap junction blocker Carbenoxolone in the bath showed that blocking electrical synapses in the l-LNvs reduces the frequency of firing of action potentials in these cells (Cao and Nitabach, 2008). Presently, it is not clear how these changes in firing frequency may alter the core molecular clock in circadian pacemakers, however studies performed on neurons from the dorsal root ganglion suggest that expression levels of many genes are highly affected by firing frequency (Fields et al., 1997; Lee et al., 2017). The effect of knockdown of *Innexin1* and *Innexin2* on membrane properties can be measured via electrophysiological recordings of LNv clock cells. However, this could be technically challenging (Fernandez-Chiappe et al., 2021, 2020). An alternate approach would be to estimate changes in membrane activity using fluorescent reporters like ArcLight or GCaMP in both control and experimental flies under constant conditions (DD 25°C). The above mentioned hypotheses need not be mutually exclusive and the actual mechanism of action of Innexins in clock neurons could be a combination of both. Future experiments intended to distinguish between these possibilities will shed light on the mechanisms by which Innexins function in clock neurons.
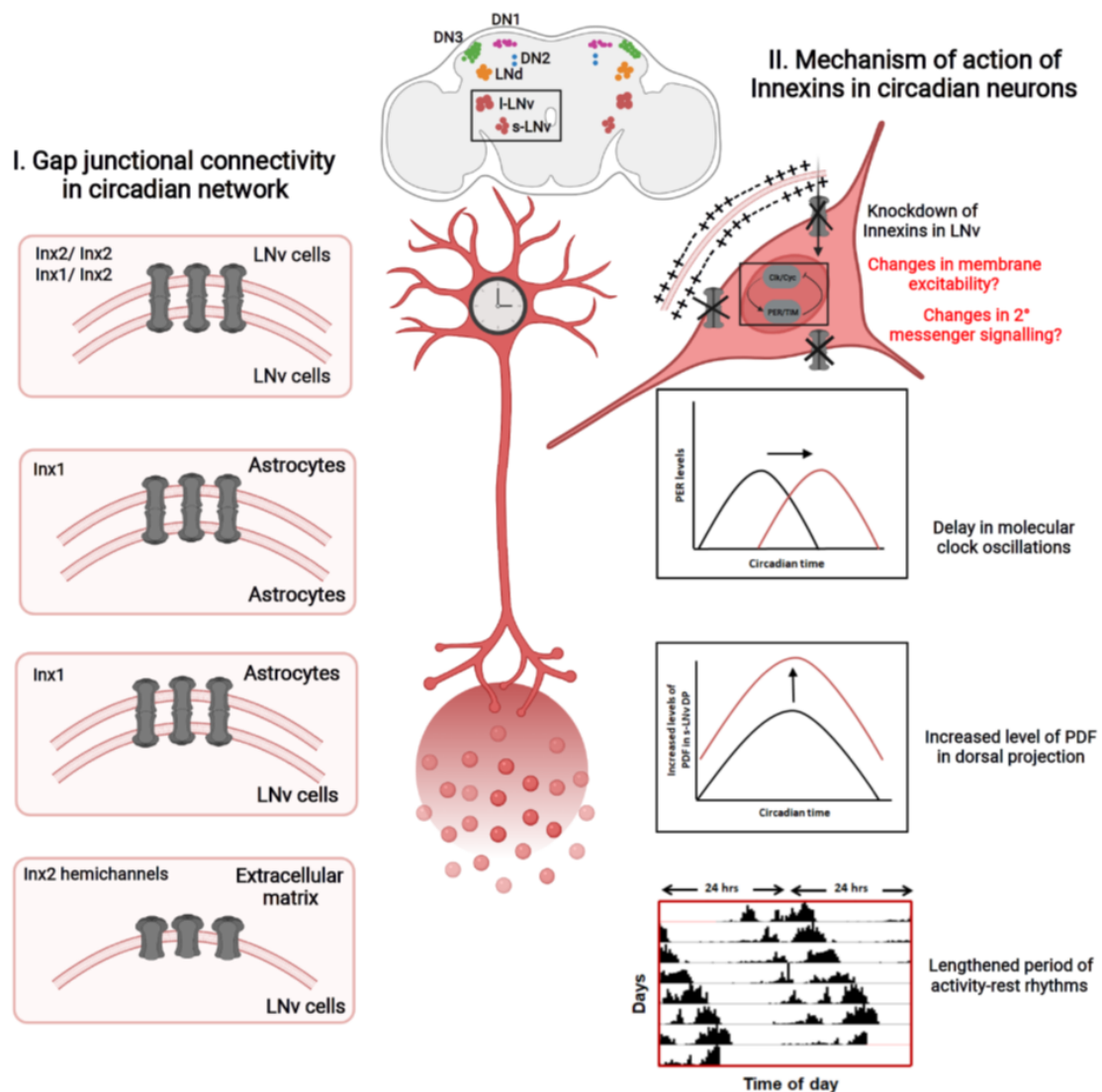
Figure 5.1: (I) Summary of all the possible combinations of gap junctions and/or hemi channels formed by Innexin1 and Innexin2 proteins in the circadian neurons and astrocytes to regulate circadian period based on my experimental results and previous reports. **(II)** Summary of the possible mechanism of action of Innexin1 and 2 in clock neurons. Knockdown of *Innexin1* or *Innexin2* could potentially affect the core clock machinery (TTFL) either by altering the membrane potential or cellular signalling via secondary messengers. This could result in a phase-delay in the oscillation of core clock protein, Period, increase in levels and amplitude of oscillation of the circadian neuropeptide PDF and, lengthening of the free-running period of activity-rest rhythms.

My behavioural studies indicate that Innexin1 could be functioning in a subset of glia, the astrocyte-like glia to modulate the free-running period. This is similar to a recent finding in mammals of the roles of gap junction protein Connexin43 in astrocytes in regulating molecular clocks and rhythmicity of SCN network under free-running conditions (Brancaccio et al., 2019); again emphasizing on the similarities between the roles of Connexins and Innexins in circadian networks. It would be pertinent to investigate the mechanisms by which Innexin1 function in astrocytes. Does Innexin1 facilitate coupling among astrocytes? Or does it facilitate coupling between astrocytes and clock neurons? (Fig. 5.1). Does astrocyte-specific knockdown of *Innexin1* affect the molecular clocks or the clock outputs? Since previous studies have shown that crosstalk between astrocytes and neurons is necessary for coherent behavioural rhythms (Kozlov et al., 2020; Ng et al., 2011), it would be interesting to examine if Innexin1 is necessary for this communication and does the loss of *Innexin1* disrupt the astrocyte-neuron communication axis.

Apart from its roles in regulating membrane potential and synchronized firing of neurons, gap junctions could also act as conduits for the passage of small molecules like secondary messengers and calcium between adjacent cells and between the cell and extracellular matrix (Nielsen et al., 2012). Calcium signalling and calcium oscillations in circadian neurons play crucial roles in regulating molecular clocks as well as behavioural rhythms in both *Drosophila* and mammalian systems (Cavieres-Lepe and Ewer, 2021). Disrupting calcium homeostasis in *Drosophila* circadian neurons results in lengthened period of behavioural rhythms (Harrisingh et al., 2007). This suggests that calcium levels are intricately linked to the behavioural period in *Drosophila*. *Drosophila* clock neurons also display spontaneous and asynchronous Ca^{+2} oscillations across cells in the network under constant conditions, and this is mediated by PDF, suggesting the importance of communication in the network for regulating these oscillations (Liang et al., 2016). It

would be interesting to assay calcium levels and oscillations in case of downregulation of *Innexin1* and *Innexin2* in clock neurons to examine if the lack of *Innexins* could affect calcium dynamics in clock neurons (Fig. 5.1).

Do Innexin1 and 2 form gap junctions together in ventral lateral neurons? (Fig. 5.1). Gap junction hemichannels can be classified as homomeric or heteromeric, composed of the same or different subunits of gap junction proteins, respectively. Intercellular channels are called homomeric if the hemichannel is made up of the same protein and heteromeric if the hemichannel is made up of different types of proteins (Faber and Pereda, 2018). Previous studies have reported that Innexin1 and Innexin2 could form functional heteromeric gap junctions or Innexin2 could form homotypic gap junctions with itself to facilitate passage of ions and/or secondary messengers or small molecules (Bauer et al., 2003; Bohrmann and Zimmermann, 2008; Holcroft et al., 2013). Alternatively, Innexin2 can also function as a hemichannel and facilitate coupling between the cell and extracellular matrix. However, this needs further validation. Co-localization of Innexin1 and Innexin2 in ventral lateral neurons could provide some evidence that these proteins could be functioning together in these cells to modulate the free-running period. The recently developed technique by Wu et al. to demonstrate functional electrical coupling among cells - PARIS (Pairing Actuators and Receivers to Optically Isolate Gap junctions) (Wu et al., 2019) could prove to be useful. Application of this method to determine functional electrical coupling among the clock neurons would be important to answer these questions. Additionally, the use of blockers that specifically disrupt hemichannels in the bath medium while recording for testing functional coupling of cells using PARIS could help distinguish the gap junction and hemichannel-based functions of Innexins in clock neurons.

Taken together, my findings highlight a hitherto unknown role for Innexins in the adult circadian pacemaker circuit of *D. melanogaster* in determining the free-running period of activity rhythms as well as phasing of activity under LD cycles and reveals that circadian timekeeping is brought about by a combination of electrical and chemical synapses in the underlying neuronal network.

References

Abhilash, L., Ramakrishnan, A., Priya, S., Sheeba, V., 2020. Waveform Plasticity under Entrainment to 12-h T -cycles in *Drosophila melanogaster* : Behavior , Neuronal Network , and Evolution J. Biol. Rhythms 35(2), 145–157.

Abhilash, L., Sheeba, V., 2019. RhythmicAlly: Your R and Shiny–Based Open-Source Ally for the Analysis of Biological Rhythms. J. Biol. Rhythms 34, 551–561.

Allada, R., White, N.E., So, W.V., Hall, J.C., Rosbash, M., 1998. A Mutant *Drosophila* Homolog of Mammalian Clock Disrupts Circadian Rhythms and Transcription of period and timeless, Cell, 93, 791–804.

Andreazzoli, M. and Angeloni, D., 2017. The amphibian clock system. In *Biological Timekeeping: Clocks, Rhythms and Behaviour* (pp. 211-222). Springer, New Delhi.

Hur, K.C., Shim, J., Johnson, R.G., 2009. Cell Communication & Adhesion A Potential Role for Cx43-Hemichannels in A Potential Role for Cx43-Hemichannels in Staurosporin-Induced Apoptosis 9061.

Attwell, D., Borges, S., Wu, S.M. and Wilson, M., 1987. Signal clipping by the rod output synapse. *Nature*, *328*(6130), pp.522-524.

Bahn, J.H., Lee, G., Park, J.H., 2009. Comparative analysis of Pdf-mediated circadian behaviors between *Drosophila melanogaster* and *D. virilis*. Genetics 181, 965–975.

Barber, A.F., Erion, R., Holmes, T.C., Sehgal, A., 2016. Circadian and feeding cues integrate to drive rhythms of physiology in *Drosophila* insulin-producing cells. Genes Dev. 30, 2596–2606.

Barrio, L.C., Suchyna, T., Bargiello, T., Xu, L.X., Roginski, R.S., Bennett, M.V. and

Nicholson, B.J., 1991. Gap junctions formed by connexins 26 and 32 alone and in combination are differently affected by applied voltage. *Proceedings of the National Academy of Sciences*, *88*(19), pp.8410-8414.

Bartos, M., Vida, I., Frotscher, M., Meyer, A., Monyer, H., Geiger, J.R. and Jonas, P., 2002. Fast synaptic inhibition promotes synchronized gamma oscillations in hippocampal interneuron networks. *Proceedings of the National Academy of Sciences*, *99*(20), pp.13222-13227.

Bauer, R., Lehmann, C., Fuss, B., Eckardt, F., Hoch, M., 2002. The *Drosophila* gap junction channel gene innexin 2 controls foregut development in response to Wingless signalling. J. Cell Sci. 115, 1859–1867.

Bauer, R., Lehmann, C., Martini, J., Eckardt, F., Hoch, M., 2004. Gap Junction Channel Protein Innexin 2 Is Essential for Epithelial Morphogenesis in the *Drosophila* Embryo. Mol. Biol. Cell 15, 2992–3004.

Bauer, R., Löer, B., Ostrowski, K., Martini, J., Weimbs, A., Lechner, H., Hoch, M., 2005. Intercellular communication: The *Drosophila* innexin multiprotein family of gap junction proteins. Chem. Biol. 12, 515–526.

Bauer, R., Martini, J., Lehmann, C., Hoch, M., 2003. Cellular Distribution of Innexin 1 and 2 Gap Junctional Channel Proteins in Epithelia of the *Drosophila* embryo. Cell Commun. Adhes. 10, 221–225.

Beckwith, E.J., Ceriani, M.F., 2015. Communication between circadian clusters: The key to a plastic network. FEBS Lett. 589, 3336–3342.

Bell-Pedersen, D., Cassone, V.M., Earnest, D.J., Golden, S.S., Hardin, P.E., Thomas, T.L. and Zoran, M.J., 2005. Circadian rhythms from multiple oscillators: lessons

from diverse organisms. *Nature Reviews Genetics*, *6*(7), pp.544-556.

Belliveau, D.J., Bani-yaghoub, M., Mcgirr, B., Naus, C.C.G., Rushlow, W.J., 2006. Enhanced Neurite Outgrowth in PC12 Cells Mediated by Connexin Hemichannels and ATP. J. Biol. Chem. 281, 20920–20931.

Beyer, E.C., Berthoud, V.M., 2018. Gap junction gene and protein families: Connexins, innexins, and pannexins. Biochim. Biophys. Acta - Biomembr. 1860, 5–8.

Bhattacharya, A., Aghayeva, U., Berghoff, E.G. and Hobert, O., 2019. Plasticity of the electrical connectome of C. elegans. *Cell*, *176*(5), pp.1174-1189.

Bittern, J., Pogodalla, N., Ohm, H., Brüser, L., Kottmeier, R., Schirmeier, S., Klämbt, C., 2021. Neuron–glia interaction in the *Drosophila* nervous system. Dev. Neurobiol. 81, 438–452.

Bittman, E.L., 2013. Does the Precision of a Biological Clock Depend upon Its Period? Effects of the Duper and tau Mutations in Syrian Hamsters. PLoS One 7.

Bittman, K., Owens, D.F., Kriegstein, A.R., Loturco, J.J., 1997. Cell Coupling and Uncoupling in the Ventricular Zone of Developing Neocortex. Journal of Neuroscience 17, 7037–7044.

Blau, J. and Young, M.W., 1999. Cycling vrille expression is required for a functional Drosophila clock. *Cell*, *99*(6), pp.661-671.

Block, G.D. and Wallace, S.F., 1982. Localization of a circadian pacemaker in the eye of a mollusc, Bulla. *Science*, *217*(4555), pp.155-157.

Bohrmann, J., Zimmermann, J., 2008. Gap junctions in the ovary of *Drosophila melanogaster*: Localization of innexins 1, 2, 3 and 4 and evidence for intercellular communication via innexin-2 containing channels. BMC Dev. Biol. 8, 1–12.

Bouskila, Y. and Dudek, F.E., 1993. Neuronal synchronization without calcium-dependent synaptic transmission in the hypothalamus. *Proceedings of the National Academy of Sciences*, *90*(8), pp.3207-3210.

Brancaccio, M., Edwards, M.D., Patton, A.P., Smyllie, N.J., Chesham, J.E., Maywood, E.S. and Hastings, M.H., 2019. Cell-autonomous clock of astrocytes drives circadian behavior in mammals. *Science*, *363*(6423), pp.187-192.

Broughton, S.J., Piper, M.D., Ikeya, T., Bass, T.M., Jacobson, J., Driege, Y., Martinez, P., Hafen, E., Withers, D.J., Leevers, S.J. and Partridge, L., 2005. Longer lifespan, altered metabolism, and stress resistance in Drosophila from ablation of cells making insulin-like ligands. *Proceedings of the National Academy of Sciences*, *102*(8), pp.3105-3110.

Bulthuis, N., Spontak, K.R., Kleeman, B. and Cavanaugh, D.J., 2019. Neuronal Activity in Non-LNv clock cells is required to produce Free-Running rest: activity rhythms in Drosophila. *Journal of biological rhythms*, *34*(3), pp.249-271.

Cao, G. and Nitabach, M.N., 2008. Circadian control of membrane excitability in Drosophila melanogaster lateral ventral clock neurons. *Journal of Neuroscience*, *28*(25), pp.6493-6501.

Cassone, V.M., Paulose, J.K., Harpole, C.E., Li, Y. and Whitfield-Rucker, M., 2017. Avian circadian organization. In *Biological Timekeeping: Clocks, Rhythms and Behaviour* (pp. 241-256). Springer, New Delhi.

Cavanaugh, D.J., Geratowski, J.D., Wooltorton, J.R.A., Spaethling, J.M., Hector, C.E., Zheng, X., Johnson, E.C., Eberwine, J.H., Sehgal, A., 2014. Identification of a circadian output circuit for rest: Activity rhythms in *Drosophila*. Cell 157, 689–701.

Cavey, M., Collins, B., Bertet, C., Blau, J., 2016. Circadian rhythms in neuronal activity propagate through output circuits. Nat. Neurosci. 19, 587–595.

Cavieres-Lepe, J., Ewer, J., 2021. Reciprocal Relationship Between Calcium Signaling and Circadian Clocks: Implications for Calcium Homeostasis, Clock Function, and Therapeutics. Front. Mol. Neurosci. 14, 1–16.

Chang, Q., Gonzalez, M., Pinter, M.J., Balice-gordon, R.J., 1999. Gap Junctional Coupling and Patterns of Connexin Expression among Neonatal Rat Lumbar Spinal Motor Neurons. Journal of Neuroscience 19, 10813–10828.

Chatterjee, A., Lamaze, A., De, J., Mena, W., Chélot, E., Martin, B., Hardin, P., Kadener, S., Emery, P., Rouyer, F., 2018. Reconfiguration of a Multi-oscillator Network by Light in the *Drosophila* Circadian Clock. Curr. Biol. 28, 2007-2017.

Chaturvedi, R., Reddig, K., Li, H.S., 2014. Long-distance mechanism of neurotransmitter recycling mediated by glial network facilitates visual function in *Drosophila*. Proc. Natl. Acad. Sci. U. S. A. 111, 2812–2817.

Chaturvedi, R., Stork, T., Yuan, C., Freeman, M.R., Emery, P., 2021. Astrocytic GABA Transporter controls sleep by modulating GABAergic signaling in *Drosophila* circadian neurons.bioRxiv [preprint].

Chen, W.F., Maguire, S., Sowcik, M., Luo, W., Koh, K. and Sehgal, A., 2015. A neuron–glia interaction involving GABA transaminase contributes to sleep loss in sleepless mutants. *Molecular psychiatry*, *20*(2), pp.240-251.

Christie, M.J., Williams, J.T. and North, R.A., 1989. Electrical coupling synchronizes subthreshold activity in locus coeruleus neurons in vitro from neonatal rats. *Journal of Neuroscience*, *9*(10), pp.3584-3589.

Chuang, C.F., VanHoven, M.K., Fetter, R.D., Verselis, V.K. and Bargmann, C.I., 2007. An innexin-dependent cell network establishes left-right neuronal asymmetry in C. elegans. *Cell*, *129*(4), pp.787-799.

Nicklas, J.A. and Cline, T.W., 1983. Vital genes that flank Sex-lethal, an X-linked sex-determining gene of Drosophila melanogaster. *Genetics*, *103*(4), pp.617-631.

Colwell, C.S., 2000. Rhythmic coupling among cells in the suprachiasmatic nucleus. J. Neurobiol. 43, 379–388.

Cornelissen, G., 2014. Cosinor-based rhythmometry. *Theoretical Biology and Medical Modelling*, *11*(1), pp.1-24.

Crocker, A., Shahidullah, M., Levitan, I.B. and Sehgal, A., 2010. Identification of a neural circuit that underlies the effects of octopamine on sleep: wake behavior. *Neuron*, *65*(5), pp.670-681.

Curti, S., Hoge, G., Nagy, J.I., Pereda, A.E., 2012. Synergy between Electrical Coupling and Membrane Properties Promotes Strong Synchronization of Neurons of the Mesencephalic Trigeminal Nucleus *Journal of Neuroscience* 32, 4341–4359.

Curtin, K.D., Huang, Z.J., Rosbash, M., 1995. Temporally Regulated Nuclear Entry of the *Drosophila* period Protein Contributes to the Circadian Clock. Neuron 14, 365–372.

Curtin, K.D., Zhang, Z., Wyman, R.J., 1999. *Drosophila* has several genes for gap junction proteins. Gene 232, 191–201.

Curtin, K.D., Zhang, Z., Wyman, R.J., 2002. Gap junction proteins are not interchangeable in development of neural function in the *Drosophila* visual system. J. Cell Sci. 115, 3379–3388.

Daan, S., 2010. A history of chronobiological concepts. In *The circadian clock* (pp. 1-35). Springer, New York, NY.

Dahdal, D., Reeves, D.C., Ruben, M., Akabas, M.H., Blau, J., 2010. *Drosophila* Pacemaker Neurons Require G Protein Signaling and GABAergic Inputs to Generate Twenty-Four Hour Behavioral Rhythms. Neuron 68, 964–977.

Davla, S., Artiushin, G., Li, Y., Chitsaz, D., Li, S., Sehgal, A. and van Meyel, D.J., 2020. AANAT1 functions in astrocytes to regulate sleep homeostasis. *Elife*, *9*, p.e53994.

Dbouk, H.A., Mroue, R.M., El-Sabban, M.E. and Talhouk, R.S., 2009. Connexins: a myriad of functions extending beyond assembly of gap junction channels. *Cell Communication and signaling*, *7*(1), pp.1-17.

Delventhal, R., O'Connor, R.M., Pantalia, M.M., Ulgherait, M., Kim, H.X., Basturk, M.K., Canman, J.C. and Shirasu-Hiza, M., 2019. Dissection of central clock function in Drosophila through cell-specific CRISPR-mediated clock gene disruption. *Elife*, *8*, p.e48308.

Depetris-Chauvin, A., Berni, J., Aranovich, E.J., Muraro, N.I., Beckwith, E.J., Ceriani, M.F., 2011. Adult-specific electrical silencing of pacemaker neurons uncouples molecular clock from circadian outputs. Curr. Biol. 21, 1783–1793.

Dewey, M.M. and Barr, L., 1964. A study of the structure and distribution of the nexus. *The Journal of cell biology*, *23*(3), pp.553-585.

Diemer, T., Landgraf, D., Noguchi, T., Pan, H., Moreno, J.L., Welsh, D.K., 2017. Cellular circadian oscillators in the suprachiasmatic nucleus remain coupled in the absence of connexin-36. Neuroscience 357, 1–11.

Dissel, S., Hansen, C.N., Özkaya, Ö., Hemsley, M., Kyriacou, C.P., Rosato, E., 2014.

The logic of circadian organization in *Drosophila*. Curr. Biol. 24, 2257–2266.

Doherty, J., Logan, M.A., Freeman, M.R., 2009. Ensheathing Glia Function as Phagocytes in the Adult *Drosophila* Brain. Journal of Neuroscience 29, 4768–4781.

Duhart, J.M., Herrero, A., de la Cruz, G., Ispizua, J.I., Pírez, N., Ceriani, M.F., 2020. Circadian Structural Plasticity Drives Remodeling of E Cell Output. Curr. Biol. 30, 5040-5048.e5.

Dunlap, J.C., Loros, J.J. and DeCoursey, P.J., 2004. *Chronobiology: biological timekeeping*. Sinauer Associates.

Duvall, L.B., Taghert, P.H., 2012. The circadian neuropeptide pdf signals preferentially through a specific adenylate cyclase isoform ac3 in m pacemakers of *Drosophila*. PLoS Biol. 10.

Duvall, L.B. and Taghert, P.H., 2011. Circadian rhythms: biological clocks work in phospho-time. *Current Biology*, *21*(9), pp.R305-R307.

Edwards, D.H., Heitler, W.J. and Krasne, F.B., 1999. Fifty years of a command neuron: the neurobiology of escape behavior in the crayfish. *Trends in neurosciences*, *22*(4), pp.153-161.

Edwards, T.N., Meinertzhagen, I.A., 2010. Progress in Neurobiology The functional organisation of glia in the adult brain of *Drosophila* and other insects. Prog. Neurobiol. 90, 471–497.

Elias, L.A. and Kriegstein, A.R., 2008. Gap junctions: multifaceted regulators of embryonic cortical development. *Trends in neurosciences*, *31*(5), pp.243-250.

Emery, P., So, W.V., Kaneko, M., Hall, J.C., Rosbash, M., 1998. Cry, a *Drosophila* clock and light-regulated cryptochrome, is a major contributor to circadian rhythm

resetting and photosensitivity. Cell 95, 669–679.

Evans, W.H., De Vuyst, E. and Leybaert, L., 2006. The gap junction cellular internet: connexin hemichannels enter the signalling limelight. *Biochemical Journal*, *397*(1), pp.1-14.

Ewer, J., Frisch, B., Hamblen-Coyle, M.J., Rosbash, M., Hall, J.C., 1992. Expression of the period clock gene within different cell types in the brain of *Drosophila* adults and mosaic analysis of these cells influence on circadian behavioral rhythms. J. Neurosci. 12, 3321–3349.

Faber, D.S., Pereda, A.E., 2018. Two forms of electrical transmission between neurons. Front. Mol. Neurosci. 11, 1–11.

Farca Luna, A.J., Perier, M., Seugnet, L., 2017. Amyloid precursor protein in *Drosophila* glia regulates sleep and genes involved in glutamate recycling. J. Neurosci. 37, 4289–4300.

Feldman, J.F. and Hoyle, M.N., 1973. Isolation of circadian clock mutants of Neurospora crassa. *Genetics*, *75*(4), pp.605-613.

Fernandez-Chiappe, F., Frenkel, L., Colque, C.C., Ricciuti, A., Hahm, B., Cerredo, K., Muraro, N.I., Ceriani, M.F., 2021. High-frequency neuronal bursting is essential for circadian and sleep behaviors in *Drosophila*. J. Neurosci. 41, 689–710.

Fernandez-Chiappe, F., Hermann-Luibl, C., Peteranderl, A., Reinhard, N., Senthilan, P.R., Hieke, M., Selcho, M., Yoshii, T., Shafer, O.T., Muraro, N.I., Helfrich-Förster, C., 2020. Dopamine signaling in wake-promoting clock neurons is not required for the normal regulation of sleep in *Drosophila*. J. Neurosci. 40, 9617–9633.

Fernández, M.D.L.P., Chu, J., Villella, A., Atkinson, N., Kay, S.A., Ceriani, M.F., 2007. Impaired clock output by altered connectivity in the circadian network. Proc. Natl. Acad. Sci. U. S. A. 104, 5650–5655.

Fernández, M.P., Berni, J. and Ceriani, M.F., 2008. Circadian remodeling of neuronal circuits involved in rhythmic behavior. *PLoS biology*, *6*(3), p.e69.

Fernandez, M.P., Pettibone, H.L., Bogart, J.T., Roell, C.J., Davey, C.E., Pranevicius, A., Huynh, K. V., Lennox, S.M., Kostadinov, B.S., Shafer, O.T., 2020. Sites of Circadian Clock Neuron Plasticity Mediate Sensory Integration and Entrainment. Curr. Biol. 30, 2225-2237.

Fields, R.D., Eshete, F., Stevens, B., Itoh, K., 1997. Action Potential-Dependent Regulation of Gene Expression: Temporal Specificity in Ca 2 , cAMP-Responsive Element Binding Proteins, and Mitogen-Activated Protein Kinase Signaling. Journal of Neuroscience, 17(19), 7252-7266.

Flourakis, M., Kula-Eversole, E., Hutchison, A.L., Han, T.H., Aranda, K., Moose, D.L., White, K.P., Dinner, A.R., Lear, B.C., Ren, D., Diekman, C.O., Raman, I.M., Allada, R., 2015. A Conserved Bicycle Model for Circadian Clock Control of Membrane Excitability. Cell 162, 836–848.

Förster, C.H., 2019. Light input pathways to the circadian clock of insects with an emphasis on the fruit fly *Drosophila melanogaster*. J. Comp. Physiol. A. 206(2), 259-272.

Frenkel, L., Muraro, N.I., Beltrán González, A.N., Marcora, M.S., Bernabó, G., Hermann-Luibl, C., Romero, J.I., Helfrich-Förster, C., Castaño, E.M., Marino-Busjle, C., Calvo, D.J., Ceriani, M.F., 2017. Organization of Circadian Behavior Relies on Glycinergic Transmission. Cell Rep. 19, 72–85.

Furshpan, E.J. and Potter, D.D., 1957. Mechanism of nerve-impulse transmission at a

    crayfish synapse. *Nature*, *180*(4581), pp.342-343.

Gaietta, G., Deerinck, T.J., Adams, S.R., Bouwer, J., Tour, O., Laird, D.W., Sosinsky,

G.E., Tsien, R.Y., Ellisman, M.H., 2002. Multicolor and electron microscopic imaging of

connexin trafficking. Science 296, 503–507.

Galarreta, M. and Hestrin, S., 2001. Electrical synapses between GABA-releasing

    interneurons. *Nature Reviews Neuroscience*, *2*(6), pp.425-433.

George, R., Stanewsky, R., 2021. Peripheral Sensory Organs Contribute to Temperature

    Synchronization of the Circadian Clock in *Drosophila melanogaster*. Front.

    Physiol. 12, 1–14.

Gerstner, J.R., Perron, I.J., Riedy, S.M., Yoshikawa, T., Kadotani, H., Owada, Y.,

    Dongen, H.P.A. Van, Galante, R.J., Dickinson, K., Yin, J.C.P., Pack, A.I., Frank,

    M.G., 2017. Normal sleep requires the astrocyte brain-type fatty acid binding

    protein FABP 7, 1–8.

Giuliani, F., Giuliani, G., Bauer, R. and Rabouille, C., 2013. Innexin 3, a new gene

    required for dorsal closure in Drosophila embryo. *PloS one*, *8*(7), p.e69212.

Goodenough, D.A. and Paul, D.L., 2009. Gap junctions. *Cold Spring Harbor*

    perspectives in biology, *1*(1), p.a002576.

Gonzalez-burgos, G., Hashimoto, T., Lewis, D.A., 2010. Alterations of Cortical GABA

    Neurons and Network Oscillations in Schizophrenia. Current psychiatry reports

    12(4), 335–344.

Gould, P.D., Locke, J.C.W., Larue, C., Southern, M.M., Davis, S.J., Hanano, S., Moyle,

    R., Milich, R., Putterill, J., Millar, A.J., Hall, A., 2006. The molecular basis of

temperature compensation in the Arabidopsis circadian clock. Plant Cell 18, 1177–1187.

Grace, A.A. and Bunney, B.S., 1983. Intracellular and extracellular electrophysiology of nigral dopaminergic neurons—1. Identification and characterization. *Neuroscience*, *10*(2), pp.301-315.

Grima, B., Chélot, E., Xia, R., Rouyer, F., 2004. Morning and evening peaks of activity rely on different clock neurons of the *Drosophila* brain. Nature 431, 869–873.

Gu, C., Li, J., Zhou, J., Yang, H., Rohling, J., 2021. Network Structure of the Master Clock Is Important for Its Primary Function. Front. Physiol. 12, 1–14.

Gu, S., Yu, X.S., Yin, X. and Jiang, J.X., 2003. Stimulation of lens cell differentiation by gap junction protein connexin 45.6. *Investigative ophthalmology & visual science*, *44*(5), pp.2103-2111.

Güiza, J., Barría, I., Sáez, J.C., Vega, J.L., 2018. Innexins: Expression, regulation, and functions. Front. Physiol. 9, 1–9.

Gummadova, J.O., Coutts, G.A., Robert, N., Glossop, J., 2009. Analysis of the *Drosophila* Clock Promoter Reveals Heterogeneity in expression between Subgroups of Central Oscillator Cells and Identifies a Novel enhancer Region. J. Biol. Rhythms 24, 353–367.

Hamasaka, Y., Rieger, D., Parmentier, M.L., Grau, Y., Helfrich-Förster, C. and Nässel, D.R., 2007. Glutamate and its metabotropic receptor in Drosophila clock neuron circuits. *Journal of Comparative Neurology*, *505*(1), pp.32-45.

Hammond, C., Bergman, H., Brown, P., 2007. Pathological synchronization in Parkinson's disease : networks , models and treatments. Trends in neurosciences 30, 357-364.

Han, Y., Xiong, L., Xu, Y., Tian, T., Wang, T., 2017. The β-Alanine transporter balaT is required for visual neurotransmission in *Drosophila*. Elife 6, 1–19.

Hardin, P.E., Hall, J.C. and Rosbash, M., 1990. Feedback of the Drosophila period gene product on circadian cycling of its messenger RNA levels. *Nature*, *343*(6258), pp.536-540.

Hardin, P.E., 2011. Molecular genetic analysis of circadian timekeeping in Drosophila. *Advances in genetics*, *74*, pp.141-173.

Harrisingh, M.C., Wu, Y., Lnenicka, G.A., Nitabach, M.N., 2007. Intracellular Ca2+ regulates free-running circadian clock oscillation in vivo. J. Neurosci. 27, 12489–12499.

Hasegawa, D.K., Turnbull, M.W., 2014. Recent findings in evolution and function of insect innexins. FEBS Lett. 588, 1403–1410.

Helfrich-Förster, C., 1998. Robust circadian rhythmicity of *Drosophila melanogaster* requires the presence of lateral neurons: A brain-behavioral study of disconnected mutants. J. Comp. Physiol. 182, 435–453.

Helfrich-Förster, C., Täuber, M., Park, J.H., Mühlig-Versen, M., Schneuwly, S., Hofbauer, A., 2000. Ectopic expression of the neuropeptide pigment-dispersing factor alters behavioral rhythms in *Drosophila melanogaster*. J. Neurosci. 20, 3339–3353.

Herberholz, J., Antonsen, B.L. and Edwards, D.H., 2002. A lateral excitatory network in the escape circuit of crayfish. *Journal of Neuroscience*, *22*(20), pp.9078-9085.

Hermann-Luibl, C., Yoshii, T., Senthilan, P.R., Dircksen, H. and Helfrich-Förster, C., 2014. The ion transport peptide is a new functional clock neuropeptide in the fruit

fly Drosophila melanogaster. *Journal of Neuroscience*, *34*(29), pp.9522-9536.

Hermann, C., Yoshii, T., Dusik, V., Helfrich-Förster, C., 2012. Neuropeptide F immunoreactive clock neurons modify evening locomotor activity and free-running period in *Drosophila melanogaster*. J. Comp. Neurol. 520, 970–987.

Herrero, A., Yoshii, T., Ispizua, J.I., Colque, C., Veenstra, J.A., Muraro, N.I., Ceriani, M.F., 2020. Coupling Neuropeptide Levels to Structural Plasticity in *Drosophila* Clock Neurons. Curr. Biol. 30, 3154-3166.e4.

Herzog, E.D., Aton, S.J., Numano, R., Sakaki, Y., Tei, H., 2004. Temporal Precision in the Mammalian Circadian System: A Reliable Clock from Less Reliable Neurons. J. Biol. Rhythms 19, 35–46.

Herzog, E.D., Hermanstyne, T., Smyllie, N.J., Hastings, M.H., 2017. Regulating the suprachiasmatic nucleus (SCN) circadian clockwork: Interplay between cell-autonomous and circuit-level mechanisms. Cold Spring Harb. Perspect. Biol. 9.

Holcroft, C.E., Jackson, W.D., Lin, W.H., Bassiri, K., Baines, R.A., Phelan, P., 2013. Innexins ogre and inx2 are required in glial cells for normal postembryonic development of the *Drosophila* central nervous system. J. Cell Sci. 126, 3823–3834.

Homyk, T., Szidonya, J. and Suzuki, D.T., 1980. Behavioral mutants of Drosophila melanogaster. *Molecular and General Genetics*, *177*(4), pp.553-565.

Hong, C.I., Conrad, E.D., Tyson, J.J., 2007. A proposal for robust temperature compensation of circadian rhythms. Proc. Natl. Acad. Sci. U. S. A. 104, 1195–1200.

Hong, C.I. and Tyson, J.J., 1997. A Proposal for Temperature Compensation of the Orcadian Rhythm in Drosophila Based on Dimerization of the Per Protein. *Chronobiology international*, *14*(5), pp.521-529.

Hyun, S., Lee, Y., Hong, S.T., Bang, S., Paik, D., Kang, J., Shin, J., Lee, J., Jeon, K., Hwang, S., Bae, E., Kim, J., 2005. *Drosophila* GPCR han is a receptor for the circadian clock neuropeptide PDF. Neuron 48, 267–278.

Iacobas, D.A., Scemes, E. and Spray, D.C., 2004. Gene expression alterations in connexin null mice extend beyond the gap junction. *Neurochemistry international*, *45*(2-3), pp.243-250.

Ito, C., Tomioka, K., 2016. Heterogeneity of the peripheral circadian systems in *Drosophila melanogaster*: A review. Front. Physiol. 7, 1–7.

Jackson, F.R., Ng, F.S., Sengupta, S., You, S. and Huang, Y., 2015. Glial cell regulation of rhythmic behavior. *Methods in enzymology*, *552*, pp.45-73.

Jiang, Z.G., Yang, Y.Q., Allen, C.N., 1997. Tracer and electrical coupling of rat suprachiasmatic nucleus neurons. Neuroscience 77, 1059–1066.

Johard, H.A.D., Yoishii, T., Dircksen, H., Cusumano, P., Rouyer, F., Helfrich-Förster, C., Nässel, D.R., 2009. Peptidergic clock neurons in *Drosophila*: Ion transport peptide and short neuropeptide F in subsets of dorsal and ventral lateral neurons. J. Comp. Neurol. 516, 59–73.

Kalra, J., Shao, Q., Qin, H., Thomas, T., Alaoui-Jamali, M.A. and Laird, D.W., 2006. Cx26 inhibits breast MDA-MB-435 cell tumorigenic properties by a gap junctional intercellular communication-independent mechanism. *Carcinogenesis*, *27*(12), pp.2528-2537.

Kandler, K. and Katz, L.C., 1995. Neuronal coupling and uncoupling in the developing nervous system. *Current opinion in neurobiology*, *5*(1), pp.98-105.

Kaneko, M., Hall, J.C., 2000. Neuroanatomy of cells expressing clock genes in

Drosophila: Transgenic manipulation of the period and timeless genes to mark the perikarya of circadian pacemaker neurons and their projections. J. Comp. Neurol. 422, 66–94.

Kaneko, M., Park, J.H., Cheng, Y., Hardin, P.E., Hall, J.C., 2000. Disruption of synaptic transmission or clock-gene-product oscillations in circadian pacemaker cells of *Drosophila* cause abnormal behavioral rhythms. J. Neurobiol. 43, 207–233.

Kidd, P.B., Young, M.W., Siggia, E.D., 2015. Temperature compensation and temperature sensation in the circadian clock. Proc. Natl. Acad. Sci. U. S. A. 112, E6284–E6292.

King, A.N., Barber, A.F., Smith, A.E., Dreyer, A.P., Sitaraman, D., Nitabach, M.N., Cavanaugh, D.J., Sehgal, A., 2017. A Peptidergic Circuit Links the Circadian Clock to Locomotor Activity. Curr. Biol. 27, 1915-1927.e5.

Klarsfeld, A., Leloup, J.C., Rouyer, F., 2003. Circadian rhythms of locomotor activity in *Drosophila*. Behav. Processes 64, 161–175.

Klose, M., Duvall, L.B., Li, W., Liang, X., Ren, C., Steinbach, J.H., Taghert, P.H., 2016. Functional PDF Signaling in the *Drosophila* Circadian Neural Circuit Is Gated by Ral A-Dependent Modulation. Neuron 90, 781–794.

Klose, M.K., Bruchez, M.P., Deitcher, D.L., Levitan, E.S., 2021. Temporally and spatially partitioned neuropeptide release from individual clock neurons. Proc. Natl. Acad. Sci. U. S. A. 118.

Kloss, B., Price, J.L., Saez, L., Blau, J., Rothenfluh, A., Wesley, C.S., Young, M.W., Virginia, W., 1998. The *Drosophila* Clock Gene double-time Encodes a Protein Closely Related to Human Casein Kinase I. Cell 94, 97–107.

Kloss, B., Rothenfluh, A., Young, M.W., Saez, L., 2001. Phosphorylation of PERIOD Is Influenced by Cycling Physical Associations of DOUBLE-TIME , PERIOD , and TIMELESS in the *Drosophila* Clock Neuron 30, 699–706.

Kondo, T., Tsinoremas, N.F., Golden, S.S., Johnson, C.H., Kutsuna, S., Ishiura, M., 1994. Circadian clock mutants of cyanobacteria. Science. 266, 1233–1236.

Konopka, R.J., Benzer, S., 1971. Clock mutants of *Drosophila melanogaster*. Proc. Natl. Acad. Sci. U. S. A. 68, 2112–2116.

Kothmann, W.W., Trexler, E.B., Whitaker, C.M., Li, W., Massey, S.C., Brien, J.O., 2012. Nonsynaptic NMDA Receptors Mediate Activity-Dependent Plasticity of Gap Junctional Coupling in the AII Amacrine Cell Network. Journal of Neuroscience 32, 6747–6759.

Kottmeier, R., Bittern, J., Schoofs, A., Scheiwe, F., Matzat, T., Pankratz, M., Klämbt, C., 2020. Wrapping glia regulates neuronal signaling speed and precision in the peripheral nervous system of *Drosophila*. Nat. Commun. 11, 1–17.

Kozlov, A., Koch, R., Nagoshi, E., 2020. Nitric Oxide Mediates Neuro-Glial Interaction that Shapes *Drosophila* Circadian Behavior. PLoS Genet. 16.

Landesman, Y., White, T.W., Starich, T.A., Shaw, J.E., Goodenough, D.A., Paul, D.L., 1999. Innexin-3 forms connexin-like intercellular channels. J. Cell Sci. 112, 2391–2396.

Landisman, C.E. and Connors, B.W., 2005. Long-term modulation of electrical synapses in the mammalian thalamus. *Science*, *310*(5755), pp.1809-1813.

Lauf, U., Giepmans, B.N.G., Lopez, P., Braconnot, S., Chen, S.C., Falk, M.M., 2002. Dynamic trafficking and delivery of connexons to the plasma membrane and

accretion to gap junctions in living cells. Proc. Natl. Acad. Sci. U. S. A. 99, 10446–10451.

Lear, B.C., Lin, J.M., Keath, J.R., McGill, J.J., Raman, I.M., Allada, R., 2005a. The ion channel narrow abdomen is critical for neural output of the *Drosophila* circadian pacemaker. Neuron 48, 965–976.

Lear, B.C., Merrill, C.E., Lin, J.M., Schroeder, A., Zhang, L., Allada, R., 2005b. A G Protein-coupled receptor, groom-of-PDF, is required for PDF neuron action in circadian behavior. Neuron 48, 221–227.

Lee Gierke, C., Cornelissen, G., 2016. Chronomics analysis toolkit (CATkit). Biol. Rhythm Res. 47, 163–181.

Lee, P.R., Cohen, J.E., Iacobas, D.A., Iacobas, S., Fields, & R.D., 2017. Gene networks activated by specific patterns of action potentials in dorsal root ganglia neurons. Scientific Reports, 7(1), 1-14.

Lewis, T.J. and Rinzel, J., 2000. Self-organized synchronous oscillations in a network of excitable cells coupled by gap junctions. *Network: Computation in Neural Systems*, *11*(4), pp.299-320.

Li, W.C. and Rekling, J.C., 2017. Electrical coupling in the generation of vertebrate motor rhythms. In *Network Functions and Plasticity* (pp. 243-264). Academic Press.

Liang, X., Holy, T.E., Taghert, P.H., 2016. Synchronous *Drosophila* circadian pacemakers display nonsynchronous Ca2+ rhythms in vivo. Science, 351, 976–981.

Lipshitz, H.D., Kankel, D.R., 1985. Specificity of gene action during central nervous system development in *Drosophila melanogaster*: Analysis of the lethal (1) optic

ganglion reduced locus. Dev. Biol. 108, 56–77.

Liu, Q., Yang, X., Tian, J., Gao, Z., Wang, M., Li, Y., Guo, A., 2016. Gap junction networks in mushroom bodies participate in visual learning and memory in *Drosophila*. Elife 5, 1–18.

Long, M.A., Jutras, M.J., Connors, B.W., Burwell, R.D., 2005. Electrical synapses coordinate activity in the suprachiasmatic nucleus. Nat. Neurosci. 8, 61–66.

Maher, B.J., McGinley, M.J. and Westbrook, G.L., 2009. Experience-dependent maturation of the glomerular microcircuit. *Proceedings of the National Academy of Sciences*, *106*(39), pp.16865-16870.

Majercak, J., Sidote, D., Hardin, P.E., Edery, I., 1999. How a circadian clock adapts to seasonal decreases in temperature and day length. Neuron 24, 219–230.

Marin-Burgin, A., Eisenhart, F.J., Kristan, W.B. and French, K.A., 2006. Embryonic electrical connections appear to prefigure a behavioral circuit in the leech CNS. *Journal of Comparative Physiology A*, *192*(2), pp.123-133.

Marin-burgin, A., Eisenhart, F.J., Baca, S.M., Jr, W.B.K., French, K.A., 2005. Sequential Development of Electrical and Chemical Synaptic Connections Generates a Specific Behavioral Circuit in the Leech. Journal of Neuroscience 25, 2478–2489.

Martin, P.E. and Evans, W.H., 2004. Incorporation of connexins into plasma membranes and gap junctions. *Cardiovascular research*, *62*(2), pp.378-387.

Martinek, S., Inonog, S., Manoukian, A.S., Young, M.W., 2001. A Role for the Segment Polarity Gene shaggy / GSK-3 in the *Drosophila* Circadian Clock. Cell 105, 769–779.

McGuire, S.E., Mao, Z., Davis, R.L., 2004. Spatiotemporal gene expression targeting

with the TARGET and gene-switch systems in *Drosophila*. Sci. Signaling (220), pl6–pl6.

Mentis, G.Z., Díaz, E., Moran, L.B., Navarrete, R., 2002. Increased incidence of gap junctional coupling between spinal motoneurones following transient blockade of NMDA receptors in neonatal rats The Journal of Physiology 544(3), 757–764.

Mertens, I., Vandingenen, A., Johnson, E.C., Shafer, O.T., Li, W., Trigg, J.S., De Loof, A., Schoofs, L., Taghert, P.H., 2005. PDF receptor signaling in *Drosophila* contributes to both circadian and geotactic behaviors. Neuron 48, 213–219.

Mezan, S., Feuz, J.D., Deplancke, B., Kadener, S., 2016. PDF Signaling Is an Integral Part of the *Drosophila* Article PDF Signaling Is an Integral Part of the *Drosophila* Circadian Molecular Oscillator Cell reports, 708–719.

Micklem, C.N., Locke, J.C.W., 2021. Cut the noise or couple up: Coordinating circadian and synthetic clocks. iScience 24, 103051.

Mills, S.L. and Massey, S.C., 1995. Differential properties of two gap junctional pathways made by AII amacrine cells. *Nature*, *377*(6551), pp.734-737.

Mizrak, D., Ruben, M., Myers, G.N., Rhrissorrakrai, K., Gunsalus, K.C., Blau, J., 2012. Electrical activity can impose time of day on the circadian transcriptome of pacemaker neurons. Curr. Biol. 22, 1871–1880.

Montoro, R.J. and Yuste, R., 2004. Gap junctions in developing neocortex: a review. *Brain research reviews*, *47*(1-3), pp.216-226.

Moore, R.Y., Bernstein, M.E., 1989. Synaptogenesis in the rat suprachiasmatic nucleus demoinstrated by electron microscopy and synapsin I immunoreactivity. J. Neurosci. 9, 2151–2162.

Moore, R.Y., Lenn, N.J., 1972. A retinohypothalamic projection in the rat. J. Comp. Neurol. 146, 1–14.

Nagy, J.I., Pereda, A.E., Rash, J.E., 2018. Electrical synapses in mammalian CNS : Past eras , present focus and future directions ☆. BBA - Biomembr. 1860, 102–123.

Nakagawa, S., Maeda, S. and Tsukihara, T., 2010. Structural and functional studies of gap junction channels. *Current opinion in structural biology*, *20*(4), pp.423-430.

Nakazawa, K., Zsiros, V., Jiang, Z., Nakao, K., Kolata, S., Zhang, S., Belforte, J.E., 2012. Neuropharmacology GABAergic interneuron origin of schizophrenia pathophysiology. Neuropharmacology 62, 1574–1583.

Narasimamurthy, R., Virshup, D.M., 2017. Molecular mechanisms regulating temperature compensation of the circadian clock. Front. Neurol. 8, 1–5.

Nettnin, E.A., Sallese, T.R., Nasseri, A., Saurabh, S., Daniel, J., 2021. Dorsal clock neurons in *Drosophila* sculpt locomotor outputs but are dispensable for circadian activity rhythms. iScience 24, 103001.

Ng, F.S., Tangredi, M.M., Jackson, F.R., 2011. Glial cells physiologically modulate clock neurons and circadian behavior in a calcium-dependent manner. Curr. Biol. 21, 625–634.

Nielsen, M.S., Axelsen, L.N., Sorgen, P.L., Verma, V., Delmar, M., Holstein-Rathlou, N.H., 2012. Gap junctions. Compr. Physiol. 2, 1981–2035.

Nikhil, K.L. and Sharma, V.K., 2017. On the origin and implications of circadian timekeeping: An evolutionary perspective. In *Biological timekeeping: Clocks, rhythms and behaviour* (pp. 81-129). Springer, New Delhi.

Nikhil, K.L., Korge, S., Kramer, A., 2020. Heritable gene expression variability and

stochasticity govern clonal heterogeneity in circadian period. PLoS Biol. 18, 1–26.

Nishiitsutsuji-Uwo, J., Pittendrigh, C.S., 1968. Central nervous system control of circadian rhythmicity in the cockroach - II. The pathway of light signals that entrain the rhythm. Z. Vgl. Physiol. 58, 1–13.

Nitabach, M.N., Blau, J., Holmes, T.C., 2002. Electrical silencing of *Drosophila* pacemaker neurons stops the free-running circadian clock. Cell 109, 485–495.

Nitabach, M.N., Wu, Y., Sheeba, V., Lemon, W.C., Strumbos, J., Zelensky, P.K., White, B.H., Holmes, T.C., 2006. Electrical hyperexcitation of lateral ventral pacemaker neurons desynchronizes downstream circadian oscillators in the fly circadian circuit and induces multiple behavioral periods. J. Neurosci. 26, 479–489.

O'Brien, J., 2014. The ever-changing electrical synapse. Curr. Opin. Neurobiol. 29, 64–72.

Osterwalder, T., Yoon, K.S., White, B.H. and Keshishian, H., 2001. A conditional tissue-specific transgene expression system using inducible GAL4. *Proceedings of the National Academy of Sciences*, *98*(22), pp.12596-12601.

Ostrowski, K., Bauer, R., Hoch, M., 2008. The *Drosophila* Innexin7 gap junction protein is required for development of the embryonic nervous system. Cell Commun. Adhes. 15, 155–167.

Page, T.L., 1982. Transplantation of the cockroach circadian pacemaker. *Science*, *216*(4541), pp.73-75.

Park, J.H., Helfrich-Förster, C., Lee, G., Liu, L., Rosbash, M., Hall, J.C., 2000. Differential regulation of circadian pacemaker output by separate clock genes in *Drosophila*. Proc. Natl. Acad. Sci. U. S. A. 97, 3608–3613.

Patke, A., Young, M.W., Axelrod, S., 2020. Molecular mechanisms and physiological importance of circadian rhythms. Nat. Rev. Mol. Cell Biol. 21, 67–84.

Peng, Y., Stoleru, D., Levine, J.D., Hall, J.C., Rosbash, M., 2003. *Drosophila* free-running rhythms require intercellular communication. PLoS Biol. 1, 32–40.

Penn, A.A., Wong, R.O. and Shatz, C.J., 1994. Neuronal coupling in the developing mammalian retina. *Journal of Neuroscience*, *14*(6), pp.3805-3815.

Pereda, A.E., 2014. Electrical synapses and their functional interactions with chemical synapses. Nat. Rev. Neurosci. 15, 250–263.

Personius, K., Chang, Q., Bittman, K., Panzer, J. and Balice-Gordon, R., 2001. Gap junctional communication among motor and other neurons shapes patterns of neural activity and synaptic connectivity during development. *Cell communication & adhesion*, *8*(4-6), pp.329-333.

Pézier, A.P., Jezzini, S.H., Bacon, J.P. and Blagburn, J.M., 2016. Shaking B mediates synaptic coupling between auditory sensory neurons and the giant fiber of Drosophila melanogaster. *PLoS One*, *11*(4), p.e0152211.

Phelan, P., Goulding, L.A., Tam, J.L.Y., Allen, M.J., Dawber, R.J., Davies, J.A., Bacon, J.P., 2008. Molecular Mechanism of Rectification at Identified Electrical Synapses in the *Drosophila* Giant Fiber System. Curr. Biol. 18, 1955–1960.

Phelan, P., Starich, T.A., 2001. Innexins get into the gap. BioEssays 23, 388–396.

Phelan, P., Stebbings, L.A., Baines, R.A., Bacon, J.P., Davies, J.A., Ford, C., 1998. *Drosophila* shaking-B protein forms gap junctions in paired Xenopus oocytes. Nature 391, 181–184.

Pírez, N., Christmann, B.L., Griffith, L.C., 2013. Daily rhythms in locomotor circuits in

Drosophila involve PDF. J. Neurophysiol. 110, 700–708.

Pittendrigh, C.S., 1960. Circadian rhythms and the circadian organization of living

systems. Cold Spring Harb. Symp. Quant. Biol. 25, 159–184.

Pittendrigh, C.S. and Daan, S., 1976. A functional analysis of circadian pacemakers in

nocturnal rodents. I. The stability and lability of spontaneous frequency. *Journal of*

comparative Physiology A, *106*(3), pp.223-252.

Prakash, P., Nambiar, A., Sheeba, V., 2017. Oscillating PDF in termini of circadian

pacemaker neurons and synchronous molecular clocks in downstream neurons are

not sufficient for sustenance of activity rhythms in constant darkness. PLoS One 12,

1–24.

Price, J.L., Blau, J., Rothenfluh, A., Abodeely, M., Kloss, B., Young, M.W., 1998.

double-time Is a Novel *Drosophila* Clock Gene that Regulates PERIOD Protein

Accumulation. Cell 94, 83–95.

Pricel, J.L., Dembinska, M.E., Youngl, M.W., Rosbash, M., 1995. Suppression of

PERIOD protein abundance and circadian cycling by the *Drosophila* clock mutation

timeless The EMBO Journal 14, 4044–4049.

Ralph, M.R., Foster, R.G., Davis, F.C. and Menaker, M., 1990. Transplanted

suprachiasmatic nucleus determines circadian period. *Science*, *247*(4945), pp.975-

978.

Rash, J.E., Pereda, A., Kamasawa, N., Furman, C.S., Yasumura, T., Davidson, K.G.V.,

Dudek, F.E., Olson, C., Li, X. and Nagy, J.I., 2004. High-resolution proteomic

mapping in the vertebrate central nervous system: close proximity of connexin35 to

NMDA glutamate receptor clusters and co-localization of connexin36 with

immunoreactivity for zonula occludens protein-1 (ZO-1). *Journal of neurocytology*, *33*(1), pp.131-151.

Rash, J.E., Curti, S., Vanderpool, K.G., Kamasawa, N., Nannapaneni, S., Palacios-prado, N., Flores, C.E., Yasumura, T., Brien, J.O., Lynn, B.D., Bukauskas, F.F., Nagy, J.I., Pereda, A.E., 2013. Molecular and Functional Asymmetry at a Vertebrate Electrical Synapse. Neuron 79, 957–969.

Rash, J.E., Olson, C.O., Pouliot, W.A., Davidson, K.G. V, Yasumura, T., Furman, C.S., Royer, S., Kamasawa, N., Nagy, J.I., Dudek, F.E., 2007. Connexin36 vs. Connexin32, "Miniature" Neuronal Gap Junctions, and Limited Electrotonic Coupling in Rodent Suprachiasmatic Nucleus, Neuroscience 149(2), 350-371.

Renn, S.C.P., Park, J.H., Rosbash, M., Hall, J.C., Taghert, P.H., 1999. A pdf neuropeptide gene mutation and ablation of PDF neurons each cause severe abnormalities of behavioral circadian rhythms in *Drosophila*. Cell 99, 791–802.

Reppert, S.M. and Schwartz, W.J., 1984. The suprachiasmatic nuclei of the fetal rat: characterization of a functional circadian clock using 14C-labeled deoxyglucose. *Journal of Neuroscience*, *4*(7), pp.1677-1682.

Revel, J.P. and Karnovsky, M., 1967. Hexagonal array of subunits in intercellular junctions of the mouse heart and liver. *The Journal of cell biology*, *33*(3), pp.C7-12.

Richard, M., Bauer, R., Tavosanis, G., Hoch, M., 2017. The gap junction protein Innexin3 is required for eye disc growth in *Drosophila*. Dev. Biol. 425, 191–207.

Richard, M., Hoch, M., 2015. *Drosophila* eye size is determined by Innexin 2-dependent Decapentaplegic signalling. Dev. Biol. 408, 26–40.

Roberts, L., Leise, T.L., Noguchi, T., Galschiodt, A.M., Houl, J.H., Welsh, D.K.,

Holmes, T.C., 2015. Light evokes rapid circadian network oscillator desynchrony followed by gradual phase retuning of synchrony. Curr. Biol. 25, 858–867.

Roenneberg, T., Morse, D., 1993. Two circadian oscillators in one cell. Nature 362, 362–364.

Ruben, M., Drapeau, M.D., Mizrak, D., Blau, J., 2012. A mechanism for circadian control of pacemaker neuron excitability. J. Biol. Rhythms 27, 353–364.

Rulifson, E.J., Kim, S.K., Nusse, R., 2002. Ablation of Insulin-Producing Neurons in Flies : Growth and Diabetic Phenotypes. Science 296, 1118–1121.

Ruoff, P., 1992. Introducing temperature-compensation in any reaction kinetic oscillator model. Journal of Interdisciplinary cycle research 23:2, 92-99.

Rutila, J.E., Suri, V., Le, M., So, W.V., Rosbash, M., Hall, J.C., 1998. CYCLE Is a Second bHLH-PAS Clock Protein Essential for Circadian Rhythmicity and Transcription of *Drosophila* period and timeless, Cell 93, 805–814.

Sahu, A., Ghosh, R., Deshpande, G., Prasad, M., 2017. A Gap Junction Protein, Inx2, Modulates Calcium Flux to Specify Border Cell Fate during *Drosophila* oogenesis. PLoS Genet. 13, 1–26.

Salome, P.A., 2010. The Role of the Arabidopsis Morning Loop Components CCA1 , LHY , PRR7 , and PRR9 in Temperature Compensation. The Plant Cell 22, 3650–3661.

Scemes, E., Spray, D.C., Meda, P., 2009. Connexins, pannexins, innexins: Novel roles of "hemi-channels." Pflugers Arch. Eur. J. Physiol. 457, 1207–1226.

Schindelin, J., Arganda-Carreras, I., Frise, E., Kaynig, V., Longair, M., Pietzsch, T., Preibisch, S., Rueden, C., Saalfeld, S., Schmid, B., Tinevez, J.Y., White, D.J.,

Hartenstein, V., Eliceiri, K., Tomancak, P., Cardona, A., 2012. Fiji: An open-source platform for biological-image analysis. Nat. Methods 9, 676–682.

Schlichting, M., Díaz, M.M., Xin, J., Rosbash, M., 2019. Neuron-specific knockouts indicate the importance of network communication to *Drosophila* rhythmicity. Elife 8, 1–20.

Schneider, N.L., Stengl, M., 2006. Gap junctions between accessory medulla neurons appear to synchronize circadian clock cells of the cockroach Leucophaea maderae. J. Neurophysiol. 95, 1996–2002.

Schotthöfer, S.K., Bohrmann, J., 2020. Analysing bioelectrical phenomena in the *Drosophila* ovary with genetic tools: Tissue-specific expression of sensors for membrane potential and intracellular pH, and RNAi-knockdown of mechanisms involved in ion exchange. BMC Dev. Biol. 20, 1–17.

Sehgal, A., Price, J.L., Man, B. and Young, M.W., 1994. Loss of circadian behavioral rhythms and per RNA oscillations in the Drosophila mutant timeless. *Science*, *263*(5153), pp.1603-1606.

Sekiguchi, M., Inoue, K., Yang, T., Luo, D.G., Yoshii, T., 2020. A Catalog of GAL4 Drivers for Labeling and Manipulating Circadian Clock Neurons in *Drosophila melanogaster*. J. Biol. Rhythms 35, 207–213.

Selcho, M., Millán, C., Palacios-Muñoz, A., Ruf, F., Ubillo, L., Chen, J., Bergmann, G., Ito, C., Silva, V., Wegener, C. and Ewer, J., 2017. Central and peripheral clocks are coupled by a neuropeptide pathway in Drosophila. *Nature communications*, *8*(1), pp.1-13.

Sengupta, S., Crowe, L.B., You, S., Roberts, M.A. and Jackson, F.R., 2019. A secreted

Ig-domain protein required in both astrocytes and neurons for regulation of Drosophila night sleep. *Current Biology*, *29*(15), pp.2547-2554.

Sepp, K.J., Schulte, J., Auld, V.J., 2001. Peripheral Glia Direct Axon Guidance across the CNS / PNS Transition Zone Developmental biology 238, 47–63.

Seugnet, L., Suzuki, Y., Merlin, G., Gottschalk, L., Duntley, S.P., Shaw, P.J., 2011. Report Notch Signaling Modulates Sleep Homeostasis and Learning after Sleep Deprivation in *Drosophila*. Curr. Biol. 21, 835–840.

Shafer, O.T., Keene, A.C., 2021. The Regulation of *Drosophila* Sleep. Curr. Biol. 31, R38–R49.

Shafer, O.T., Kim, D.J., Dunbar-Yaffe, R., Nikolaev, V.O., Lohse, M.J., Taghert, P.H., 2008. Widespread Receptivity to Neuropeptide PDF throughout the Neuronal Circadian Clock Network of *Drosophila* Revealed by Real-Time Cyclic AMP Imaging. Neuron 58, 223–237.

Shafer, O.T., Rosbash, M., Truman, J.W., 2002. Sequential nuclear accumulation of the clock proteins period and timeless in the pacemaker neurons of *Drosophila melanogaster*. J. Neurosci. 22, 5946–5954.

Shafer, O.T., Yao, Z., 2014. Pigment-dispersing factor signaling and circadian rhythms in insect locomotor activity. Curr. Opin. Insect Sci. 1, 73–80.

Shang, Y., Donelson, N.C., Vecsey, C.G., Guo, F., Rosbash, M., Griffith, L.C., 2013. Short Neuropeptide F Is a Sleep-Promoting Inhibitory Modulator. Neuron 80, 171–183.

Sharma, V.K., Chandrashekaran, M.K., 1999. Precision of a mammalian circadian clock. Naturwissenschaften 86, 333–335.

Sheeba, V., 2008. The *Drosophila melanogaster* circadian pacemaker circuit. J. Genet. 87, 485–493.

Sheeba, V., Gu, H., Sharma, V.K., O'Dowd, D.K., Holmes, T.C., 2008b. Circadian- and light-dependent regulation of resting membrane potential and spontaneous action potential firing of *Drosophila* circadian pacemaker neurons. J. Neurophysiol. 99, 976–988.

Sheeba, V., Sharma, V.K., Gu, H., Chou, Y.T., O'Dowd, D.K., Holmes, T.C., 2008c. Pigment dispersing factor-dependent and -independent circadian locomotor behavioral rhythms. J. Neurosci. 28, 217–227.

Shibata, S. and Moore, R.Y., 1987. Development of neuronal activity in the rat suprachiasmatic nucleus. *Developmental Brain Research*, *34*(2), pp.311-315.

Shiga, S., 2013. Photoperiodic plasticity in circadian clock neurons in insects. Front. Physiol. 4 AUG, 1–4.

Shyu, W.H., Lee, W.P., Chiang, M.H., Chang, C.C., Fu, T.F., Chiang, H.C., Wu, T., Wu, C.L., 2019. Electrical synapses between mushroom body neurons are critical for consolidated memory retrieval in *Drosophila*. PLoS Genet. 15, 1–20.

Siegmund, T. and Korge, G., 2001. Innervation of the ring gland of Drosophila melanogaster. *Journal of Comparative Neurology*, *431*(4), pp.481-491.

Singh, S., Giesecke, A., Damulewicz, M., Fexova, S., Mazzotta, G.M., Stanewsky, R., Dolezel, D., 2019. New *Drosophila* Circadian Clock Mutants Affecting Temperature Compensation Induced by Targeted Mutagenesis of Timeless. Front. Physiol. 10.

Siwicki, K.K., Eastman, C., Petersen, G., Rosbash, M., Hall, J.C., 1988. Antibodies to

the period gene product of *Drosophila* reveal diverse tissue distribution and rhythmic changes in the visual system. Neuron 1, 141–150.

Smith, P., Buhl, E., Tsaneva-Atanasova, K., Hodge, J.J.L., 2019. Shaw and Shal voltage-gated potassium channels mediate circadian changes in *Drosophila* clock neuron excitability. J. Physiol. 597, 5707–5722.

Spéder, P., Brand, A.H., 2014. Gap junction proteins in the blood-brain barrier control nutrient-dependent reactivation of *Drosophila* neural stem cells. Dev. Cell 30, 309–321.

Srivastava, M., Varma, V., Abhilash, L., Sharma, V.K., Sheeba, V., 2019. Circadian Clock Properties and Their Relationships as a Function of Free-Running Period in *Drosophila melanogaster*. J. Biol. Rhythms 34, 231–248.

Stains, J.P. and Civitelli, R., 2005. Gap junctions regulate extracellular signal-regulated kinase signaling to affect gene transcription. *Molecular biology of the cell*, *16*(1), pp.64-72.

Stains, J.P., Lecanda, F., Screen, J., Towler, D.A., Civitelli, R., 2003. Gap Junctional Communication Modulates Gene Transcription by Altering the Recruitment of Sp1 and Sp3 to Connexin-response Elements in Osteoblast Promoters . J. Biol. Chem. 278, 24377–24387.

Stanewsky, R., Kaneko, M., Emery, P., Beretta, B., Wager-Smith, K., Kay, S.A., Rosbash, M., Hall, J.C., 1998. The cry(b) mutation identifies cryptochrome as a circadian photoreceptor in *Drosophila*. Cell 95, 681–692.

Stavropoulos, N., Young, M.W., 2011. Article insomniac and Cullin-3 Regulate Sleep and Wakefulness in *Drosophila*. Neuron 72, 964–976.

Stebbings, L.A., Todman, M.G., Phelan, P., Bacon, J.P., Davies, J.A., 2000. Two *Drosophila* innexins are expressed in overlapping domains and cooperate to form gap-junction channels. Mol. Biol. Cell 11, 2459–2470.

Stokkan, K.A., Yamazaki, S., Tei, H., Sakaki, Y., Menaker, M., 2001. Entrainment of the circadian clock in the liver by feeding. Science 291, 490–493.

Stoleru, D., Nawathean, P., Fernández, M. de la P., Menet, J.S., Ceriani, M.F., Rosbash, M., 2007. The *Drosophila* Circadian Network Is a Seasonal Timer. Cell 129, 207–219.

Stoleru, D., Peng, Y., Agosto, J., Rosbash, M., 2004. Coupled oscillators control morning and evening locomotor behaviour of *Drosophila*. Nature 431, 862–868.

Stoleru, D., Peng, Y., Nawathean, P., Rosbash, M., 2005. A resetting signal between *Drosophila* pacemakers synchronizes morning and evening activity. Nature 438, 238–242.

Stork, T., Bernardos, R. and Freeman, M.R., 2012. Analysis of glial cell development and function in Drosophila. *Cold Spring Harbor Protocols*, *2012*(1), pp.pdb-top067587.

Hastings, J.W. and Sweeney, B.M., 1957. On the mechanism of temperature independence in a biological clock. *Proceedings of the National Academy of Sciences of the United States of America*, *43*(9), p.804.

Swenson, K.I., Jordan, J.R., Beyer, E.C., Paul, D.L., 1989. Formation of gap junctions by expression of connexins in Xenopus oocyte pairs. Cell 57, 145–155.

Szabo, T.M., Faber, D.S., Zoran, M.J., 2004. Transient Electrical Coupling Delays the Onset of Chemical Neurotransmission at Developing Synapses. Journal of

Neuroscience 24, 112–120.

Thaben, P.F., Westermark, P.O., 2014. Detecting Rhythms in Time Series with RAIN. J. Biol. Rhythms 29, 391–400.

Todd, K.L., Jr, W.B.K., French, K.A., 2010. Gap Junction Expression Is Required for Normal Chemical Synapse Formation. Journal of Neuroscience 30, 15277–15285.

Troup, M., Yap, M.H.W., Rohrscheib, C., Grabowska, M.J., Ertekin, D., Randeniya, R., Kottler, B., Larkin, O., Munro, K., Shaw, P.J., van Swinderen, B., 2018. Acute control of the sleep switch in *Drosophila* reveals a role for gap junctions in regulating behavioral responsiveness. Elife 7, 1–22.

Vanderheyden, W.M., Goodman, A.G., Taylor, R.H., Frank, M.G., Van Dongen, H.P. and Gerstner, J.R., 2018. Astrocyte expression of the Drosophila TNF-alpha homologue, Eiger, regulates sleep in flies. *PLoS genetics*, *14*(10), p.e1007724.

Vanin, S., Bhutani, S., Montelli, S., Menegazzi, P., Green, E.W., Pegoraro, M., Sandrelli, F., Costa, R., Kyriacou, C.P., 2012. Unexpected features of *Drosophila* circadian behavioural rhythms under natural conditions. Nature 484, 371–375.

Vecsey, C.G., Pírez, N., Griffith, L.C., 2014. The *Drosophila* neuropeptides PDF and sNPF have opposing electrophysiological and molecular effects on central neurons. J. Neurophysiol. 111, 1033–1045.

Verselis, V.K., Ginter, C.S. and Bargiello, T.A., 1994. Opposite voltage gating polarities of two closely related onnexins. *Nature*, *368*(6469), pp.348-351.

Veruki, M.L. and Hartveit, E., 2002. AII (Rod) amacrine cells form a network of electrically coupled interneurons in the mammalian retina. *Neuron*, *33*(6), pp.935-946.

Vitaterna, M.H., King, D.P., Chang, A.M., Kornhauser, J.M., Lowrey, P.L., McDonald, J.D., Dove, W.F., Pinto, L.H., Turek, F.W. and Takahashi, J.S., 1994. Mutagenesis and mapping of a mouse gene, Clock, essential for circadian behavior. *Science*, *264*(5159), pp.719-725.

Wang, M.H., Chen, N., Wang, J.H., 2014. The coupling features of electrical synapses modulate neuronal synchrony in hypothalamic superachiasmatic nucleus. Brain Res. 1550, 9–17.

Wang, Y., Belousov, A.B., 2011. Deletion of neuronal gap junction protein connexin 36 impairs hippocampal LTP. Neurosci. Lett. 502, 30–32.

Watanabe, A., 1958. The interaction of electrical activity among neurons of lobster cardiac ganglion. *The Japanese journal of physiology*, *8*, pp.305-318.

Watanabe, T., Kankel, D.R., 1990. Molecular cloning and analysis of l(1)ogre, a locus of *Drosophila melanogaster* with prominent effects on the postembryonic development of the central nervous system. Genetics 126, 1033–1044.

Watanabe, T. and Kankel, D.R., 1992. The l (1) ogre gene of Drosophila melanogaster is expressed in postembryonic neuroblasts. *Developmental biology*, *152*(1), pp.172-183.

Welsh, D.K., Reppert, S.M., 1996. Gap junctions couple astrocytes but not neurons in dissociated cultures of rat suprachiasmatic nucleus. Brain Res. 706, 30–36.

Welsh, J.P., Ahn, E.S., Placantonakis, D.G., 2005. Is autism due to brain desynchronization ? International journal of developmental neuroscience 23, 253–263.

Whitmore, D., Foulkes, N.S., Strähle, U., Sassone-Corsi, P., 1998. Zebrafish Clock

rhythmic expression reveals independent peripheral circadian oscillators. Nat. Neurosci. 1, 701–707.

Wu, C.L., Shih, M.F.M., Lai, J.S.Y., Yang, H.T., Turner, G.C., Chen, L., Chiang, A.S., 2011. Heterotypic gap junctions between two neurons in the *Drosophila* brain are critical for memory. Curr. Biol. 21, 848–854.

Wu, L., Dong, A., Dong, L., Wang, S.Q., Li, Y., 2019. PARIS, an optogenetic method for functionally mapping gap junctions. Elife 8, 1–22.

Wülbeck, C., Grieshaber, E., Helfrich-Förster, C., 2008. Pigment-dispersing factor (PDF) has different effects on *Drosophila*'s circadian clocks in the accessory medulla and in the dorsal brain. J. Biol. Rhythms 23, 409–424.

Xia, X., Mills, S.L., 2004. Gap junctional regulatory mechanisms in the AII amacrine cell of the rabbit retina. Visual neuroscience 791–805.

Yaksi, E., Wilson, R.I., 2010. Electrical Coupling between Olfactory Glomeruli. Neuron 67, 1034–1047.

Yamazaki, S., Numano, R., Abe, M., Hida, A., Takahashi, R.I., Ueda, M., Block, G.D., Sakaki, Y., Menaker, M., Tei, H., 2000. Resetting central and peripheral circadian oscillators in transgenic rats. Science, 288, 682–685.

Yang, Z., Sehgal, A., 2001. Role of molecular oscillations in generating behavioral rhythms in *Drosophila*. Neuron 29, 453–467.

Yao, Z., Bennett, A.J., Clem, J.L., Shafer, O.T., 2016. The *Drosophila* Clock Neuron Network Features Diverse Coupling Modes and Requires Network-wide Coherence for Robust Circadian Rhythms. Cell Rep. 17, 2873–2881.

Yao, Z. and Shafer, O.T., 2014. The Drosophila circadian clock is a variably coupled

network of multiple peptidergic units. *Science*, *343*(6178), pp.1516-1520.

Yoo, S.H., Yamazaki, S., Lowrey, P.L., Shimomura, K., Ko, C.H., Buhr, E.D., Siepka, S.M., Hong, H.K., Oh, W.J., Yoo, O.J., Menaker, M., Takahashi, J.S., 2004. PERIOD2::LUCIFERASE real-time reporting of circadian dynamics reveals persistent circadian oscillations in mouse peripheral tissues. Proc. Natl. Acad. Sci. U. S. A. 101, 5339–5346.

Yoshii, T., Heshiki, Y., Ibuki-Ishibashi, T., Matsumoto, A., Tanimura, T., Tomioka, K., 2005. Temperature cycles drive *Drosophila* circadian oscillation in constant light that otherwise induces behavioural arrhythmicity. Eur. J. Neurosci. 22, 1176–1184.

Yoshii, T., Wülbeck, C., Sehadova, H., Veleri, S., Bichler, D., Stanewsky, R., Helfrich-Förster, C., 2009. The neuropeptide pigment-dispersing factor adjusts period and phase of *Drosophila*'s clock. J. Neurosci. 29, 2597–2610.

Yuste, R., Peinado, A. and Katz, L.C., 1992. Neuronal domains in developing neocortex. *Science*, *257*(5070), pp.665-669.

Yu, Y.C., He, S., Chen, S., Fu, Y., Brown, K.N., Yao, X.H., Ma, J., Gao, K.P., Sosinsky, G.E., Huang, K. and Shi, S.H., 2012. Preferential electrical coupling regulates neocortical lineage-dependent microcircuit assembly. *Nature*, *486*(7401), pp.113-117.

Zerr, D.M., Hall, J.C., Rosbash, M., Siwicki, K.K., 1990. Circadian fluctuations of period protein immunoreactivity in the CNS and the visual system of *Drosophila*. J. Neurosci. 10, 2749–2762.

Zhang, L., Chung, B.Y., Lear, B.C., Kilman, V.L., Liu, Y., Mahesh, G., Meissner, R.A., Hardin, P.E., Allada, R., 2010. DN1p Circadian Neurons Coordinate Acute Light

and PDF Inputs to Produce Robust Daily Behavior in *Drosophila*. Curr. Biol. 20, 591–599.

Zhang, S.L., Yue, Z., Arnold, D.M., Artiushin, G., Sehgal, A., 2018. A Circadian Clock in the Blood-Brain Barrier Regulates Xenobiotic Efflux. Cell 173, 130-139.e10.

Appendices

Appendix 1

Fly Strains	Source
UAS *Innexin1* RNAi	BL 44048, BDSC
UAS *Innexin2* RNAi	BL 42645, BDSC
UAS *Innexin3* RNAi	BL 60112, BDSC
UAS *Innexin4* RNAi	BL 27674, BDSC
UAS *Innexin5* RNAi	BL 28042, BDSC
UAS *Innexin6* RNAi	BL 44663, BDSC
UAS *Innexin7* RNAi	BL 26297, BDSC
UAS *Innexin8* RNAi	BL 57706, BDSC
UAS *Innexin2* RNAi	BL 80409, BDSC
Innexin2 mutant	111858, DGRC
UAS eGFP	BL 6874, BDSC
timGal4	Todd Holmes, UC Irvine
pdfGal4	Todd Holmes, UC Irvine
Clk856Gal4	Orie Shafer, ASRC, CUNY
Clk4.1MGal4	BL 36316, BDSC
UAS *tubGal80^{ts}*	BL 7017, BDSC
pdfGal80	Charlotte Helfrich-Förster, University of Würzburg
dvpdfGal4	Michael Rosbash, Brandeis University
LNdGal4	Daniel Cavanaugh, Loyola University
UAS *RFP-Inx2*	Andrea Brand, Cambridge University
UAS *Inx2-GFP*	Michael Hoch and Reinhard Bauer, University of Bonn
UAS *Innexin1* RNAi	BL 27283, BDSC
ogre KO	BL 53719, BDSC
UAS *dicer-2* (II chromosome)	BL 24650, BDSC
UAS *dicer-2* (III chromosome)	BL 24651, BDSC
Clk4.5Gal4	BL 37526, BDSC
R77H08Gal4	BL 39981, BDSC
R51H05Gal4	BL 41275, BDSC
R64A07Gal4	BL 39288, BDSC
Kurs58Gal4	BL 80985, BDSC
alrmGal4	BL 67032, BDSC
NP2222Gal4	112830, DGRC
NP0076Gal4	103516, DGRC
pdfGal4(Gene switch)	Fernanda Ceriani, Leloir Institute Foundation
elavGal4	NCBS
Dilp2Gal4	Amita Sehgal, University of Pennsylvania
Mai301Gal4	Gunter Korge, Freie University of Berlin
UAS *Inx1-GFP*	Andrea Brand, University of Cambridge
UAS *GFP-Inx1*	Andrea Brand, University of Cambridge
UAS *Inx1-myc*	Michael Hoch and Reinhard Bauer, University of Bonn

Appendix 1: A list of all the fly lines used along with their sources is mentioned here. BDSC- Bloomington *Drosophila* Stock centre, IN, USA, DGRC: *Drosophila* Genomics Resource Centre, Japan, NCBS- National Centre for Biological Sciences, Bangalore, India.

Appendix 2.1

Driver	F-statistic	p value
tim > Inx1 RNAi	$F_{2,79} = 778$	0.0000
tim > Inx2 RNAi	$F_{2,83} = 191$	0.0000
tim > Inx3 RNAi	$F_{2,86} = 6$	0.00451
tim > Inx4 RNAi	$F_{2,70} = 0.706$	0.4974
tim > Inx5 RNAi	$F_{2,81} = 37$	0.0000
tim > Inx6 RNAi	$F_{2,90} = 10$	0.00012
tim > Inx7 RNAi	$F_{2,82} = 5$	0.01148
tim > Inx8 RNAi	$F_{2,91} = 5$	0.0137

Appendix 2.1: One-way ANOVA with genotype as a fixed factor conducted for free-running period of flies with each of the eight *Innexin* genes downregulated using *timGal4* driver. $F_{(k-1), (N-k)}$ where k = number of genotypes, N = number of replicates. F-statistic and p-value of the main effect of genotype are indicated here. Specific differences between genotypes determined after post-hoc Tukey's test are represented by different alphabets in the respective graphs and specific p-values for the post-hoc test are mentioned in the respective figure legends.

Appendix 2.2

Driver	F-statistic	p value
tim > Inx1 RNAi	$F_{2,79} = 1.736$	0.1835
tim > Inx2 RNAi	$F_{2,83} = 2.557$	0.0847
tim > Inx3 RNAi	$F_{2,86} = 3.077$	0.0516
tim > Inx4 RNAi	$F_{2,70} = 16.284$	0.0000
tim > Inx5 RNAi	$F_{2,81} = 21.145$	0.0000
tim > Inx6 RNAi	$F_{2,90} = 4.981$	0.0089
tim > Inx7 RNAi	$F_{2,82} = 12.292$	0.00002
tim > Inx8 RNAi	$F_{2,91} = 2.121$	0.1260

Appendix 2.2: One-way ANOVA with genotype as a fixed factor conducted for power of rhythm of flies with each of the eight *Innexin* genes downregulated using *timGal4* driver. $F_{(k-1), (N-k)}$ where k = number of genotypes, N = number of replicates. F-statistic and p-value of the main effect of genotype are indicated here. Specific differences between genotypes determined after post-hoc Tukey's test are represented by different alphabets in the respective graphs and specific p-values for the post-hoc test are mentioned in the respective figure legends.

Appendix 2.3

Driver	F-statistic	p value
tim > Inx1 RNAi	$F_{2,77} = 6.567$	0.0023
tim > Inx2 RNAi	$F_{2,71} = 0.211$	0.8101

Appendix 2.3: One-way ANOVA with genotype as a fixed factor conducted for onsets of precision of flies with *Innexin1* and *Innexin2* genes downregulated using *timGal4* driver. $F_{(k-1),\ (N-k)}$ where k = number of genotypes, N = number of replicates. F-statistic and p-value of the main effect of genotype are indicated here. Specific differences between genotypes determined after post-hoc Tukey's test are represented by different alphabets in the respective graphs and specific p-values for post-hoc are mentioned in the respective figure legends.

Appendix 2.4

Driver	F-statistic	p value
tim > Inx1 RNAi	$F_{2,85} = 5.692$	0.0048
tim > Inx2 RNAi	$F_{2,85} = 3.3457$	0.0401

Appendix 2.4: One-way ANOVA with genotype as a fixed factor conducted for offsets of precision of flies with *Innexin1* and *Innexin2* genes downregulated using *timGal4* driver. $F_{(k-1),\ (N-k)}$ where k = number of genotypes, N = number of replicates. F-statistic and p-value of the main effect of genotype are indicated here. Specific differences between genotypes determined after post-hoc Tukey's test are represented by different alphabets in the respective graphs and specific p-values for post-hoc are mentioned in the respective figure legends.

Appendix 2.5

Driver	F-statistic	p value
tim > Inx1 RNAi	$F_{2,57} = 29.937$	0.0000
tim > Inx2 RNAi	$F_{2,61} = 162.29$	0.0000

Appendix 2.5: One-way ANOVA with genotype as a fixed factor conducted for difference in free-running period values at temperatures of 29°C and 25°C of flies with *Innexin1* and *Innexin2* genes downregulated using *timGal4* driver. $F_{(k-1),\ (N-k)}$ where k = number of genotypes, N = number of replicates. F-statistic and p-value of the main effect of genotype are indicated here. Specific differences between genotypes determined after post-hoc Tukey's test are represented by different alphabets in the respective graphs and specific p-values for post-hoc are mentioned in the respective figure legends.

Appendix 2.6

Driver	F-statistic	p value
tim > Inx1 RNAi	$F_{1,33} = 15.771$	0.000352
tim > Inx2 RNAi	$F_{1,44} = 34.085$	0.000001
tim > Inx3 RNAi	$F_{1,41} = 1.9496$	0.1699
tim > Inx4 RNAi	$F_{1,27} = 0.0802$	0.7791
tim > Inx5 RNAi	$F_{1,25} = 2.2247$	0.1478
tim > Inx6 RNAi	$F_{1,25} = 0.15$	0.7009
tim > Inx7 RNAi	$F_{1,30} = 2.7415$	0.1081
tim > Inx8 RNAi	$F_{1,41} = 0.4937$	0.4861

Appendix 2.6: One-way ANOVA with regime as a fixed factor conducted for values of phase of onsets of flies with each of the eight *Innexin* genes downregulated using *timGal4* driver. $F_{(k-1),\,(N-k)}$ where k = number of regimes, N = number of replicates. F-statistic and p-value of the main effect of regime are indicated here.

Appendix 2.7

Driver	F-statistic	p value
tim > Inx2 RNAi	$F_{2,76} = 10.584$	0.000085
tim > Inx4 RNAi	$F_{2,79} = 43.81$	0.00000

Appendix 2.7: One-way ANOVA with genotype as a fixed factor conducted for onsets of evening activity of flies with *Innexin2* and *Innexin4* genes downregulated using *timGal4* driver. $F_{(k-1),\,(N-k)}$ where k = number of genotypes, N = number of replicates. F-statistic and p-value of the main effect of genotype are indicated here. Specific differences between genotypes determined after post-hoc Tukey's test are represented by different alphabets in the respective graphs and specific p-values for post-hoc are mentioned in the respective figure legends.

Appendix 2.8

Driver	F-statistic	p value
tim > Inx2 RNAi	$F_{2,82} = 1.624$	0.2070
tim > Inx4 RNAi	$F_{2,72} = 5.562$	0.0071

Appendix 2.8: Welch's one-way ANOVA with genotype as a fixed factor conducted for morning anticipation values of flies with *Innexin2* and *Innexin4* genes downregulated using *timGal4* driver. $F_{(k-1),\,(N-k)}$ where k = number of genotypes, N = number of replicates. F-statistic and p-value of the main effect of genotype are indicated here. Specific differences between genotypes determined after post-hoc Tukey's test are represented by different alphabets in the respective graphs and specific p-values for post-hoc are mentioned in the respective figure legends.

Appendix 2.9

Driver	F-statistic	p value
tim > Inx2 RNAi	$F_{2,82} = 8.192$	0.00080
tim > Inx4 RNAi	$F_{2,72} = 35.05$	8.31E-10

Appendix 2.9: Welch's one-way ANOVA with genotype as a fixed factor conducted for evening anticipation values of flies with *Innexin2* and *Innexin4* genes downregulated using *timGal4* driver. $F_{(k-1), (N-k)}$ where k = number of genotypes, N = number of replicates. F-statistic and p-value of the main effect of genotype are indicated here. Specific differences between genotypes determined after post-hoc Tukey's test are represented by different alphabets in the respective graphs and specific p-values for post-hoc are mentioned in the respective figure legends.

Appendix 3.1

Driver	F-statistic	p value
timgal4	$F_{2,84} = 121.4$	0.000
Clk856Gal4	$F_{2,68} = 64.7$	0.000
tim; tubgal80^{ts} (DD 29°C)	$F_{2,65} = 68$	0.000
tim; tubgal80^{ts} (DD 19°C)	$F_{2,70} = 2.2$	0.113
pdf(GS)Gal4 (vehicle)	$F_{2,49} = 4.5$	0.016
pdf(GS)Gal4 (RU food)	$F_{2,53} = 26.99$	0.000

Appendix 3.1: One-way ANOVA with genotype as a fixed factor conducted for free-running period of flies with *Innexin2* downregulated using each of the indicated drivers. $F_{(k-1), (N-k)}$ where k = number of genotypes, N = number of replicates. F-statistic and p-value of the main effect of genotype are indicated here. Specific differences between genotypes determined after post-hoc Tukey's test are represented by different alphabets in the respective graphs and specific p-values for post-hoc are mentioned in the respective figure legends.

Appendix 3.2

Driver	F-statistic	p value
timGal4	$F_{2,84} = 2.587$	0.0812
Clk856Gal4	$F_{2,68} = 0.095$	0.9096
tim; tubgal80^{ts} (DD 29°C)	$F_{2,65} = 22.67$	0.0000
tim; tubgal80^{ts} (DD 19°C)	$F_{2,70} = 0.609$	0.5470

Appendix 3.2: One-way ANOVA with genotype as a fixed factor conducted for power of rhythm of flies with *Innexin2* downregulated using each of the indicated drivers. $F_{(k-1), (N-k)}$ where k = number of genotypes, N = number of replicates. F-statistic and p-value of the main effect of genotype are indicated here. Specific differences between genotypes

determined after post-hoc Tukey's test are represented by different alphabets in the respective graphs and specific p-values for post-hoc are mentioned in the respective figure legends.

Appendix 3.3

Driver	F-statistic	p value
dvpdfGal4	$F_{2,62} = 127$	0.000
pdfGal4	$F_{2,82} = 338$	0.000
LNdGal4	$F_{2,69} = 11.1$	0.000069
Clk4.1MGal4	$F_{2,53} = 11.7$	0.000064
tim; pdfGal80	$F_{2,83} = 10.5$	0.000089
Clk856; pdfGal80	$F_{2,61} = 12.8$	0.000023

Appendix 3.3: One-way ANOVA with genotype as a fixed factor conducted for free-running period of flies with *Innexin2* downregulated using each of the indicated drivers. $F_{(k-1), (N-k)}$ where k = number of genotypes, N = number of replicates. F-statistic and p-value of the main effect of genotype are indicated here. Specific differences between genotypes determined after post-hoc Tukey's test are represented by different alphabets in the respective graphs and specific p-values for post-hoc are mentioned in the respective figure legends.

Appendix 3.4

Driver	F-statistic	p value
dvpdfGal4	$F_{2,62} = 16.02$	0.000002
pdfGal4	$F_{2,82} = 3.262$	0.04333
LNdGal4	$F_{2,69} = 19.948$	0.0000
Clk4.1MGal4	$F_{2,53} = 1.009$	0.3713
tim; pdfGal80	$F_{2,83} = 3.248$	0.0438

Appendix 3.4: One-way ANOVA with genotype as a fixed factor conducted for power of rhythm of flies with *Innexin2* downregulated using each of the indicated drivers. $F_{(k-1), (N-k)}$ where k = number of genotypes, N = number of replicates. F-statistic and p-value of the main effect of genotype are indicated here. Specific differences between genotypes determined after post-hoc Tukey's test are represented by different alphabets in the respective graphs and specific p-values for post-hoc are mentioned in the respective figure legends.

Appendix 3.5

Driver	F-statistic	p value
tim > Inx2-GFP	$F_{2,68} = 5.3$	0.0073
pdf > Inx2-GFP	$F_{2,61} = 21.5$	0.0000
tim > RFP-Inx2	$F_{2,82} = 32.6$	0.0000
pdf > RFP-Inx2	$F_{2,84} = 44$	0.0000

Appendix 3.5: One-way ANOVA with genotype as a fixed factor conducted for free-running period of flies with *Innexin2* overexpressed using each of the indicated drivers. $F_{(k-1), (N-k)}$ where k = number of genotypes, N = number of replicates. F-statistic and p-value of the main effect of genotype are indicated here. Specific differences between genotypes determined after post-hoc Tukey's test are represented by different alphabets in the respective graphs and specific p-values for post-hoc are mentioned in the respective figure legends.

Appendix 3.6

Driver	F-statistic	p value
tim > Inx2-GFP	$F_{2,68} = 18.353$	0.0000
pdf > Inx2-GFP	$F_{2,61} = 13.119$	0.000018
tim > RFP-Inx2	$F_{2,82} = 6.819$	0.00182
pdf > RFP-Inx2	$F_{2,82} = 3.287$	0.0422

Appendix 3.6: One-way ANOVA with genotype as a fixed factor conducted for power of rhythm of flies with *Innexin2* overexpressed using each of the indicated drivers. $F_{(k-1), (N-k)}$ where k = number of genotypes, N = number of replicates. F-statistic and p-value of the main effect of genotype are indicated here. Specific differences between genotypes determined after post-hoc Tukey's test are represented by different alphabets in the respective graphs and specific p-values for post-hoc are mentioned in the respective figure legends.

Appendix 3.7

Driver	Z score	p value
tim > Inx2 RNAi (s-LNv)	3.6987	0.00021
tim > Inx2 RNAi (l-LNv)	2.0981	0.0358

Appendix 3.7: Mann-Whitney U-test with genotype as a factor conducted for Innexin2 intensity values in both small ventral lateral neurons (s-LNv) and large ventral lateral neurons (l-LNv) when *Innexin2* is downregulated using the *timGal4* driver. Z-score and p value of the main effect of genotype are indicated here for both the cell types.

Appendix 3.8

Driver	F-statistic	p value
Inx2 oscillations in s-LNv	$F_{5,24} = 6.2506$	0.000033
Inx2 oscillations in l-LNv	$F_{5,29} = 7.710$	0.000002

Appendix 3.8: One-way ANOVA with time point as a fixed factor conducted for Innexin2 intensity values in both small (s-LNv) and large ventral neurons (l-LNv). $F_{(k-1), (N-k)}$ where k = number of genotypes, N = number of replicates. F-statistic and p-value of the main effect of genotype are indicated here. Specific differences between timepoints determined after post-hoc Tukey's test are represented by asterisks in the respective graphs and specific p-values for post-hoc are mentioned in the respective figure legends.

Appendix 4.1

Driver	F-statistic	p value
timGal4	$F_{2,84} = 139.3$	0.000
Clk856Gal4	$F_{2,75} = 216.3$	0.000
tim; tubgal80^{ts} (DD 29°C)	$F_{2,64} = 82.4$	0.000
tim; tubgal80^{ts} (DD 19°C)	$F_{2,62} = 120.4$	0.000
pdf(GS)Gal4 (vehicle)	$F_{2,49} = 1.6$	0.2161
pdf(GS)Gal4 (RU food)	$F_{2,51} = 23.45$	0.000

Appendix 4.1: One-way ANOVA with genotype as a fixed factor conducted for free-running period of flies with *Innexin1* downregulated using each of the indicated drivers. $F_{(k-1), (N-k)}$ where k = number of genotypes, N = number of replicates. F-statistic and p-value of the main effect of genotype are indicated here. Specific differences between genotypes determined after post-hoc Tukey's test are represented by different alphabets in the respective graphs and specific p-values for post-hoc are mentioned in the respective figure legends.

Appendix 4.2

Driver	F-statistic	p value
timGal4	$F_{2,84} = 3.830$	0.02558
Clk856Gal4	$F_{2,75} = 0.77$	0.46668
tim; tubgal80^{ts} (DD 29°C)	$F_{2,64} = 32.428$	0.0000
tim; tubgal80^{ts} (DD 19°C)	$F_{2,62} = 1.5391$	0.2226

Appendix 4.2: One-way ANOVA with genotype as a fixed factor conducted for power of rhythms of flies with *Innexin1* downregulated using each of the indicated drivers. $F_{(k-1), (N-k)}$ where k = number of genotypes, N = number of replicates. F-statistic and p-value of the main effect of genotype are indicated here. Specific differences between genotypes determined after post-hoc Tukey's test are represented by different alphabets in the

respective graphs and specific p-values for post-hoc are mentioned in the respective figure legends.

Appendix 4.3

Driver	F-statistic	p value
dvpdfGal4	$F_{2,62} = 1081.3$	0.000
pdfGal4	$F_{2,80} = 226$	0.000
LNdGal4	$F_{2,73} = 14$	0.000005
tim; pdfGal80	$F_{2,69} = 65.1$	0.000

Appendix 4.3: One-way ANOVA with genotype as a fixed factor conducted for free-running period of flies with *Innexin1* downregulated using each of the indicated drivers. $F_{(k-1), (N-k)}$ where k = number of genotypes, N = number of replicates. F-statistic and p-value of the main effect of genotype are indicated here. Specific differences between genotypes determined after post-hoc Tukey's test are represented by different alphabets in the respective graphs and specific p-values for post-hoc are mentioned in the respective figure legends.

Appendix 4.4

Driver	F-statistic	p value
dvpdfGal4	$F_{2,62} = 32.545$	0.0000
pdfGal4	$F_{2,80} = 0.396$	0.6741
LNdGal4	$F_{2,73} = 10.058$	0.000143
tim; pdfGal80	$F_{2,69} = 0.2357$	0.79068

Appendix 4.4: One-way ANOVA with genotype as a fixed factor conducted for power of rhythms of flies with *Innexin1* downregulated using each of the indicated drivers. $F_{(k-1), (N-k)}$ where k = number of genotypes, N = number of replicates. F-statistic and p-value of the main effect of genotype are indicated here. Specific differences between genotypes determined after post-hoc Tukey's test are represented by different alphabets in the respective graphs and specific p-values for post-hoc are mentioned in the respective figure legends.

Appendix 4.5

Driver	F-statistic	p value
Clk4.1MGal4	$F_{2,48} = 30$	0.000
Clk4.5FGal4	$F_{2,49} = 8.8$	0.000549
R77H08Gal4	$F_{2,80} = 1.5$	0.2354
R51H05Gal4	$F_{2,68} = 4.8$	0.0111
R64A07Gal4	$F_{2,61} = 23$	0.000
Kurs58Gal4	$F_{2,71} = 1.5$	0.2357
Dilp2Gal4	$F_{2,50} = 0.1$	0.8654
Mai301Gal4	$F_{2,48} = 9.3$	0.00041

Appendix 4.5: One-way ANOVA with genotype as a fixed factor conducted for free-running period of flies with *Innexin1* downregulated using each of the indicated drivers. $F_{(k-1), (N-k)}$ where k = number of genotypes, N = number of replicates. F-statistic and p-value of the main effect of genotype are indicated here. Specific differences between genotypes determined after post-hoc Tukey's test are represented by different alphabets in the respective graphs and specific p-values for post-hoc are mentioned in the respective figure legends.

Appendix 4.6

Driver	F-statistic	p value
Clk4.1MGal4	$F_{2,48} = 0.4668$	0.6298
Clk4.5FGal4	$F_{2,49} = 1.2894$	0.28461
R77H08Gal4	$F_{2,80} = 0.03$	0.97
R51H05Gal4	$F_{2,68} = 10.171$	0.000135
R64A07Gal4	$F_{2,61} = 20.9864$	0.0000
Kurs58Gal4	$F_{2,71} = 4.960$	0.009635
Dilp2Gal4	$F_{2,50} = 0.72$	0.4919
Mai301Gal4	$F_{2,48} = 29.875$	0.0000

Appendix 4.6: One-way ANOVA with genotype as a fixed factor conducted for power of rhythms of flies with *Innexin1* downregulated using each of the indicated drivers. $F_{(k-1), (N-k)}$ where k = number of genotypes, N = number of replicates. F-statistic and p-value of the main effect of genotype are indicated here. Specific differences between genotypes determined after post-hoc Tukey's test are represented by different alphabets in the respective graphs and specific p-values for post-hoc are mentioned in the respective figure legends.

Appendix 4.7

Driver	F-statistic	p value
elav; pdfGal80	$F_{2,51} = 2.2$	0.1177
alrmGal4	$F_{2,66} = 10.4$	0.000119
NP2222Gal4	$F_{2,61} = 15.9$	0.000004

Appendix 4.7: One-way ANOVA with genotype as a fixed factor conducted for free-running period of flies with *Innexin1* downregulated using each of the indicated drivers. $F_{(k-1), (N-k)}$ where k = number of genotypes, N = number of replicates. F-statistic and p-value of the main effect of genotype are indicated here. Specific differences between genotypes determined after post-hoc Tukey's test are represented by different alphabets in the respective graphs and specific p-values for post-hoc are mentioned in the respective figure legends.

Appendix 4.8

Driver	F-statistic	p value
elav; pdfGal80	$F_{2,51} = 0.188$	0.8293
alrmGal4	$F_{2,66} = 18.188$	0.0000
NP2222Gal4	$F_{2,61} = 3.381$	0.04134

Appendix 4.8: One-way ANOVA with genotype as a fixed factor conducted for power of rhythms of flies with *Innexin1* downregulated using each of the indicated drivers. $F_{(k-1), (N-k)}$ where k = number of genotypes, N = number of replicates. F-statistic and p-value of the main effect of genotype are indicated here. Specific differences between genotypes determined after post-hoc Tukey's test are represented by different alphabets in the respective graphs and specific p-values for post-hoc are mentioned in the respective figure legends.

Appendix 4.9

Driver	F-statistic	p value
tim > Inx1-GFP	$F_{2,66} = 10.6$	0.000105
pdf > Inx1-GFP	$F_{2,65} = 28.1$	0.00000
pdf > Inx1-myc	$F_{2,87} = 57.3$	0.0000
pdf > Inx1-myc; Inx2-GFP	$F_{2,79} = 17.3$	0.0000
tim > GFP-Inx1	$F_{2,80} = 29.9$	0.00000
pdf > GFP-Inx1	$F_{2,59} = 42.5$	0.0000

Appendix 4.9: One-way ANOVA with genotype as a fixed factor conducted for free-running period of flies with *Innexin1* overexpressed using each of the indicated drivers. $F_{(k-1), (N-k)}$ where k = number of genotypes, N = number of replicates. F-statistic and p-value of the main effect of genotype are indicated here. Specific differences between genotypes

Appendix 4.10

Driver	F-statistic	p value
tim > Inx1-GFP	$F_{2,66} = 3.384$	0.03988
pdf > Inx1-GFP	$F_{2,65} = 2.414$	0.09730
pdf > Inx1-myc	$F_{2,87} = 0.591$	0.555873
pdf > Inx1-myc; Inx2-GFP	$F_{2,79} = 7.706$	0.00087
tim > GFP-Inx1	$F_{2,80} = 7.030$	0.0015
pdf > GFP-Inx1	$F_{2,59} = 12.784$	0.000023

Appendix 4.10: One-way ANOVA with genotype as a fixed factor conducted for power of rhythms of flies with *Innexin1* overexpressed using each of the indicated drivers. $F_{(k-1), (N-k)}$ where k = number of genotypes, N = number of replicates. F-statistic and p-value of the main effect of genotype are indicated here. Specific differences between genotypes determined after post-hoc Tukey's test are represented by different alphabets in the respective graphs and specific p-values for post-hoc are mentioned in the respective figure legends.

Appendix 4.11

	p-value	phase	Peak shape	period
control	4.011243E-18	4	8	24
experimental	1.015176E-16	8	8	24

Appendix 4.11: Table obtained from RAIN analysis indicating the p-value, phase, peak shape and period of PER protein oscillations in small ventral lateral neurons (s-LNv) of both control (*dcr; Inx1* RNAi) and experimental (*Clk856 > dcr; Inx1* RNAi) flies dissected on day 3 of constant darkness (DD day3).

Appendix 4.12

	p-value	phase	Peak shape	period
control	0.1124613	20	20	24
experimental	5.62E-06	4	12	24

Appendix 4.12: Table obtained from RAIN analysis indicating the p-value, phase, peak shape and period of PER protein oscillations in large ventral lateral neurons (l-LNv) of both control (*dcr; Inx1* RNAi) and experimental (*Clk856 > dcr; Inx1* RNAi) flies dissected on day 3 of constant darkness (DD day3).

Appendix 4.13

	p-value	phase	Peak shape	period
control	7.07E-06	4	16	24
experimental	0.00018	8	4	24

Appendix 4.13: Table obtained from RAIN analysis indicating the p-value, phase, peak shape and period of PDF oscillations in the dorsal projections of small ventral lateral neurons of both control (*dcr; Inx1* RNAi) and experimental (*Clk856 > dcr; Inx1* RNAi) flies dissected on day 3 of constant darkness (DD day3).

Appendix 4.14

Driver	Z-score	p value
Cont vs expt (CT3)	0.00	1.00
Cont vs expt (CT7)	-2.02564	0.04282
Cont vs expt (CT11)	3.97273	0.000071
Cont vs expt (CT15)	1.0639	0.2873
Cont vs expt (CT19)	4.1606	0.000032
Cont vs expt (CT23)	3.7969	0.000146

Appendix 4.14: Pairwise comparisons made using the Mann-Whitney U-test with genotype as a factor conducted for PER protein intensity values in the small ventral lateral neurons (s-LNv) for all six time points in both control (*dcr; Inx1* RNAi) and experimental (*Clk856 > dcr; Inx1* RNAi) flies. Z-score and p values are indicated in this table.